EXPLORING FLOWERING AND PHOTOPERIOD RESPONSE MECHANISMS IN LEGUMES

by

Beatriz Contreras Planesas

MSc in Plant Biotechnology

School of Natural Sciences

Submitted in fulfilment of the requirements for the Doctor of

Philosophy University of Tasmania, February 2022

Author declarations

Declaration of Originality

This thesis contains no material which has been accepted for a degree or diploma by the University or any other institution, except by way of background information and duly acknowledged in the thesis, and to the best of my knowledge and belief no material previously published or written by another person except where due acknowledgement is made in the text of the thesis, nor does the thesis contain any material that infringes copyright.

Authority of Access

This thesis may be made available for loan. Copying and communication of any part of this thesis is prohibited for two years from the date this statement was signed; after that time limited copying and communication is permitted in accordance with the Copyright Act 1968.

Beatriz Contreras Planesas

University of Tasmania, Hobart

21st of October 2021

Acknowledgements

I would like to take this opportunity to thank all those that have encouraged and supported me throughout my PhD, specially at the end. First and foremost, I would like to express my sincere gratitude to my supervisors, Jim Weller and Valérie Hecht, for giving me this exciting opportunity. I am deeply grateful for all their support, guidance and extensive knowledge. I would like to give a special thanks to the other amazing members of the Pea Flowering Group (past and present) who have been a delight to work with and always helpful and supportive; Jackie Vander Schoor, Laura James, Jak Butler, Raul Ortega, Andy Rubenach, Kelsey Picard and Chantelle Beagley.

I would also like to thank all the PhD candidates and staff at the School of Biological Sciences for providing a friendly and welcoming environment. A special thanks to Michelle Lang and Tracey Winterbottom for keeping my plants alive, Dr Frances Sussmilch and Dr Lu Wang for their kind and extremely useful assistance in Yeast-Two-Hybrid and Western Blot techniques, and Adam Smolenski and Sharee McCammon for their technical support and advice in the molecular laboratory. I would like to extend my appreciation to the University of Tasmania and the Graduate Research Scholarship for supporting this research.

I am extremely grateful to all my friends in Tasmania and abroad who have always supported and encouraged me during this wild adventure. To James Pay, Laura Rood, Cat Butler, Kelsey Picard, Jak Butler, Owen Williams, Kirstin Proft and Candice Untiedt, thanks for sharing the good and the bad times (and all my tears) and always be there for me. A big thank you to Jackie, Sam-girl, Sam-boy and Gerry, for their encouraging and caring friendship. I am also deeply grateful for my friends abroad Marta, Gemma, Marta, Katie and Cris, who have dealt with many intermittent conversations due to time difference but have unconditionally had my back. I am immensely grateful for my Spanish friends in Tasmania, Raul, Tere, Patri and Mara, who have become my Spanish family in Australia.

Lastly, I would like to thank my family for their endless support and encouragement. Even without being clear on what I have been working on, they have supported me in every single decision of my life. Mum and dad have been my role models for resilience and hard work, which have been fundamental pillars for this thesis. I am forever indebted for all their kind support and daily text messages for the last 5 years reminding me of all their love and encouragement.

Table of content

List of figures

List of tables

Abbreviations

This list contains commonly used abbreviations in this thesis. Other abbreviations are explained in the specific sections used.

BC	Backcross
bp	Nucleotide base pairs
bZIP	Basic leucine zipper domain
CAPS	Cleaved Amplified Polymorphic Sequences
CDFs	*CYCLING DOF FACTORs*
cDNA	Complementary DNA
CDS	Coding sequence
CEF	Controlled Environment Facility
CF	24h of Continuous cool-white Fluorescent light
CO	*CONSTANS*
COL	*CONSTANS-LIKE*
COP1	*CONSTITUTIVE PHOTOMORPOGENIC 1*
CRF	Controlled release fertilizer
cv.	Cultivar
DNA	Deoxyribonucleic acid
dNTPs	Deoxynucleotide triphosphates
DTF	Days to flowering
ELF3	*EARLY FLOWERING 3*
EMS	Ethyl methanesulfonate
E1	*E1 gene*

FKF1	*FLAVIN-BINDING, KELCH REPEAT, F-BOX 1*
FLR	Flower-Leaf Relativity
FT	*FLOWERING LOCUS T*
gDNA	Genomic DNA
GI	*GIGANTEA*
HR	*HIGH RESPONSE*
HRM	High Resolution Melt
IL	Internode Length
I_1	Primary inflorescence
I_2	Secondary inflorescence
kB	1000 nucleotide base pairs
LATE1	*LATE BLOOMER 1*
LATE2	*LATE BLOOMER 2*
LB	Lurio-Bertani media
LD	Long day(s)
LDF	LD photoperiod extended with Fluorescent light
LDI	LD photoperiod extended with Incandescent light
LDP	Long Day flowering Plant
LIP1	*LIGHT INDEPENDENT PHOTOMORPHOGENESIS 1*
LOV	Light–Oxygen–Voltage domain
NBs	Nuclear Bodies
NCBI	National Center for Biotechnology Information
NFI	Node of flower initiation

NLS	Nuclear Localizing Signal
NV	Non-Vernalised treatment
ORF(s)	Open Reading Frame(s)
PCR	Polymerase Chain Reaction
PHYA	PHYTOCHROME A
PHYB	PHYTOCHROME B
qPCR	Quantitative Polymerase Chain Reaction
QTL	Quantitative Trait Loci
RN	Reproductive nodes
RNA	Ribonucleic acid
RT-PCR	Reverse-Transcription Polymerase Chain Reaction
SD	Short Day(s)
SDP	Short Day flowering Plant
SDW	Sterile Milli-Q water
SE	Standard error
SNP	Single Nucleotide Polymorphism
TAE	Tris acetate ethylenediamine tetra-acetic acid
TAIR	The *Arabidopsis* Information Resource
Tm	Melting temperature
TN	Total nodes
TOR	Torsdag cultivar
UV	Ultraviolet light
V	Vernalised treatment

WT	Wild-type

Abstract

Flowering defines the reproductive stage of a plant, and its timing is regulated by environmental factors to align reproduction with favourable conditions to maximise the success of a plant. Daylength (photoperiod) and temperature are the two primary factors that signal seasonal changes and drive plant responses. The genetic pathways through which these factors act to influence flowering time has been extensively studied in model plants like *Arabidopsis*, and underlying molecular mechanisms have been substantially elucidated. The molecular knowledge regarding flowering time control is helping to describe and predict the adaptation of plants and crops, and is particularly useful in an agricultural context.

The molecular pathway conferring photoperiod-responsiveness of flowering was first described in the model *Arabidopsis* and involves a central role for the hormone-like florigen protein FT that integrates environmental information and signals from leaf to shoot apex. Under LD conditions, *FT* gene expression is highly induced by *CO*, a direct *FT* regulator and key element of the pathway, that integrates input from light and from the circadian clock to determine photoperiod sensitivity. While many other genes participate in the regulation of flowering, research across diverse angiosperm crop and model species plants seem to support the conserved nature of this central mechanism, in which light perceived by photoreceptors is translated to photoperiod-specific *CO* expression, which in turn activates *FT*, providing the ultimate inductive signal for flowering to occur. However, other evidence suggests that this conservation may not be universal.

In legumes, the *FT* gene family is expanded, but several genes show strong photoperiod-dependent expression and promotive effects on flowering, similar to *Arabidopsis FT*. In contrast, *CO-like* genes are present, but have not been shown to have any clear or substantial role in regulation of flowering, at least in the temperate LD legumes. An increasing number of other legume flowering gene homologs have also been examined, but this is ongoing, and many potential components still remain to be characterised. Also, the finding that the role of *CO* may not be conserved in legumes raises questions about how photoperiod-specific *FT* expression occurs. This thesis explores this question by characterising several loci implicated in photoperiod sensitive flowering in other systems.

In the case of soybean, a SD legume, the integrating role of *CO* may instead be played by *E1*, a legume specific gene encoding a transcription factor that directly represses *FT* gene expression under LD. *E1* is also the most important locus explaining latitudinal variation for flowering time across different cultivars. Chapter 3 of this thesis examines *E1* phylogeny, compares E1 protein

structures and investigates the potential role of *E1* genes in two temperate LD legumes, pea and *Medicago*, through the characterization of mutants obtained by reverse genetics.

Protein-level control is an important feature of the photoperiod pathway, and is critical for the precise timing of the activity of some elements in the pathway, most notably *CO*. In *Arabidopsis*, COP1 is the main E3 ubiquitin ligase involved in the regulation of CO protein abundance. *COP1* has been shown to participate in diverse light-mediated processes and it is particularly well characterised for its role in photomorphogenesis. Its participation in flowering regulation includes a direct interaction with CO but also with other components such as photoreceptors, GIGANTEA (GI) and ELF3 thereby also modulating transcriptional regulation of *CO*. In pea, the *LIP1* gene has been characterized as the *COP1* ortholog, and Chapter 4 examines its potential role in flowering time control and developmental rate, including how it might interact genetically with key elements of the pea flowering network such as *LATE1* (*PsGI*), *HR* (*PsELF3a*) and *PHYA* through the characterisation of the double and triple mutants with *lip1*. In addition, the predicted protein structure of LIP1 was compared to COP1 to identify any possible functionally-significant differences.

Another important component in the *Arabidopsis* photoperiod pathway is *FKF1*, which is able to perceive blue light and participates in the transcriptional and post-transcriptional regulation of *CO*. Its function is associated with the formation of protein complexes controlling protein degradation. One such complex, formed between FKF1 and GI, is able to regulate members of the CDF transcription factor family, which are repressors of *CO* transcription. This complex serves as one important point in the integration of light and circadian clock regulation for the response to photoperiod in *Arabidopsis*. Chapter 5 investigates whether *FKF1* might participate in flowering time control in pea and *Medicago*, through isolation of mutants and examination of potential effects on flowering and photomorphogenesis. A phylogenetic study of the legume *FKF1* family is included together with an examination of the possible physical interaction of FKF1 and LATE1 using a yeast two-hybrid assay.

Results from the thesis suggest that some regulatory factors of the pathway are conserved and participate in flowering control, but others have minimal regulatory roles. *E1* in pea and *Medicago* has a small promoting effect on flowering, opposite to that observed in the SD legume, soybean. Thus, although potentially retaining a role in flowering time regulation, it is not the sole point of integration for the photoperiod response. *LIP1* also has a small effect on flowering time due in part to a slow developmental rate (plastochron). Genetic interactions with important flowering components like *LATE1* and *HR* suggest it is unlikely to have a role in the photoperiod response

similar to *Arabidopsis COP1*. Finally, FKF1 protein is able to interact with LATE1 in pea but its flowering effect in both pea and *Medicago* seems to be limited, with a minimal late-flowering phenotype in some photoperiod conditions. Overall, this research makes a significant contribution to the current understanding of photoperiod regulation of flowering time in temperate long-day legumes.

Chapter 1 - General introduction

1.1 Control of flowering time by photoperiod

The transition from vegetative to reproductive phase (flowering) is a major developmental change, and in order to ensure a successful life cycle, is highly coordinated and regulated with internal/endogenous factors like plant age, hormone signalling or developmental stage, and with external inputs such as temperature, light quality and daylength (Andrés and Coupland, 2012; He et al., 2020; Kinoshita and Richter, 2020). The concept that plants could respond to external signals was first described in 1920's by Garner and Allard 1920, but the nature and integration of internal signals mediating these changes has been a more complicated subject to describe (Song et al., 2015). Photoperiod (or daylength) operates as an excellent guide of seasonal changes for sessile organisms like plants due to its stable and predictable nature. Many regulatory networks emerged in plants able to integrate the seasonal information captured in the leaves (as light duration, light quality and light quantity) and transform it into a molecular network directing many developmental processes (Brambilla and Fornara, 2017a; Thomas, 2006).

Flowering essentially involves the transformation of meristems to produce flowers instead of shoots and is associated with other developmental changes such as stem elongation, plant maturity, lateral branching, resource distribution among others (Weller and Ortega, 2015). This transition is strictly regulated and highly coordinated with the most favourable environmental conditions. Temperature and daylength are the main seasonal factors regulating flowering time through molecular signalling cues (Andrés and Coupland, 2012; Li et al., 2016). In some cases exposure to a prolonged temperature event is required in order to permit response to photoperiod and induce flowering in the following seasons (Kim et al., 2009; Quiroz et al., 2021; Song et al., 2013). The exposure to a cold event is known as vernalization and it is commonly associated with a release of flowering inhibition as an adaptation to temperate climates, but the range of temperature and response is highly variable between species, varieties and/or environmental niches (Kim et al., 2009; Sung and Amasino, 2005). Plants are able to follow changes in daylength through an endogenous timekeeper which contributes to tracking of dark and light periods (Johansson and Staiger, 2015). Daily light duration is perceived in the leaves inducing an internal signal commonly termed florigen, which travels to the shoot apex to promote flowering (Johansson and Staiger, 2015; Lang et al., 1977; Romanov, 2012). Therefore, a mechanistic framework for photoperiod control of flowering can be divided into three components: light input in leaves, circadian clock and timekeeper tracking and the output signal

known as florigen. Genes and gene interactions mediating photoperiodic changes and guiding the time of flowering have been extensively studied and described, pointing to a complex gene network (Johansson and Staiger, 2015; Shim et al., 2017; Song et al., 2015).

1.1.1 Relation of photoperiod and flowering time

Depending on the onset of flowering in relation to photoperiod, plants can be divided in three groups. Long-day plants (LDP) flower when the day exceeds a certain length, whereas short-day plants (SDP) flower when the period of light in the day is shorter than a critical threshold, and Day-Neutral Plants (DNP) flower independently of daylength. These three photoperiodic flowering responses are commonly associated with latitudinal distribution (Andrés and Coupland, 2012; Johansson and Staiger, 2015). The model plant examples for these groups include: *Arabidopsis thaliana* as LDP system in which photoperiodic flowering molecular network has been described in the greatest detail (Koornneef et al., 1991; Quiroz et al., 2021); *Oryza sativa* (rice) which is a facultative SDP in which the genetic network regulating flowering has similarities to the *Arabidopsis* model but also features unique components and interactions (Brambilla and Fornara, 2013; Izawa, 2007); and finally tomato (*Solanum lycopersicum)* which has served as a DNP genetic model for flowering studies (Lifschitz and Eshed, 2006; Silva et al., 2019).

1.1.2 Adaptation to photoperiod

To match plant developmental transitions with the best environmental conditions, many plant systems have incorporated great levels of plasticity in their genetic networks (Blackman, 2017), and there is a wide range of natural variation and variety of flowering responses in relation to diverse photoperiod conditions and extended geographical distribution. Modification of flowering time in relation to photoperiod has also been an important feature of domestication and breeding in which human selection has been applied to this natural variation (Blackman, 2017; Jung and Muller, 2009; Leijten et al., 2018). The knowledge acquired from the flowering genetic network and the photoperiodic response is highly valuable for agricultural practices due to its link with latitudinal adaptation (Nakamichi, 2015; Weller et al., 2019). In many species this adaptation has required an adjustment and relaxation in photoperiod sensitivity and included great levels of natural variation in flowering genes and their regulation as well, documented in rice and soybean (Brambilla and Fornara, 2013; Fuller et al., 2010; Huang et al., 2012b; Izawa, 2007; Olsen and Wendel, 2013). It is common to find parallel adaptation in different species in relation to flowering

time traits that has been subjected to selection (Olsen and Wendel, 2013). An example of latitudinal adaptation and domestication facilitated by a relaxation in photoperiod response is rice, which originated in lower latitudes and is now grown more broadly (Andrés and Coupland, 2012; Purugganan and Fuller, 2009). Similarly, in soybean at least 10 flowering-related loci have undergone a relaxation in photoperiod sensitivity with some high-latitude adaptation related to natural variation in a key flowering gene (He et al., 2020; Watanabe et al., 2011; Weller and Ortega, 2015). Despite the natural variation in flowering genes and their photoperiod response related to adaptation, flowering promotion is still determined by inductive light and circadian clock conditions leading to a genetic signalling cascade which induces expression of *FT (FLOWERING LOCUS T)* genes (Andrés and Coupland, 2012; Brambilla and Fornara, 2013; Lv et al., 2021; Song et al., 2013, 2015).

1.2 Photoperiod regulation of flowering in *Arabidopsis*

Most molecular-genetic research on flowering time has focused on *Arabidopsis thaliana,* a model plant species that is widely distributed in the north hemisphere (Koornneef et al., 1991). It is a facultative LD flowering species with a short life cycle and easily-measurable flowering traits and provides the facility to isolate flowering-time mutants, and readily generate transgenic lines. These useful research characteristics made *Arabidopsis* the flowering genetics model species and increasingly contributed to unravelling the response to daylength and control of flowering initiation (Andrés and Coupland, 2012).

The isolation of photoperiod responsive mutants and their flowering characterization in *Arabidopsis* led to the gradual development of a genetic model for the mechanism of photoperiodism, in which activation of photoreceptors in the leaves are able to interact with outputs of the internal circadian clock to confer expression control on a key signalling component, the zinc-finger transcription factor CONSTANS (CO). This protein is thought to act as a central integrator that converts light and circadian clock information to a LD-specific induction of *FT* expression (Andrés and Coupland, 2012; Kinoshita and Richter, 2020). The FT protein considered as "florigen", is synthesized in the leaves, and moves to the shoot apical meristem where it induces expression of floral identity genes and subsequently flowering (Andrés and Coupland, 2012; Shim et al., 2017; Song et al., 2015).

1.2.1 Regulation of flowering at the transcriptional level

CO is considered the main regulator of photoperiod-dependent *FT* expression in *Arabidopsis* (Shim et al., 2017; Song et al., 2015), and is subject to regulation at both the transcriptional and at a protein level, that confers LD-specificity on its control of *FT* (Shim et al., 2017). When CO protein is stabilised, it is able to bind in the promoter region of the *FT* gene, inducing its expression and leading to a *FT* peak of expression on the afternoon of LD (Tiwari et al., 2010). In addition to CO, *FT* expression is also strongly regulated by other components acting either as activators or repressors of its transcription (Song et al., 2015). It is important to note that the tissue-specific regulation of the different components like clock genes or *CO* or *FT* plays an important role in flowering promotion (Hearn and Webb, 2020; Nimmo et al., 2020; Sawa and Kay, 2011).

CO expression is highly regulated as it plays an important role joining different inputs of regulation like circadian clock, light, and temperature (Putterill et al., 1995; Suárez-López et al., 2001). The upstream regulatory pathway of *CO* involves the circadian clock and photoperiod components participating in a sophisticated network of regulation (Kinoshita and Richter, 2020) leading to a peak of *CO* expression around 12-16 h after light stimulation and, linking with a CO protein stabilization at the end of Long Days (12-16h) (Andrés and Coupland, 2012). During the morning, CO protein interacts with other protein complexes which regulates its protein stability and function.

Starting with the transcriptional control of *CO*, CYCLING DOF FACTORs (CDFs) directly repress *CO* transcription acting redundantly in the morning (Fornara et al., 2009; Imaizumi et al., 2005; Renau-Morata et al., 2020). CDFs are able to bind in the promoter region *CO* and are precisely regulated by a complex formed by GIGANTEA (GI) and FLAVIN KELCH BOX 1 (FKF1) proteins (Fornara et al., 2009; Sawa et al., 2007). Both *GI* and *FKF1* like *CDFs,* show circadian rhythms of expression under the control of circadian clock and light (Renau-Morata et al., 2020; Song et al., 2014). GI is a plant-specific protein that links circadian clock regulation into the photoperiodic pathway acting together with FKF1, a chromophore protein with ubiquitin ligase activity and regulated by blue light (Song et al., 2012, 2014). Light-activated FKF1 is able to be stabilised by GI protein during the afternoon of LD, forming a protein complex which precisely regulates the degradation of CDFs, releasing the repression of *CO* and allowing *FT* expression (Andrés and Coupland, 2012; Song et al., 2014). Once the CDFs are removed from *CO* promoter, other transcriptional activating factors named FBHs (FLOWERING BHLH1, FBH2, FBH3 and FBH4) are able to bind the promoter region resulting in a high expression of *CO* from late afternoon to dawn (Ito et al., 2012b; Shim et al., 2017). *CO* expression is also regulated by other mechanisms, one of them is direct GI binding in

CO promoter, which is mediated by ELF4 (EARLY FLOWERING 4) controlling GI localization by nuclear bodies formation (Kim et al., 2013c; Mishra and Panigrahi, 2015).

The transcriptional control of flowering involves the rigorous regulation of *FT* expression by external and internal factors (Johansson and Staiger, 2015; Song et al., 2015). The role of *CO* is to bind in a proximal CO response element (CORE) region in the promoter of *FT,* together with NF-Y protein and FE protein, forming a protein complex (Gnesutta et al., 2017; Shibuta and Abe, 2017; Tiwari et al., 2010), which leads to DNA looping in the *FT* promoter region facilitating the access of other regulators and sustaining the transcriptional activation of *FT* in LD (Gnesutta et al., 2017; Shibuta and Abe, 2017). CRYPTOCHROME-INTERACTING BASIC HELIX-LOOP-HELIX (CIB) transcription factor proteins also activate *FT* gene expression in long days, in a blue-light dependent manner through the action of cryptochromes (Liu et al., 2013). GI is another direct regulator of *FT* expression by directly binding in *FT* promoter region. *GI* is also described as a *FT* activator in mesophyll tissue (Sawa and Kay, 2011). Moreover, GI is the main regulator of direct *FT* repressors like *TEMPRANILLO (TEM1* and *TEM2)* genes and *SHORT VEGETATIVE PHASE (SVP)* (Castillejo and Pelaz, 2008; Mishra and Panigrahi, 2015; Sawa and Kay, 2011). CDF1 can also act as a *CO*-independent repressor of *FT* in the morning, being directly controlled by FKF1 (Song et al., 2012).

1.2.2 Regulation of flowering at the protein level

Similarly, there is a precise and accurate regulation of protein levels, stability and protein subcellular localization involved in photoperiod flowering. CO protein levels exhibit daily oscillation patterns and seasonal changes depending on daylength and as previously mentioned, CO protein stability in LD afternoon leads to the expression of *FT* and induction of flowering (Andrés & Coupland, 2012; Shim et al., 2017). CO protein stability is regulated by light through the action of different photoreceptors and multiple E3 ubiquitin ligases, reaching a CO protein stabilization and accumulation in the late afternoon of LD (Shim et al., 2017). A well-described CO regulator is COP1 (CONSTITUTIVE PHOTOMORPHOGENIC 1), an E3 ubiquitin ligase that interacts with SPA (SUPPRESSOR OF PHYA-105) proteins to form the COP1-SPA complex which can direct CO to degradation (Jang et al., 2008; Liu et al., 2008). COP1 action mainly occurs at night and it is prevented in the evening through the action of photoreceptors CRYPTOCHROME 1 (CRY1) and CRYPTOCHROME (CRY2) which interact with SPA proteins in a blue light dependent manner to suppress COP1-SPA complex formation and ubiquitin activity (Liu et al., 2011; Zuo et al., 2011). Phytochrome photoreceptors are also regulators of CO stability (Shim et al., 2017; Valverde et al.,

2004), but different phytochromes may act in different ways. On one hand, PHYTOCHROME B (PHYB) is able to destabilize CO protein together with a ubiquitin ligase protein named HIGH EXPRESSION OF OSMOTICALLY RESPONSIVE GENES 1 (HOS1). In the morning, PHYB physically interacts with HOS1 and CO in order to destabilize CO (Lazaro et al., 2015). On the other hand, PHYB also regulates CO protein in the afternoon, in this case through a positive regulator of flowering named PHL (PHYTOCHROME-DEPENDENT LATE-FLOWERING) which interacts with PHYB and CO under red-light conditions to reduce the activity of the CO destabilization complex (Endo et al., 2013). PHYTOCHROME A (PHYA) is also responsible for maintaining CO stability in the afternoon through a possible disruption of the COP1-SPA complex (Sheerin et al., 2015). More recently, the blue-light photoreceptor FKF1 has been characterised as an inhibitor of COP1-dependent CO degradation, altering COP1 homodimerization and affecting COP1 multimeric complex formation and ubiquitin degradation activity (Lee et al., 2017; Song et al., 2012). This role of FKF1 as a photoreceptor regulating COP1 function seems to have a direct effect in photoperiodic flowering regulation (Lee et al., 2019). Moreover, a direct interaction between FKF1 and CO has been reported to be dependent on blue light and leading to CO protein stabilization in the afternoon of LD (Song et al., 2012). The characterization of this direct interaction led to a model in which FKF1 and ZTL (ZEITLUPE), which is an homolog of *FKF1*, together with GI (Hwang et al., 2019) confer a bimodal pattern of CO expression in LD. The model incorporates a ZTL-mediated degradation of CO in the morning by direct interaction and later in the day, a GI-dependent inactivation of ZTL (Song et al., 2014). ZTL is also capable of interact with FKF1 inhibiting its stabilization of CO in the afternoon, but the preferential interaction of GI-ZTL leads to an inactivation of ZTL and a maintenance of FKF1-dependent stabilization of CO and therefore, an accumulation of CO protein in the afternoon of LD (Hwang et al., 2019; Song et al., 2014). Overall, this regulation, summarized in Figure 1.1, leads to a specific CO protein accumulation in the late afternoon of long days and thus to *FT* activation (Shim et al., 2017).

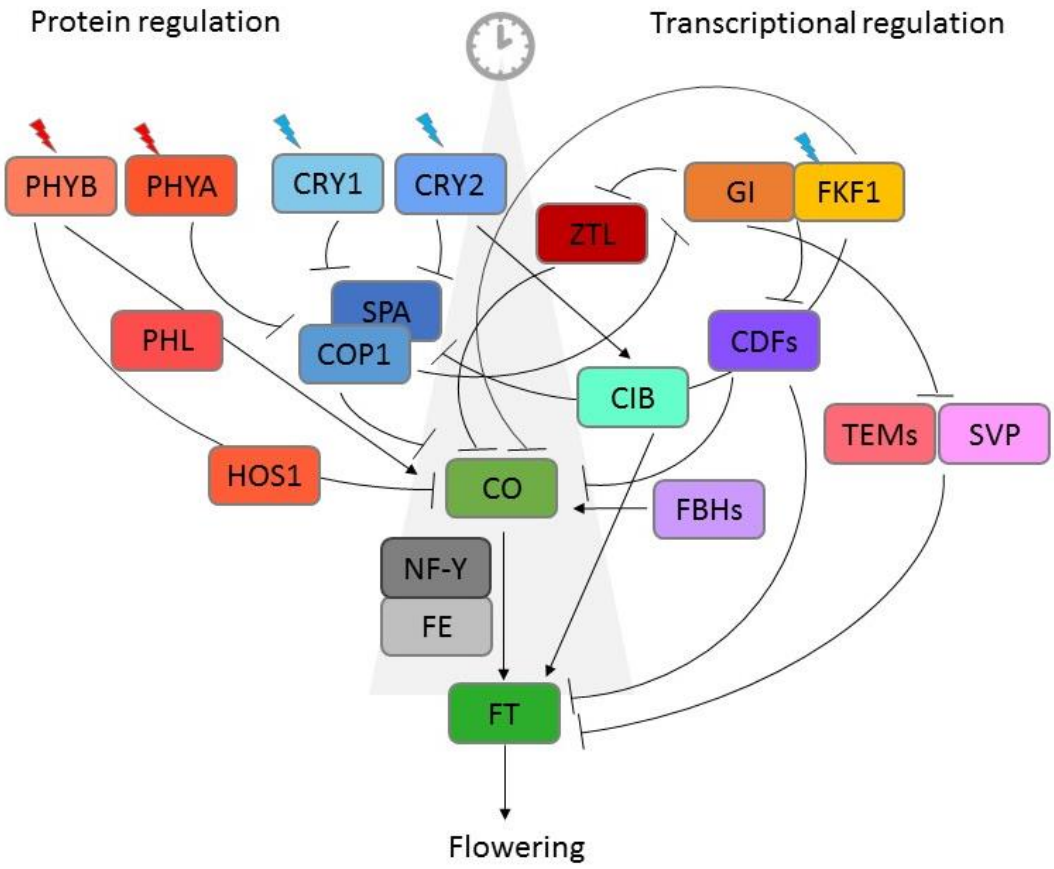

Figure 1.1 Diagram representing flowering genetic network in *Arabidopsis*.

Diagrammatic representation of *Arabidopsis* flowering model. Components of the pathway are represented in boxes with the acronym names described above. The left side represents the components involved in protein regulation and the right side represents transcriptional regulation. Circadian clock involvement is represented by a grey clock. Flat solid arrows indicate direct repression and solid pointy arrows indicate induction. The blue or red lighting represents red or blue light activation.

1.3 Conservation and divergence in the photoreceptor-clock-CO-FT pathway

In general, the photoreceptor-clock-CO-FT module seems to be the most important component of photoperiodic flowering in *Arabidopsis* and has served as a model on which to base investigations of other species like rice (Izawa et al., 2002; Lee and An, 2015; Shim and Jang, 2020), wheat (Kamran et al., 2014; Kitagawa et al., 2012; Li and Dubcovsky, 2008; Xiang et al., 2005), tomato (Cao et al., 2016; Pnueli et al., 2001; Shibuya et al., 2021; Silva et al., 2019), potato (Abelenda and Navarro, 2014; González-Schain et al., 2012; Navarro et al., 2015) or poplar (*Populus deltoides*) (Blümel et al., 2015; Böhlenius et al., 2006; Leijten et al., 2018). The general model is conserved among species but with great diversification in the regulation and connection between the components of the pathway. There are high levels of conservation in these molecular components and their molecular structure, but with differences in regulatory function in flowering or, in the case of *CO,* even its participation in photoperiod flowering regulation in some species (Figure 1.2).

1.3.1 *FT*

Among many plant species studied, one common feature is the regulation by daylength of *FT* expression (Andrés and Coupland, 2012). *FT* is first expressed in leaves and then acts as a graft-transmissible signal moving through the phloem as a small protein directed to the shoot apical meristem (SAM) to induce flowering by triggering floral meristem gene expression (Chen et al., 2018; Qin et al., 2017; Zeevaart, 2006). In the SAM, FT associates with other components to promote flowering, especially transcription factors like FD, a bZIP factor (Abe et al., 2005). FT belongs to the CETS (CENTRORADIALIS [CEN], TERMINAL FLOWER1 [TFL1] and FT) protein family and has been characterised as a member of transcriptional complexes (Andrés and Coupland, 2012; Qin et al., 2017). FT is a component in flowering pathways among plants but with some diversification regarding specific role, interactions and regulators, and movement (Putterill and Varkonyi-Gasic, 2016; Qin et al., 2017).

There are multiple studies giving evidence of *FT-like* genes playing a universal role in regulating flowering in diverse species like rice (Tamaki et al., 2007; Tsuji et al., 2011), tomato (Lifschitz and Eshed, 2006), apple (Tränkner et al., 2010), wheat (Yan et al., 2006) or poplar (Blümel et al., 2015; Leijten et al., 2018). Interestingly, most of these species contain multiple *FT-like* gene orthologs

and meanwhile some participate in flowering induction like in *Arabidopsis*, other orthologs differ on their function or it is still not defined. For instance, only 2 *FT-like* genes in rice from a total of 13 identified are known to play a role in flowering regulation (Komiya et al., 2008; Ogiso-Tanaka et al., 2013). In the legume family, most of the species contain 5-6 *FT-like* orthologs categorised in three clades but only some have been shown to have a flowering regulatory role (Weller and Macknight, 2019; Weller and Ortega, 2015). In some cases, the *FT-like* genes can act antagonistically like in sugar beet, where *FT1* is a floral repressor and *FT2* acts as floral promoter (Pin et al., 2010) or in tomato, where there are 6 *FT-like* genes characterised of which 3 act as floral inhibitors and only one participates in floral induction (Cao et al., 2016). Soybean has also antagonistic *FT-like* genes with *GmFT2a* and *GmFT5a* inducing flowering in SD (Kong et al., 2010; Weller and Macknight, 2019) and *GmFT4* repressing flowering in LD (Zhai et al., 2014a). There is also growing evidence for diversification in the role of *FT-like* genes in plant developmental processes including tuber formation in potato (Navarro et al., 2015) or bulb formation in onion (Lee et al., 2013).

Expression of *FT* in the leaves and movement of FT protein trough phloem cells is conserved in other species as rice or tomato, where the *FT* orthologs *Hd3a* in rice or *SlSPs* in tomato move through the phloem and are received in the shoot apical meristem by components like bZIP factors or 14-3-3 isoforms (Aki et al., 2008; Cao et al., 2016; Corbesier et al., 2007; Pnueli et al., 2001; Tamaki et al., 2007; Taoka et al., 2011). In barley and wheat, where flowering induction requires exposure to vernalization, some *VRN* genes participate in flowering regulation acting as florigen (Li and Dubcovsky, 2008; Yan et al., 2006). For instance, VRN3 proteins which included TaFT in wheat and HvFT in barley, are the homologs of rice and/or *Arabidopsis* florigens, moving from leaves to the apical meristem and promoting flowering in the same characterised fashion (Brambilla et al., 2017b; Li and Dubcovsky, 2008). VRN3 responds to photoperiod and vernalization under the regulation of other vernalization genes, *VRN1* as floral promoter and *VRN2* as a floral repressor similar to the rice *GRAIN NUMBER, PLANT HEIGHT AND HEADING DATE7 (Ghd7)* (Brambilla et al., 2017b; Ream et al., 2012).

The diversification in the flowering models also includes regulators and interactors of *FT,* which tend to be the same components but with variation in function among plants species. For instance in wheat, the majority of *FT-like* genes are regulated by genes containing CCT (CONSTANS, CO-like, and TOC1) or B-box domain like *PPD1 (PHOTOPERIOD RESPONSE 1)* (Brambilla and Fornara, 2017a; Shaw et al., 2013) or in rice where *OsPRR37 (Pseudo-Response Regulator 37)* regulates *Hd3a (Heading Date 3a)* expression (Hu et al., 2021), but the nature of these regulations is different,

resulting in flowering promotion under LD in wheat and under SD in rice. Moreover, some plants like rice have a parallel flowering induction system in which the *Ehd1 (EARLY HEADING DATE1)* gene, which is a B-type response regulator of *FT* rice genes under both LD and SD, activates another functional *FT* homolog, *RFT1 (RICE FLOWERING LOCUS T 1* (Doi et al., 2004; Komiya et al., 2008; Shrestha et al., 2014; Song et al., 2015). *Ehd1* is highly regulated by a CCT domain protein Ghd7, which is under the control of circadian clock and represses flowering in LD trough the module *Ehd1-RFT1* (Shim and Jang, 2020; Shrestha et al., 2014; Xue et al., 2008; Zhao et al., 2012) (Figure 1.2).

1.3.2 Circadian clock

The plant circadian clock is understood to consist of an intricate connection of molecular regulatory feedback loops that generate a 24h rhythmicity (Johansson & Staiger, 2015). Certain clock components are also regulated by light resulting in a synchronization with day and night periods. Clock genes collectively have output targets implicated in many developmental processes including photosynthetic activity, metabolism, growth, or photoperiodic flowering (Dodd et al., 2005; Johansson and Staiger, 2015).

Circadian clock components are understood to have a key regulatory contribution in flowering regulation. Of particular interest is *GI,* a circadian clock element with a key role in regulation of flowering at transcriptional level together with *FKF1* (Sawa et al., 2007; Song et al., 2012, 2014). *ELF3 (EARLY FLOWERING 3)* and *ELF4* are also circadian clock components involved in flowering regulation in *Arabidopsis* (Johansson and Staiger, 2015; Yu et al., 2008). Many circadian clock components first identified in *Arabidopsis* have been shown to have a conserved role in flowering regulation in diverse plant species like *OsGI or OsELF3-1* in rice (Hayama et al., 2003; Yang et al., 2013; Zhao et al., 2012), and *ELF3* or *PRR7* orthologs in barley (Campoli et al., 2012; Faure et al., 2012; Song et al., 2015). The same circadian clock components are involved in flowering regulation but their function differs among systems. For instance, in barley *Ppd-H1 (PRR7* ortholog in barley) can induce *HvFT* expression (*FT* ortholog in barley) without the participation of *HvCO1* (CO ortholog in barley)(Campoli et al., 2012). Another *PRR7* ortholog in beetroot (*BcBTC1- BOLTING TIME CONTROL1* gene) participates in the direct regulation of *FT* orthologs with implications in bolting (Pin and Nilsson, 2012), and the rice *OsPRR37* regulates *Hd3a* expression in rice flowering (Hu et al., 2021).

The rice genome also contains an ortholog for *GI*, *OsGI,* which integrates circadian clock regulation into rice flowering regulation trough the two main pathways, OsGi-Ghd7-Edh1-RFT1 and OsGI-Hd1-Hd3a (Hayama et al., 2003; Zhao et al., 2012)(Figure 1.2). The functional conservation of GI is expanded in the plant kingdom, with *GI* orthologs in distant species like the liverwort *Marchantia polymorpha* which is able to rescue flowering phenotype in *Arabidopsis* mutants (Kubota et al., 2014). The characterised *GI* orthologs are functionally conserved, participating in circadian clock and flowering regulation. Moreover, there are many *FKF1* and *GI* orthologs described in various plant systems, conserving rhythmic patterns of expression, and giving support to a high level of conservation in the module FKF1-GI with flowering regulatory participation (Brambilla et al., 2017b; Mishra and Panigrahi, 2015).

1.3.3 Photoreceptors

The ability of a plant to detect and respond to daylength implies a role for photoreceptors in sensing differences in the light environment. Photoreceptors have been extensively studied in *Arabidopsis*, in which four out of the five phytochromes genes (PHYA, B, D, E), two cryptochromes (CRY1 and CRY2) and FKF1 have been shown to have a significant role in the control of flowering. These photoreceptors all mainly appear to act through the regulation of *CO* expression and CO protein stability (Endo et al., 2013, 2016; Franklin and Quail, 2010; Kong and Okajima, 2016; Liu et al., 2011).

Not surprisingly, key roles for photoreceptors in plant photoperiod responses are widely conserved. For instance, mutations in the sorghum *PHYB* ortholog are insensitive to photoperiod, having early flowering in any daylength (Brambilla et al., 2017b; Yang et al., 2014b), and PHYA has been shown to regulate flowering in species like soybean (Watanabe et al., 2009) and pea (Weller et al., 2004). There is also some diversification in function, like the rice PHYC which requires PHYB to act as photo-sensing component, finding PHYB-PHYC heterodimers acting in PHYC -mediated responses regulating seedling development and flowering (Xie et al., 2014). Interestingly, another phytochrome in barley, HvPhyC, is able to regulate *HvFT1* and flowering induction independently of circadian clock and *HvCO* participation (Johansson and Staiger, 2015; Nishida et al., 2013). Cryptochrome orthologs also maintain flowering regulatory roles but with some diversification in function. In rice, which contains three cryptochrome genes, OsCRY2 is involved in flowering promotion but it is also characterised to be negatively regulated by blue-light (Hirose et al., 2006). And the two studied cryptochromes in soybean conserved blue light regulation but contrary to the *Arabidopsis* model GmCRY1 participates in flowering promotion (Zhang et al., 2008).

1.3.4 *CO*

As seen in previous sections, the basic *Arabidopsis* photoreceptor/clock-FT pathway appears to be generally conserved across a number of species, but the function of *CO* genes as mediators although conserved, does not appear universal. Similarly to the rest of components of the pathway, *CO* is present in many species, with *CO* orthologs in species like barley, rice or pea (Song et al., 2015; Valverde, 2011), but their role in flowering regulation, if any, differs from *Arabidopsis* (Song et al., 2010; Wu et al., 2014).

For instance, *CO* has been described as an essential component responsive to photoperiod in potato, having a weak effect on flowering but with a major participation in tuberization trough the regulation of a similar gene to *FT* (González-Schain et al., 2012). Interestingly, many photoperiod components are present in this network like *StGI*, *StFKF1* or *StCDF* and even more interestingly, the role of *StCO* in this network is different to the *Arabidopsis* model: *StCO* acts as a repressor of photoperiodic tuberization (Abelenda and Navarro, 2014). Rice provides another good example in which some major components of the molecular network are different (e.g., for *Ehd1* and *Ghd7* described above) while others are conserved (*OsGI*, *OsCO* and *OsFT*), although aspects of their regulation are quite distinct. In particular, the rice *CO* ortholog *CO/Hd1* acts to repress the expression of *FT* homologs, and is thus reversed relative to *Arabidopsis*, resulting in suppression rather than activation of flowering in LD (Hayama et al., 2003; Johansson and Staiger, 2015). In other cases like the LDP barley, *HvCO1* promotes flowering but does so independently of photoperiod (Campoli et al., 2012; Johansson and Staiger, 2015). In these cases, *CO* orthologs clearly participate in direct regulation of *FT* and flowering*,* but this is not seen in other models (Brambilla and Fornara, 2017a).

In several species, there is evidence of photoperiod-dependent regulation of *FT* expression without any apparent involvement of *CO* homologs (Cockram et al., 2007; Johansson and Staiger, 2015; Song et al., 2015). Examples include barley (Campoli et al., 2012), wheat (Beales et al., 2007), morning glory (Hayama et al., 2007) and the legumes *Lotus japonicus* (Yamashino et al., 2013), *Medicago truncatula* (Wong et al., 2014) and pea (Hecht et al., 2007). Even in *Arabidopsis* there are subpathways of flowering regulation where *CO* is not functionally active like the direct regulation of *FT* by GI binding in the promoter region (Sawa and Kay, 2011).

The *Arabidopsis* CO sub-family of CCT genes contains 16 other *CO-like* genes grouped in three clades (Brambilla and Fornara, 2017a; Wong et al., 2014), and are typified by the presence of one

or two B-box domains, an N-terminal Zinc (Zn) finger region and a CCT terminal domain structure. CCT domains are required for nuclear localization and are involved in interaction with other proteins (Li and Xu, 2017). Phylogenetic studies of the *CO-like (COL)* family indicate substantial independent diversification with, for example, up to 25 *COL* genes in *Brassica rapa* also grouped in three clades (Xu et al., 2015b). The study of *COL* genes and their functional role has been extensive in legumes indicating the absence of photoperiodic flowering regulatory role in this family (Hecht, 2005; Wong et al., 2014; Zhu et al., 2019).

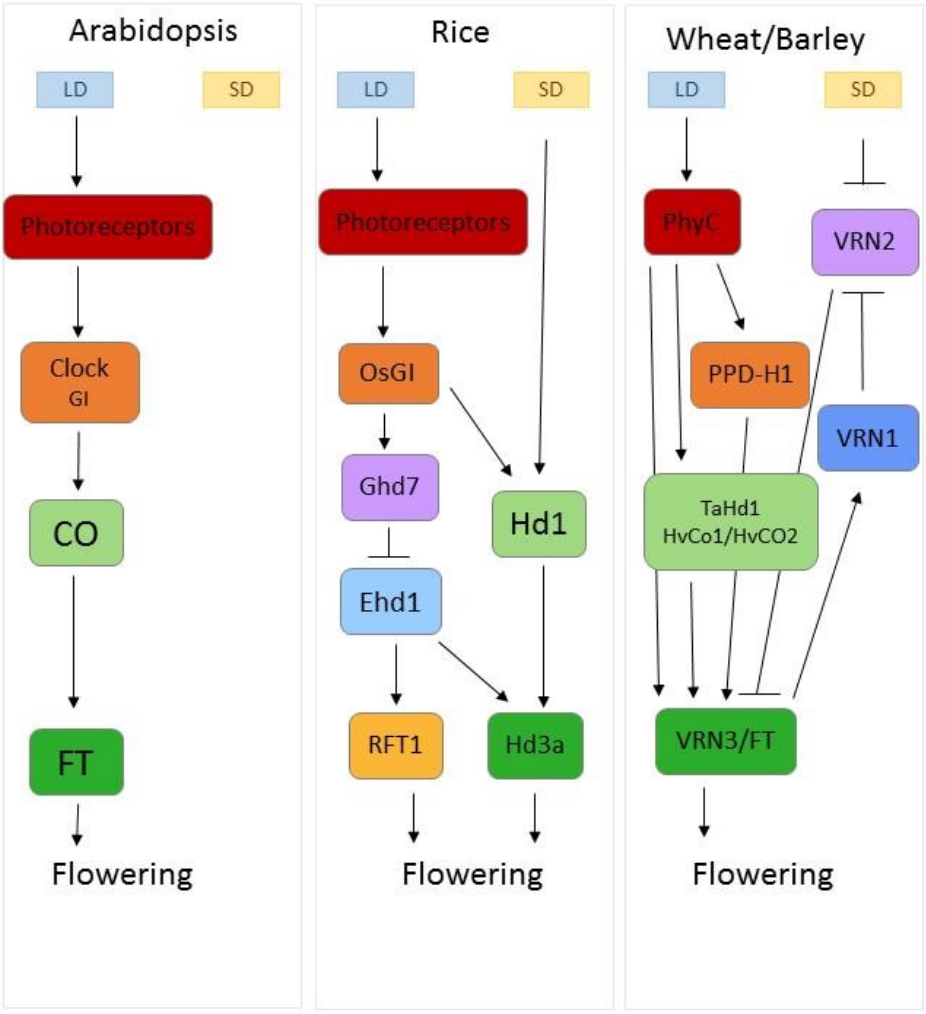

Figure 1.2 Simplified flowering regulatory network in *Arabidopsis*, rice and the cereals wheat and barley.

Simplified diagrammatic representation of flowering models in *Arabidopsis*, rice, wheat and barley. Components of the pathway are represented in boxes with the acronym names described in the text. The same box color indicates ortholog genes and LD or SD indicate the photoperiod response. Flat solid arrows indicate direct repression and solid pointy arrows indicate induction.

1.4 Photoperiod regulation of flowering in legumes

The legume family features many crop species of substantial economic value in global agriculture, including soybean, beans, chickpeas, peas, lentils and faba beans. The understanding of legume control of flowering time is relevant for crop production and the generation of new varieties by breeding and includes great potential for the genetic improvement of the legume species (Blümel et al., 2015; Foyer et al., 2016; Weller and Macknight, 2019; Weller and Ortega, 2015). Among legume crop species there are both LD-responsive plants like chickpea, pea or *Medicago truncatula*, and those which flower in response to SD like soybean or beans (Summerfield et al., 1985; Weller and Ortega, 2015). Of these, soybean and pea in particular have become valuable models for understanding the control of flowering time and differences between relatively closely-related SDP and LDP (Weller and Macknight, 2019; Weller and Ortega, 2015). The investigation of flowering genetic network in legume families has identified many *Arabidopsis* orthologs (Hecht, 2005; Weller and Ortega, 2015; Xia et al., 2012) but there are important differences in molecular structure and/or functionality. The most remarkable differences in legumes include the lack of *FLC* orthologs (Hecht, 2005; Kim et al., 2013b), the presence of only three phytochromes (PHYA, PHYB and PHYE) (Hecht, 2005; Weller and Ortega, 2015), the expansion and diversification of the *FT* family in three legume-specific clades (*FTa, FTb* and *FTc*)(Hecht et al., 2011; Weller and Ortega, 2015), and the apparent absence of any functional homologue of *CO* in most legume species (Fudge et al., 2018; Wong et al., 2014).

1.4.1 A short day legume model: Soybean *(Glycine max)*

Soybean flowering and maturity is controlled by numerous loci (*E1-E9* and *J* genes), of which four (*E1- E4*) are responsible for the majority of natural variation in flowering (Jiang et al., 2014; Lu et al., 2017; Miladinović et al., 2018; Tsubokura et al., 2013, 2014). Three of these are known to be orthologs of *Arabidopsis* flowering genes: *E2* is *GI* ortholog (Watanabe et al., 2011), and both *E3* and *E4* are PHYA orthologs (Tsubokura et al., 2013; Watanabe et al., 2009). In contrast, the fourth gene, *E1,* is a novel legume-specific flowering repressor with a key role in photoperiodic flowering (Xia et al., 2012). It is subject to light-dependent regulation through E3 and E4 and is itself able to directly regulate *GmFT2a* and *GmFT5a* (*FT* orthologs in soybean) resulting in flowering induction under SD conditions (Kong et al., 2010; Xia et al., 2012; Xu et al., 2015b) as shown in Figure 1.3. Of the 12 *FT* genes in soybean, two (*GmFT2a* and *GmFT5a)* have a particularly prominent role in

flowering, and both are up-regulated in SD conditions to induce flowering (Kong et al., 2010; Weller and Macknight, 2019). Interestingly, another *FT* gene *GmFT4* is reported to have a divergent role, with regulatory characteristics and a potential function in repression of flowering in LD (Zhai et al., 2014a). Soybean contains 26 *CO* orthologs and four of them (*COL1a/COL1b* and *COL2a/COL2b)* have been reported to contribute to flowering regulation (No et al., 2021; Wu et al., 2014). *COL1a* and *COL1b* display as floral suppressors in LD, (i.e., the opposite role to *AtCO)* and, all four genes can complement a *co* mutant in *Arabidopsis* (Wu et al., 2014). However, there is no evidence supporting a role for these genes in natural variation for flowering time in this species and it is not yet clear how their function may relate to that of *AtCO* (Cao et al., 2015; Zhu et al., 2019). Thus, this model supports the idea that *PHYA* (photoreceptors), *GI* (circadian clock) and *FT* orthologs are essential components of the photoperiodic flowering mechanism, but highlights potential areas of divergence, as presented in Figure 1.3.

1.4.2 Long Day legumes

1.4.2.1 Photoperiod flowering research in Pea (Pisum sativum)

In pea, the genetic network inducing flowering under LD conditions has been extensively studied. For instance, pea genetic research has examined the *FT* family expansion with five *FT-like* genes divided in three groups (*FTa*, *FTb* and *FTc*), where *FTb2* is the main photoperiod-controlled *FT* ortholog (Hecht, 2005; Hecht et al., 2011; Weller and Ortega, 2015). The genetic model of the control of flowering in pea involves PHYA which is one of the main photoreceptors regulating pea flowering, proven by the null-mutant being highly insensitive to LD and a dominant photoperiod insensitive mutant with early flowering phenotype (Weller et al., 2004; Weller et al., 1997a). There are indications of the participation of other photoreceptors, particularly PHYB and cryptochromes regulating far-red and blue light flowering promotion respectively, but their characterization needs some more understanding (Platten et al., 2005; Weller et al., 2001; 2009a). Other well-characterized components include *LATE1 (LATE BLOOMER1)* and *LATE2 (LATE BLOOMER 2)* which are homologs of the key *Arabidopsis* regulators *GI* and *CDF1* respectively (Hecht et al., 2007; Ridge et al., 2016). The *late1* mutant is late-flowering, regulated by circadian clock and able to regulate expression of a number of circadian clock genes. Its flowering participation alters pea *FT* gene expression, mainly *FTb2*, without influencing the transcript levels of pea *CO-like* genes (Hecht et al., 2007; Liew et al., 2014; Ridge et al., 2016). The *late2* mutant is also late-flowering with a reduced photoperiod response. Similarly to the *late1* mutant, *late2* also shows altered *FT* genes expression but lacks any obvious effect on expression of *CO-like* genes (Ridge et al., 2016)(Figure

1.3). However, similar to *Arabidopsis* CDF proteins, the LATE2 protein was shown to interact with the pea FKF1 in yeast-two-hybrid experiments indicating a possible conserved role for the FKF1/GI/CDF module in pea (Ridge et al., 2016).

1.4.2.2 Medicago truncatula

Medicago truncatula is a temperate legume which flowers in response to LD photoperiods and vernalization exposure (Weller and Macknight, 2019). Genetic characterization has described the expansion of *FT* family in *Medicago*, containing five *FT-like* genes divided in three groups, following the classification previously characterised in pea (Laurie et al., 2011; Putterill et al., 2013). Their genomic structure is conserved and they are located close to each other in the same chromosome with *FTb1* and *FTb2* clustered together, similarly to other legumes genomic structure (Hecht, 2005; Ortega et al., 2019; Putterill et al., 2013). But the expression patterns differ between *FT-like* genes; only *MtFTa1* is up-regulated by photoperiod and vernalization, acting as a promoter of flowering in *Medicago* (Laurie et al., 2011), meanwhile the other *FTs* could be also involved in photoperiod flowering induction (Laurie et al., 2011; Putterill et al., 2013). Similar to the pea system, *MtFTb* genes are responsive to LD photoperiod (but not vernalization), supporting a conserved role as floral activator in LDP (Laurie et al., 2011). Remarkably, the characterization of *Medicago COL* genes by several genetic approaches evidences the lack of a flowering regulatory role of this family in *Medicago* (Weller and Macknight, 2019; Wong et al., 2014). Additionally, *MtE1L* gene, the homolog of soybean *E1* has been described in this system with a mild flowering phenotype in the mutant (Jaudal et al., 2020; Zhang et al., 2016; 2019). There are other similarities to the conserved core of *Arabidopsis* flowering model since components related with circadian clock are also preserved in *Medicago* like the participation of *MtCDFd1_1* inducing flowering in LD (Zhang et al., 2019)(Figure 1.3).

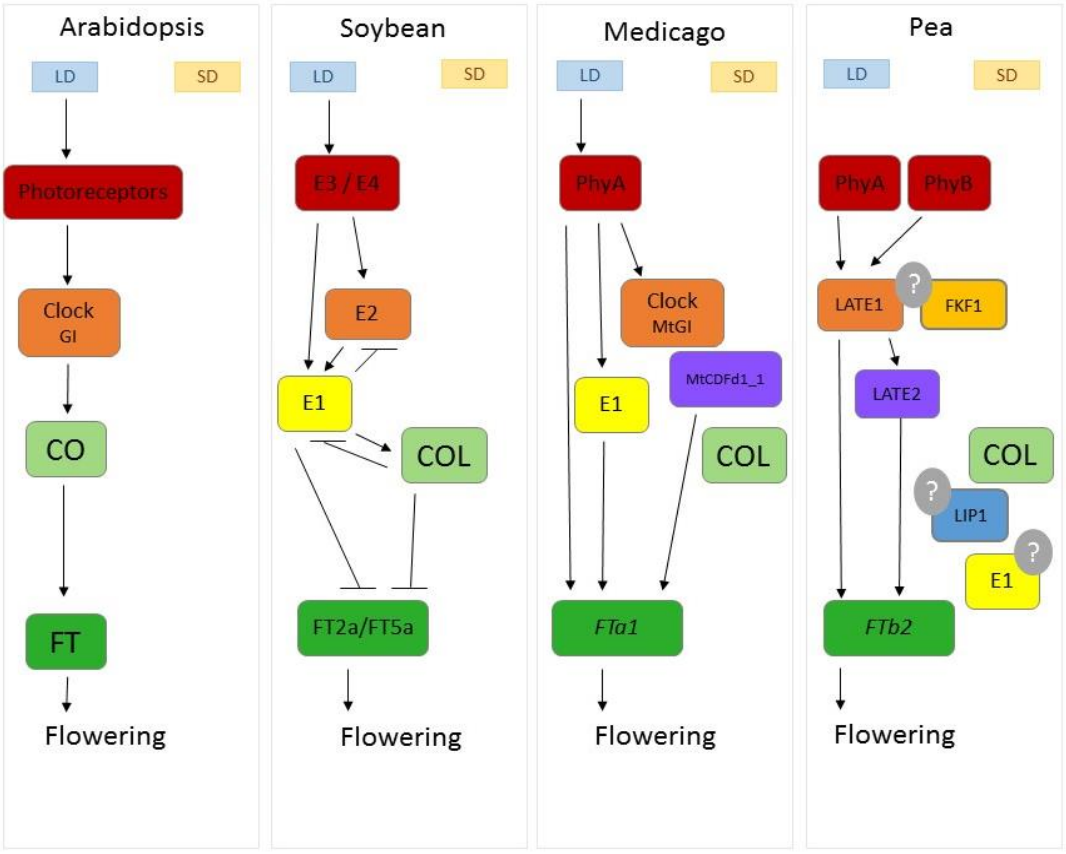

Figure 1.3 Simplified flowering regulatory network in *Arabidopsis* and legume models.

Simplified diagrammatic representation of flowering models in *Arabidopsis* and the legume soybean (SDP), *Medicago* (LDP) and pea (LDP). Components of the pathway are represented in boxes with the acronym names described in the text. The same box color indicates ortholog genes and LD or SD indicate the photoperiod response. Flat solid arrows indicate direct repression and solid pointy arrows indicate induction. Question mark bubbles indicate chapter questions discussed in thesis aims in section 1.5.

1.5 Thesis aims

The legume family offers an excellent system to evaluate flowering responses to photoperiod, as it incorporates a comparison between related SD and LD models which are supported by significant genetic resources and a history of physiological and molecular research. Moreover, the detailed characterization of the *Arabidopsis* model also serves as a valuable guide particularly for LD legumes. This study aims to further understand the LD flowering legume model, focusing primarily on the pea system.

Chapter 3 presents an investigation into the possible role of the *E1* gene in temperate legumes, and specifically to examine whether it might have a role as a "missing link" connecting light and clock regulation with *FT* genes, as in soybean, a question raised by the lack of a role for *COL* genes

in flowering regulation in temperate legumes. This work includes a characterization of mutants in both pea and *Medicago*.

The *LIP1* gene in pea has been characterised as the ortholog of *COP1* in *Arabidopsis* and shown to have a strongly conserved role downstream of phytochromes in photomorphogenic responses. However, it is not known whether it might also have a role in flowering time control similar to that of COP1. **Chapter 4** examines this question an includes and analysis of genetic interactions with known components of the pea flowering pathway including PHYA, *LATE1 (PsGI)* and *HR (PsELF3a)*, for which orthologs in *Arabidopsis* all show some functional interaction with COP1.

Chapter 5 examines two other components in flowering regulation, focussing on FKF1 and its interaction with GI. The potential function of *FKF1* in flowering time and photomorphogenesis is examined through the characterization of *Medicago* and pea mutants. It also attempts to extend our knowledge of FKF1-LATE1-LATE2 interactions in pea and their potential flowering regulatory implications.

This thesis concludes with a general discussion in Chapter 6, assessing the key findings of each individual chapter and summarizing the overall contribution to the understanding of flowering control in temperate legumes.

Chapter 2 - General Materials and Methods

This chapter describes the general materials and methods used for all research presented in this thesis. The description of specific materials and methods of explicit experiments will be detailed in the materials and methods sections of individual chapters.

2.1 Plant material and growth conditions

This research has been focused on two legume species: *Pisum sativum* (pea) and *Medicago truncatula* (*Medicago*).

2.1.1. *Pisum sativum* material

Details of the specific lines and mutants studied in this research are explained in each chapter. The wild-type (WT) line referred in this thesis is the pea line NGB5839, a gibberellin deficient dwarf mutant carrying a mutation in *LE* gene (*le-3*) of cultivar Torsdag which facilitates and eases the growth in glasshouse conditions (Lester et al., 1997). Mutants used in this thesis were either originated by EMS mutagenesis in NGB5839 or in another cultivar and introgressed into NGB5839. The general details of the pea mutants used for this thesis are described in Table 2.1. Once introgressed in NGB5839 background, lines were crossed to generate populations segregating for single and double mutants. Genotype and phenotype screening were used in F_2 and F_3 segregating populations to generate single or double mutants used for this research. These F_2 and F_3 populations were previously generated at University of Tasmania by Jim Weller and Jackie Vander Schoor.

Table 2.1 Details of the pea lines and the origin of the flowering mutants used in this study.

Line	Description	Reference
NGB5839	Wild-type pea line originally used in mutagenesis programmes. Gibberellin deficient (*le-3*) dwarf of cv. Torsdag	(Lester et al., 1997)
cv. Torsdag (TOR)	Wild-type line originally used in mutagenesis programmes. Tall line from which NGB5839 is derived.	Hobart Line 107
cv. Cameor	Wild type line of the TILLING population.	(Dalmais et al., 2008)
e1	Created by EMS mutagenesis of cv. *Cameor* and obtained by TILLING screen. These lines were introgressed into NGB5839 by back-crossing (BC_5). *E1* is the candidate pea ortholog gene of soybean *E1* with seven mutant alleles described in Chapter 3.	This study
lip1	Spontaneous mutant of cv. *Alaska* and introgressed in NGB5839 and TOR by backcrossing from the original *lip1* line. *LIP1* has been characterized as a *COP1* ortholog and there is only one mutant allele described in Chapter 4.	(Frances et al., 1992; Sullivan and Gray, 2000; Weller et al., 2009b)
late1	Created by EMS mutagenesis in NGB5839. *LATE1* was characterized as the *GIGANTEA* ortholog with six mutant alleles of which details are included in Chapter 5.	(Hecht et al., 2007; Liew et al., 2009)
fkf1	Created by EMS mutagenesis of cv. *Cameor* and obtained by TILLING screen. These lines were introgressed into NGB5839 by back-crossing (BC_5). *FKF1* is the ortholog gene of *FKF1* in *Arabidopsis*, includes two mutant alleles described in Chapter 5.	This study
HR	Introgressed in NGB5839 by backcrossing from the original *HR* line. *HR* was characterized as *ELF3a* ortholog.	(Murfet, 1973; Weller et al., 2012)
phyA	Created by EMS mutagenesis of cv. Torsdag and selected in a dwarf background by crossing into NGB5839.	(Weller et al., 1997a)

	PHYA was characterized as the *Arabidopsis PHYA* ortholog. Two mutant alleles are included in this thesis, specified in Chapter 3 and Chapter 4.	

All plants described in this thesis were grown in controlled-environment growth cabinets or phytotrons at the University of Tasmania. Seeds were coated with Thiram fungicidal powder, and then sown in 14cm pots which contain 1:1 mixture of gravel/vermiculite and topped with 3-5cm of sterilized potting containing controlled release fertilizer (CRF) (Horticultural and Landscape Supplies, Brighton, Tas, Australia). Plants were regularly watered according to needs (growth phase and growing season) and supplied with nutrients on a weekly basis. Pesticide and fungicide treatments were performed on a regular basis according to plant state and need.

Phytotron temperature was maintained at approximately 24°C during the day and 16°C at night and plants were exposed to a base photoperiod of 8 hours of natural light in combination with darkness or extended lighting to create different photoperiod conditions. Unless otherwise indicated in any individual chapters, photoperiod conditions for the different experiments were as follows: Plants under short day (SD) conditions received 8 hours of natural daylight and 16 hours of total darkness, while those in long day (LD) conditions received natural daylight extended before dawn and after dusk with artificial light (50 µmol m^{-2} s^{-1}) to provide a total photoperiod of 16 h.

Growth cabinets were used for all experiments in which highly accurate temperature or photoperiod were required. Growth cabinets were maintained at a constant temperature of 20°C and white light provided by cool-white fluorescent tubes (L40 W/20S cool white; Osram Germany) at an irradiance of 120-140 µmol m^{-2} s^{-1} unless otherwise specified.

2.1.2. *Medicago truncatula* material

Information about the *Medicago* lines and mutants studied in this thesis are described in each specific chapter. Seeds were identified and ordered in the *Medicago Tnt1* mutant database (Medicago-mutant.noble.org/mutant/database.php) and obtained from the Noble foundation (Lee and Mysore, 2018; Sun et al., 2018; Tadege et al., 2008).

Before sowing, seeds were scarified and imbibed overnight in sterile water and plated on wet sterile paper in a petri dish sealed with parafilm. When vernalization was necessary, petri dishes

were stored at 4°C in the dark for 2 weeks. After imbibition or vernalization process, germinating seeds were exposed to 48h of LD photoperiod (16h light/8h dark) prior to sowing (Laurie et al., 2011). *Medicago* seedlings were sown in 12 cm slim-pots containing 1:1 mixture of sand and sterilized potting mix containing controlled release fertilizer (CRF) (Horticultural and Landscape Supplies, Brighton, Tas, Australia). Slim-pots were confined in trays containing soil mixture to facilitate root development. Plants and trays were watered regularly depending on the growth stage and nutrient was supplied weekly (Laurie et al., 2011).

All *Medicago* plants described in this thesis were grown in controlled-environment glasshouse cells in the Biological Sciences Biosecurity facilities of University of Tasmania. Biosecurity glasshouse cells were maintained at approximately 24°C during the day and 16°C at night with LD photoperiods including natural light and white light provided by cool-white fluorescent tubes (L40 W/20S cool white; Osram Germany) at an irradiance of 120-140 µmol m^{-2} s^{-1} unless otherwise specified.

2.2 Plant measurements

Details of traits measured on pea plants grown in this study are shown in Table 2.2 . All traits were measured on the main stem, unless otherwise stated and all lengths were measured to the nearest millimetre. Data from any plants which exhibited stunted or abnormal growth were excluded. For all traits involving numbering of nodes, the lowest scale leaf was counted as node 1. For measurement of internodes, internodes were numbered with internode 1 between the first and second scale leaf. When reproductive nodes were numbered, the node of floral initiation (NFI) was counted as reproductive node 1.

Table 2.2 Details of pea plant traits measured in this study.

Trait	Description
Days to first open flower (DTF)	Number of days between sowing and first fully developed/open flower with standard and wing petals fully unfurled.
Internode length (IL)	Length between the base of a node and the base of the next higher node (mm).
Node of flower initiation (NFI)	Node of first secondary inflorescence (I_2) on main stem, regardless of whether a fully developed flower is borne on this I_2.
Reproductive nodes (RN)	Number of nodes on the main stem bearing an axillary I_2. Measured from NFI (inclusive) to the last node (TN).
Total nodes (TN)	Total number of nodes with fully expanded leaves on the main stem.
Flower-Leaf Relativity (FLR)	Measurable relation between expanding leaf and NFI. The leaf expansion level is measured in relation to the opening of the leaf and scored on a decimal scale when NFI occurs. FLR is calculated as a subtraction between leaf expansion level and NFI. If the developing leaf is in the same or later node than the NFI, FLR will be a positive number between 0- 4. If the developing leaf is in an earlier node, FLR will be a negative number (Murfet, 1985).
Node developing rate	Rhythm of node development measured as the level of leaf expansion (opening) at consecutive time points.
Leaf length	Distance between the base of the leaf and the apex. Measured used to calculate leaf area.
Leaf width	Distance between the sides of the leaf relative to its expansion level. Measured used to calculate leaf area.

For *Medicago* plants, flowering time was measured as the number of days from germination to first fully opened flower was observed and labelled as Days To First open flower (DTF).

2.3 Photomorphogenesis

For photomorphogenesis experiments, pea plants were grown in pots for 2 weeks in specific light conditions (specified in each chapter) or darkness. Plants were grown following the conditions previously mentioned in growth conditions section and placed in growth rooms in a double-door isolated space at the University glasshouse where temperature and water regime were controlled. At 14 days, four traits were measured: Internode 1-2 length, Internode 2-3 length, Leaf width and Leaf length. Leaf area was calculated by multiplying leaf width by leaf length. Photographs of the photomorphogenesis experimental plants were taken at 14 days.

2.4 Online sequence resources

Online sequence databases were used for identification, analysis of gene homologs and primer design. Where genes were not annotated or were found to be incorrectly annotated based on expressed sequences or alignments between species, coding and protein sequences were corrected accordingly for use in phylogenetic analyses. BLAST searches were performed to identify homologous genes using the resources seen in Table 2.3.

Table 2.3 Online resources used for sequence information.

Species	Database name	Website	Reference
Pea (*Pisum sativum*)	GeneBank PsCam Transcriptome Database Pea genome Project Legume Information System Ensembl	www.ncbi.nlm.nih.gov bios.dijon.inra.fr/FATAL/cgi/PsUniLowCopy.cgi urgi.versailles.inra.fr/Species/Pisum/Pea-Genome-project legumeinfo.org asia.ensembl.org/index.html	(Alves-Carvalho et al., 2015; Dash et al., 2016; Franssen et al., 2011; Kaur et al., 2012; Kreplak et al., 2019; Ruffier et al., 2017)
Chickpea (*Cicer arietinum*)	Phytozome Genebank Legume Information System Ensembl	phytozome.jgi.doe.gov www.ncbi.nlm.nih.gov legumeinfo.org asia.ensembl.org/index.html	(Dash et al., 2016; Goodstein et al., 2012; Ruffier et al., 2017)
Common bean (*Phaseolus vulgaris*)	Phytozome Genebank Legume Information System Ensembl	phytozome.jgi.doe.gov www.ncbi.nlm.nih.gov legumeinfo.org asia.ensembl.org/index.html	(Dash et al., 2016; Goodstein et al., 2012; Ruffier et al., 2017)
Soybean (Glycine max)	Phytozome Genebank Legume Information System Ensembl	phytozome.jgi.doe.gov www.ncbi.nlm.nih.gov legumeinfo.org asia.ensembl.org/index.html	(Dash et al., 2016; Goodstein et al., 2012; Ruffier et al., 2017)
Medicago truncatula	Phytozome Genebank Legume Information System Ensembl	phytozome.jgi.doe.gov www.ncbi.nlm.nih.gov legumeinfo.org asia.ensembl.org/index.html	(Dash et al., 2016; Goodstein et al., 2012; Ruffier et al., 2017)
Red clover (*Trifolium pretense*)	Phytozome Genebank Legume Information System Ensembl	phytozome.jgi.doe.gov www.ncbi.nlm.nih.gov legumeinfo.org asia.ensembl.org/index.html	(Dash et al., 2016; Goodstein et al., 2012; Ruffier et al., 2017)
Lotus japonicus	Phytozome Genebank Legume Information System Ensembl	phytozome.jgi.doe.gov www.ncbi.nlm.nih.gov legumeinfo.org asia.ensembl.org/index.html	(Dash et al., 2016; Goodstein et al., 2012; Ruffier et al., 2017)
Pigeon pea (*Cajanus cajan*)	Phytozome Genebank Legume Information System Ensembl	phytozome.jgi.doe.gov www.ncbi.nlm.nih.gov legumeinfo.org asia.ensembl.org/index.html	(Dash et al., 2016; Goodstein et al., 2012; Ruffier et al., 2017)
Mungbean (*Vigna angularis*)	Phytozome Genebank Legume Information System Ensembl	phytozome.jgi.doe.gov www.ncbi.nlm.nih.gov legumeinfo.org asia.ensembl.org/index.html	(Dash et al., 2016; Goodstein et al., 2012; Ruffier et al., 2017)

***Arabidopsis* (*Arabidopsis thaliana*)**	Phytozome Genebank TAIR	phytozome.jgi.doe.gov www.ncbi.nlm.nih.gov www.Arabidopsis.org	(Berardini et al., 2015; Goodstein et al., 2012)
Tomato (*Solanum lycopersicum*)	Phytozome Genebank	phytozome.jgi.doe.gov www.ncbi.nlm.nih.gov	(Goodstein et al., 2012)
Maize (*Zea mays*)	Phytozome Genebank	phytozome.jgi.doe.gov www.ncbi.nlm.nih.gov	(Goodstein et al., 2012)

2.5 Primer design

Primers were designed from pea sequence using the web-based software Primer3 (primer3.wi.mit.edu/) (Koressaar and Remm, 2007; Untergasser et al., 2012). They were optimised for primer length (18-25bp), product length, G/C content, annealing temperature, minimal self-compatibility and cross-compatibility and the presence of a GC clamp at the 3' end. Details for all the primers used in this research are given in the material and methods section of each individual chapters.

2.6 DNA and RNA extractions and processing

2.6.1 Standard genomic DNA (gDNA) extraction

For extraction of gDNA, tissue samples were collected in liquid nitrogen and stored at -80°C until processing. Frozen tissue samples were ground using either mortar and pestle or carbide beads, and a mechanical homogeniser (Retsch MM30 or Qiagen TissueLyserII), depending on sample sizes. Samples were stabilised with 500µL of 2x Extraction Buffer (100mM Tris-HCl, 1.4M NaCl, 20mM EDTA, 2% w/v CTAB, pH 8 with HCl) and incubated for 10-15 minutes at 60°C with gentle agitation. Solvent extraction was performed twice using chloroform-isoamyl alcohol (24:1) solution. DNA was precipitated with 1mL of Precipitation Buffer (50mM Tris-HCl, 10mM EDTA, 1% w/v CTAB, pH 8 with HCl), pelleted by centrifugation for 10 minutes at 10,000g and resuspended in 300µL 1.5M NaCl containing 1µg RNase A (25mg/mL) and incubated for 10-15 minutes at 50°C. DNA was precipitated in chilled 95% ethanol, pelleted by centrifugation at 10,000g for 15 minutes, washed in 70% ethanol, air dried and dissolved in autoclaved Milli-Q water (Milli-Q Plus, Merck Millipore, Billerica, MA, USA). Dilutions of 50ng/µL gDNA were used for PCR and HRM analysis.

2.6.2 RNA extraction and cDNA synthesis

Frozen tissue samples were ground using either mortar and pestle or carbide beads and mechanical homogeniser (Retsch MM30 or Qiagen TissueLyserII), depending on sample size. Total RNA was extracted using the Promega SV Total RNA Isolation System (Promega, Madison, WI) in accordance with the manufacturer's instructions.

First strand cDNA was synthesised from 1µg RNA using Tetro Reverse Transcriptase (Bioline, Australia) in a total volume of 20µL, in accordance with the manufacturers' instructions. To check for gDNA contamination, a negative control without reverse transcriptase (RT-) was included in each sample. The cDNA product was diluted 1/5 by adding 80 µL of water to the first strand cDNA and used for PCR or qRT-PCR.

2.7 PCR

2.7.1 Standard PCR

Standard PCR was performed in a 50µL volume, comprising 5µL of template DNA at 25ng/µL, 10µL of 5x reaction buffer, 1µL of dNTPs (10mM), 1µL of forward primer (10µM), 1µL of reverse primer (10µM), 1.5µL $MgCl_2$ (50mM), and 0.2µL of MangoTaq™ DNA polymerase (Bioline, Australia), with autoclaved Milli-Q water to final volume. Reactions were conducted in a thermal cycler with heated lid as follows: 94°C for 5 minutes, 35-40 cycles of [94°C for 45 seconds, primer annealing temperature for 45 seconds, 72°C for 1 minute per Kb according to expected product size], 72°C for 5 minutes. A no-template control (containing water instead of DNA) was included for each run to check for contamination.

2.7.2 High Fidelity PCR

High fidelity PCR was performed using the same reaction mix as for standard PCR except using 0.2µL of Phusion® DNA polymerase (Finnzymes, Espoo, Finland), with 5x Phusion HF Buffer and without addition of $MgCl_2$, in accordance with the manufacturer's instructions. Reactions were conducted in a thermal cycler with heated lid as follows: 98°C for 30 seconds, 25-35 cycles of [98°C for 10 seconds, primer annealing temperature + 3°C for 30 seconds, 72°C for 30 seconds per Kb of PCR product], 72°C for 5 minutes. A no-template control (containing water instead of DNA) was included for each run to check for contamination.

2.7.3 Colony PCR

Colony PCR was carried out using bacterial colonies suspended in 5µL autoclaved Mili–Q water. Bacteria cells were first lysed by 5min at 94°C. PCR conditions were the same that those described in the standard PCR with the following program: initial denaturation at 94°C for 5 minutes followed by 30 cycles (1 minute at 94°C, annealing temperature for 1 minute, extension of 1 minute/Kb of PCR product at 72°C) and a final extension of 5 minutes at 72°C. A no-template control (containing water instead of DNA) was included for each run to check for contamination.

2.7.4 Quantitative reverse transcription PCR (qRT-PCR)

For analysis of relative gene expression, qRT-PCR was conducted using a Rotor-Gene 3000 Real-time Thermal Cycler with Rotor-Gene 6 Version 6.1 (Corbett Research, Australia). A PIRO Pipetting Robot (Lindauer DORNIER GmbH, Germany) with Dornier PIRO Version PR-01.00.0206 software was used to prepare reactions. Each 10µL reaction comprised 2µL cDNA template, 5µL 2x SensiMixPlus SYBR reagent (Bioline, Australia), 0.3µL each of forward and reverse primer (10µM) and 2.4µL autoclaved Milli-Q water. A no- template control (containing water instead of cDNA) was included for each run to check for contamination, and each sample was run in replicate for increased accuracy. Reactions were run for 50 cycles.

A standard curve for the target gene was included in every run. Standard curves were generated from a 10-fold dilution series from 10^{-2} to 10^{-6} ng/µL. Standard curve regression was considered acceptable if the R^2 value was equal to or higher than 0.99. *TFIIa* was chosen as the reference constitutive gene for evaluating relative transcript levels of flowering genes as previously described (Foo et al., 2005; Hecht et al., 2011). Calculations of gene expression relative to *TFIIa* were based on non-equal amplification efficiencies and deviation in threshold cycle using the means for two technical replicates (Pfaffl, 2001).

2.7.5 Visualisation of nucleic acid

To visualise PCR products and check DNA/RNA integrity, samples were separated on agarose gel in TAE buffer (40mM Tris Acetate and 1mM EDTA), containing Acridine orange (Sigma), alongside an appropriate DNA ladder (Bioline, Australia) and visualized under UV light.

2.7.6 Purification of PCR products

Prior to cloning and/or sequencing, PCR products were purified using Promega Wizard® SV Gel and PCR Clean-Up System (Promega, Madison, WI, USA) and eluted in sterile, nuclease free water in accordance with the manufacturer's instructions.

2.8 Quantification of DNA, RNA and PCR products

Concentration of DNA, RNA and PCR products was measured with a NanoDrop 8000 Spectrophotometer (Thermo Fisher Scientific, Wilmington, DE, USA) in accordance with the manufacturer's instructions.

2.9 Sequencing and sequence analysis

Purified DNA was sent for sequencing to Macrogen Inc. (Seoul, Korea). Sequences were edited manually using Geneious v8.1.8 (www.geneious.com) (Kearse et al., 2012) to correct falsely identified bases, remove unreadable sequence at the 3' and 5' ends and group sequences in contigs. Sequence identity was confirmed by BLAST search or alignment with existing sequence. Sequences were annotated using Geneious v8.1.8.

2.10 Design of genotyping markers

For genotyping purposes, High resolution melt (HRM) markers were designed to target indels and C/T, G/A, C/A and G/T SNPs with primers designed to amplify small fragments (<200 bp). After characterising the mutation and genomic location by sequencing, primers were designed in the flanking region to include the SNP in the amplification. HRM markers were tested and scored in segregating populations using a Rotorgene Q HRM machine (Qiagen). A PIRO Pipetting Robot (Lindauer DORNIER GmbH, Germany) and Dornier PIRO Version PR-01.00.0206 software was used to prepare reactions containing 100ng template, 0.5µM of each primer, 7.5µL SensiFAST™ HRM Mix (Bioline, Australia), and sterile milli-Q water to complete 15 µL. Conditions were as follows: 95°C for 5 minutes, 50x [95°C for 10 seconds, annealing temperature (Tm; 50-60°C) for 30 seconds], 95°C for 5 minutes, 50°C for 5 minutes, HRM (temperature increasing with 0.1°C

increments from 60-90°C, or from product melt temperature -5°C to +5°C). HRM results were analyzed with Rotor-Gene® ScreenClust HRM® Software (Qiagen).

2.11 Genotyping PCR for *Medicago*

Medicago lines were genotyped by standard PCR involving two reactions with primer details specified in the material and methods section of each individual chapter. A first gene specific PCR reaction using gene-specific primers with binding sites in the flanking region of the insertion site of the *Tnt1* retrotransposon. Therefore, the amplification product includes the insertion site. And secondly, the insertion specific PCR reaction which include one of the flanking primers (gene specific) combined with a *Tnt1* specific primer. In some mutants, a third insertion specific PCR reaction was included as a reassurance of the genotyping, including the other flanking gene specific primer combined with another *Tnt1* specific primer. The categorization of genotypes is then analyzed after the PCRs product visualization finding the three possible genotypes represented in Table *2*.4.

Table 2.4 Genotype categorization for *Medicago* lines after PCR analysis with gene specific and insertion specific primers.

Gene specific reaction	Insertion specific reaction	Genotype
Amplification	NO amplification	**Homozygote WT** – No *Tnt1* insertion
Amplification	Amplification	**Heterozygote** – There is DNA with *Tnt1* insertion and DNA without the insertion
NO amplification	Amplification	**Homozygote mutant** – *Tnt1* insertion

2.12 Construction of alignments and phylogenetic trees

For phylogenetic analyses, amino acid sequences of proteins or coding DNA sequences were aligned using ClustalX (Thompson et al., 1994) and adjusted manually, where necessary, using Geneious v8.1.8 (www.geneious.com) (Kearse et al., 2012) and Genedoc (Nicholas and Nicholas, 1997). Using these alignments, distance-based methods were used for phylogenetic analyses in PAUP* 4.0b10 (http://paup.csit.fsu.edu/). For comparison of homologous proteins, percentage

identity at the amino acid level was calculated in Geneious from full-length protein alignments constructed using ClustalX.

2.13 Protein structure prediction software

For protein structure prediction, protein sequences were analysed by I-TASSER (zhanglab.ccmb.med.umich.edu/I-TASSER) (Yang et al., 2014a; Yang and Zhang, 2015), an online public software which predicts protein function from the automated structure prediction of protein sequences. Structural protein models were built from diverse threading configurations by iterative fragment assembly of simulations which were based on recognised templates from protein databases. A functional annotation to each structural model was predicted from known proteins databases and a confident score (C-score) was assigned for each model. Some protein predictions were analysed by SWISS-MODEL (swissmodel.expasy.org) (Waterhouse et al., 2018) which predicts structure and stoichiometry of amino acid sequences by homology inferred modelling.

2.14 Statistical analysis

All statistical analysis were conducted using GraphPad Prism v6.01 (www.graphpad.com), using a significant level of 0.05. For comparisons between only two groups, two-tailed t-tests were conducted and for comparisons between three or more groups, one-way ANOVA was conducted. To further study the significant differences between groups a Multiple Comparisons (Tukey's multiple comparisons test) analysis was conducted. *p*-values are reported in text for each statistical analysis.

Chapter 3 - Investigating the flowering role of the candidate *E1* gene in temperate legumes

3.1 Introduction

3.1.1 Conservation of the *CO-FT* module

Understanding variation in plant photoperiod responses and the study of the conserved and/or novel genes involved in photoperiodic genetic networks is a key focus in flowering time research. Extensive previous studies in plant models as *Arabidopsis thaliana* and rice have characterized genetic networks that responds to different day length and circadian clock (Andrés and Coupland, 2012; Brambilla and Fornara, 2013). In both systems, the main and ultimate targets of this photoperiodic regulation are genes in the *FLOWERING LOCUS T (FT)* family (Ishikawa et al., 2005; Song et al., 2013). The degree of *FT* expression is dependent on photoperiod, in *Arabidopsis* this regulation is mainly achieved by the transcriptional regulator *CONSTANS (CO)* (Suárez-López et al., 2001). In the *Arabidopsis* model, the CO-FT interaction has been understood as the main key regulatory step for flowering induction, and the point at which inputs from light signalling and the circadian clock regulation are integrated to control CO activity (Turck et al., 2008; Valverde, 2011). However, more recent research indicates that this model is unlikely to be tightly conserved, and has highlighted differences in the regulation and importance of CO (Wong et al., 2014). In some cases, this module is functionally conserved for photoperiod responsiveness but is primarily important for processes other than flowering, such as photoperiodic tuberization in potato (González-Schain et al., 2012). In other cases *CO* homologs appear to have less importance, or function in parallel with other genes. For instance, in rice the *Hd1* locus encodes a *CO* ortholog that regulates a rice *FT* ortholog *Hd3a*, but a second pathway featuring the *Ehd1* gene is able to regulate flowering without the intervention of *CO* (Hayama et al., 2002; Hayama and Coupland, 2004; Hori et al., 2016; Tsuji et al., 2011). Barley provides another example, in which a *CO* ortholog (*HvCO1)* participates in *FT* regulation and flowering time control but other flowering genes such as the pseudo-response regulator *Ppd-H1* (ortholog of *PPR7* in *Arabidopsis*) can control flowering independently of *HvCO1* action (Campoli et al., 2012). Other plant groups may show a greater degree of diversification. For example, within the legume family, *CO* orthologs in the LD species *Medicago, Lotus* and pea appear to have no role in control of flowering time (Hecht et al., 2011; Ridge et al., 2017; Wong et al., 2014; Yamashino et al., 2013). In SD legumes such as soybean,

while *CO* orthologs may contribute to flowering time control (Cao et al., 2015), a more prominent role is seen for the legume-specific E1 transcription factor which can regulate *FTs* without the participation of *CO* in this regulation (Xia et al., 2012).

Legume species therefore constitute an interesting system in which to explore *CO* functions and potential alternative mechanisms, and how these might be adapted to provide SD or LD-type responses. In this respect, the two key species are the LDP pea, and the SDP soybean, as in both systems, numerous flowering time loci have been identified and characterized at the molecular level (Weller and Ortega, 2015). In soybean, most of the known loci (*E1* to *E9*) have been described as orthologs of flowering genes and among these, *E1-E4* are known to be involved in photoperiodic control (Langewisch et al., 2017; Miladinović et al., 2018). For instance, *E2* is *GIGANTEA (GmGIa)* ortholog (Watanabe et al., 2011) and *E3* and *E4* are *PHYA* orthologs. Other important flowering genes that have been characterised in soybean include *GmFT2a* and *GmFT5*a as homologues of *FT* and important targets of this genetic regulation (Kong et al., 2010).

3.1.2 Fundamental nature of *E1* in soybean

E1 is one of the most important soybean loci controlling natural variation for flowering time and maturity, and was initially identified as a new legume-specific gene and putative transcription factor (Xia et al., 2012; Xu et al., 2015b). Molecular identification of the gene and its variants has confirmed its contribution as a major component of the flowering time variation and photoperiod adaptation in soybean cultivars, together with *E3, E4* and more recently *E7* (Jiang et al., 2014; Xia et al., 2012; Zhao et al., 2016). *E1* is an intron-free gene that encodes a protein related to the plant-specific B3 domain, a domain present in several genes participating in flowering regulation in other species. These B3 genes include the *TEMPRANILLO* genes in *Arabidopsis* (Castillejo and Pelaz, 2008; Osnato et al., 2012; Xia et al., 2012) which operates as direct repressors of *FT* balancing the inductive regulation of *CO* to regulate premature flowering. They also include the rice gene *OsLFL1* (*LEC2 and FUSCAS3 Like1* gene containing B3 domain) which is able to bind in the promoter region of *Ehd1* and regulate flowering time (Peng et al., 2007). E1 protein contains a putative bipartite nuclear localization signal. The nuclear localization signal is key for its function, as its disruption in several mutant alleles (natural mutants or EMS induced mutants) display defective localization and early flowering (Xia et al., 2012).

E1 acts as a transcription factor able to repress flowering by directly regulating the two homologous *FT* genes in soybean, *GmFT2a* and *GmFT5a* (Xia et al., 2012; Zhai et al., 2014a). This

E1 dependent repression of *FT* genes occurs in LD, meanwhile in SD, *E1* expression is suppressed allowing flowering to occur. The control of *E1* expression appears to be a key mechanism for flowering control in soybean and its activity is regulated by photoperiod. This is achieved through phytochrome A photoreceptors E3 and E4, which strongly suppress *E1* expression under SD to permit flowering (Zhai et al., 2014a). Under LD, this suppression is relieved and *E1* is expressed with a bimodal diurnal pattern and prevents flowering through its repression of *GmFT2a* and *GmFT5*a (Xia et al., 2012). In addition to *E1* itself, soybean also contains two other *E1* homologs, *E1La* (*E1-like-a)* and *E1Lb* (*E1-like-b*), which are similarly regulated by photoreceptors and participate in the regulation of *GmFT2a* and *GmFT5* in some cultivars (Xu et al., 2015b). *CONSTANS* homologs (*GmCOLs*) have been characterized in soybean, and there is some evidence that they may influence flowering (Cao et al., 2015; Wu et al., 2014; Zhang et al., 2016). However, considering that the phytochrome (E3/E4) -E1- FT pathway is proposed to be the key engine for photoperiod flowering adaptation in soybean (Cao et al., 2015; Tsubokura et al., 2014), it is not yet clear whether there is any potential regulatory link between *GmE1* and *GmCOL* genes.

3.1.3 Possible *E1* role in other legumes

The potential role of *E1*-like genes in other legume species has not yet been explored in detail. A couple of recent studies have suggested that *E1* may participate in flowering regulation and could have an important role controlling flowering time in other legumes (Jaudal et al., 2020; Zhang et al., 2016). For instance, the *E1* ortholog in *Lotus japonicus* (*LjE1*) was proposed as a candidate to explain latitudinal variation in flowering time, based on sequence differences (Wakabayashi et al., 2014). In *Medicago,* two mutant lines for *E1* show a flowering phenotype and in the case of common bean, ectopic overexpression of *PvE1* in soybean was able to induce a flowering phenotype (Zhang et al., 2016). The study of legume *E1* homologs and their participation in flowering regulation is of great interest and important relevance to explain the regulatory connectivity of the legume system with the lack of *CO* role.

3.1.4 Aims

In view of these recent studies, it becomes interesting to understand whether *E1* may contribute to flowering time control in pea, an important LD legume model in which numerous flowering genes have been characterised (Weller et al., 2009a; Weller and Ortega, 2015). In particular, considering that there is no clear evidence supporting the function of *CO-like* genes as mediators

of photoperiod-dependent *FT* induction in pea, there is an important question around how this regulation is achieved and whether *CO-like* function may be carried out by other unrelated genes, such as *E1*. However, pea *E1* has not been characterised and its role in flowering regulation has not yet been examined. This chapter aims to address this question by examining the possible function of *E1* in pea using a reverse genetic study and including the possible regulation of PHYA in flowering time control. It also presents a deeper examination of *E1* in *Medicago* in order to allow comparison of potential *E1* roles in LD legume species and complements the *E1* phylogeny study with protein structural analysis in diverse SDP and LDP legumes.

3.2 Specific material and methods

This section describes specific details of materials and methods for research included in this chapter. General materials and methods that are also relevant are described in Chapter 2.

3.2.1 Plant material

The research in this chapter is based on *Pisum sativum* and *Medicago truncatula.* Details of the pea plant lines used for the experiments presented in this chapter are outlined in Table 3.1.

Table 3.1 Details of pea plant material presented in this chapter.

Target gene	Genotype	Purpose
E1	*e1-3*	Mutant containing a premature stop codon for *E1* gene. Originated by EMS mutagenesis of cv. *Cameor* and obtained by TILLING screen. This line was introgressed into NGB5839 by back-crossing (BC_5). Further mutation description and mutant characterization regarding flowering response, photoperiodic development and gene expression is included in this chapter.
E1	*e1-4*	Mutant containing a substitution in a conserved region for *E1* gene. Originated by EMS mutagenesis of cv. *Cameor* and obtained by TILLING screen. This line was introgressed into NGB5839 by back-crossing (BC_3). Genotype used for *E1* characterization in flowering time and photoperiodic response.
PHYA	*phyA-3D*	Dominant mutant for *PHYA* gene described by (Weller et al., 2004). Originated by EMS mutagenesis of cv. Torsdag and crossed into NGB5839. Genotype analysed for *E1* expression studies.
PHYA	*phyA-1*	Null mutant for *PHYA* gene described by (Weller et al., 2004). Originated by EMS mutagenesis of cv. Torsdag and crossed into NGB5839. Genotype analysed for *E1* expression studies.

Details of the *Medicago* plant lines used for the experiments presented in this chapter are described in Table 3.2.

Table 3.2 Details of *Medicago* plant material presented in this chapter.

Target gene	Genotype	Original line	Purpose
E1	*MtE1*	NF16583	WT genotype for *E1 o*riginated from *Medicago Tnt1* database. Genotype used for *Medicago* flowering and vernalization characterization analysis.
E1	*Mte1*	NF16583	Mutant containing a *Tnt1* retrotransposon in its exon. Mutant genotype for *E1 o*riginated from *Medicago Tnt1* database. Genotype used for *Medicago* flowering and vernalization characterization analysis.
PHYA	*MtPHYA*	NF1583	WT genotype for *PHYA* originated from *Medicago Tnt1* database. Genotype used for *Medicago* flowering and vernalization characterization analysis.
PHYA	*Mtphya*	NF1583	Mutant containing a *Tnt1* retrotransposon in its first intron. Mutant genotype for *PHYA* originated from *Medicago Tnt1* database. Genotype used for *Medicago* flowering and vernalization characterization analysis.

3.2.2 Plant growth conditions

Plants were either grown in the University of Tasmania Controlled Environment Facility (CEF) phytotron with the photoperiod conditions described in Chapter 2 or in controlled environment growth cabinets at 20°C under fluorescent light for the full photoperiod.

For the different photoperiod experiment in this chapter, plants were grown in pots in different light conditions specified in Table 3.3, with temperature and water regime controlled.

Table 3.3 Photoperiod conditions details studied in this chapter.

Photoperiod label	Location	Conditions
LDI	Top Phytotron Bay 1	12h LD extended with 8h on Incandescent light
LDF	Top Phytotron Bay 2	12h LD extended with 8h on Fluorescent light
Natural LD	Main Glasshouse apron	Natural LD from the apron in the glasshouse facility
CF	Controlled environment growth cabinet	24h of continuous cool-white fluorescent light at 20°C
SD	Controlled environment growth cabinet	8h of light with 12hr of darkness

3.2.3 Plant measurement

Due to the earlier observations on the effect of the *lip1* mutant in Chapter 4*,* the rate of node development was also examined in this chapter. This assesses the rate at which leaf expansion (opening) occurs through multiple measurements of the total number of nodes/leaves over a number of weeks until flowering. In this case it was measured every week for 6 weeks (until flowering) in both WT, heterozygotes and *e1-3* plants from a BC_3F_3 segregating population grown simultaneously and exposed to the same photoperiods.

3.2.4 Genotyping

Most of the genotyping of the different *e1* mutant alleles was performed with HRM markers specified in section 3.2.5. Exceptionally, e*1-3* genotyping was performed by CAPS marker (Cleaved Amplified Polymorphic Sequence) using the digestion enzyme protocol of NcoI. A PCR with primers specified in Table 3.4 was designed to amplify a 400pb region containing the substitution G>A of the *e1-3* mutant. After PCR purification, 20µL of PCR product were incubated at 37°C overnight with 1µL of NcoI enzyme (BioLab, Australia) and 10x Buffer 3.1 in a 50µL reaction. The digested fragments were visualised with a High-Resolution Agarose gel of 3%, revealing a 400bp band for the *e1-3* mutant, two bands of 250bp and 150bp for WT (*E1)* and therefore, three bands of 400bp, 250bp and 150bp for Heterozygotes.

3.2.5 Primer details

Information of the primers used for this chapter is found in Table 3.4. For expression analysis, levels of *E1* in relation to *TFIIa* gene were measured in developmental node series material by qRT-PCR.

Table 3.4 Details of primers used in this chapter.

Gene	Purpose	Primer name	Primer sequence	Temp
E1	PCR for genotyping by CAPS marker	PsE1-7F	CAATTTCTGAAGAAGAGGAAATCA	58ºC
		PsE1-8R	CGAAATCTTGATTCCACTTTCC	
E1	*e1-4* HRM genotyping	PsE1-4F	AACCGACAGCGATCTAGGAA	60ºC
		PsE1-5R	CCATGTCGAAAACCTGAACC	
E1	Expression experiment	PsE1-7F	CAATTTCTGAAGAAGAGGAAATCA	58ºC
		PsE1-7R	GGACACTGATCCCTTGCTGT	
TFIIa	Expression experiment	PsTFIIA-1F	CGGTGGAAATGCTGATGTTA	60ºC
		PsTFIIA-1R	GCTCCCTCCACATACCTCAA	
MtE1	Expression experiment	MtE1-5F	GCGATCTTGGAATCTTGAGC	58ºC
		MtE1-5R	GAACCTTCCTCGGTTTCTGC	
MtE1	PCR gene specific reaction for genotyping	MtE1-F	AGAGTGTAATTGGGAGTGT	58ºC
		MtE1-R2	TTGAAAGCGCGGTTAAAAGG	
	PCR insertion specific reaction for genotyping	MtE1-F	AGAGTGTAATTGGGAGTGT	58ºC
		MtTnt1-R	CAGTGAACGAGCAGAACCTGTG	
	PCR insertion specific reaction for genotyping	MtTnt1-F	ACAGTGCTACCTCCTCTGGATG	58ºC
		MtE1-R2	TTGAAAGCGCGGTTAAAAGG	

3.3 Results

3.3.1 Functional analysis of *PsE1*

The pea *E1* gene (Psat1g027960 - genome v.1a) (Kreplak et al., 2019) has the same structure as the well-characterized *GmE1*, with a single exon of 892bp, as seen in Figure 3.1. We made use of the pea TILLING platform for reverse genetics (Alves-Carvalho et al., 2015; Dalmais et al., 2008) to target the entire *E1* gene in a single screen, and identified seven alleles with mutations distributed throughout the gene as shown in Figure 3.1. Among these, four (*e1-4, e1-5, e1-6* and *e1-7*) specified amino acid substitutions in the conserved region (represented by numbered red triangles in Figure 3.16) that could potentially affect E1 protein function. However, a fifth allele (*e1-3*) carried a premature stop codon, and was therefore prioritized for genetic analysis.

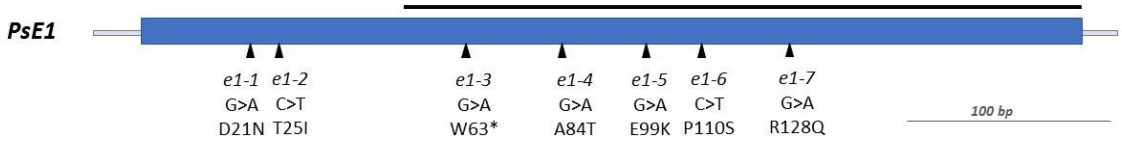

Figure 3.1 *E1* pea gene diagram.

Diagrammatic representation of the *E1* gene in pea containing no introns and a unique exon represented with a blue box and showing the location and nature of mutations in *e1* mutants. The black line represents the highly conserved region with other legume species.

In the absence of any prior knowledge of *E1* function in LD legume species such as pea, it was not clear how it might be influencing photoperiodic flowering. In particular it was not clear whether, like in soybean, it might act to delay flowering under non-inductive conditions (which would predict an early-flowering phenotype in pea under SD) or might act under the same photoperiod conditions as in soybean (LD) but in an opposite manner (i.e. promoting rather than inhibiting flowering). In view of the possibility that it might play a LD-promotive role analogous to CO, mutant phenotypes were examined under both LD and SD conditions, focusing initially on the *e1-3* mutants. The *e1-3* allele was selected for the genetic studies and therefore primers were created for HRM genotyping purposes (details in 3.2.5 Primer details section) together with other HRM markers for other alleles. There were some analytical problems in the genotyping of *e1-3* allele, finding a double peak in the melting curve with no relation to another nucleotide substitution since the DNA sequences were analysed. Due to the impossibility of genotyping by HRM analyses,

an enzymatic digestion protocol was designed for *e1-3* genotyping using NcoI enzyme after a specific *E1* PCR (details included in 3.2.4 Genotyping section).

The pea *e1* mutants were obtained from an EMS mutagenesis screening in the cultivar *Cameor* and then they were introgressed in NGB5839 background by five backcrossing. A preliminary comparison of wild-type (WT) line NGB5839 and an *e1-3* near-isogenic line (NIL) revealed that the growth and development of *e1-3* mutant was overall very similar to the WT, under both photoperiod conditions (Figure 3.2). Both genotypes initiated flowering at a similar node with a respective mean node of flower initiation (NFI) in WT and *e1-3* of 17 and 17.7 in LD, and 20 and 20.7, in SD, but with no significant statistical difference between genotypes as seen in Figure 3.2 B. In pea, as in other species flowering is often assessed both in terms of node number (e.g. NFI) and date of flowering (DTF) and these traits are often correlated across genotypes, although there can be exceptions, as seen for the *lip1* mutant in Chapter 4. In the case of *E1,* the time of flowering was also similar for both genotypes. As described in Figure 3.2 C, in LD conditions both genotypes flowered around 41 days, and in SD around 58 days. This preliminary result seemed to provide a clear indication that *PsE1* might not have a major or distinctive role in flowering time control, somewhat contrary to expectation.

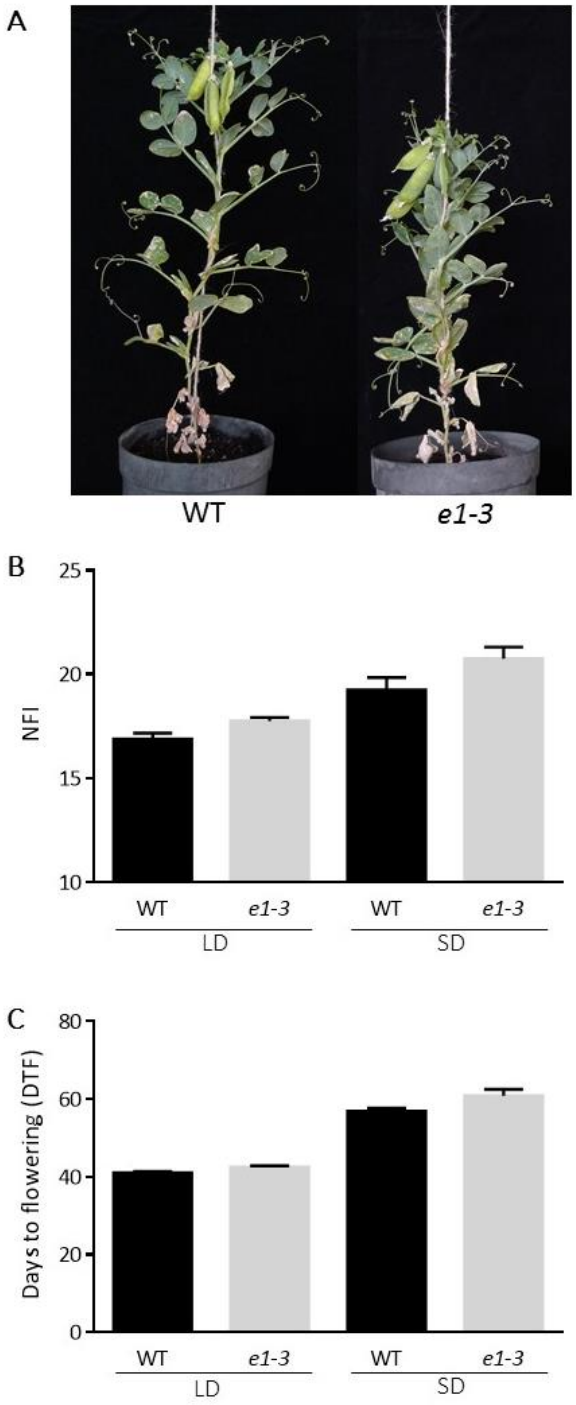

Figure 3.2 Phenotypic comparison of WT (5839) and *e1-3* in flowering time.

A) Phenotypic representation of both genotypes under LD development. B) Node of floral initiation in both genotypes under LD and SD conditions. Values represent mean ± SE for n=8 plants in each condition. There are not significant differences within photoperiod treatment (p-value>0.05). C) Date of flowering in both genotypes under both photoperiods. Values represent mean ± SE for n=8 plants in each condition. No significant differences are found within photoperiod treatment (p-value>0.05).

Another mutant allele (*e1-4*) was also examined, with a similar lack of clear difference from WT for NFI or Reproductive Nodes (RN), as shown in Figure 3.3. To also rule out the possibility that *e1* might affect other aspects of development known to be associated with the flowering transition in pea, several other diverse vegetative-stage traits were examined, including leaf expansion rate and vegetative branching, but no clear differences were identified.

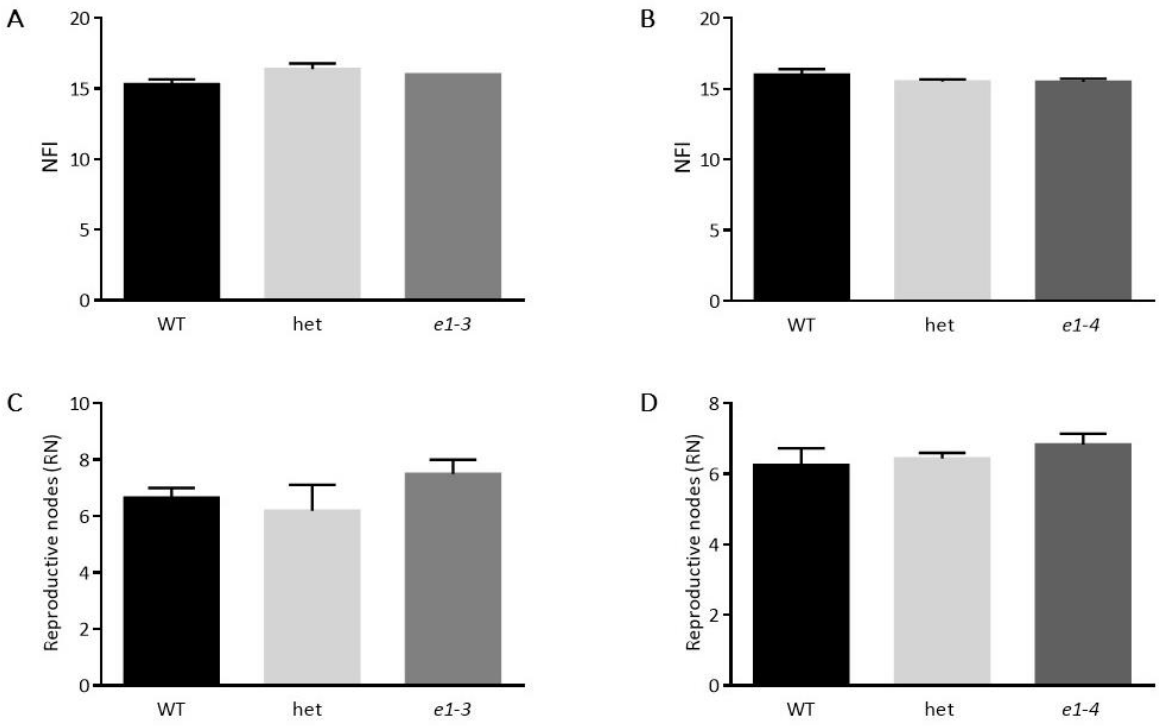

Figure 3.3 Flowering node and reproductive node in LD of the *e1*-3 and *e1-4* BC_3F_2 population mutants.

A) Flowering node of a BC_3F_2 segregating population of *e1-3* mutant. Values represent mean ± SE for n =2-5 plants in each genotype. There are not statistical differences between the groups (p=0.214) B) Flowering node of an BC_3F_2 segregating population of *e1-4* mutant. Values represent mean ± SE for n =4-18 plants in each genotype. There are not statistical differences between the groups (p=0.395) C) Reproductive node of an BC_3F_2 segregating population of *e1-3* mutant. Values represent mean ± SE for n =2-5 plants in each genotype. There are not statistical differences between the groups (p=0.349) D) Reproductive node of an BC_3F_2 segregating population of *e1-4* mutant. Values represent mean ± SE for n =4-18 plants in each genotype. There are not statistical differences between the groups. (p=0.58).

The potential phenotypic effect of the *e1-3* allele was further assessed in additional experiments using a BC_3F_3 population segregating for *e1-3* (to control for any effect of genetic background and allow for examination of heterozygous genotypes (Figure 3.4). As in the preliminary experiment, analysis of the segregating F_3 indicated that although *e1-3* mutants appeared to flower at a marginally later node, this difference was not statistically significant (Figure 3.4 A). We also assessed Reproductive nodes (RN) in Figure 3.4 B, which is another photoperiod-responsive trait that may in some cases be a more sensitive indicator of responsiveness than flower initiation. Once again, despite an apparent small increase in RN in *e1-3* relative to WT, this difference did not achieve statistical significance. The same was also true for flowering time (Figure 3.4 C) and Flower-Leaf Relativity (FLR) (Figure 3.4 D). These observations agree with data from the preliminary NIL comparison together indicating that *E1* may have at most a very minor effect on flowering in pea, at least in the NGB5839 genetic background.

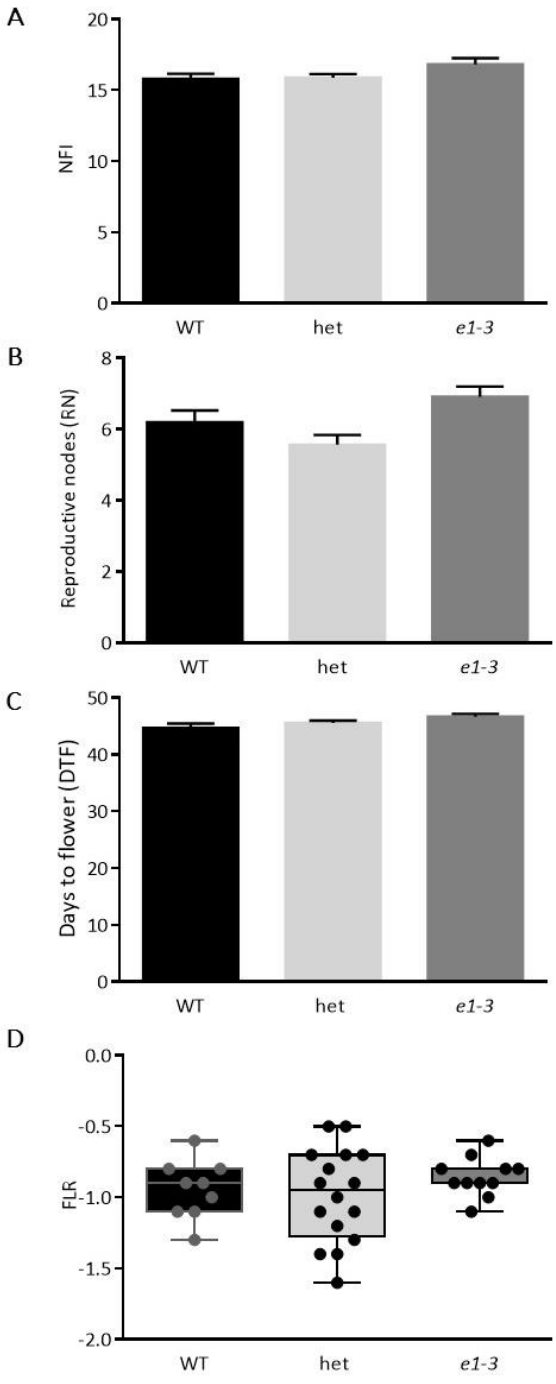

Figure 3.4 Phenotypic comparison of flowering time in LD of an F_3 segregating population for *e1-3*.

A) Flowering node of an F_3 segregating population of *e1-3* mutant. Values represent mean ± SE for n =10-16 plants in each genotype. There are not statistical differences between the groups (p=0.125) B) Reproductive node of an F_3 segregating population of *e1-3* mutant. Values represent mean ± SE for n =10-16 plants in each genotype. There are statistical differences between groups (p=0.021) but not significant difference between *e1-3* and WT groups. C) Flowering date of an F_3 segregating population of *e1-3* mutant. Values represent mean ± SE for n =10-16 plants in each genotype. There are not statistical differences between the groups (p=0.075) D) Flower-Leaf Relativity (FLR) of an F_3 segregating population of *e1-3* mutant. Values represent mean ± SE for n =10-16 plants in each genotype. There are not statistical differences between the groups. (p=0.426).

In order to investigate whether the role of *E1* on flowering is due to a difference in rate of development of the plant, rather than to developmental change in the initiation of flowering, the developmental node rate of WT, *e1-3* mutants and heterozygotes were compared during two weeks in the same segregating F_3 population under LD conditions. As shown in Figure 3.5, there was no evidence for any significant difference among genotypes.

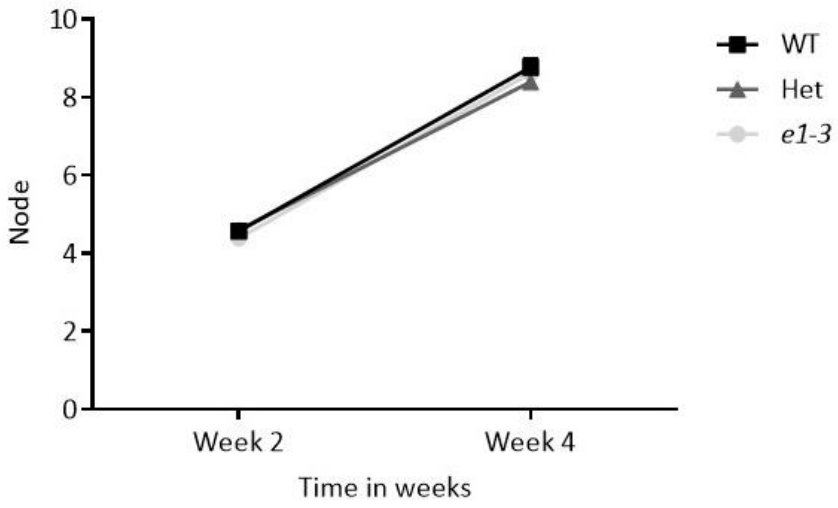

Figure 3.5 Leaf expansion rate of an F_3 segregating population for *e1-3.*

Representation of the developmental rhythm of the plant by node development and leaf expansion from an F_3 population segregating for *e1-3* allele. Values represent mean ± SE for n =10-16 plants in each genotype. There are not significant differences (p=0.997) between the genotypes.

We also considered that the apparent lack of any substantial *E1* effect might also reflect the limited range of environmental conditions tested, and therefore examined the *e1-3* mutant under a wider range of light conditions (Figure 3.6), using only homozygous WT and mutant segregant families, with NGB5839 as an additional comparison. Conditions used are detailed in Table 3.3 and include 8h SD, continuous cool-white fluorescent light (CF), and three different 16-h LD environments with differing light quantity and quality (LDI, LDF and Natural LD).

Flower initiation shown in Figure 3.6 A, occurred at around node 16 in all three LD conditions with at most, only small differences between *E1* and *e1-3* segregants. Under LD with an extension with FR-rich tungsten-filament light (LDI) the difference in mean flowering node was approx. 1.5 nodes (16 for *E1 vs* 17.5 for *e1-3*). Under constant light conditions, flowering was slightly later than in LDF but a similar difference in mean FNI was observed between *E1* (17.3 nodes) and *e1-3* (18.3 nodes). In LDF, flowering was accelerated, and FNI overall was a node earlier than under LDI. The difference between *E1* (mean FNI of 15.3) and *e1-3* genotypes (15.6) was smaller than in LDI, but again, was not statistically significant (p =0.3190). The most distinctive phenotypic effect was seen in SD conditions, where *e1-3* flowered significantly later (27.6 nodes) than the corresponding *E1* sibling plants (20.1 nodes) or 5839 (21.5 nodes) (p=0.0018).

The total node (TN) trait is another indicator of photoperiod responsiveness in pea (Weller et al., 1997b) and showed a similar pattern of variation with *E1* genotype for the different light conditions (Figure 3.6 B). No significant difference was seen for any of the conditions except SD, where the *e1-3* mutants produced more nodes overall than the WT (42 vs. 38 respectively) (p=0.0004). Under all LD conditions there were at most minor differences between the genotypes, the largest being a 2-node increase in mean TN in *e1-3* relative to *E1* under CF and none were statistically significant.

The days to flower (DTF) trait was the most uniform across the genotypes and conditions examined displayed in Figure 3.6 C. In contrast with node-based measurements, there was no statistically significant effect of the *e1-3* mutant under any conditions, although minor differences were observed. Under the various LD conditions the flowering date range was only 6 days (41 to 47 DTF), with plants in LDI conditions the latest to flower (46 and 48 DTF in *E1* and *e1-3* respectively). Plants in LDF flowered a few days earlier, around 44 days for *E1* WT and 45 days for the mutants. In constant and natural light conditions flowering was slightly earlier still, with *E1* flowering at an average of 42 days in both conditions and *e1-3* one to two days later. Some indication of later flowering in *e1-3* relative to *E1* under SD was seen, in line with the node measurements, but the difference of six days between the *E1* (65 DTF) and *e1-3* (71 DTF) was not significant (p=0.2444).

Regarding the Flower-Leaf Relativity (FLR) shown in Figure 3.6 D, there are no statistical differences between genotypes grown in any LD conditions. In most of the photoperiod conditions all genotypes display a similar range of leaf expansion in relation to NFI, suggesting that plants are developing and opening the leaves at the same node as the flower. The only statistically interesting pattern is observed in SD conditions, similar to NFI and TN trend, there is suggestive

difference between the *e1-3* mutant and the WT (p>0.005). In this case, *E1* WT is flowering at 20th node and the expanded leaf corresponds to the node 19th meanwhile the *e1-3* mutant flowers at 27.6 node, same node that is currently expanding the leaf, showing a big difference regarding the genotypes but without a significant difference between NFI and the current expanded leaf.

The NGB5839 genotype (*E1*) is used as a control for this experiment and does not give statistically support for any difference in NFI, TN, DTF or FLR in any photoperiod condition. The majority of differences observed are between the segregants from backcross studied - *E1* (WT) and *e1-3* genotypes- and are similar to the control NGB5839 (*E1*). This result suggests that *e1-3* may be having an effect just in SD, having a swiftly later flowering time regarding FNI and it is correlated with the developmental aim of the plant. This lateness does not have enough statistical support when analysed by date of flowering, even though the mutant shows a slight delay.

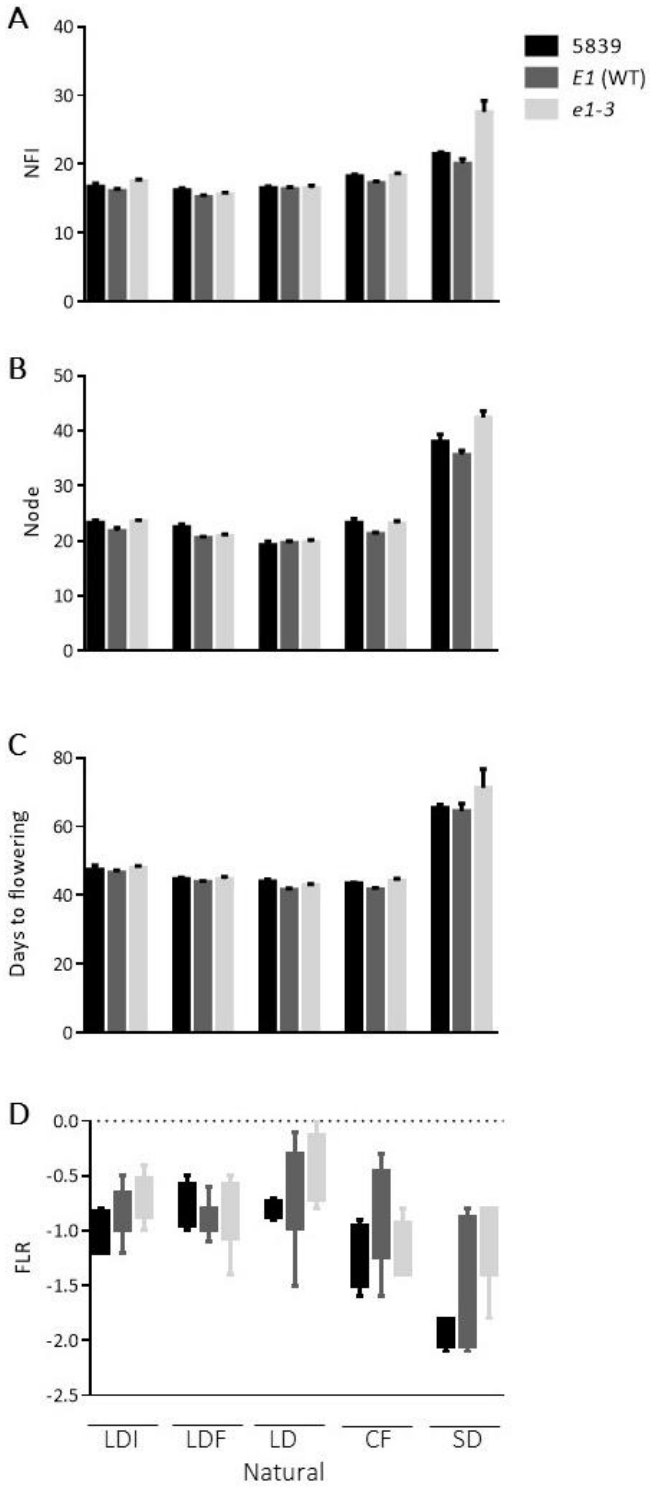

Figure 3.6 Phenotypic comparison of flowering time in different photoperiod conditions for *e1-3* BC_3F_3 families.

E1 WT plants and *e1-3* plants from a BC_3F_3 population were exposed to 5 different photoperiods detailed in Table 3.3 and consisting on: 12h LD+ 8h Incandescent extension (LDI), 12h LD+ 8h Fluorescent extension (LDF), continuous cool-white fluorescent light (CF) for 24h at 20°C, Natural LD from the apron in the glasshouse facility and SD (8h light/16h dark). Values represent mean ± SE for n =8 plants in each genotype. In the case of *E1* (WT) and *e1-3,* values represent n=8 including 4 plants from each identified segregant family. A) Flowering node of WT and *e1-3* mutant in comparison with 5839. There are no statistical differences between

the groups except for SD conditions (p=0.0018) B) Total node of WT and *e1-3* mutant in comparison with 5839. There are not statistical differences between the groups except for SD conditions (p=0.0004) C) Date of flowering of WT and *e1-3* mutant in comparison with 5839. There are no statistical differences between the groups neither for SD conditions (p=0.2444). D) Flower-Leaf Relativity (FLR) of WT and *e1-3* mutant in comparison with 5839. There are not statistical differences between the groups.

3.3.2 Expression analysis of *E1* gene in WT and *phyA* developmental series.

As outlined earlier in this thesis, the *E1* gene has a central role in flowering time and photoperiod response in soybean. Several studies indicate that under LD the PHYA photoreceptor genes *E3* and *E4* play an important role in the induction of *GmE1* expression, which then delays flowering through the repression of *FTs* (Kong et al., 2010; Xia et al., 2012). Under SD, however, *GmE1* expression is not induced and therefore there is no repression of flowering (Zhai et al., 2014a). It has recently been suggested that in LDP legumes such as *Medicago, E1* may have a role that is opposite to that in soybean, inducing *FT* expression for promotion of flowering in LD, but may itself retain a similar regulation and be induced by photoreceptor action under LD (Zhang et al., 2016). This genetic pathway for regulation of *E1* expression in soybean has been characterized in considerable detail (Miladinović et al., 2018; Tsubokura et al., 2014), but little is known about the characteristics of *E1* regulation in a LD legume model. In an attempt to gain further insight to the role of *E1* in pea, its expression pattern was queried in the Pea Gene Atlas (Alves-Carvalho et al., 2015). This data showed that *E1* expression is overall very low across the different tissue types featured in the Atlas (Figure 3.7) consistent with similar results from soybean (Xia et al., 2012). Consistent with soybean and with a potential role as a regulator of *FT* genes, the highest level of *PsE1* expression was seen in leaf tissue, and expression studies were therefore focused on leaf tissue.

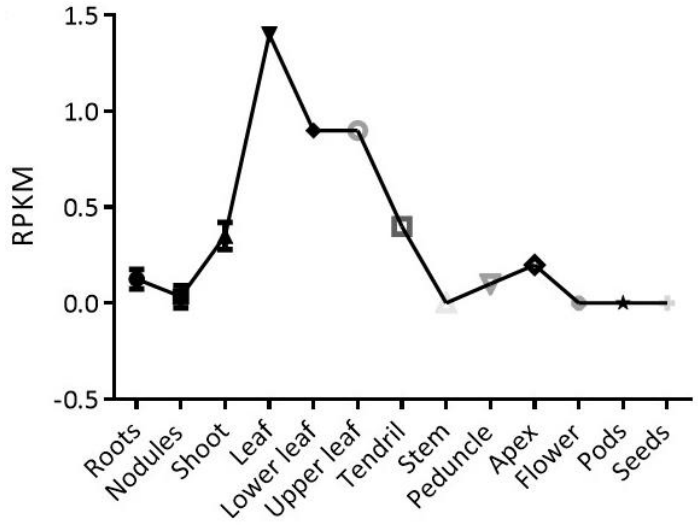

Figure 3.7 Expression profile of pea *E1* (PsCam02161).

Reads Per Kilobase Million (RPKM) calculated from RNA-seq data in (Alves-Carvalho et al., 2015) This profile shows the *E1* expression in different pea plant tissues.

Thus, in an initial attempt to test whether the regulation of *E1* by PHYA seen in soybean might be conserved in pea, two developmental series comparing WT and *phyA* mutant alleles were examined – a LD series comparing WT NGB5839 and the isogenic late-flowering *phyA-1* null mutant (Weller et al., 2004) and a SD series comparing WT NGB5839 with the early-flowering *phyA-3D* gain of function mutant (Weller et al., 2004). The results in Figure 3.8 show that under LD, the level of *E1* expression in both genotypes was very low, relative to two different constitutive pea genes, *TFII* and *ACTIN*. There is lot of variability represented by the error bars (Figure 3.8 A) and there is higher expression of *E1* in the WT than in the *phyA-1* mutant (null mutant), which is not supported by statistical power, but suggests that *PHYA* acts as an inducer of *E1* expression as seen in *Medicago*. In SD conditions, there is a high level of variability as well (Figure 3.8 B), but it seems that *E1* expression is reduced in WT in comparison with the gain of function mutant (*phyA-3D*) suggesting that, in SD there is no induction of *E1* expression (Figure 3.8 B). These expression results show low gene expression with high levels of variation and therefore, their interpretation can only be suggestive. But also, these results agree with the model of Zhang et al., 2016 suggesting that the photoperiodic regulation applied on *E1* is similar in all the legume species but the role of *E1* in the control of flowering could be opposite in Long Day vs Short Day plants.

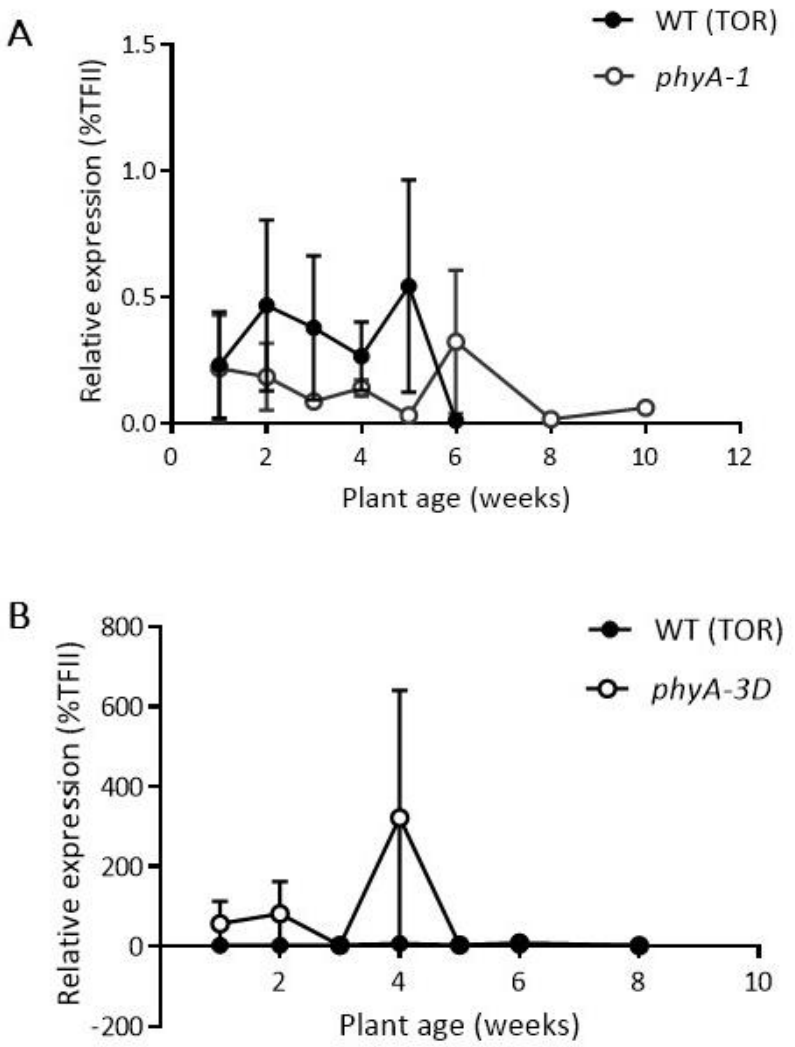

Figure 3.8 *E1* expression in developmental series in both photoperiods.

E1 expression in developmental series. A) *E1* relative expression in a LD for 10 weeks. Two leaf replicates of a *phyA-1* mutant (null mutant) and WT (TOR background). B) *E1* relative expression in a SD for 8 weeks. Two leaf replicates of a *phyA-3D* (gain of function) mutant and WT (TOR background).

3.3.3 *Medicago e1* mutant flowering characterization in LD conditions with vernalization.

The two separate analyses in pea are inconclusive but suggestive of the possibility that *E1* might promote flowering and be regulated by PHYA. However, this effect is at best minimal, and as such is opposite to the strong role of *E1* in soybean. Further evidence of a role for *E1* orthologs in LD legumes might come from an examination of other species. In *Medicago truncatula*, an effect of *E1* on promotion of flowering under LD was recently reported in a study using reverse genetics (Zhang et al., 2016) but this was again mild relative to the soybean effect. Here we performed an independent characterization of the effect of *MtE1* including the characterization of the vernalisation effect in flowering. *Medicago* is emerging as a legume model used for genetics studies and flowering response characterization since it has a fully sequenced and annotated genome and substantial genetic resources, including a large scale *Tnt1* retrotransposon insertion mutant platform (Sun et al., 2018, 2019). Zhang et al., 2016 reported the isolation of two such mutants for *E1*, of which one was independently characterized in this study.

Line NF16583 and line NF20110 were obtained from the *Tnt1* platform at the Noble foundation (Sun et al., 2018, 2019). These lines were reported by Zhang et al., 2016 to carry *Tnt1* insertions towards the 5' end of the single *E1* exon at position 218pb (line NF16583) and towards the centre of the exon at position 259bp (line NF20110) as presented in Figure 3.9.

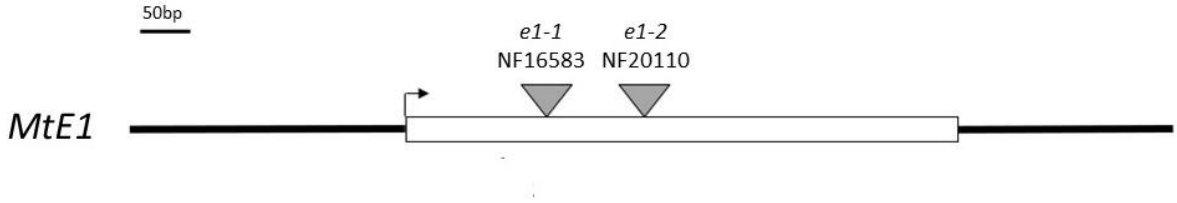

Figure 3.9 *Medicago E1* gene scheme and lines representation.

Diagrammatic representation of the *E1* gene in *Medicago* containing no introns and showing the *Tnt1* insertions (grey triangle) in each *e1* line mutants.

The sequence analysis confirmed the presence of the *Tnt1* insertion in each line and line NF16583 was selected for the consequent studies, where it is referred to as *e1-1.* The following analysis and characterization presented in this section is focalised in the *e1-1* line after the screening of useful heterozygote families to analyse *E1* role and due to the prediction of a significant disruption to E1 protein sequence and activity. From the original segregating progeny received, the line *e1-1* was

propagated by recurrent selection for heterozygosity of the insertion, and progenies generated from homozygous WT and mutant *(e1)* siblings were used for phenotypic comparisons.

The *Tnt1* insertion in *e1-1* line, located around 218pb in the first and unique exon, affects the expression of the *E1* gene, finding expression in the WT segregants which produce viable E1 protein but no *E1* expression is detected in the *e1-1* plants containing the insertion, as seen in Figure 3.10. Therefore, the line *e1-1* seems to be a good candidate for the following genetic analysis since the mutant is not expressing *E1* gene.

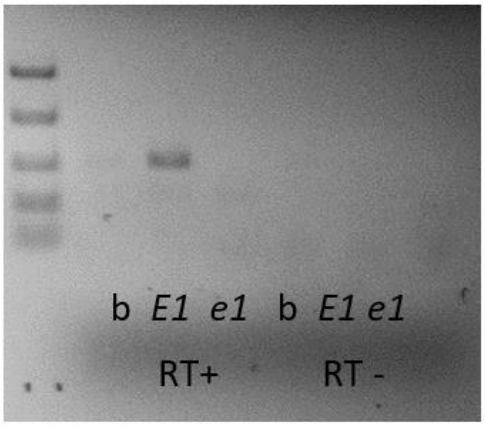

Figure 3.10 *E1* expression analysis for WT and *e1* plants siblings originated from the *e1-1* line.

Agarose gel image of a RT-PCR with gene specific primers for *MtE1*. There is *E1* amplification just in the WT line (band around 500bp). Both RT+ and RT- reactions are presented, RT- was performed as control.

Like *Arabidopsis*, flowering in *Medicago* is promoted both by exposure to LD photoperiods and exposure to cold (Clarkson and Russell, 1975; Jaudal et al., 2020; Laurie et al., 2011; Putterill et al., 2013). Relative to untreated (non-vernalized or LD+NV treatment) plants exposed to vernalization (LD+V treatment) flower earlier after producing fewer leaves and display an elongated primary shoot with fewer, longer branches as seen in Figure 3.11 and previously described by (Laurie et al., 2011). Although it appears that the vernalization (V) and photoperiod (P) responses are partially independent (Jaudal et al., 2016; Putterill et al., 2013; Weller and Ortega, 2015), it was not certain whether any effect of mutants might be exposed more clearly in LD+V or in LD+NV plants so both treatments were included in the study.

Figure 3.11 *Medicago* WT plants exposed to LD+NV and LD+V treatment.

Phenotypic differences of a WT *Medicago* plant (NF1583, MtPHYA WT) exposed to LD+NV treatment (on the left) and LD+V treatment for two weeks after germination (right). Both plants were grown under LD conditions. The LD+NV plants seem to focus their resources on vegetative development for longer, producing more and bigger leaves (red arrow), shorter shoots (yellow arrow) and flower later in time than the LD+V plants. The LD+V plants tend to focus their developing towards a reproductive phase, finding an earlier onset of flowering, longer shoots (yellow arrow) with less leaf total mass (red arrow) and when comparing both at the same time point, the LD+V plants have induced flowering and already present flowers and well-developed seed pots (blue arrow).

Under LD conditions the effect of the vernalization treatments on general growth habit was clearly evident and the two genotypes were overall very similar in appearance in LD+V or LD+NV treatments (Figure 3.12), with no obvious or consistent phenotypic difference. This was also specifically true for flowering time (recorded as days to flower) where no statistically significant differences were observed between genotypes for either treatment, despite a 3-4 week promotion of flowering by the LD+V treatment as shown in Figure 3.12 C and D graphs.

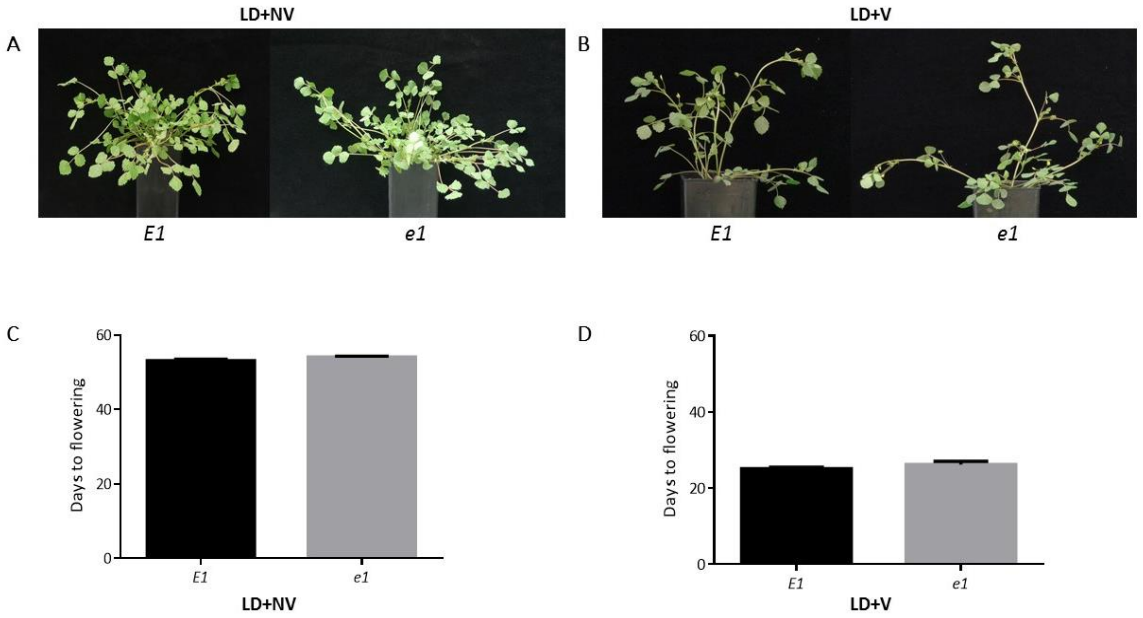

Figure 3.12 Phenotype and flowering time comparison of *MtE1* plants in LD+NV and LD+V treatment.

A) Phenotype of LD+NV *E1* (WT) and *e1* (mutant line NF16583) *Medicago* plants. Both have a short, bushier look with a heavy leaf mass, short shoots and without evidence of floral buds. B) Phenotype of LD+V *E1* (WT) and *e1* (mutant line NF16583) *Medicago* plants. Both *E1* and *e1* present long shoot with few leaves and some yellow flowers have opened already. Photos were taken 30 days after sowing. C) Flowering time for LD+NV treatment. Both *E1* and *e1* have similar flowering time dates around 54 DTF. There are no significant differences in flowering time between the two genotypes ($p=0.0653$). Values represent mean ± SE for $n>40$ plants in each condition. D) Flowering time for LD+V treatment. Both *E1* and *e1* flower around 25 DTF and there are no significant differences in flowering time between the two genotypes ($p=0.2855$). Values represent mean ± SE for n= 14-30 plants in each condition.

This result differs from that of Zhang et al., 2016 who reported that the same *E1* mutant line (NF16583) flowered approximately 5 days later under LD conditions (it was reported WT flowering approximately at 35 DTF and mutant lines around 40 DTF in LD conditions). For this reason, a second evaluation was conducted in which the *E1* mutant line (NF16583) was also compared with a mutant for *MtPHYA* (NF1583). This line was obtained from the same *Tnt1 Medicago* database and it contains a *Tnt1* insertion in the first intron of the *MtPHYA* gene as shown in Figure 3.13. As described earlier (in Chapter 1) PHYA is a strong promoter of flowering in the related LDP legume pea, where *phyA* mutants are late-flowering and effectively insensitive to LD (Weller et al., 1997a, 2004). *PHYA* genes *E3* and *E4* are also major regulators of *E1* in soybean (Xia et al., 2012; Zhang et al., 2016). Also, recent research characterised *MtphyA-1* line as a late flowering mutant in LD+NV and LD+V conditions (Jaudal et al., 2020). Thus, if *E1* is indeed important in *Medicago*, it might be expected that *e1* and *phyA* mutants would have similar phenotypes.

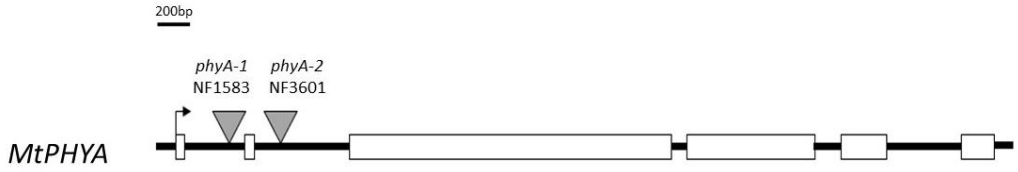

Figure 3.13 *MtPHYA* gene scheme and lines representation.

Diagrammatic representation of the *MtPHYA* gene containing 6 exons (white boxes) and 5 introns (black lines between exons). The grey triangles represent the two locations of the *Tnt1* insertions found in this gene. The first insertion is named *phyA-1* for the insertion line NF1583 was used in this study and referred to as *Mtphya* mutant line, and the second insertion is named *phyA-2* for the line NF3601.

Instead of the homozygous progenies used in both the initial experiment and by Zhang et al., 2016, this second evaluation compared the effects of the mutations in segregating progenies, to ensure that any other variation was adequately accounted for. In each case, progenies were genotyped for the presence of the insertion by PCR using insertion- and gene-specific primers detailed in section 3.2.5.

The result in Figure 3.14 shows that the *Mtphya* mutant segregants were clearly flowering later than the WT (*MtPHYA*) segregants under both LD+V and LD+NV conditions. This difference was ≈15 days in LD+NV ($p<0.0001$) and ≈4 days in LD+V ($p= 0.0061$), where the overall range in flowering time was much narrower.

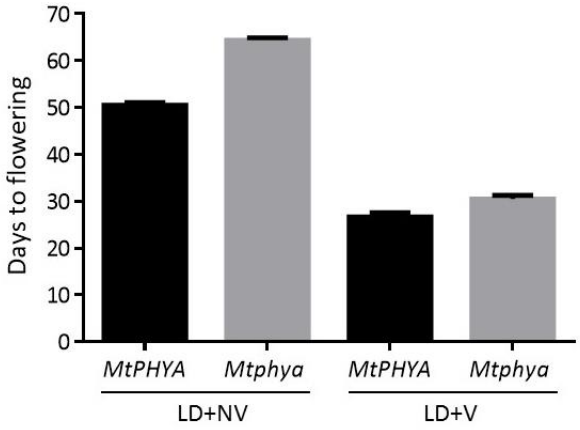

Figure 3.14 Flowering time in *Medicago PHYA* genotypes exposed to LD+NV and LD+V photoperiods.

Representation of flowering time as DTF in two genotypes, WT *MtPHYA* and mutant line *Mtphya* for both vernalisation treatments (LD+NV and LD+V). Values represent mean ± SE for n=18-20 plants for LD+NV treatment and n=8-10 plants for LD+V treatment. There are significant differences in flowering time between *MtPHYA* and *Mtphya* in both treatments.

In contrast to this strong *phyA* phenotype, the *e1* mutation again showed a minimal effect, with *e1* mutant segregants flowering on average only three days later than *E1* WT segregants (Figure 3.15 A), but this difference was only marginally significant (p=0.042). Moreover, the heterozygote segregants displayed an intermediate date of flowering without any statistical difference between either of the homozygote genotypes. Frequency distributions for flowering date in each of the segregating *E1* genotypes showed a broad overlap, with a very similar range (Figure 3.15 B-D) in contrast to the *phyA* mutant and WT genotypes, that flowered over discrete time ranges (Figure 3.15 E). This result is consistent with the initial experiment, indicating that the magnitude of the effect of the *Mte1-1* mutation on flowering, if any, is minimal, and also shows that the *E1* gene is unlikely to play an important role as a major regulator of flowering downstream of PHYA.

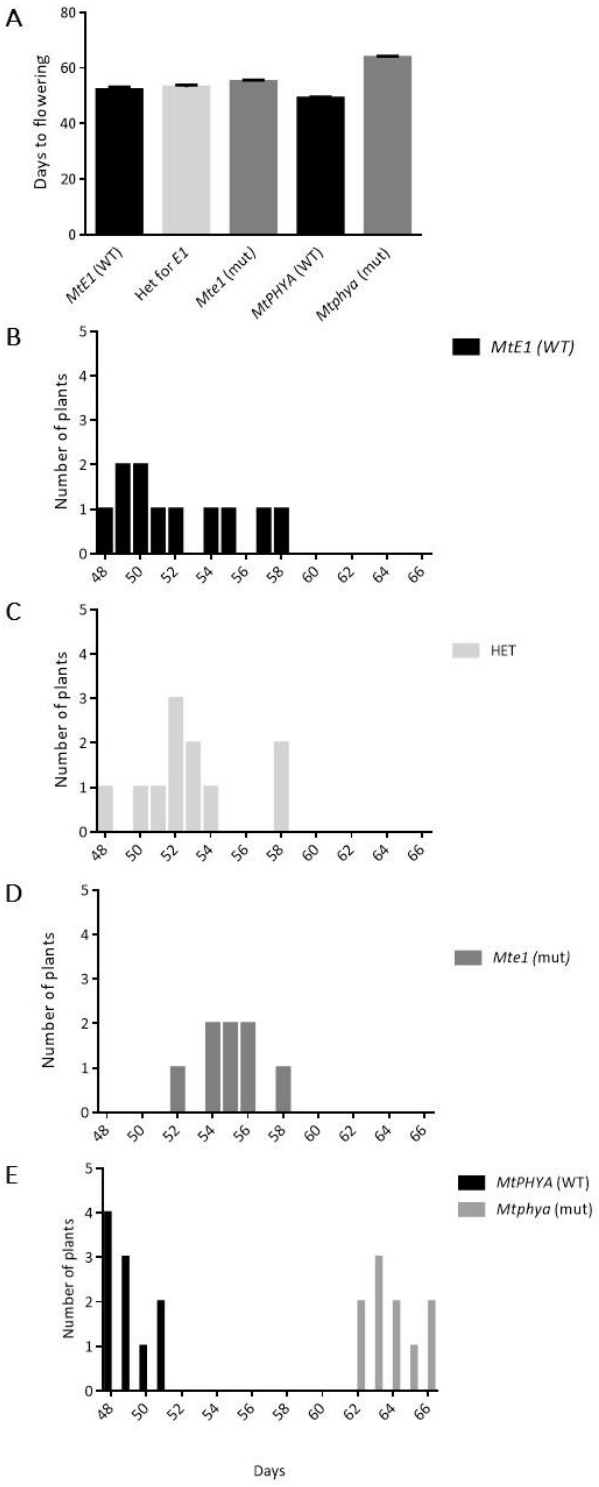

Figure 3.15 Distribution of flowering time of the segregating *MtE1* family and *MtPHYA* controls.

Representation of flowering time as DTF with a n= 8-13 plants per genotype. Plants were grown under LD+NV conditions. A) Flowering time representation based on days to flower. There are no significant differences between the genotypes segregating in the *E1* family (p=0.1051). B) Number of plants for *MtE1* segregants. All of them flowered between 48 and 58 DTF similar to *MtPHYA (WT)*. C) Frequency of plants for Hets segregants. All of them flowered before between 48-58 DTF as WT. D) Frequency of plants for *Mte1* segregants. They flowered between 52-58 DTF. E) *Mtphya* and *MtPHYA* distribution is shown for

comparison with a strong flowering mutant. *MtPHYA (WT)* flowered between 48-51 DTF and *Mtphya (mut)* flowered between 62-67 DTF showing a late flowering phenotype.

3.3.4 *E1* legume family: phylogeny and protein characterization

Since the results of the previous sections together suggest that *E1* does not have a central role in the photoperiod response of LD legumes and it was mentioned earlier the important role in the control of flowering of soybean *E1,* it was of interest to examine in more detail the molecular evolution of the *E1* family in legumes. *E1* was first characterized in soybean and suggested to carry a domain distantly related to the plant-specific B3 DNA binding domain that is distinctive of many plant transcriptional factors, as well as a putative bipartite nuclear localizing signal (NLS) (Xia et al., 2012).

An earlier report presented a limited phylogenetic tree for E1 proteins in legumes (Zhang et al., 2016) and here, a more extensive analysis was performed, incorporating sequences from a wider range of both SD and LD legume groups, specified in Table 3.5.

Table 3.5 Legume E1 sequences identified by blast in online sequences resources.

Name	Species	Locus ID
MtE1	*Medicago truncatula*	Medtr2g058520
GmE1	*Glycine max*	*Glyma.06G207800.1*
GmE1La	*Glycine max*	Glyma.04G156400.1
GmE1Lb	*Glycine max*	Glyma.04G143300.1
LjE1L	*Lotus japonicus*	*Lj5g3v2221340.1*
PvE1	*Phaseolus vulgaris*	*Phvul.009G204600*
CaE1	*Cicer arietinum*	*Ca_21849*
CcE1L1	*Cajanus cajan*	*C.cajan_45915*
CcE1L2	*Cajanus cajan*	*Ca_21849*
PsE1	*Pisum sativum*	PsCam021612
TpE1	*Trifolium pratense*	Tp57577
VaE1	*Vigna angularis*	*Vang09g03420.1*

E1 gene structure was seen to be well conserved among legumes, with all genes featuring a single exon encoding a protein that ranged from 163 (LjE1L) to 182 amino acids in length (MtE1 and

VaE1). The predicted amino acid sequence is highly conserved, with the minimum pairwise identity within this set of sequences being over 64%. The region of high conservation extends from the centre across most of the C-terminus of the protein, corresponding to positions 60-160 in the consensus represented in Figure 3.16. Two putative bipartite nuclear localization signals (NLS) were found in the non-conserved region, one of these sequences is strongly conserved in all the legume E1 proteins (shown in green letters in Figure 3.16) and the second NLS formed by RRR aminoacids (represented in pink letters in Figure 3.16) is also highly conserved showing and R>K substitution in pea or chickpea sequences, which are still functional NLS motifs.

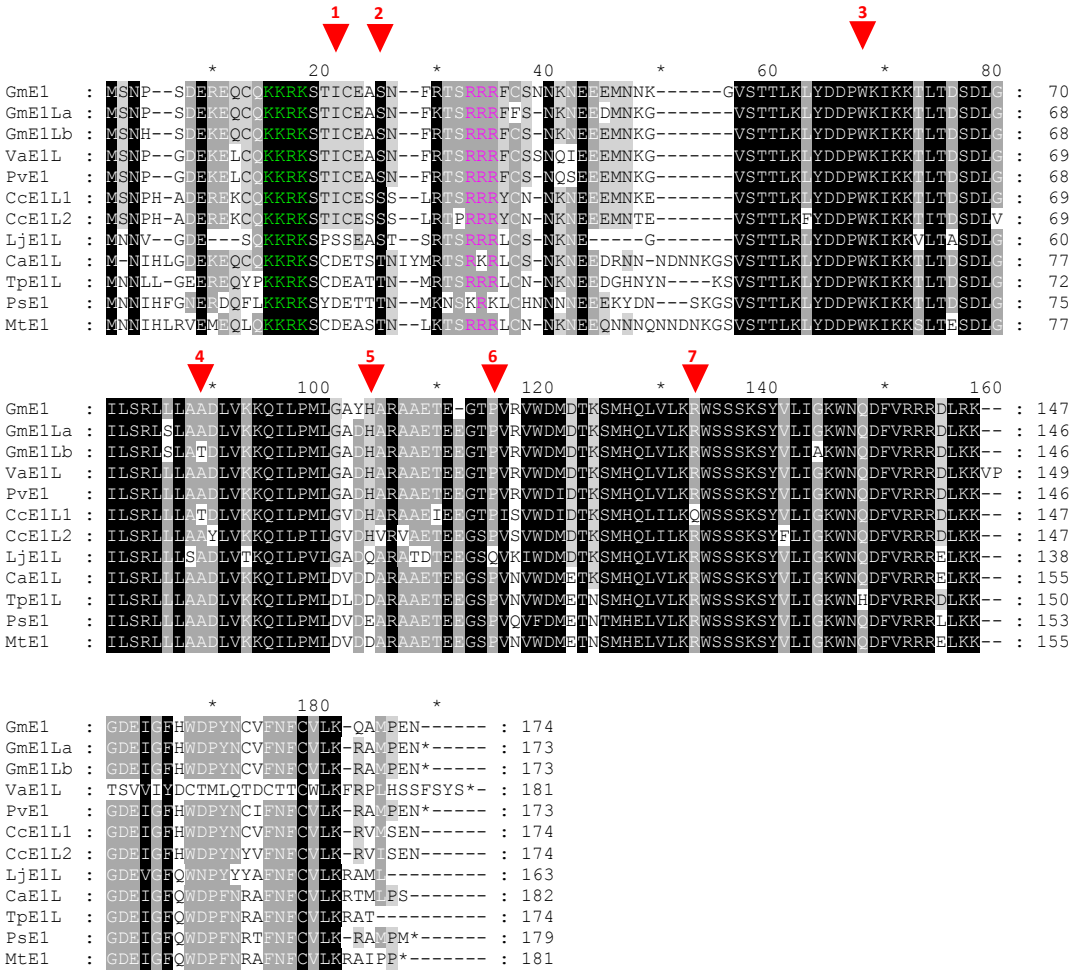

Figure 3.16 Protein sequence alignment of E1 protein of different legume species.

A ClustalX alignment (Thompson et al., 1994) was conducted with full-length predicted protein sequences and adjusted with GeneDoc (Nicholas and Nicholas, 1997). The degree of conservation for the aminoacids are identified with shade degree: black for 100% conserved, dark grey for 80% conserved and light grey for 60% conserved. The abbreviation names followed Table 3.5. Locations are indicated for putative bipartite nuclear localization signals (NLS) identified by (Zhang et al., 2016) with green and pink letters. The numbered red triangles indicate the location of mutations in different pea *e1* alleles.

A phylogenetic tree was conducted including the alignment sequences. The phylogenetic analysis shows a clear distinction between SD and LD legume sequences, and within each group the structure of the tree in general reflects the known phylogenetic relationships among the species included. The SD-legume group includes soybean (GmE1, GmE1La and GmE1Lb), being closely related to red mung bean (VaE1) and common bean (PvE1). This SD group also includes pigeon pea (CcE1L1 and CcE1L2). The other group is clustering the LD legumes finding pea (PsE1) close related to *Medicago* (MtE1). Together, the closest LD legume appears to be red clover (TrE1), followed by chickpea (CaE1L) and *Lotus* (LjE1L) as shown in Figure 3.17.

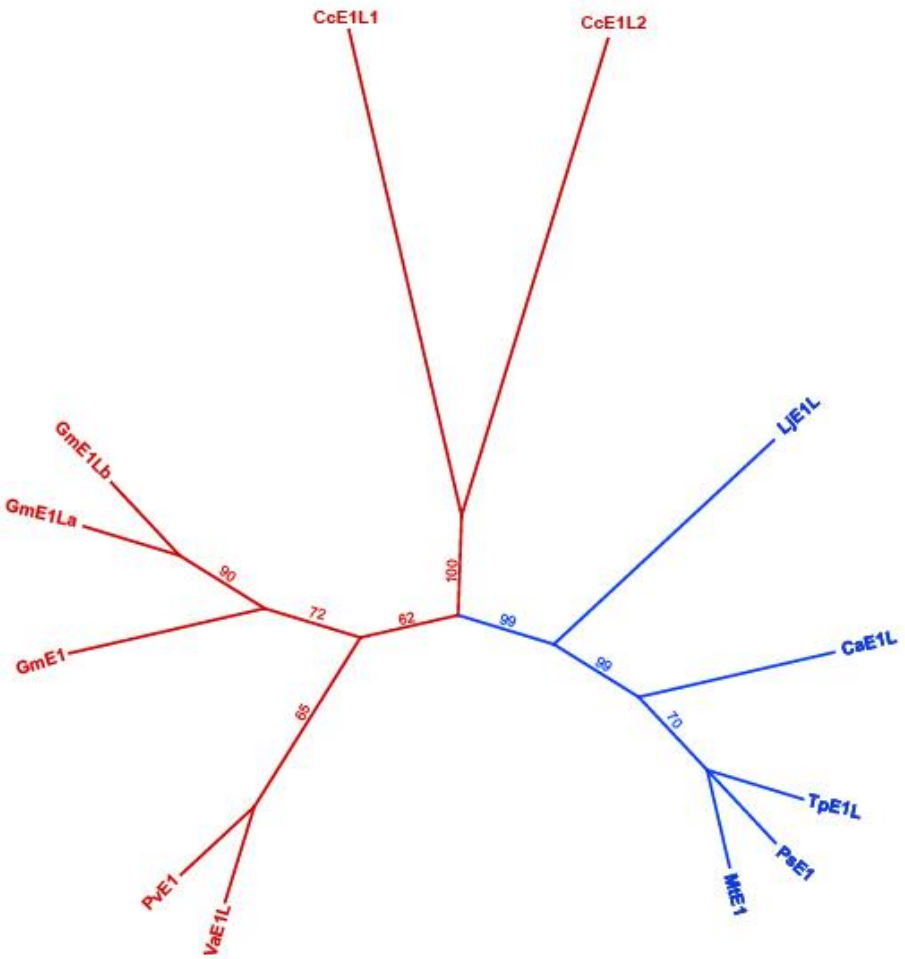

Figure 3.17 Phylogenetic neighbour-joining tree of E1 protein sequences from legumes species.

The phylogram was constructed from full length predicted protein sequences of *E1* genes identified in Table 3.5 and align in Figure 3.16. Species names are indicated in Table 3.5. The phylogenetic tree was performed using a neighbour-joining method and with a bootstrap of 1000. Blue color indicates LD legume groups and red color indicates SD legume species.

The phylogenetic classification suggests that there are differences between the two subclades of legumes, SD and LD legumes, giving enough statistical power to separate the two legume groups. Most of the protein is highly conserved among legumes but there are aminoacid differences, specially at the N-terminal of the sequence like the aminoacid TICE sequence present in SD legumes at position 20 in the alignment (Figure 3.16), which could contribute to differences in protein structure between these two groups. These SD/LD differences are mostly in the less-conserved N-terminal region but there are also some within the conserved region; for example a characteristic G/D substitution at position 101 or a K/N at position 124 (Figure 3.16), which could potentially lead to important functional changes in DNA-binding.

The initial characterization of *GmE1* identified the substantial similarity of its most conserved region to plant-specific B3 DNA binding domains, suggesting that it might act as a transcription factor able to bind promoter region of flowering genes. Further characterization confirmed the ability of E1 to bind to the *GmFTa1* promoter (soybean *FT* homolog) and regulate photoperiodic flowering (Liu et al., 2018; Zhai et al., 2014a). This B3 domain is present in a gene superfamily of transcription factors which are involved in different developmental processes, including some related to flowering control and floral development. For instance, the RAV family in *Arabidopsis* includes the proteins *AtRAV1*, *AtTEM1* and *AtTEM2/RAV2*, which have all been characterised belonging to this B3 superfamily and participating in the regulation of flowering time (Matías-Hernández et al., 2014).

An extensive phylogenetic analysis between legume E1 proteins and the B3 superfamily revealed a large phylogenetic distance and indicated that E1 closest related family seem to be the RAV family, a highly characterised family containing many flowering regulators (Matías-Hernández et al., 2014; Osnato et al., 2012). In *Arabidopsis*, *AtRAV1* is known to be a transcription factor related with flowering regulation and which structure is composed of an AP2/ERF domain, a NLS region followed by the B3 domain (Hu et al., 2004; Matías-Hernández et al., 2014), similar to the known structure of *GmE1*. Therefore, a further study was performed including legume E1 protein family (protein sequence details found in Table 3.5) together with RAV sequences, involving legume species and other characterised RAV proteins like maize (ZmRAV1) and tomato (SlRAV1 and SlRAV2), specified in Table 3.6.

Table 3.6 RAV legume genes orthologs to AtRAV1.

Name	Species	Locus ID	B3 domain family
AtRAV1	*Arabidopsis thaliana*	>AT1G13260	RAV
AtRAV1like	*Arabidopsis thaliana*	>AT3G25730	RAV
AtTEM1	*Arabidopsis thaliana*	>AT1G25560	RAV
AtTEM2/RAV2	*Arabidopsis thaliana*	>AT1G68840	RAV
AtRAV3	*Arabidopsis thaliana*	>AT1G50680	RAV
AtRAV3like	*Arabidopsis thaliana*	>AT1G51120	RAV
PvRAV-like1	*Phaseolus vulgaris*	>Phvul.003G111800.1	RAV
PvRAV-like2	*Phaseolus vulgaris*	>Phvul.007G102800.1	RAV
MtRAV-like1	*Medicago truncatula*	>Medtr5g053920.1	RAV
MtRAV-like2	*Medicago truncatula*	>Medtr1g093600.1	RAV
GmRAV-like1	*Glycine max*	>Glyma.01G087500.1	RAV
GmTEM1-like1	*Glycine max*	>Glyma.02G099500.1	RAV
GmRAV-like3	*Glycine max*	>Glyma.20G186200.1	RAV
GmRAV-like4	*Glycine max*	>Glyma.10G204400.1	RAV
PsRAV-like2	*Pisum sativum*	>PsCam037110_1_AA	RAV
ZmRAV1	*Zea mays*	>NP_001151105.2	RAV
SlRAV1	*Solanum lycopersicum*	>ABY57634.1	RAV
SlRAV2	*Solanum lycopersicum*	>ABY57635.1	RAV

The phylogenetic analysis seen in Figure 3.18 displays a phylogenetic tree constructed with RAV and TEM sequences and E1 sequences. It shows a clear separation between the E1 legume protein group and all the other RAV and TEM sequences, suggesting that E1 does not belong to the RAV legume family. The closest related sequences to the E1 legume group seems to be AtRAV3 and AtRAV3like sequences followed by the maize RAV protein (ZmRAV1) as seen in Figure 3.18. The phylogenetic analysis also describes a clear distinction between the legume orthologs and the other group of characterized RAV genes (*Arabidopsis*, tomato and maize). In this second group, there is a division with a similar phylogenetic pattern as described previously between RAVs and TEMs (Matías-Hernández et al., 2014). Regarding the legume group, soybean (GmTEM1-like1 and

GmRAV-like1) seems to follow the family pattern including a clear differentiation between the two subgroups belonging to RAVs and TEMs. The phylogenetic RAV relationship within legumes seem to be conserved, finding a differentiation between SD and LD legumes and having a duplication in soybean genes. As previously described, this phylogenetic analysis gives support to the presence of a B3 domain in *E1* sequences very distantly related to the B3 domain characterized superfamily which probably does not share functional conservation.

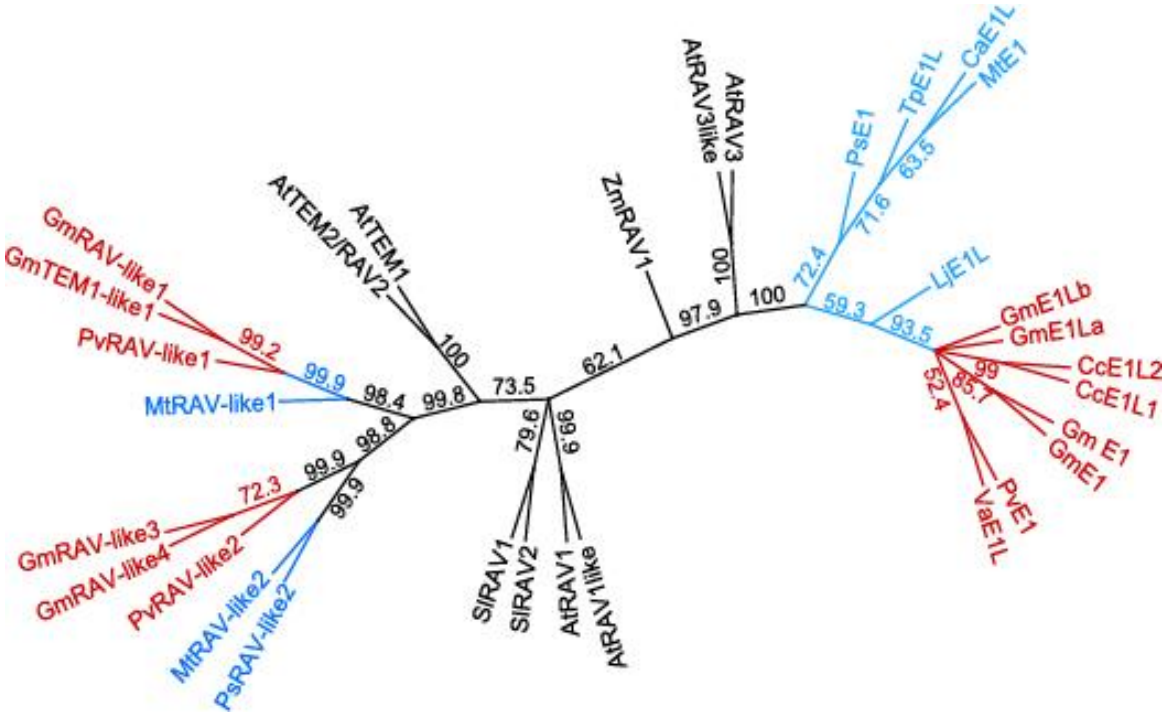

Figure 3.18 Phylogenetic neighbour-joining tree of RAV protein sequences and E1 legume group.

The phylogenetic tree was performed using a neighbour-joining method and with a bootstrap of 1000. The phylogram was constructed from full length predicted protein sequences of E1 genes identified in Table 3.5 and RAV sequences identified in Table 3.6. Species names are indicated in Table 3.5 and Table 3.6. The phylogenetic tree was performed using a neighbour-joining method and with a bootstrap of 1000. Blue color indicates LD legume groups and red color indicates SD legume species.

In order to have a better look at protein structure and possible protein differences between legume E1 in these two legume groups, a 3D protein prediction was conducted for a GmE1 and PvE1 belonging to the SD group and for PsE1 and MtE1 belonging to the LD group using I-TASSER and shown in Figure 3.19.

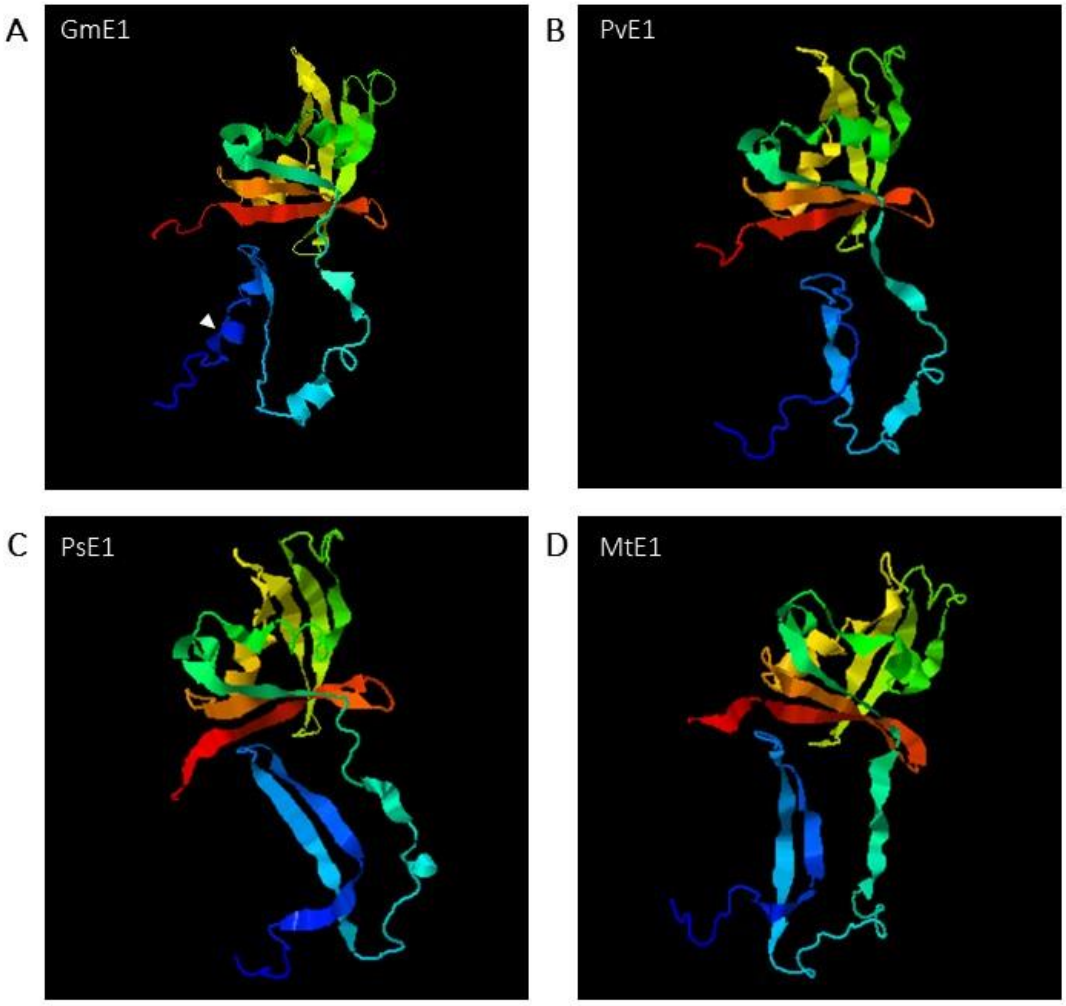

Figure 3.19 Protein structural model prediction for GmE1, PvE1, PsE1 and MtE1.

Protein prediction was performed with I-TASSER that simulates different structural models and predicts the most confident structural protein model based on C-score (C-score is a confidence measurement of the quality of the protein prediction that is in the range of [-5 to 2]. A high C-score implies a high confidence in the prediction). A) GmE1 3D protein simulation with a C-score = -0.63. Approximate position of the conserved NLS marked by white triangle. B) PvE1 3D protein simulation with a C-score =-0.52 C) PsE1 3D protein simulation with C-score = -0.10. D) MtE1 3D protein simulation with a C-score=-0.39.

In the protein structure prediction, there are some clear distinctions to consider. GmE1 protein prediction estimates a helix-turn-helix structure for the N-terminal (aqua and blue region in Figure 3.19 A) and a B-fold structure for the C-terminal region (red-orange-yellow region in Figure 3.19 A). The most significative difference is in the blue region, the helix-turn-helix structure in GmE1 (Figure 3.19 A) that is completely lost in the other legume predictions. In the case of PvE1 (Figure 3.19 B), the fold in this blue coloured region is preserved but the helix structure is lost, and it is

totally missing for both PsE1 and MtE1 (Figure 3.19 C and D). This region corresponds with the poorly conserved region in the alignment (Figure 3.16) and contains the NLS marked in Figure 3.19 A with a white triangle. The C-terminal region of the polypeptide sequence seems to be more similar between the polypeptide predictions (Green, yellow, orange and red region in Figure 3.19) corresponding with the highly conserved region in the alignment (Figure 3.16). The folds and turns in this region are more conserved but the end part (red colour region) which corresponds with the final- not so well conserved- aminoacid sequence differs between predictions. In the SD group, including GmE1 and PvE1, the B-fold structure is mostly conserved (Figure 3.19 A and B) but it is lacking in the LD legumes PsE1 and MtE1 (Figure 3.19 C and D). These variations in the predicted structure together with a clear distinction on the phylogeny between SD and LD legumes suggest that the E1 polypeptide structure, and probably function, is not fully conserved between legumes, requiring a deep analysis of the action and role of E1 in a LD legume model as pea or *Medicago* to fully characterised E1 role in the legume family.

3.4 Discussion

The molecular characterization of the soybean *E1* gene has defined a legume-specific protein that participates as a key repressor of flowering and maturity, and that regulates *GmFT4, GmFT2a* and *GmFT5a* (*FT* homologs) and is under photoperiodic control by phytochromes (E3 and E4 in soybean) (Xia et al., 2012; Zhai et al., 2014a). These studies have revealed an alternative mechanism of flowering regulation in a legume model, in which a legume-specific regulator may replace the prominent role for *CO-like* genes seen in *Arabidopsis* (Zhai et al., 2014a; Zhang et al., 2016). Moreover, *E1* allelic variation has been described as a decisive factor determining soybean adaptation to diverse latitudes and photoperiods, including the biggest effect on flowering time determination in field conditions (Miladinović et al., 2018; Xia et al., 2012; Zhai et al., 2014b). Given the importance of *E1* in soybean regulatory photoperiodic-flowering pathway, the understanding of its role and participation in other legume systems is highly valuable.

More recent studies have given some indication of possible roles for *E1* in flowering time regulation in other legume species, including preliminary examination of the function of *E1* genes from common bean and *Medicago* (Zhang et al., 2016). The characterization of *e1* mutants in pea was anticipated to provide an important additional test of this possibility, whether *PsE1* has a similar function to soybean *E1* delaying flowering under non-inductive conditions (early-flowering in SD for pea) or having an effect in the same photoperiod conditions (LD) but promoting flowering in pea (opposite to soybean: inhibiting LD flowering). There were some suggestions of the promoting possibility since *MtE1-like* is described as promoting flowering in LD+V (Zhang et al., 2016). Additionally, the pea genetic network is simpler and less redundant than soybean, with a unique *PsE1* homolog instead of three functional *E1* in soybean, making the study of *PsE1* flowering role more straightforward trough reverse genetics.

3.4.1 Effect of *E1* on pea development and flowering

Among a number of different mutant alleles (Figure 3.1) this characterization was mainly performed using the allele *e1-3,* a premature stop codon mutant expected to be the strongest mutant allele and likely to provide a definitive loss-of-function. However, the initial study of vegetative growth and reproductive traits in both LD and SD photoperiods suggested a minimal, if any, flowering regulatory role of *E1* in this long-day legume. Although there was no statistical support for any differences in NFI, RN, DTF or FLR for any LD/SD comparison in the *e1-3* mutant (Figure 3.2), it was observed that across the analysis there was a slight trend toward lateness in

the *e1-3* mutant (Figure 3.2), more specifically in LD (Figure 3.4). Examination of a second mutant allele, *e1-4,* which contained a substitution in the conserved region of the protein (Figure 3.1), indicated at most an even more subtle effect on NFI or RN (Figure 3.3), further supporting the conclusion that *E1* has at most a very minor effect in flowering regulation in pea.

These unexpected observations were further explored in segregating F_3 families (Figure 3.4) which allowed both a validation of the initial comparison, and the opportunity for addition control on any additional effect of background genetic variation. However, NFI and RN trait values in mutant segregants again did not differ statistically from WT, strengthening the conclusion that *E1* has little if any role as a flowering regulator in pea. Measurements of leaf expansion and vegetative development also detected no significant differences between genotypes (Figure 3.5).

In view of preliminary results from *Medicago*, where *E1* may act as a relatively weak flowering activator in LD (Zhang et al., 2016), and the slight trend towards lateness in the pea *e1-3* mutant, a further detailed examination of potential flowering phenotypes under different light conditions was conducted. The specific aim was to test whether a subtle flowering phenotype in *e1-3* under natural light could be accentuated by manipulating the light quality of the photoperiod extension (Figure 3.6). Under natural LD conditions, *e1-3* again displayed a minimal effect on flowering time, both in node and date, consistent with Figure 3.2. Similarly, under both LDI and LDF conditions the *e1* mutant showed a slight trend toward lateness more noticeable in NFI or RN than DTF, but again did not reach the threshold of statistical significance. Under continuous cool-white fluorescent light (CF) for 24h the mutant also displayed a slight lateness trend without statistical implication. Overall, however, both the *E1* and *e1* near-isogenic lines were very similar to the pure NGB5839 *E1* control genotype under LD. There is therefore no evidence that *E1* contributes significantly to the LD promotion of flowering typical of the NGB5839 reference line.

In contrast, under SD conditions in both experiments, the mutant showed a small but significant delay in flowering node relative to the WT. The consistent results obtained in three different LD and two different SD experiments indicate that *E1* may participate weakly in promotion of flowering under SD, but not substantially under LD. Thus at least in the NGB5839 genetic background, *E1* does not appear to be acting as a LD-specific promoter of flowering in the way initially imagined.

Another insight from comparison of the results from different conditions and repeated experiments is that date of flowering (DTF) is a more consistent flowering trait to use when comparing different generations, seasons, or genetic backgrounds than flowering node (NFI), which seems to have more plasticity, an unexpected observation affecting this mutant. This contrasts with many other observations and also with the results in Chapter 4 in which the *lip1* mutant is shown to affect developmental rate and therefore the relation between NFI and DTF, making NFI a more robust indicator of flowering.

3.4.2 Participation of *PHYA* in *E1* regulation

The important role of *E1* in soybean flowering control is also evident in the regulation of its expression. *GmE1* is expressed specifically in leaf tissue and at a very low but detectable level in LD and displays a bimodal pattern with two peaks of expression at ZT4 and ZT16 but is not detectable in SD (Xia et al., 2012). In pea, *E1* expression also seems to be low and following soybean pattern, the highest level of expressions was localised in leaf tissue (Figure 3.7). In soybean, *E1* expression is repressed by a PHYA signalling pathway under SD and this is a key interaction determining SD-specific *GmFT expression* and flowering induction (Thakare et al., 2011; Xia et al., 2012; Zhai et al., 2014a). In pea, PHYA is also an essential component for LD-inductive flowering and also participated in seedling deetiolation (Weller et al., 2004). Therefore, it is an important photoreceptor for this system, able to regulate flowering induction trough the regulation of *FT* genes expression (Hecht et al., 2007; Weller and Ortega, 2015). We found no significant effect of *phyA* mutations on *E1* expression, although the very low expression levels again introduce some uncertainty (Figure 3.8) and the trend indicated a possibly reduced level in the *phyA-1* loss-of function mutant and an increase in the *phyA-3D* gain-of-function mutant. These results, if confirmed, would be consistent with soybean and *Medicago* models in placing *E1* downstream of *PHYA*, but might also suggest that this interaction is less significant in pea than in these other species. Further research and verification are needed to fully describe the role of *E1* in pea, especially after being characterised in a domesticated NGB5839 genetic background carrying important mutation like in *HR/ELF3a* gene and therefore having a limited photoperiod response and with a not fully introgressed mutant.

3.4.3 High conservation of E1 in legumes with NLS variation

In addition to understanding how this entire sub-clade evolved, an understanding of the history of the legume E1 family may also be highly valuable, as it could potentially hold an important key to understanding the diversity of flowering responses. Whereas *E1* soybean, a SD legume model, acting as a repressor of flowering in LD conditions (Xia et al., 2012; Zhai et al., 2014a), but unexpectedly in pea, a LD legume system, it does not seem to participate in the photoperiod response pathway; it is not acting as a repressor in SD nor an activator in LD conditions. The highest conservation level in E1 protein sequences from different SD and LD legumes (Figure 3.16) suggested that the proteins will be broadly similar in their structure-function relationships. Firstly, at the amino acid sequence level with high degree of conservation among legumes sharing over 64% identity specifically in the C-terminal region and the two highly conserved N-terminal NLS domains (Figure 3.16). With respect to their tertiary structure, the structural prediction of E1 protein conformation revealed similar conformations between SD legume species (soybean-GmE1 and bean-PvE1) and LD legume species (pea -PsE1 and *Medicago* -MtE1) (Figure 3.19). The tertiary structure prediction also illustrates some substantial differences between the legume E1 conformations. For instance, in the N-terminal region, a helix-turn-helix is formed in soybean (Figure 3.19 A) but is lacking in the other protein predictions, and considering this is the region that contains the NLS, it is possible that such differences could affect *E1* functionality.

E1 is reported to belong to the superfamily of B3 domain proteins, which contain DNA binding motifs and capability of acting as transcription factors (Xia et al., 2012), however, most characterization has focused only on soybean. The B3 superfamily phylogenetic analysis performed in this study (Figure 3.18) highlights the novelty and specificity of E1 as a legume component. Legume E1 protein sequences share minimal sequence similarity with other members of the B3 superfamily, being closest related (but still distant) to AtRAV3, belonging to the RAV/TEM family with functions related to flowering regulation by transcriptional repression due to their multiple DNA binding domains and targets (Causier et al., 2012; Matías-Hernández et al., 2014).

Taken together, the protein and phylogenetic analysis supports high conservation in E1 legume proteins with differences between legume groups, leading to a distinction among SD and LD E1 sequences following the legume phylogeny (Figure 3.17) previously reported by Zhang et al., 2016. The similarities in sequence and protein conformation within legume group (SDP similarities vs. LDP) supports that there could be differences on functionality and *E1* role could differ in LD legumes and not remain as a repressor of flowering.

3.4.4 Potential role of *E1* in *Medicago*

As the closest "model" legume to pea, the comparison with *Medicago* is also of great interest, particularly as recent research has suggested *MtE1* as an activator of flowering in LD (Zhang et al., 2016), which contrasts with the repressive role of the soybean genes. These authors observed a moderately delayed flowering time in *Mte1* mutants in comparison to the WT (Zhang et al., 2016). This mild *MtE1* flowering effect was supported in a second report published during the preparation of this thesis (Jaudal et al., 2020). However, in the present study, the same mutant lines exhibited essentially no clear phenotype (Figure 3.12), and flowered in a manner very similar to WT lines in vernalized LD conditions, differing from the previous observations (Zhang et al., 2016). This was also confirmed in segregating progenies (Figure 3.15) and it was also confirmed that that *E1* expression was lacking, as expected, in the mutant line (Figure 3.10). To provide a context for comparison, the analysis of *Medicago e1* mutant lines was complemented with a *MtPHYA* mutant line (Figure 3.13)(Figure 3.14) which in contrast developed a clear late flowering phenotype in LD conditions under both vernalization treatments. This shows that the lack of a clear phenotype of the *Mte1* mutant does not merely reflect the nature of the growth conditions. It also indicates that *E1* is not essential, or even particularly important, for the promotion of flowering by *MtPHYA*. The comparisons made of other phenotypic traits related to plant architecture support previous observations by Laurie et al., (2011) that vernalization results in accelerated flowering and a narrower flowering window, and also a reduction in leaf biomass, increased elongation of the primary shoot and the initiation of fewer branches (Figure 3.11).

3.4.5 Conclusions and future directions

E1 in both *Medicago* and pea has a minimal effect in flowering suggesting that its role is not as important in LDP flowering regulation as in soybean. Remarkably, soybean has three *E1* homologs with functional redundancy and the loss of function of just one of them has a big impact in flowering, inducing early flowering in LD (Xia et al., 2012; Xu et al., 2015b), contrary to the loss of function of non-redundant *E1* in any LDP, where the effect, if any, is a mild lateness in LD flowering for *Medicago*. The absence of *Mte1* flowering phenotype observed in this study could be explained by the photoperiod conditions used since the reported phenotype was studied in cool-white fluorescent light (Jaudal et al., 2020) instead of LED light with some Far-Red content, as used in this thesis. The spectral quality of light is well known to be important in both LDP and SDP (Song et al., 2018). Different photoperiod conditions to fully explore the *MtE1* flowering response are of potential interest to further characterise its role, but, in the case of pea, diverse photoperiod

conditions were explored without giving any evidence of a flowering phenotype, suggesting that the *E1* role in LDP is much less than might be expected from its central role in soybean. Diverse light conditions should be included for *Medicago* characterization together with an extension in pea description including more than just one mutant allele and analysing a fully introgressed mutant.

In future, it will also be of interest to investigate *E1* function in diverse legumes including more species from SDP and LDP, either using mutant alleles or, where possible, transformation. This will help to further test the current model with differential action of *E1* in SDP and LDP: floral repressor in LD for SDP and a floral promoter in LD for LDP (Jaudal et al., 2020; Zhang et al., 2016). It is also possible that reciprocal analyses of SDP *E1* in LDP and vice versa may be informative, as well as characterizing the binding of different E1 proteins to diverse *FT* promoter sequences from both LDP and SDP. However, without such further verification, current results collectively support a conserved regulatory pathway upstream of *E1* among legume species (i.e. PHYA is conserved as a regulator of *E1* under LD conditions), with a specification of action downstream at *E1* level (*E1* acting as repressor of promoter of flowering in different systems)(Jaudal et al., 2020; Xu et al., 2015b; Zhang et al., 2016). Therefore, further investigation is required to unravel the molecular mechanism downstream of *E1* in order to know its target genes, its role in the genetic pathway and supplementary roles in legume vegetative and reproductive development.

Chapter 4 - Examining the potential roles and interactions of the LIP1/COP1 ubiquitin ligase in pea flowering

4.1 Introduction

4.1.1 Characterization and fundamental nature of *COP1*

The *CONSTITUTIVE PHOTOMORPHOGENIC 1* (*COP1*) gene was initially identified in *Arabidopsis* for its key role as a repressor of seedling photomorphogenesis (Deng et al., 1991; Wei and Deng, 1996), with several *cop1* mutant alleles showing a light-grown seedling phenotype in darkness, that included short hypocotyls, expanded and open leaves and anthocyanin accumulation. This phenotype was accompanied by the constitutive expression of many light-regulated genes, and overall indicated a broad role for *COP1* in regulation of responses to light.

Interestingly, some mutant alleles also showed an early-flowering phenotype described in the weak *cop1* mutant alleles, *cop1-4* and *cop1-6,* while other alleles seem to be adult lethal when homozygous (McNellis et al., 1994). The study of the flowering phenotype suggested an involvement in photoperiodic regulation of many plant responses like control of flowering time, primarily in the inhibition of flowering under non-inductive short day (SD) conditions (Jang et al., 2008; McNellis et al., 1994). Subsequent research investigated the role of *COP1* in more detail, focusing particularly on the link between how light and photoreceptor signalling regulated the expression of the flowering gene *CONSTANS* (*CO*) at the transcriptional and protein stability level (Valverde et al., 2004). Demonstration of the role of *COP1* in proteasome-dependent degradation of CO, and the *CO*-dependent early-flowering phenotype of *cop1* mutants confirmed the characterization of *COP1* as a key regulator of CO protein stability (Jang et al., 2008).

In addition to its role in photomorphogenesis (Deng et al., 1991; Lau and Deng, 2012) and photoperiodic flowering (Jang et al., 2008; Liu et al., 2008), further physiological and molecular studies also revealed roles for *COP1* in a diverse range of light responses including germination (Yu et al., 2016), organ development (Kang et al., 2009; Mao et al., 2005), response to low temperature stress (Catalá et al., 2011), shade avoidance (Crocco et al., 2010; McNellis et al., 1994), and circadian rhythm (Yu et al., 2008) among others (Huang et al., 2014; Lau and Deng, 2012; McNellis et al., 1994). Its molecular identity as a E3 ubiquitin ligase indicates an important

function controlling proteolysis in light signalling pathways regulating these diverse processes (Huang et al., 2014; Ordoñez-Herrera et al., 2015; Xu et al., 2016).

Although very conserved in plants, *COP1* orthologs are also present in animals, where they seem to participate in the control of cell cycle by protein regulation mechanisms. Animal *COP1* is reported to affect the progression of certain cancers, suppressing tumours in certain cases (Migliorini et al., 2011) while promoting them in others (Choi et al., 2015; Dornan et al., 2004). As in plants, the role of animal *COP1* is connected with its participation in multimeric ubiquitin ligase regulatory complexes (Yi and Deng, 2005), with the c-Jun oncoprotein. Other studies have explored the regulation of p53 (tumour suppressor gene in mammals) through COP1 (Dornan et al., 2004).

The important role in cellular processes in both animals and plants reflects the critical part this regulatory protein exercises in the cell, with COP1 participating in numerous protein complexes primarily acting to regulate stability of other protein (Huang et al., 2014). Focussing on plants, the nature of COP1 complexes is relatively well-characterised with known specific roles in diverse multimeric complex participating in photomorphogenesis, flowering and/or UV-B response (Hoecker, 2017; Lau and Deng, 2012; Yin and Ulm, 2017).

4.1.2 Molecular identity and associations

Arabidopsis COP1 is a single copy gene composed of 13 exons that encodes a E3 ubiquitin ligase, an enzyme that attaches ubiquitin molecules to proteins and tags them for degradation. The COP1 protein has multiple targets, many of which are transcription factors, and imparts light-dependent regulation of the stability of these proteins. Ubiquitin ligase complexes are typically multimeric, with various components contributing target specificity, and COP1 commonly associates with SPA (SUPPRESSOR OF PHYA-105) proteins to regulate the stability of diverse photomorphogenesis-transcriptional factors (Podolec and Ulm, 2018). The SPA family in *Arabidopsis* includes four members (SPA1-4) which have some functional redundancy and are able to interact with COP1 under specific light conditions (Hoecker et al., 1998; Laubinger et al., 2004). The structure of SPA proteins is quite similar to COP1, including central coiled-coil and C-terminal WD40 repeat domains, but featuring a protein kinase domain instead of the ubiquitin ligase domain in the N-terminal region (Hoecker and Quail, 2001). The COP1-SPA complex is tetrameric, comprising two COP1 (homodimer) and two SPA proteins, forming a complex with ubiquitin ligase activity, regulated by light and participating in photomorphogenesis and flowering time regulation (Uljon

et al., 2016; Xu et al., 2016). The SPA proteins are the primary partners of COP1 (Hoecker, 2017; Ordoñez-Herrera et al., 2015), and the role of COP1 role *in planta* is dependent on its interaction with SPAs (Podolec and Ulm, 2018). Like COP1, SPA protein contribution to the active multimeric complex is regulated by light and the different light-dependent mechanisms of COP1-SPA regulation include different subcellular localization of SPAs and COP1, leading to an indirect regulation without COP1 degradation (Balcerowicz et al., 2017; Podolec and Ulm, 2018). COP1 subcellular localization is light-dependent and central to its light-dependent function. In darkness, active COP1 protein accumulates in the nucleus, and forms a functional COP1-SPA complex, whereas in light, COP1 remains in the cytoplasm and is unavailable for complex formation (Podolec and Ulm, 2018; Wang et al., 2019a). This subcellular localization is a key regulatory mechanism in COP1 but not present in SPA proteins which are constitutively localized in the nucleus (Balcerowicz et al., 2017; Laubinger et al., 2004).

4.1.3 Regulation by light

COP1 is a central component in the photoregulation of many different developmental processes and is involved in signalling from several different photoreceptors (Galvão and Fankhauser, 2015) including phytochromes, cryptochromes and the UV-A/B photoreceptor *UV RESISTANCE LOCUS 8* (*UVR8*) (Lau and Deng, 2012; Podolec and Ulm, 2018). These photoreceptors contribute to the regulation of COP1 activity across a wide spectral range and do so via several distinct molecular mechanisms as seen in Figure 4.1.

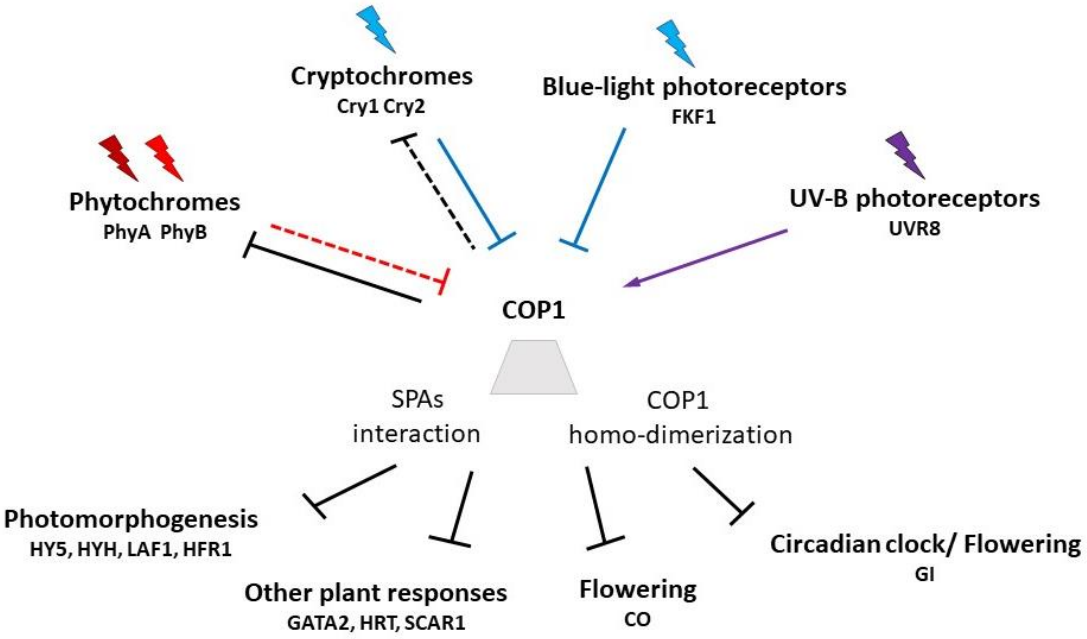

Figure 4.1 COP1 signaling pathway.

COP1 integrates light-regulation from various photoreceptors and transfers the signalling through different changes in protein interaction finally targeting for degradation diverse proteins. Different colours represent the different light spectra that the photoreceptors absorb: Far-Red light (burgundy color), Red light (Red color), Blue light (Blue color), UV-B light (Purple color). Arrow indicates induction and flat lines indicate repression. Solid line indicates physical and direct interaction.

Photoactivation of phytochromes by absorption of red or far-red light results in their movement from the cytoplasm to the nucleus and enables interaction with other nuclear proteins, including COP1 (Kim et al., 2017). This light-mediated protein interaction of phytochrome with COP1 sequesters it away from its primary role in proteolytic protein complexes (like COP1-SPA complex) and thereby inhibits their activity, resulting in a repression of COP1-dependent proteolysis activity under light (Lu et al., 2015; Podolec and Ulm, 2018). In the case of cryptochromes, the blue light photoreceptors in plants known to be able to regulate COP1 activity through the protein-protein interaction with SPA proteins that is able to dismantle COP1-SPA complexes in a similar way to phytochromes (Liu et al., 2011; Zuo et al., 2011). A coaction between phytochromes and cryptochromes in regulation COP1 activity has also been observed, and is suggested to reflect the phytochrome regulation of BICs (BLUE-LIGHT INHIBITORS OF CRYPTOCHROME 1) which are direct regulators of cryptochrome activity (Wang et al., 2018).

More recently, UV-B regulation of COP1 activity was shown to result from a direct interaction between the activated forms of UVR8 and COP1 proteins (Galvão and Fankhauser, 2015; Yin and Ulm, 2017). For two further classes of photoreceptors, phototropin proteins (blue light photoreceptor) and LOV-Kelch domain proteins (UV-A photoreceptor), the evidence of interactions with COP1 seems less clear. Recent literature indicates that the FLOWERING KELCH FACTOR 1 (FKF1) protein, is able to interact with COP1 directly and interfere in the formation of COP1-SPA complex in a light-dependent manner (Lee et al., 2017, 2019), similar to other photoreceptors. Interestingly, FKF1-family proteins also possess an E3-ubiquitin ligase activity, but it is not clear how this relates to the similar property of COP1, and whether it is significant for their interaction (Ito et al., 2012a; Podolec and Ulm, 2018).

4.1.4 Protein structure and interactions

COP1 is a single-copy gene in most plant species, and the COP1 protein structure is highly conserved with three major domains understood to participate in aspects of its function (Figure 4.2). The first is an N-terminal RING finger domain that is the site for recruitment of conjugative enzymes like E2 ubiquitin ligases when forming the larger ubiquitin ligase complex (Huang et al., 2014; Yi and Deng, 2005). The central coiled-coil domain recruits other regulatory subunits needed for protein complex formation and is the site for the light-dependent binding to SPA proteins (Zhu et al., 2008). Lastly, the C-terminal WD40 repeat domain determines the interaction with different substrates, most of which appear to be transcription factors (Lau et al., 2019). This domain is also the region that supports the physical interaction with the majority of the photoreceptors, including phytochromes, cryptochromes, and UVR8 (Hoecker, 2017; Ordoñez-Herrera et al., 2015; Uljon et al., 2016). In contrast, the LOV-domain photoreceptor FKF1 was recently reported to interact with COP1 via the RING finger domain, blocking COP1 homodimerization in a light-dependent manner (Lee et al., 2017)(Figure 4.2).

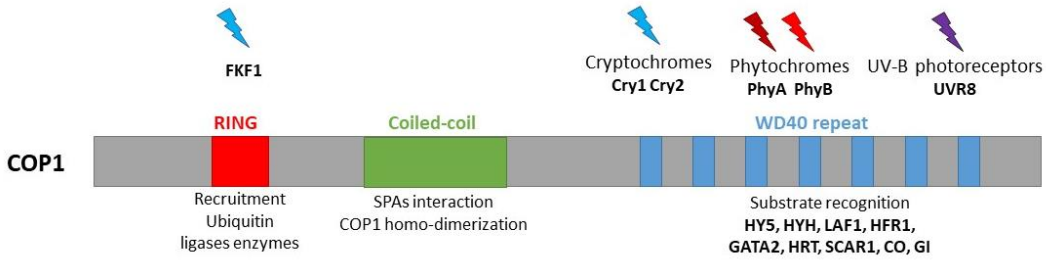

Figure 4.2 COP1 protein domains and interactors.

COP1 protein contains three main domains: RING finger domain (red), a Coiled-coil domain (green) and a WD40 repeat domain (blue). The RING finger domain is characterised as the recruitment site for other conjugative enzymes of the ubiquitin ligase complex. Recently, it was characterised as the interactive domain between FKF1 and COP1, affecting COP1 protein complex formation. The coiled-coil domain participates in protein interaction helping with the formation of multimeric protein complexes, like SPA-COP1 complex or homo-dimer COP1 interaction. The WD40 repeat domain is characterised as the interactive region between COP1 and different targets. Also, most of the photoreceptors are described interacting in the WD40 domain.

As mentioned above, COP1 is known to interact with multiple factors and substrates through its WD40 repeat domain and targets its substrates for degradation via its E3 ubiquitin ligase activity. Known COP1 target proteins participate in a range of diverse light-mediated responses. One of the first identified and best characterised targets in *Arabidopsis* is HY5 (ELONGATED HYPOCOTYL 5), a bZIP transcription factor that is able to directly bind to the promoter region of genes leading to an induction of photomorphogenesis. COP1 interacts directly with the HY5 protein to accelerate its degradation and thereby reduce its activity (Osterlund et al., 2000). Many other similar transcription factors have subsequently been characterised as substrates of COP1, including another bZIP factor named HYH (HY5 HOMOLOG) (Holm et al., 2002), another transcription factor from the myb family, LAF1 (LONG AFTER FAR-RED LIGHT 1) (Soo Seo et al., 2003), and a bHLH transcription factor identified as HFR1 (LONG HYPOCOTYL IN FAR RED 1) (Yang et al., 2005) among others. Other COP1 targets include GATA2, involved in with light-mediated brassinosteroid pathways (Luo et al., 2010; Wang et al., 2019b), HRT (HYPERSENSITIVE RESPONSE TO TCV) which has roles in plant defence (Jeong et al., 2010), and SCAR1, which participates in root development pathways (Dyachok et al., 2011).

Several prominent proteins in circadian clock and photoperiod response networks are also regulated in part through COP1 also has a prominent role in protein-level regulation of components in *Arabidopsis* circadian rhythm and/or flowering networks, including CO, ELF3 and GI (See 4.1.5 section) (Jang et al., 2008; Liu et al., 2008; Yu et al., 2008). The influence of COP1 also

extends to the regulation of photoreceptors including the blue-light receptor FKF1 (Lee et al., 2019) and phytochromes PHYA and PHYB, which are known to directly interact with COP1 and may act as regulators and/or as targets (Jang et al., 2010; Seo et al., 2004).

COP1 and SPA proteins interact through their coiled-coil domains forming homo- and hetero-dimers and such complexes are considered to be the active form in many biological responses, such as hormone signalling through the regulation of HFR1 (Wang et al., 2019a), photomorphogenesis through the regulation of HY5 (Yu et al., 2013) and photoperiodic flowering through the regulation of CO (Hoecker, 2017; Xu et al., 2016).

Recently, different substrates of COP1 have been suggested to share a common VP (Val-Pro) motif for binding of the COP1 WD40 domain, and to compete for interaction depending on the specific binding affinity of this motif. This has led to the concept of a conserved mechanism in which competition for COP1 binding is regulated by light-mediated binding affinity of potential target proteins. Considering that some of these competitor substrates are photoreceptors capable of inactivating COP1, such an interaction therefore establishes an autoregulatory light-dependent feedback loop (Lau et al., 2019; Wang et al., 2019a).

4.1.5 *COP1* role in flowering

4.1.5.1 COP1 flowering role in Arabidopsis

In addition to the role of *COP1* in photomorphogenesis, its role in flowering time regulation has also been extensively studied in *Arabidopsis* (Lau and Deng, 2012). This role was first reported in a study by McNellis et al., (1994) who observed that the weak *cop1-6* mutant allele was able to achieve reproduction in complete darkness, suggesting a *COP1* role in light-regulated flowering control. Further allele characterization in different photoperiods revealed that *cop1-1*, *cop1-4,* and *cop1-6* flowered in SD as if growing in LD conditions, indicating a specific role in the response to photoperiod (McNellis et al., 1994).

As discussed in Chapter 1, activation of the *Arabidopsis FT (FLOWERING LOCUS T)* gene is a key step in flowering induction, and this occurs under LD mainly through the action of the *CONSTANS (CO)* gene, which is tightly regulated by the circadian clock at a transcriptional level and by light at both the transcriptional and the protein level (Fornara et al., 2010). *COP1* has been shown to contribute to direct and indirect regulation of *CO*, by regulating the protein stability of CO itself and several of its upstream regulators (Jang et al., 2008). *COP1* participation in *Arabidopsis* flowering is represented in Figure 4.3 showing that daily patterns of CO protein expression are

partly conferred by COP1-SPA dependent degradation of CO protein at night, and the relief of this degradation during the day to allow CO accumulation when light suppresses COP1 activity (Jang et al., 2008). COP1 is also known to regulate protein stability of GIGANTEA (GI), a protein participating in the circadian clock function and has a positive effect on *CO* transcription (Jang et al., 2015). This GI-COP1 protein interaction is mediated by another circadian clock factor, ELF3 (EARLY FLOWERING 3), which acts as a substrate adaptor, helping COP1 to regulate GI protein. *ELF3* was firstly characterised as one of the three components of the so-called Evening Complex (EC) of the *Arabidopsis* circadian clock, together with *EARLY FLOWERING 4 (ELF4)* and *LUX ARRYTHMO* (*LUX*) which regulate expression patterns of clock genes (Hicks et al., 2001; Huang et al., 2016; Nimmo et al., 2020). ELF3 can form protein complexes with other components, like GI and COP1 and is considered to be an important linking point between circadian clock and photoperiod control of flowering (Huang et al., 2016; Yu et al., 2008). Therefore, *COP1* participates in a direct protein level regulation and also, controls an indirect transcriptional level when its role results in a variation of *CO* transcription (Jang et al., 2015; Yu et al., 2008).

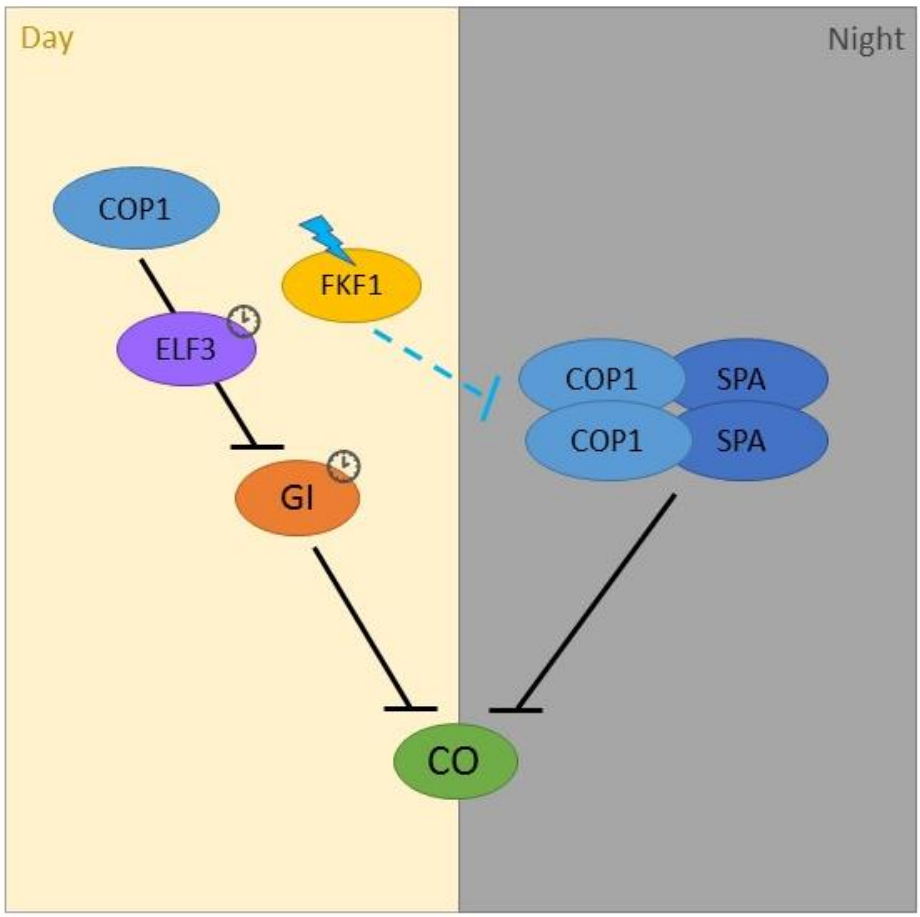

Figure 4.3 COP1 participation in *Arabidopsis* flowering regulation.

Diagrammatic representation of COP1 protein interactions and its function as a regulator in *Arabidopsis* flowering pathway. COP1 is represented in light blue, able to interact with SPA proteins (dark blue) in a tetrameric complex and regulate CO protein (green) during the night (represented as grey background). Light conditions (represented as yellow background) facilitate the blue light dependent regulation of COP1 homodimerization by FKF1 (yellow). The COP1-dependent regulation of GI (orange) mediated by ELF3 (purple) also controls CO protein levels under photoperiod and circadian clock (represented by a grey clock) control. Flat solid arrows indicate direct repression and dash lines indicate impairment of homo-dimerization.

Arabidopsis elf3 mutants were first reported to develop long hypocotyls and being early flowering regardless of daylength, suggesting that *ELF3* might have a role in light signalling to the clock that is manifested in both flowering and photomorphogenic responses (Hicks et al., 2001). *ELF3* was characterised as participating in flowering regulation through the control of *CO* expression in *Arabidopsis* (Suárez-López et al., 2001). Later research also proposed a participation in flowering regulation through a *CO*-independent pathway (Kim et al., 2005; Yu et al., 2008). The characterization of its function and effects revealed its ability to interact with many other photoperiod related proteins like PHYB and COP1 (Huang et al., 2016). Despite this evidence, ELF3

protein interaction with PHYB was shown to be important in the control of photomorphogenesis, but not for the regulation of flowering time (Xing et al., 2001). *ELF3* is believed to control flowering through the regulation of the GIGANTEA protein-level, by working as an adaptor facilitating the interaction of other proteins like COP1. ELF3 promotes the formation of nuclear bodies (NBs) in darkness, in which it mediates the interaction between COP1 and GI to facilitate GI protein degradation (Mishra and Panigrahi, 2015; Yu et al., 2008). Other evidence suggests that transcriptional repression by the EC (including *ELF3*) is the basis for a direct temperature-dependent regulation of *GI* (Mizuno et al., 2014). Circadian clock and flowering genes form an extremely connected network, and these three important components present a high level of interconnection in many layers, with a well-characterised effect in CO protein after the regulation of GI protein trough the ELF3 mediated GI-COP1 interaction.

These two mechanisms of flowering regulation have been extended with the discovery of another important factor in the flowering network, FKF1 which is a novel interactor of COP1 also represented in Figure 4.3 (Lee et al., 2017). FKF1 is a blue-light photoreceptor and co-operates with GI in a transcriptional complex to repress the expression of members of the CYCLING DOF FACTOR (CDF) protein family, which are in turn transcriptional repressors of *CO.* It is now known that FKF1 also acts as a regulator of COP1 activity, and when activated by light, interferes with COP1 homodimerization. This results in a reduction in COP1-dependent degradation of CO in LD leading to a photoperiodic flowering regulation in *Arabidopsis* (Lee et al., 2017, 2019). All of these protein interactions with COP1 suggested an interconnected network which strongly regulates flowering induction in relation with light conditions.

4.1.5.2 COP1 flowering role in other species

In *Arabidopsis*, one consequence of altered *COP1* function is disrupted rhythmic expression of multiple flowering genes under SD conditions, including *ELF3, GI, CO* and *FT* (Yu et al., 2008). These genes are understood to have a broadly-conserved role in flowering regulation through the study of their orthologs in other species such as barley and rice, where the regulation of *FT* and *CO* orthologs by *ELF3* orthologs appears important for photoperiodic flowering control (Faure et al., 2012; Yang et al., 2013).

COP1 orthologs have also been found in other plant species but without a clear functional characterization, outstandingly in comparison with other flowering orthologs (Huang et al., 2014). For instance, the rice *PPS (PETER PAN SYNDROME*) gene participates in vegetative-reproductive

phase change (Tanaka et al., 2011). Mutants lacking *PPS* activity are early flowering both in SD and LD, and the early induction of flowering is independent from an early induction of expression of *CO-FT* rice orthologs. Another interesting characteristic is that *pps* mutants are dwarf plants, have a very short 'adult' phase and, like *Arabidopsis cop1* mutants, show photomorphogenic development in darkness.

In apple (*Malus domestica)*, *COP1* orthologs participate in the anthocyanin biosynthesis regulated by light and red fruit coloration pathway (Li et al., 2012). An orthologous gene has also been described having a similar COP1 protein function in light-regulated development in soybean (Shin et al., 2016).

There is little exploration of *COP1* in the legume family except for pea. *LIP1 (LIGHT-INDEPENDENT PHOTOMORPHOGENESIS 1)* was initially characterised in the study of a spontaneous single allele mutant showing a light-grown development in complete darkness in pea (Frances et al., 1992). Some other phenotypic characteristics of the *lip1* mutant were similar to *Arabidopsis* photomorphogenic mutants like *det1, det2* or *cop1* (Frances et al., 1992), and *lip1* mutants were also described as having a dwarf phenotype and a light-mediated regulatory role in gibberellin biosynthesis with a possible interference in the phytochrome signal transduction (Sponsel et al., 1996; Weller et al., 2009b). The gibberellin participation in the phenotype of *lip1* was studied in order to elucidate *LIP1* implication in photocontrol of stem elongation (Sponsel et al., 1996) and in 2000, Sullivan and Gray characterized *LIP1* as the ortholog of *COP1* in *Arabidopsis*. This study revealed that *lip1* phenotype was originated by a partial duplication of the *LIP1* gene and was able to produce both wild-type and partial transcripts of *LIP1* (Sullivan and Gray, 2000). More characterization of the role of *LIP1* in gibberellin pathway in pea was performed showing its genetic interaction with *LONG1* in the light-mediated regulation of gibberellin biosynthesis and photomorphogenic development (Weller et al., 2009b).

Until this study, *LIP1* characterization in pea was focussed on hormone pathway and photomorphogenic development but flowering characterization is still not investigated, despite of having most of the *Arabidopsis COP1* interacting partners identified in pea and other legumes. For instance, research in legumes has also revealed the conserved function of *ELF3* orthologs, exposing a direct regulation to photoreceptors and flowering regulators in soybean (Lu et al., 2017) and regulation of *FT* genes in chickpea without a role in circadian clock control (Ridge et al., 2017). In pea, *ELF3* ortholog genes have been described affecting flowering and photoperiod sensitivity that explains the adaptation variability in germplasms (Rubenach et al., 2017; Weller et al., 2012). In particular, *HIGH RESPONSE TO PHOTOPERIOD (HR),* one of the pea *ELF3* orthologs

(*PsELF3a*), is involved in circadian clock function and is responsible for an enormous flowering time variation and photoperiod responsiveness in different cultivars (Weller et al., 2012). Other pea EC genes have been also described such as *DNE,* the pea ortholog of *ELF4* and *SN,* the pea ortholog of *LUX* (Liew et al., 2009, 2014). For both these genes, the mutants show an early flowering phenotype regardless of photoperiod with increased levels of *FT* genes expression (Liew et al., 2014). *DNE/PsELF4* was described as a regulator of circadian genes, leading to a *LATE1*-dependent flowering regulation and without the implication of *CO*-like genes in pea (Liew et al., 2009). The characterisation of *SN/PsLUX* suggested a different conservation in the regulatory connection of EC members in pea due to the lack of alteration on *DNE* expression in the *hr* mutant and the pattern of expression of *HR* during light/dark cycles (Bendix et al., 2015; Liew et al., 2014). Therefore, since the identity and interactions of *HR* as part of the EC are well-established, it is of interest to expand our understanding to examine its interactions with other known members of the photoperiodic flowering pathway as *LIP1* and *LATE1,* which in the *Arabidopsis* model are really relevant.

4.1.6 Aims

This chapter aims to give insight in the role of *LIP1* in photoperiodic control of flowering in pea and its genetic interaction with main regulators of the pathway as photoreceptors like *PHYA* and other key components like *LATE1 (PsGIGANTEA)* and *HR (PsELF3a),* implicated in circadian clock regulation. This chapter characterises *lip1* mutant and its effects on flowering, photomorphogenesis and vegetative growth rhythm and as well as the expression pattern of *FT* genes in relation to developmental stage. It also describes *LIP1* and *PHYA* genetic interaction in flowering response and photomorphogenesis, together with the genetic interaction of the flowering regulatory complex formed by *LIP1*, *HR* and *LATE1* in pea, and concludes with an examination of legume COP1 phylogeny and predicted protein structures.

4.2 Specific material and methods

This section describes specific details of materials and methods for research included in this chapter. General materials and methods that are also relevant are described in Chapter 2.

4.2.1 *Pisum sativum* lines used

The research in this chapter has only focused on *Pisum sativum.* Details of the plant lines used for the experiments presented in this chapter are outlined in Table 4.1.

Table 4.1 Details of pea plant material presented in this chapter.

Target gene	Genotype	Purpose
LIP1	*lip1 (lip1 hr)*	Mutant containing a partial duplication within *LIP1* locus described by (Sullivan and Gray, 2000). Studied to characterize the flowering phenotype and *LIP1* role in pea. Background is *hr*/*elf3a* in NGB5839 line *(le-3)* or TOR background *(LE)*.
HR/ELF3a	*HR/ELF3a*	Line developed by Jackie Vander Schoor by several back-crosses from the *HR* line JI-1771 to NBG5839. The resulting line contains an introgressed form of the WT *HR*/*ELF3a* gene from line JI-1771 into a NGB5839 background. Genotype used for genetic interaction studies of flowering regulation.
LIP1 & HR	*lip1 HR*	F_3 segregating families originated by Jackie Vander Schoor from a *lip1 le-3 x HR* cross. The segregating families were used in this chapter to analyse the genetic interaction of *LIP1* and *HR.* Background is *HR*/*ELF3a* in NGB5839 line.
PHYA	*phyA-1*	Null mutant for *PHYA* gene described by (Weller et al., 2004) Originated by EMS mutagenesis of cv. Torsdag and crossed into NGB5839. Genotype control for genetic interaction studies including flowering characterization and photomorphogenesis response.
LIP1 & PHYA	*lip1 phyA-1 double mutant*	Double mutant generated by Jackie Vander Schoor from a *lip1 LE x phyA le* cross. The segregating families were selected for *lip1* segregants germinating in dark and genotyped for *phyA-1* and *le-3.* The F_3 families were used as plant material for photomorphogenesis experiment and flowering characterization in a NGB5839 background (*le-3*).

LATE1	*late1-2*	Null mutant for *LATE1* gene described by (Hecht et al., 2007). Originated by EMS mutagenesis of NGB5839. Genotype control for genetic interaction studies of flowering regulation. Background is *hr*/*elf3a* in NGB5839.
LATE1 & HR	*late1-2 HR*	F_3 segregating families originated by Jackie Vander Schoor from a *late1-2 x HR* cross. The segregant families were used in this chapter to analyse the genetic interaction of *LATE1* and *HR.* Background is *HR*/*ELF3a* in NGB5839.
LIP1 & LATE1	*lip1 late1-2*	Double mutant obtained from a *lip1 x late1-2* cross. Background is *hr/elf3a* in NGB5839.

4.2.2 Plant growth conditions and measurements

Plants were either grown in the University of Tasmania Controlled Environment Facility (CEF) phytotron with the photoperiod conditions described in Chapter 2 or in controlled environment growth cabinets at 20°C under fluorescent light for the full photoperiod.

For the specific photomorphogenesis experiment in this chapter, plants were grown in pots for two weeks at constant 20°C under continuous far red (FR) light provided by a Heliospectra RX30 LED lighting unit, at an irradiance of 10 µmol m^{-2} s^{-1}. After 14 days, photos of the plants were taken together with the respective photomorphogenesis measurements explained in Chapter 2.

To fully capture the developmental differences observed in *lip1* mutants, the rate of node development was also quantified. Node developing rate represents the level of leaf expansion (opening) of the latest node in consecutive weeks in order to illustrate the development of the plant in a timeframe until flowering. It was calculated every week for a total period of 6 weeks (until flowering) in both WT and *lip1* plants grown simultaneously and exposed to the same photoperiods.

4.2.3 Genotyping details

Lip1 mutants were identified by their characteristic dwarf phenotype in any photoperiod conditions. The genotyping of other mutants (*late1-2, HR, phyA-1)* was performed by HRM and *LIP1* genotyping was performed by PCR. The details are specified in section 4.2.4 Primer details.

4.2.4 Primer details

Information of the primers used for this chapter is found in Table 4.2. For expression analysis, levels of diverse flowering genes in relation to *TFIIa* gene were measured in developmental node series material by qRT-PCR.

Table 4.2 Details of pea primers used in this chapter.

Gene	Purpose	Primer name	Primer sequence	Temp
LATE1	HRM genotyping	late1.2-F	TGGATGCTACTGGATGATATGC	60ºC
		late1.2-R	CTATTGCACGCAAGAAATGC	
LIP1	PCR genotyping	lip1-F	CTGAAGCTCCATGCTCTGC	60ºC
		lip1-R	GTCCGTACAGGGCTTTATGC	
PHYA	HRM genotyping	PsPHYA-1-HRM-F1	CTGGTTTAGGTCGCACACTG	58ºC
		PsPHYA-1-HRM-R1	TGATGATCTTGGATGCATCTTCCT	
HR/ELF3a	HRM genotyping	ELF3-HR-F	ACTAACACTTTATTGGCAAGTG	58ºC
		ELF3-HR-R	GCGGAAAGTATCGTCATTTTG	
FTa1	Expression experiment	FTL-A-6F	GCCCAAGCAACCCTACTTTT	60ºC
		FTL-A-2R	CCATCCTGGAGCGTAAACCC	
FTb2	Expression experiment	FTLE-1F	TCAATGAGCAAAATCATCAAAGC	60ºC
		FTLE-1R	GGTGACATGACACTTTGTTTGC	
FTc	Expression experiment	FTL-L1-8F	GATATTCCAGCCACAACAAGC	62ºC
		FTL-L1-7R	TTATGACGCCACTCTGGAGCAA	
TFIIa	Expression experiment	PsTFIIA-1F	CGGTGGAAATGCTGATGTTA	60ºC
		PsTFIIA-1R	GCTCCCTCCACATACCTCAA	

4.3 Results

4.3.1 *LIP1* flowering phenotypic description.

The *lip1* mutation appeared spontaneously in the photoperiod insensitive cultivar Alaska where it was characterised as a photomorphogenic gene (Frances et al., 1992). Since light conditions can affect the gibberellin content of the stem and shoot and *lip1* is a dwarf mutant, it was proposed as a candidate signalling intermediate in the photocontrol of gibberellin-mediated stem elongation (Sponsel et al., 1996). In view of the potential influence of gibberellin status on aspects of reproductive development, the mutant was introgressed into several different genetic pea backgrounds in order to characterise its developmental effects (see Weller et al., 2009b), *Pisum sativum* cv Torsdag (TOR) which carries a functional allele of Mendel's *LE* gene with long internodes, and its derivative NGB5839 carrying the *le-3* mutation, which impairs gibberellin synthesis and stem elongation (Lester et al., 1997, 1999). However, the nature of the *COP1* partial duplication in the *lip1* mutant meant that there was no reliable molecular marker or other way to distinguish the heterozygote (*lip1/LIP1)* and WT (*LIP1/LIP1)* without extensive progeny testing, and the "WT" segregants therefore include both genotypes. As the *lip1* mutants show a characteristic dwarf phenotype, plant height provided a clear and convenient means of identifying the mutant homozygotes (Sullivan and Gray, 2000; Weller et al., 2009b).

As a previous photoperiodic study in *Arabidopsis* revealed that *cop1* mutants flowered earlier than WT in SD (Jang et al., 2008; Yu et al., 2008), we investigated the potential effects of *LIP1* on flowering time in pea in the two near-isogenic genetic backgrounds TOR and its derivative NGB5839. Both genetic backgrounds carry a mutant *hr* allele, which confers an intermediate photoperiod response (Weller et al., 2012). Eight F_2 families originating from a cross between the WT NGB5839 line and its near-isogenic *lip1* mutant were grown in LD and SD conditions. Half of the individuals from each family were grown in LD and the other half in SD. The flowering time phenotype was assessed both as flowering node (Node of Flowering Initiation, NFI) and date of flowering (Days to Flowering, DTF). Data was initially analysed separately for each family, but as genotype means were not significantly different between families, data were subsequently merged and analysed together. The results obtained are presented in Figure 4.4.

In the NGB5839 background, *lip1* mutants developed the expected dwarf phenotype under both LD (Figure 4.4 A) and SD conditions. Node of flowering initiation (NFI) differed significantly between genotypes in both photoperiods. In LD conditions, WT/Het flowered at around node 16 and *lip1* around node 13, whereas in SD, WT/Het flowered at node 23 and *lip1* around node 19

(Figure 4.4 B). Regarding Days To open first Flower (DTF), all genotypes, WT/Het and *lip1* mutants, flowered at a similar date under LD (around 44 days) and SD (around 64 days), suggesting that the *lip1* mutant had no effect on flowering time or on the degree of photoperiod responsiveness (Figure 4.4 C). The comparison between these two types of measurement of flowering indicates that WT/Het and *lip1* may have different rates of leaf production/node development.

To investigate this possibility, the effect of *lip1* on vegetative development was examined in more detail, including effects on the rate of node development and on internode elongation. Figure 4.4 D shows that the rate of node development was in general slower in *lip1* than in WT plants under both LD and SD. This difference did not become statistically significant until week 3, and by week 4 *lip1* mutants had produced 3 fewer expanded nodes than WT, under both photoperiods. Observations over the entire six-week period indicated around a 20% reduction in rate of node development in *lip1* relative to WT (finding a 20.69% reduction in week 4, 19.72% reduction in week 5 and 19.55% reduction in week 6).

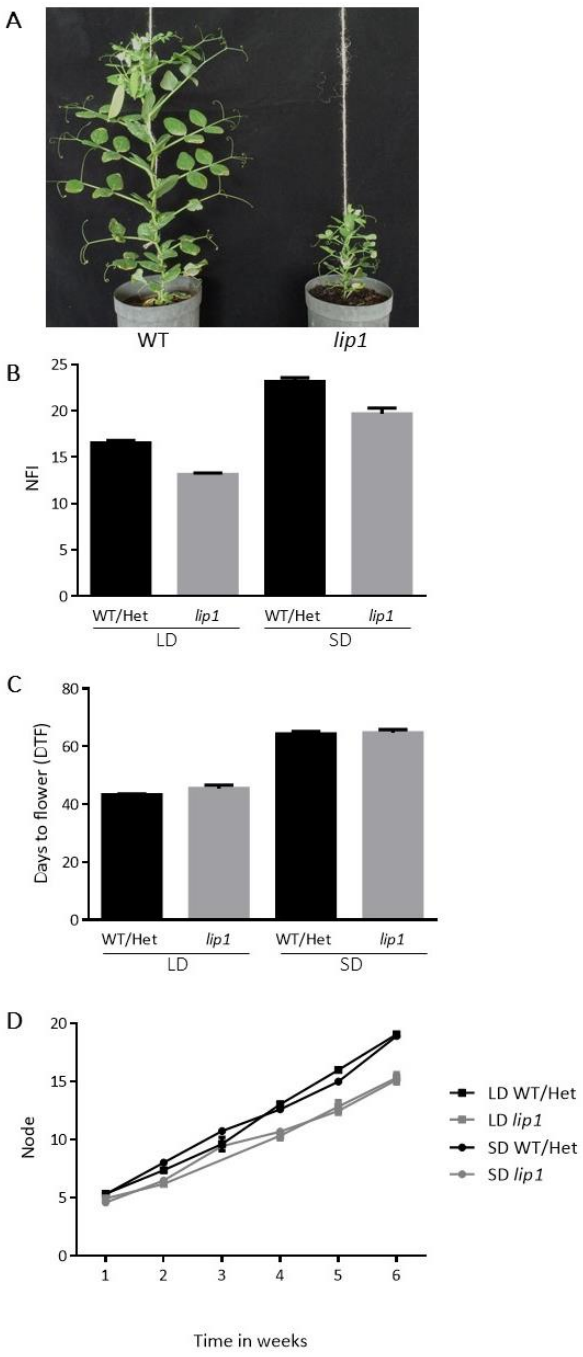

Figure 4.4 Flowering phenotype and node development rate of *lip1* in NGB5839 genetic background

A) Phenotype representation of WT and *lip1* mutant plants in a NGB5839 genetic background at 8 weeks of age in LD conditions. A distinctive difference in plant height and internode length is shown between genotypes. B) Flowering node initiation of a F_2 population segregating for WT/Het and *lip1* under LD and SD conditions. Values represent mean ± SE for N=8-38 plants per genotype. There are significant differences between genotypes (p-value<0.05). C) Date of flowering of WT/Het and *lip1* genotypic classes in F_2 populations under LD and SD photoperiods. Values represent mean ± SE for N=8-38 plants per genotype. There is no significant difference between genotypes (p-value>0.05). D) Node developing rate for WT/Het (black) and *lip1* (grey) growing in LD (square) and SD (circle) conditions for 6 weeks. Values represent mean ± SE for N=8-38 plants per genotype. There are significant differences between genotypes from week 3 onwards (p-value>0.05).

A reduction in active gibberellin levels caused by the *le-1* and the *le-3* mutant alleles of the *LE* gibberellin biosynthesis gene do not significantly impair the flowering response to photoperiod (Sponsel and Reid, 1992) and NGB5839 (*le-3*) has been extensively used as a photoperiod-responsive progenitor for isolation of photoperiod response mutants (e.g Hecht et al., 2007; Liew et al., 2014). However, it is possible that the observed effect of *lip1* on node development could be due in part to an interaction with the reduced gibberellin level in the NGB5839 background. In order to investigate this hypothesis, the effect of *lip1* mutation was also examined in the cv Torsdag (TOR) genetic background, carrying the WT *LE* gene. This experiment was conducted in seven F_3 families segregating for the *lip1* mutation, where *lip1* mutants were also easily identified by their dwarf phenotype. As previously presented before, the segregating families were grown in LD and SD with 10 individuals of each family in each condition and the data was grouped as *lip1* and WT/Het genotypes and it is presented in Figure 4.5.

The results obtained show that the effect of the *lip1* mutation on flowering time in a TOR background is similar to the effect previously observed in the NGB5839 background, with the mutant flowering at an earlier node (node 13 in LD and node 19 in SD) than WT/Het (node 19 in LD and node 26 in SD) under both light conditions (Figure 4.5 A). There is no significant effect of *lip1* mutation on the date of flowering under either photoperiod finding that both groups flowered around 45 days in LD and around 62 days in SD (Figure 4.5 B). Nevertheless, the *lip1* mutant clearly retained a significant response to photoperiod that was similar to WT, in terms of both flowering node and days to flower.

The effect of *lip1* on the rate of node development was also examined in the TOR background, where a significant reduction was first detected after 2 weeks, and a reduced rate of development was maintained over subsequent weeks (Figure 4.5 C). This pattern of reduced node development rhythm in the *lip1* mutants suggests a direct role of *LIP1* in node development rate regardless of the *LE* genetic background.

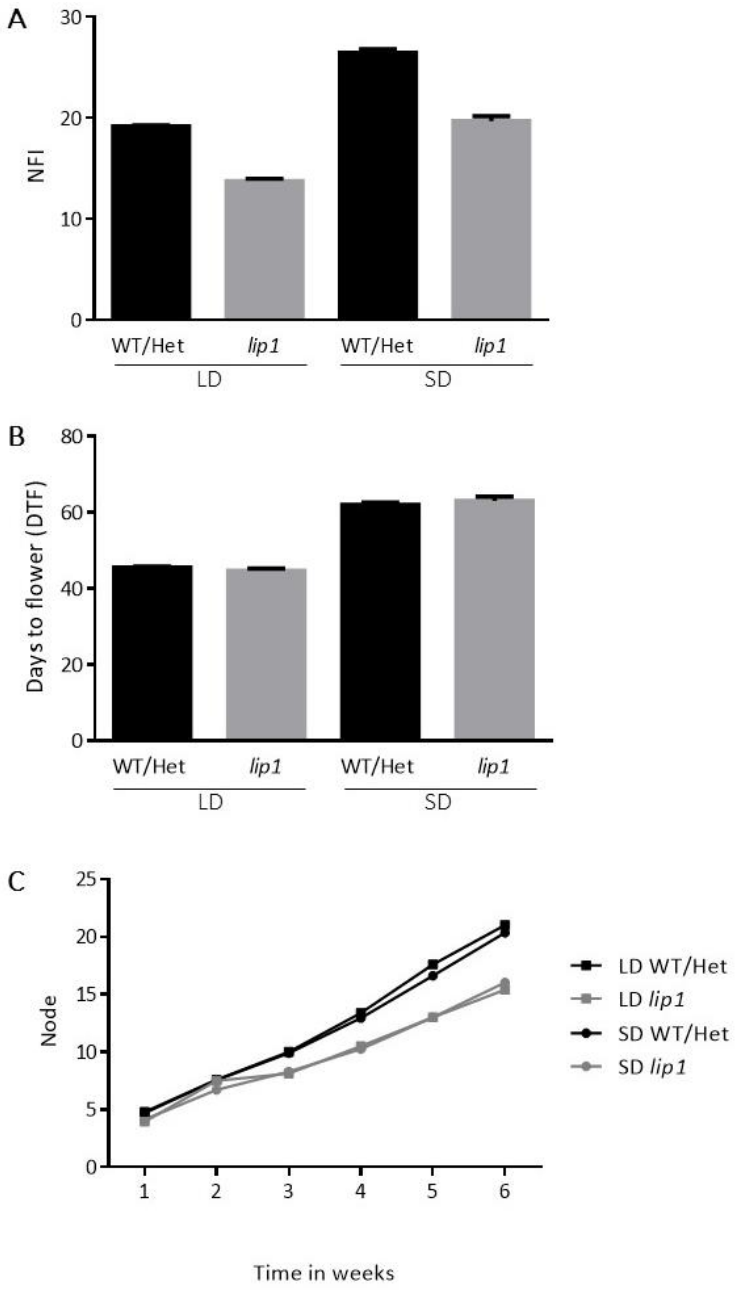

Figure 4.5 Flowering phenotype and node development rate of *lip1* in TORSDAG genetic background.

A) Flowering node initiation phenotype of a F_3 population segregating for WT/Het (TOR) and *lip1* under LD and SD conditions. Values represent mean ± SE for N=19-54 plants. Significant differences were found between genotype and within photoperiods ($p<0.05$). B) Date of flowering representation of WT/Het (TOR) and *lip1* under LD and SD. N=19-54 plants per condition. There is not significant difference between genotypes within photoperiod treatment (p-value>0.05). C) Rate of node development for WT/Het (black) and *lip1* (grey) growing in LD (square) and SD (circle) conditions for 6 weeks. Values represent mean ± SE for N=19-54 plants per genotype. There are significant differences between genotypes from week 3 onwards (p-value>0.05).

In both *LE* backgrounds (TOR and NGB5839), the time necessary for flowering (DTF) is not significantly different between WT and *lip1* mutant while the node of flowering initiation (NFI) is earlier in the mutant. But some differences were observed between autumn and summer sowings. For example, in a summer sowing (Figure 4.6), *lip1* mutants had a statistically significant earlier node of flowering initiation (Figure 4.6 A), but flowered several days later (Figure 4.6 B) than WT under SD. The NFI reduced the difference between genotypes, finding flowering to occur at node 16 and node 15 in LD and node 19 and node 18 in SD for WT and *lip1* respectively (Figure 4.6 A). Days to Flower (DTF) measurements revealed a different pattern, showing similar days for LD conditions between genotypes (43 days and 44 days for WT and *lip1* respectively) and a greater difference between genotypes in SD (58 days for WT and 65 days for *lip1*). Since the glasshouse location and photoperiods conditions of the phytotrons used were the same in all experiments, these differences suggest that some seasonal environmental variables might influence the expression of the *lip1* mutation effects. One possibility might be the glasshouse temperature, which can be variable during the year (the average daily temperature in Hobart in June was 5-12°C vs. the average daily temperature in January was 11-21°C with glasshouse temperatures generally 5-10°C higher than these figures).

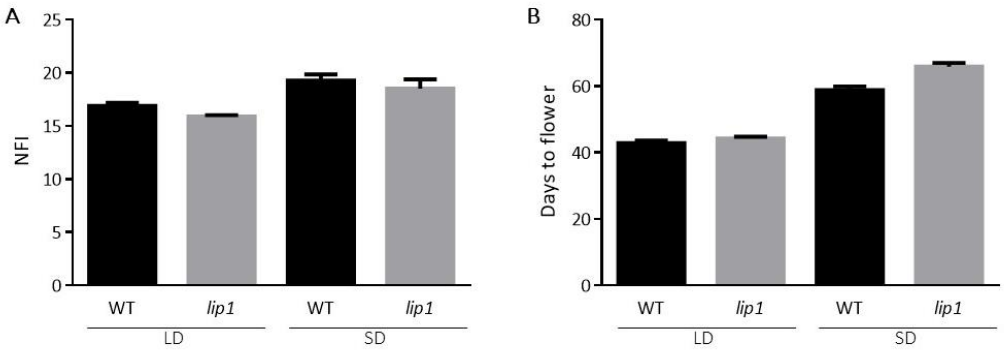

Figure 4.6 Flowering node and date of WT and *lip1* plants in a hot summer sowing.

Flowering phenotype of WT (NGB5839 background) and *lip1* affected by high temperatures in the glasshouse. A) Node of flowering in LD and SD photoperiods for WT and *lip1* mutant. N= 8 plants in each condition. There is not statistical support for a difference in NFI between genotypes (p-value>0.05). B) Date of flowering in LD and SD photoperiods for WT and *lip1* mutant. N= 8 plants in each condition. There is statistical support for a difference in date of flowering in SD between genotypes (p-value=0.0013).

To further examine the regulation of flowering by *LIP1*, the expression of key flowering genes was examined, focusing on expression of florigen (*FT*) genes during a developmental time-course. Whereas similar experiments examining flowering gene expression in pea have generally compared genotypes at similar timepoints, this experiment aimed to compare expression in WT and *lip1* at an equivalent developmental stage in terms of the number of nodes developed.

Previous investigation of florigen genes expression have shown that out of the six *FT* genes in pea, two (*FTb2* and *FTa1*) are strongly expressed and responsive to photoperiod, and likely to participate in the induction of flowering. Both genes are mainly induced in leaf tissue and *FTb2* expression coincides with the commitment to flowering (Hecht et al., 2011). Leaf samples were harvested from WT and *lip1* plants at four different developmental stages, corresponding to full expansion of the leaf at node 3, 5, 8 and 13, with sampling of *lip1* leaf tissue for the relevant node performed later than WT (Table 4.3) due to the slower leaf development rate.

Table 4.3 Harvest times for equivalent developmental nodes in WT and *lip1*.

Days between sowing and harvesting	**Node 3**	**Node 5**	**Node 8**	**Node 13**
WT	12	14	25	41
lip1	12	18	33	53

FTb2 and *FTa1* expression was analyzed in all samples, and as in previous reports, *FTb2* was found to be more strongly expressed than *FTa1*. Figure 4.7 shows that for both genes, the expression levels are similar in WT and *lip1* samples, except at node 13 where the *lip1* mutant shows higher expression of both genes.

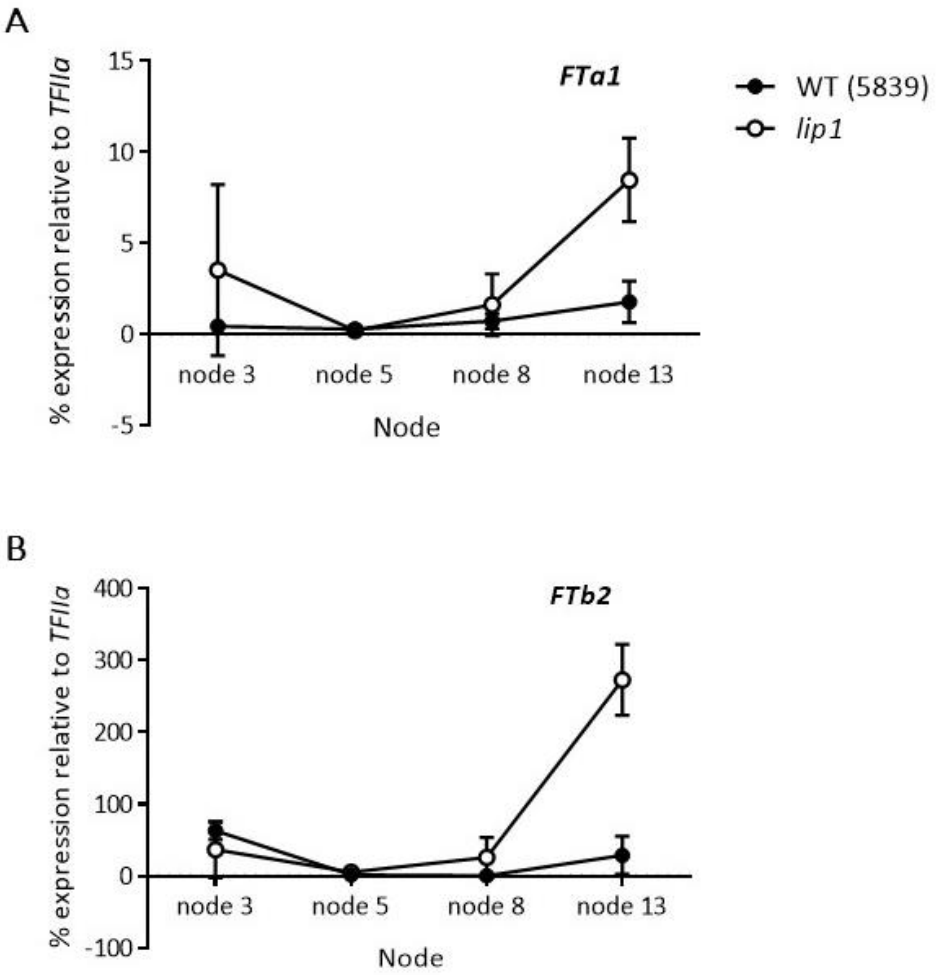

Figure 4.7 *FTa1* and *FTb2* expression in *WT* and *lip1* at the same developing node stage.

A) *FTa1* expression in leaves at four different nodes. The developmental nodes studied are: node 3, node 5, node 8 and node 13. The genotypes studied are WT (5839) with closed circles and *lip1* (5839 background) with open circles. Plants were grown in LD conditions. Values have been normalised to the transcript level of *TFIIa* gene and represent mean ± SE for N= 3 biological replicates. B) *FTb2* expression in four different developmental nodes. The developmental nodes studied are: node 3, node 5, node 8 and node 13. The genotypes studied are WT (5839) with closed circles and *lip1* (5839 background) with open circles. Plants were grown in LD conditions. Values have been normalised to the transcript level of *TFIIa* gene and represent mean ± SE for N= 3 biological replicates.

4.3.2 *LIP1* genetic interaction with *PHYA*

To further characterize the role of *LIP1* in the photoperiod genetic pathway, it is of potential interest to analyse its genetic interaction with other key components of the pathway. One of the most relevant groups are photoreceptors, as these perceive light and presumably act upstream of *COP1* orthologs. The best understood photoreceptor acting in photoperiodic flowering in pea is *PHYTOCHROME A* (*PHYA*), where both loss-of-function (*phyA-1* and *phyA-2*) and gain-of-function (*phyA-3D*) mutants have been previously described (Weller et al., 1997a, 2004). The pea *phyA-1* null mutant is late-flowering under LD and effectively photoperiod-insensitive (Weller et al., 1997a). In terms of flowering and other photoperiod-responsive traits such as reduced lateral branching and a reduction in the length of the reproductive phase, the *phyA-1* mutant closely phenocopies a SD-grown WT plant (Weller et al., 1997a, 2004).

In *Arabidopsis*, *COP1* is known to mediate signalling from multiple photoreceptors during photomorphogenesis and flowering time regulation, and a regulatory connection between *PHYA* and *COP1* is well-known. As outlined above, COP1 protein is primarily active in the nucleus, and is "inactivated" via a light-induced relocation to the cytosol (Kim et al., 2017). This regulation is in part dependent on a direct interaction between light-activated PHYA and COP1, but at the same time, PHYA itself seems to be subject to protein-level regulation by COP1 (Seo et al., 2004). In addition, PHYA is also able to regulate the activity of COP1 indirectly, by regulating the availability of other components of the COP1 multi-protein complex, the SPA proteins which are essential cofactors for COP1 (Podolec and Ulm, 2018; Xu et al., 2016).

To examine the genetic interaction between *LIP1* and *PHYA*, a double mutant *lip1 phyA-1* was generated as described in Table 4.1. The flowering behaviour of single and double mutants in LD conditions is shown in Figure 4.8. The *lip1* single mutant developed its typical dwarf phenotype, meanwhile the *lip1 phyA-1* double mutant showed a similar overall phenotype to the *phyA-1* single mutant, with well-developed lateral branches in basal nodes and without any formed and opened flower (Figure 4.8 A). This similarity was also seen in the height of the plants, with *phyA-1* and double mutant *lip1 phyA-1* intermediate in height between *lip1* and WT. WT and *lip1* mutants have opened flowers at this stage of development (6-week-old plants), while both *phyA-1* and double mutant *lip1 phyA-1* are still not at flowering stage. As shown previously, *lip1* flowered at an earlier node than WT (13 vs. 16) and *phyA-1* flowered later, at node 22 (Figure 4.8 B). The double mutant *lip1 phyA-1* flowered at node 24, statistically not significantly different than the *phyA-1* single mutant. This genetic interaction shows that the effects of *phyA-1* are epistatic to *lip1*, meaning that *lip1* has no detectable effect in the absence of *phyA*. This would normally

suggest that *PHYA* is acting in the same pathway as *LIP1*. However, it would also imply that *PHYA* is acting downstream of *LIP1* to regulate flowering.

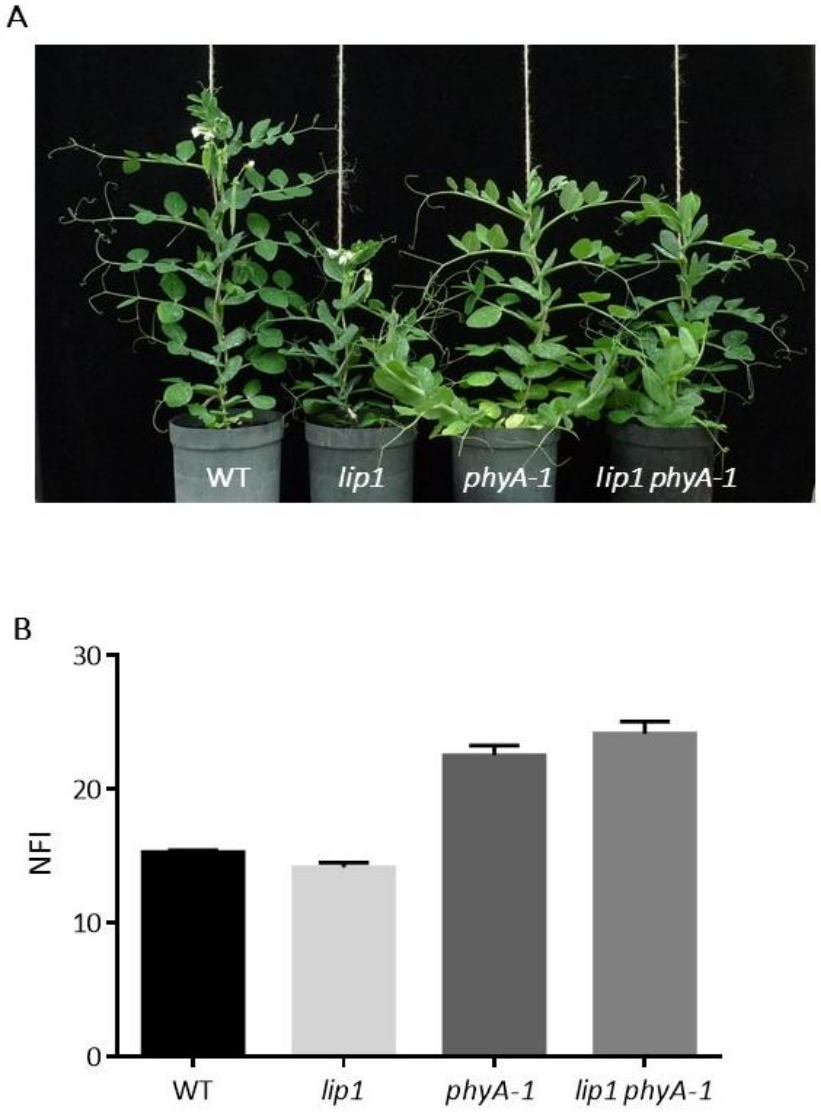

Figure 4.8 Flowering phenotype of *lip1* and *phyA-1*, single and double mutants.

Flowering phenotype of *lip1*, *phyA-1* and double mutant *lip1 phyA-1* in NGB5839 background under LD conditions. A) 6 weeks old plants with flowers and seed pods distinguished in both WT and *lip1* mutant meanwhile *phyA-1* and double mutant *lip1 phyA-1* do not show any flower. B) Node of Flowering Initiation for *lip1*, *phyA-1* and double mutant *lip1 phyA-1*. N=8 plants per genotype. Significant differences were found for all the genotypes in relation to WT ($p<0.05$) except for *phyA-1* single mutant in relation with double mutant.

To examine the genetic interaction for photomorphogenic responses, the same genotypes were grown under far-red (FR) light and shown in Figure 4.9. The two single mutants *phyA-1* and *lip1*

are known to have opposite effects on photomorphogenesis development. The *phyA-1* mutant displaying long internodes and low leaf surface area under FR, typical of WT seedlings in dark conditions (Weller et al., 1997a). In contrast, the *lip1* single mutant under FR showed a phenotype of exaggerated photomorphogenic characteristics relative to WT, with a shorter stem and fully expanded leaves typical of a WT seedling grown under broad-spectrum white light (Weller et al., 2009b). The same phenotypes were observed under FR conditions in this study (Figure 4.9). The *lip1 phyA-1* double mutant developed shorter internodes than the single *phyA-1* mutant comparable to WT seedlings (Figure 4.9 A, B, C), and has expanded leaves resembling the single *lip1* mutant (Figure 4.9 A, D). Both *lip1* and *lip1 phyA-1* had a significant increase in leaflet area relative to WT and did not differ from each other in this trait (Figure 4.9 D). The internode lengths of the double mutant were intermediate between the two single mutants, but overall, more similar to WT. This phenotypic data suggests that *LIP1* acts downstream of *PHYA* to mediate photomorphogenic effects.

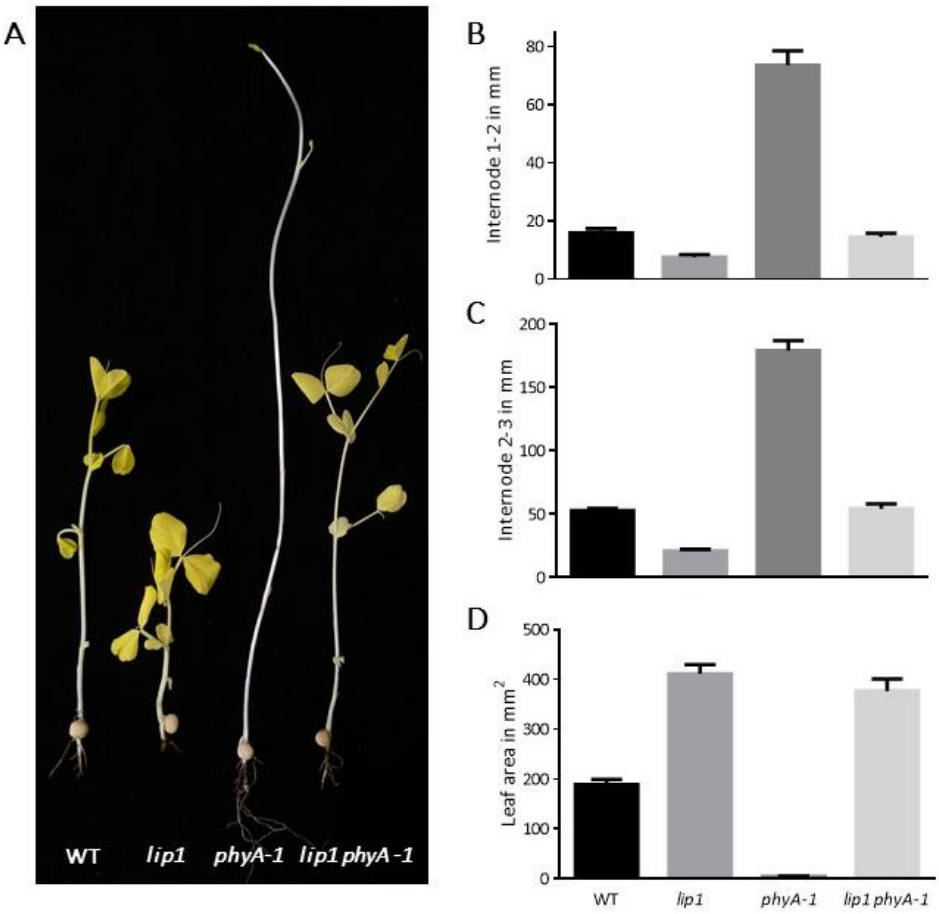

Figure 4.9 Photomorphogenic phenotype of *lip1* and *phyA-1*, single and double mutants under FR light.

The photomorphogenic development under Far Red (FR) light was studied for 12 plants of each genotype: NGB5839 (WT), *lip1*, *phyA-1* and double mutant *lip1 phyA-1*. A) Representative seedling for each genotype after 12 days under FR light conditions. B) Internode 1-2 length under FR light conditions. Significant differences were found between *phyA-1* and the other genotypes (p-value<0.05). C) Internode 2-3 length under FR light conditions. Significant differences were found between all the genotypes (p-value<0.05), except for the analysis between WT and double mutant. D) Leaf area under FR light conditions. Significant differences were found between all the genotypes (p-value<0.05) except for the analysis of *lip1* single mutant and double mutant *lip1 phyA-1.*

4.3.3 Genetic interactions of *LIP1*, *LATE1* and *HR* in pea.

The extended research of *COP1* in *Arabidopsis* has revealed its importance in flowering regulation through diverse mechanisms (Jang et al., 2008): a direct regulation of CO protein by COP1-SPA complex affecting flowering induction and, an indirect mechanism where COP1 forms a protein complex with EARLY FLOWERING 3 (ELF3) to regulate GIGANTEA (GI), a circadian clock and flowering regulator of *CO* and *FT* expression (Jang et al., 2015). The pea orthologs of these genes have been characterized and loss-of-function mutants are available: *HR* is an *ELF3* ortholog (*PsELF3a*) (Weller et al., 2012) and *LATE1* is the *GIGANTEA* ortholog (Hecht et al., 2007).

To analyse the genetic relationship between *LIP1 (PsCOP1), LATE1 (PsGIGANTEA)* and *HR (PsELF3a)* in control of flowering time, a number of segregating populations for *lip1* and *late1-2* in a *HR* background were examined under LD conditions.

4.3.3.1 LIP1 (PsCOP1) and LATE1 (PsGIGANTEA) interactions

In models like pea, where CO does not appear to have a central role in flowering time regulation, it is likely that other forms of regulation may be more prominent. The known interaction of COP1 and GI, promoting the degradation of GI protein and facilitated by ELF3 in nuclear bodies (Mishra and Panigrahi, 2015; Yu et al., 2008), becomes then an interesting key point of study. Despite its importance in *Arabidopsis,* it is not clear whether this mechanism is relevant in other species but, the understanding of the functions and interaction of these three proteins and how their protein life-span is regulated is still relevant to understanding the mechanism as a whole.

In order to examine the genetic interaction between *LATE1* (*PsGIGANTEA*) and *LIP1*(*PsCOP1*), a cross between *lip1* and *late1-2* mutants was made, and double mutants were obtained in a *hr* background (NGB5839). Flowering phenotypes and data scored are shown in Figure 4.10, showing plants at seven weeks old. Both WT and *lip1* genotypes have already flowered and the single mutant *late1-2* and double mutant do not show any flower development. In Figure 4.10 A, the phenotype also reveals a dwarf plant for *lip1* single mutant, and an even shorter phenotype for the double mutant *lip1 late1-2*. The scoring of node of flowering initiation reveals an early flowering node for *lip1* around node 13, and a late flowering node for *late1-2* around node 19 in relation to node 16 of flowering of the WT (5839) (Figure 4.10 B). The double mutant *lip1 late1-2* has a flowering node intermediate between the single mutants, around node 17, more similar to the WT. Regarding date to flowering (Figure 4.10 C), WT flowers around 47 days after emerging while the single mutants *lip1* and *late1-2* flower around 54 and 62 respectively. This data

corresponds to a summer sowing were the higher temperatures strongly affect the development and flowering response of the weak mutant *lip1*. The double mutant took longer to flower than any of the single mutants, 71 days. Finally, Figure 4.10 D shows the data for Reproductive Nodes (RN) revealing that WT develops around 4 reproductive nodes, and the single mutants *lip1* and *late1-2* develop around 3 and 8 reproductive nodes respectively. The double mutant develops 6 reproductive nodes, an intermediate phenotype similar to WT.

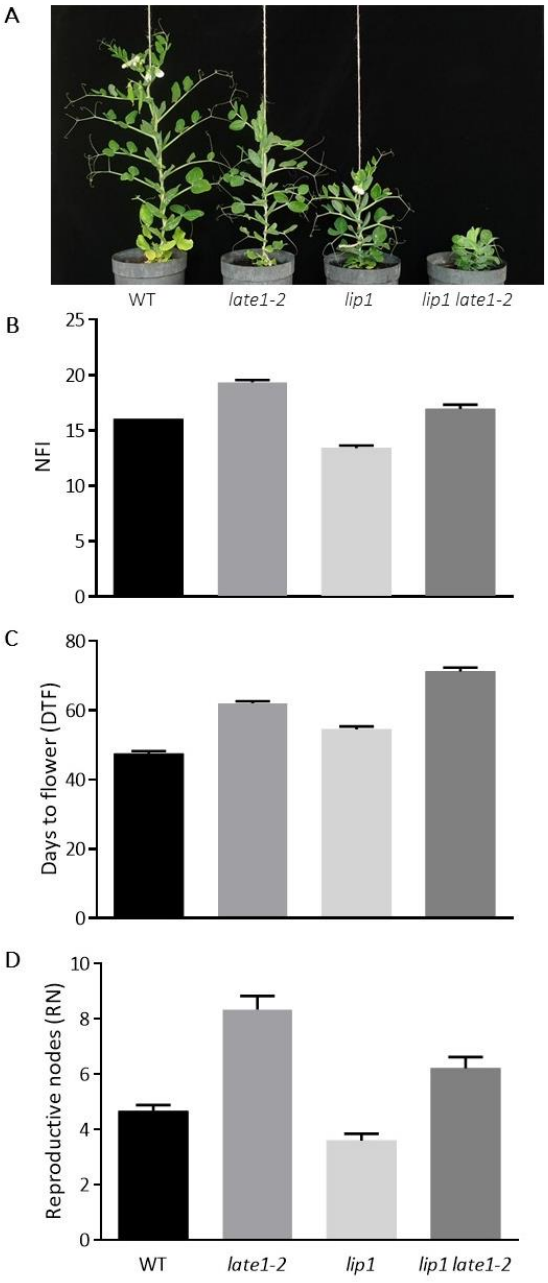

Figure 4.10 Flowering phenotype of *lip1* and *late1-2* single and double mutants.

A) Representative plants of WT (NGB5839), *late1-2, lip1* and double mutant *lip1 late1-2* at 7 weeks. The double mutant *lip1 late1-2* developed an extremely dwarf phenotype. B) Flowering Node Initiation (NFI) description of *late1-2, lip1* and double mutant *lip1 late1-2* in 5839 background under LD conditions. N= 6– 52 plants per genotype belonging to and F_3 segregating family. Significant differences were found between all the genotypes in relation to WT ($p<0.05$) except for WT in relation with double mutant. C) Date of flowering description of *late1-2, lip1* and double mutant *lip1 late1-2* in 5839 background under LD conditions. N= 6– 52 plants per genotype belonging to and F_3 segregating family. Significant differences were found for all the genotypes in relation to WT ($p<0.05$) and there are significant differences in date of flowering between single and double mutants ($p<0.05$). D) Reproductive Nodes (RN) description of *late1-2, lip1* and double mutant *lip1 late1-2* in 5839 background under LD conditions. N= 6– 52 plants per genotype belonging to and F_3 segregating family. Significant differences were found between all the genotypes in relation to WT ($p<0.05$) except for WT in relation with double mutant.

4.3.3.2 LIP1 (PsCOP1) and HR (PsELF3a) interactions

In previous sections of this chapter, the *lip1* phenotype has been characterized in NGB5839 and cv Torsdag backgrounds both carrying a *hr/elf3a* allele (Weller et al., 2012). A line containing the WT *HR/ELF3a* gene in a NGB5839 background was developed prior to this work (J Vander Schoor, unpublished; details in Table 4.1). A cross between lines *lip1 hr* (*lip1* in NGB5839 background) and *LIP1 HR* (*HR* in NBG5839 background) was made and F_2 individuals carrying the *HR* allele were selected. From these, several segregating F_3 populations were grown in LD conditions together with control NGB5839 (*LIP1 hr*) and *lip1* mutants in NGB5839 background (*lip1 hr*).

The difference in flowering behaviour between the two *LIP1* genotypes (*HR* and *hr*) has already been described (Weller et al., 2012) and is not the focus of this section. Here we characterise the effect of the *lip1* mutation on the flowering phenotype according to its *HR* background. The results for NFI in Figure 4.11 A indicate that the *LIP1 HR* genotype had the latest flowering phenotype (around node 25) where the *lip1 HR* genotype flowered some nodes earlier (around node 23). The same pattern is observed for *LIP1 hr* (flowering around node 16) and *lip1 hr* (flowering around node 13), indicating that in both *HR* backgrounds, the *lip1* mutation reduces the node of flowering initiation. Figure 4.11 B shows the characterization of RN in which *LIP1 HR* is the genotype with more reproductive nodes (around 14 reproductive nodes developed) followed by *lip1 HR* which develops around 7 reproductive nodes. In this case, both genotypes with a *hr* genetic background develop similar number of reproductive nodes (both *LIP1 hr* and *lip1 hr* develop 4 reproductive nodes). Thus, for this trait, there is a slightly different interaction, in which the presence of *lip1* substantially reduces the length of the reproductive phase in an *HR* genetic background. This may identify a distinct role for *lip1* in regulating post-flowering reproductive growth and suggests an additive effect from *LIP1* in the phenotype of node development in *HR* genetic background. This result also indicates that the effect of the *lip1* mutation is weaker in presence of the WT *ELF3a*, and might suggest a degree of functional redundancy between *LIP1* and *HR*.

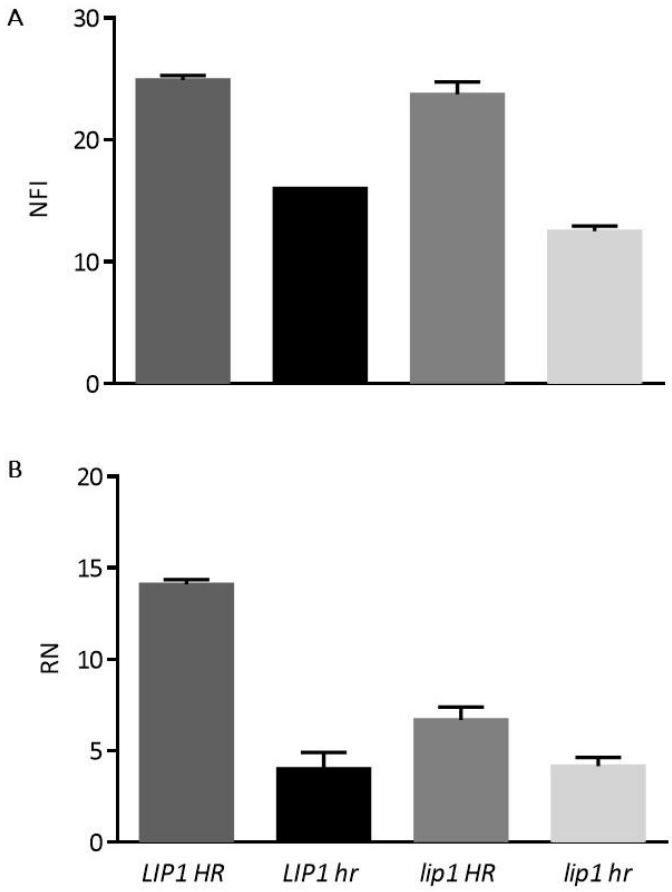

Figure 4.11 Flowering node and reproductive node phenotype of the *lip1* and *HR* F_3 segregating population.

A) Node of Flowering Initiation for *lip1* in a *HR/hr* backgrounds. Values represent mean ± SE for n =6-40 plants in each genotype. Statistical support indicating significant difference is found between all genotypes ($p<0.05$) except for *LIP1 HR* vs. *lip1 HR* and *LIP1 hr* vs. *lip1 hr.* B) Reproductive nodes of an F_3 segregating population for *lip1* in a *HR* background. Values represent mean ± SE for n =6-40 plants in each genotype. There are statistical differences between all genotypes ($p<0.05$) except between *LIP1 hr* vs. *lip1 hr.*

4.3.3.3 LATE1(PsGIGANTEA) and HR(PsELF3a) interactions

A cross between *late1-2 hr* (*late1-2* in NGB5839 background) and *LATE1 HR* (*HR* line in NGB5839 background) was made and F_2 individuals carrying the *HR* allele were selected. From these, several F_3 populations segregating the *late1-2* allele were grown in LD conditions next to some NGB5839 (*LATE1 hr*) and *late1-2* mutants (*late1-2 hr*). The plants were genotyped for the *late1-2* mutation. Flowering time phenotype was scored as node of flowering initiation (NFI) and reproductive node (RN) and results are presented in Figure 4.12. The study of NFI revealed the latest flowering genotype to be *late1-2 HR* (flowering around node 39) as seen in Figure 4.12 A. *LATE1 HR* genotype

is relatively late flowering (flowering around 25th node) suggesting an additive effect of *LATE1* in *HR* background. In the case of *LATE1 hr* and *late1-2 hr,* the NFI difference is not that bigger, finding the node of flowering initiation to be 16 and 19 respectively, displaying the characterised late-flowering effect of *late1* in flowering induction in pea in *hr* background. Plants carrying *late1-2* were late flowering in both *HR/hr* genetic backgrounds but the response to photoperiod is controlled by *HR* leading to an extremely late flowering phenotype in *late1-2 HR* genotype. The reproductive node analysis shown in Figure 4.12 B indicates that the genotype with more reproductive nodes is *LATE1 HR* (displaying 13 reproductive nodes) followed by *late1-2 HR* (developing 10 reproductive nodes). The genotypes in *hr* genetic background display less reproductive nodes, *LATE1 hr* develops 4 reproductive nodes and *late1-2 hr* develops around 8 reproductive nodes. This analysis confirms the strong role of *HR* in photoperiod response in pea and indicates an intermediate phenotype for both NFI and RN in the double mutant suggesting an additive effect of *LATE1* in *HR* background.

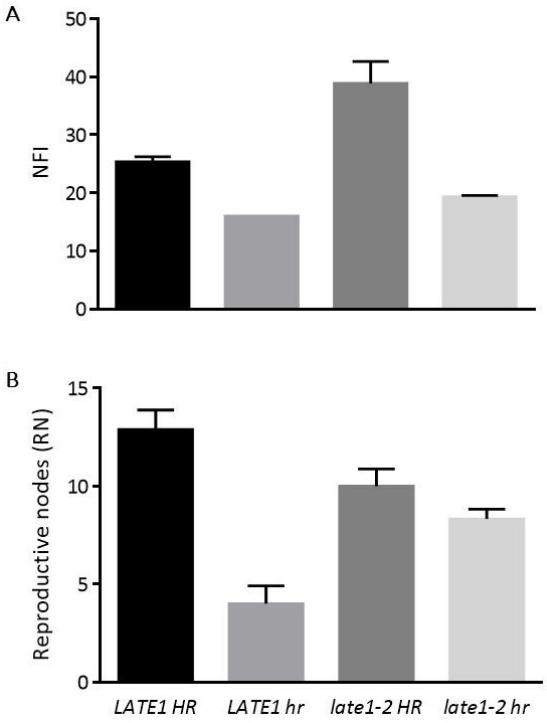

Figure 4.12 Flowering node and total node of the *late1-1* and *HR* F_3 segregating population.

A) Node of Flowering Initiation for *late1-2* in a *HR/hr* background. Values represent mean ± SE for n =6-9 plants. There are statistical differences between all genotypes ($p<0.05$). B) Reproductive nodes for *late1-2* in a *HR/hr* background. Values represent mean ± SE for n =6-9 plants in each genotype. There are statistical differences between all genotypes ($p<0.05$) except for *late1-2 HR* vs. *late1-2 hr.*

4.3.4 *LIP1* phylogeny in legumes

To complement the functional characterizations of *LIP1* described above and elsewhere, a study of the phylogeny of this gene and comparative aspects of protein structure is also of interest. The initial molecular characterization revealed that *LIP1* is a gene containing 13 exons and 12 introns, being present as a single copy gene in the pea genome (Sullivan and Gray, 2000) now designated as Psat2g025120 in the recently published pea genome (Kreplak et al., 2019). The *lip1* mutation has been described as a partial duplication of exons 1 to 7 (Sullivan and Gray, 2000), consistent with the retention of partial protein activity in the mutant, a feature also found in viable *cop1* mutant alleles in *Arabidopsis* (McNellis et al., 1994). More broadly, *COP1* protein function as an ubiquitin ligase appears to be highly conserved among plants and other species, but despite this, it is not clear the extent of structural variation that exists within and between plant groups. This high level of functional conservation in distant protein families gives support to a key and vital role for *COP1* in cell life and important biological processes. Hence, viable mutant alleles of *COP1* commonly keep functional protein activity but there are many lethal alleles (McNellis et al., 1994; Tanaka et al., 2011).

The conserved functions of *LIP1* suggest a conservation of the *COP1* role in pea (Sullivan and Gray, 2000; Weller et al., 2009b) but the presence and conservation of *COP1/LIP1* in other legumes has not yet been characterised. To further examine the level of conservation of *COP1/LIP1* among legumes, a protein comparison was performed, using *COP1* orthologs retrieved from NCBI GenBank and other sources. Target species (Table 4.4) included SD and LD legumes species such as soybean *(Glycine max)*, *Medicago truncatula*, *Lotus japonicus*, common bean *(Phaseolous vulgaris)*, chickpea *(Cicer arietinum),* pigeon pea *(Cajanus cajan)* and pea *(Pisum sativum),* and also the non-legumes *Arabidopsis* , tomato (*Solanum lycopersicum*), rice (*Oryza sativa),* maize (*Zea mays)* and apple (*Malus domestica)* as more diverse comparisons.

Table 4.4 COP1 protein sequences identified in online sequences resources.

Name	Species	Locus ID
AtCOP1	*Arabidopsis thaliana*	NP_180854.1
CaCOP1_1	*Cicer arietinum*	XP_004491092.1
CcCOP1_1	*Cajanus cajan*	XP_020233903.1
GmCOP1_1	*Glycine max*	XP_003545597.1
GmCOP1_2	*Glycine max*	XP_003519446.1
LjCOP1_1	*Lotus japonicus*	Lj0g3v0114209.1
MdCOP1	*Malus domestica*	BAM08276.1
MtCOP1_1	*Medicago truncatula*	Medtr5g085250.1
OsCOP1(PPS)	*Oryza sativa*	XP_015627602.1
PsLIP1	*Pisum sativum*	Psat2g025120
PvCOP1_1	*Phaseolus vulgaris*	Phvul.008G214400.2
SlCOP1	*Solanum lycopersicum*	NP_001234047.2
ZmCOP1	*Zea mays*	NP_001152482.1

The COP1 protein alignment contains sequences that range in length from 646 aminoacids (MdCOP1) to 693 aminoacids (ZmCOP1), with most of this variation located in a highly variable region towards the N-terminus (Figure 4.13). Outside this region, the protein sequence is highly conserved among legumes with amino acid sequence similarity between 89%-95%, dropping to 61% across all species including non-legumes. Areas of particular conservation are the two COP1 domains (RING finger domain and WD40 repeats, see Figure 4.2) which in *Arabidopsis* contribute the most to the ubiquitin ligase activity. The RING finger domain, marked with a red line, is located in the N-terminal region and it is highly conserved among the sequences. WD40 repeat domain is forming all the C-terminal region indicated with a blue letters. The level of conservation in this domain is extremely high and this remark is well-described among other species, including human COP1, where the WD40 repeat domain is sufficient for the Trib binding and the COP1 function (Uljon et al., 2016). The last domain, coiled-coil domain indicated with a green line is also well conserved among species but the least conserved domain from the three.

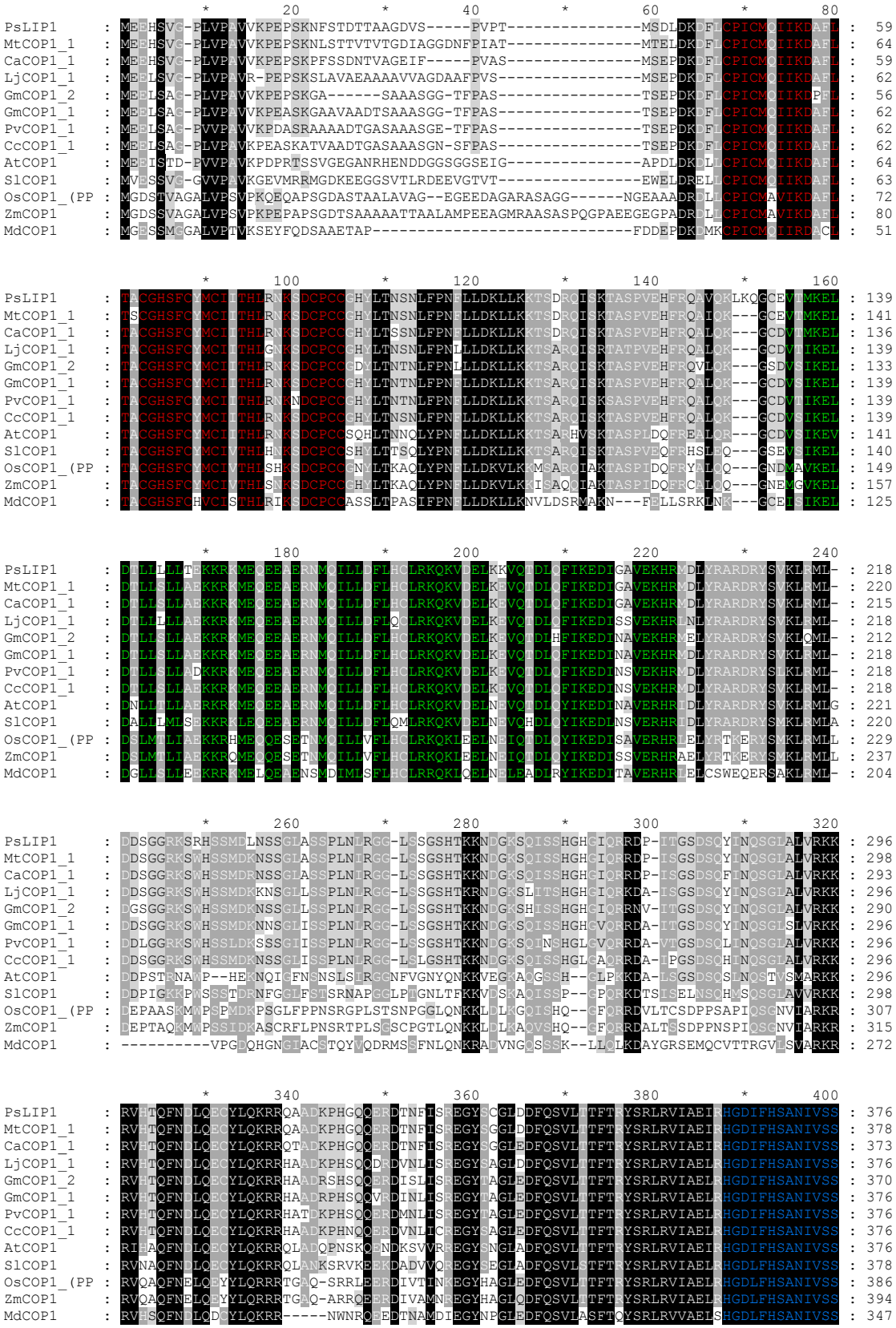

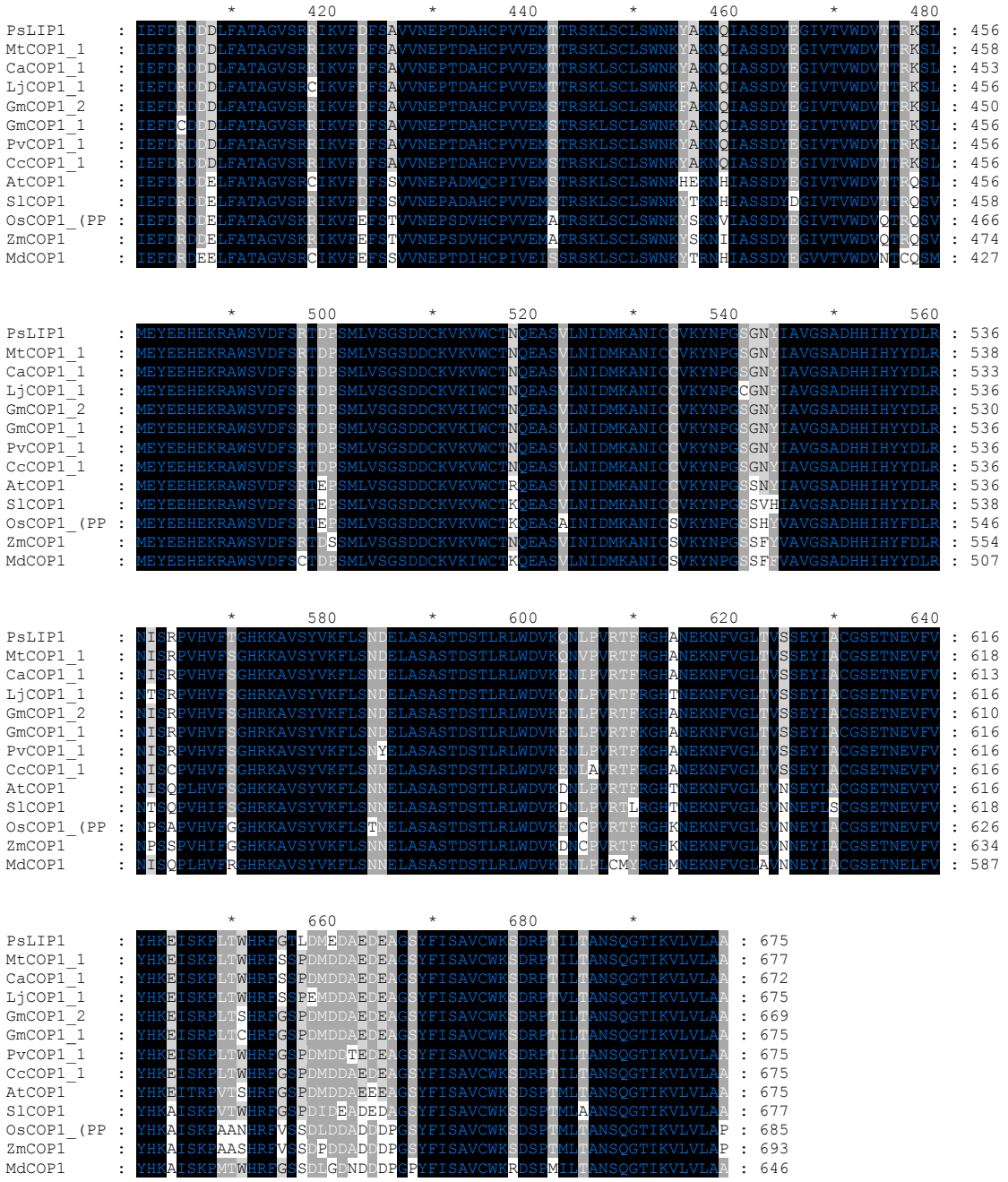

Figure 4.13 Protein sequence alignment of COP1 in different species.

COP1 protein alignment for *Arabidopsis*, tomato, rice, maize, apple and legumes homologs. Locations are indicated for RING Finger domain with red letters, coiled-coil domain in green and for WD40 repeat domain in blue letters. A ClustalX alignment (Thompson et al., 1994) was conducted with full-length predicted protein sequences and adjusted with GeneDoc (Nicholas and Nicholas, 1997). The degree of conservation for the aminoacids are identified with shade degree: black for 100% conserved, dark grey for 80% conserved and light grey for 60% conserved. The abbreviation names followed the previous described species in Table 4.4.

A phylogenetic tree was subsequently constructed from the alignment and presented in Figure 4.14, which indicated the expected distinction between SD and LD legume species. In general, the structure of this tree also supported the known species relationships. Overall, the only anomalies were the apparent closer similarity of common bean to pigeon pea than to soybean, and the unexpected distance of apple, which as a member of the Rosaceae, might be expected to be the most similar to the legume sequences.

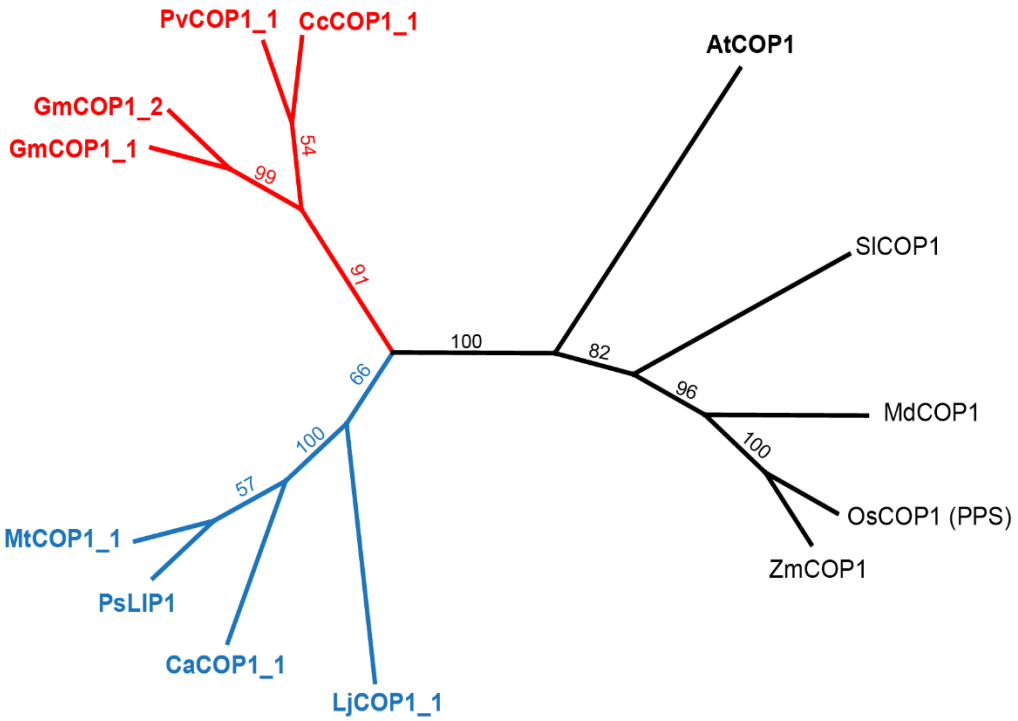

Figure 4.14. Phylogenetic neighbour-joining tree of COP1 protein sequences from selected legume and non-legume species.

The phylogram was constructed from full length predicted protein sequences of COP1 genes identified in Table 4.4 and Figure 4.13. Species names are indicated in Table 4.4. The phylogenetic tree was performed using a neighbour-joining method and with a bootstrap of 1000. Blue colouring indicates Long-Day (LD) legumes ad red colouring indicated Short-Day (SD) legumes.

The phylogenetic analysis and protein alignment suggest that COP1 is highly conserved among species. Sequence similarity normally considered to be closely related to in protein structure, function and substrate recognition as illustrated for the comparison of *Arabidopsis* and human *COP1* orthologs (Uljon et al., 2016). In order to further compare the similarity of LIP1 with COP1, a protein structural prediction was performed in I-TASSER (Yang et al., 2014a) for both proteins (Figure 4.15).

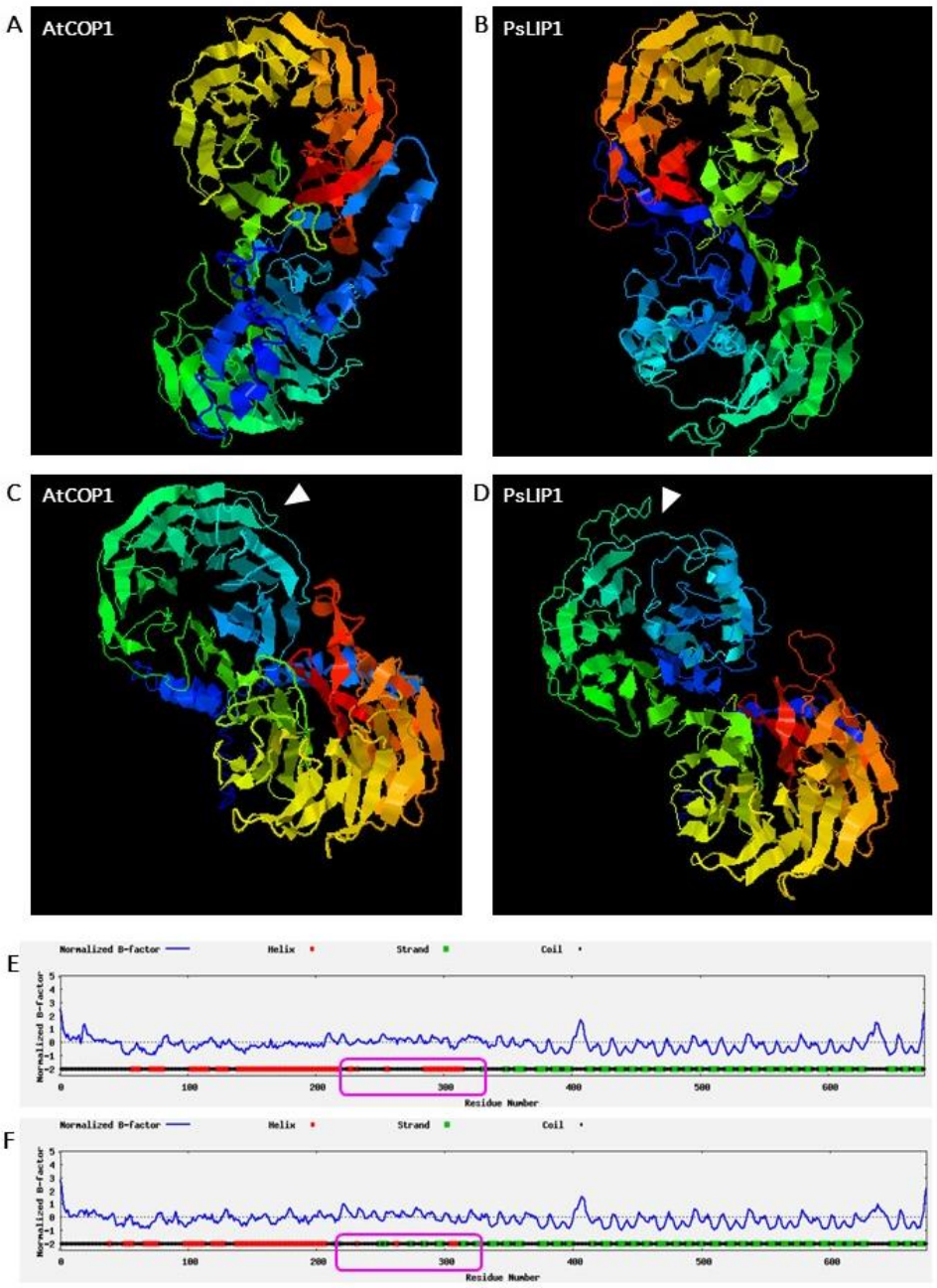

Figure 4.15. Protein structural model prediction for AtCOP1 and PsLIP1.

Protein prediction was performed with I-TASSER that simulates different structural models and predicts the most confident structural protein model based on C-score (C-score is a confidence measurement of the quality of the protein prediction that is in the range of [-5 to 2]. A high C-score implies a high confidence in the prediction). A) AtCOP1 3D protein simulation with a C-score = -2.02. B) PsLIP1 3D protein simulation with C-score = -1.45. C) AtCOP1 3D protein simulation, different angle with a C-score =-2.02. White arrow indicates region with different structure between models. D) PsLIP1 3D protein simulation, different angle with a C-score=-1.45. White arrow indicates region with different structure between models. E) AtCOP1 normalised B-factor (blue line) and secondary structure prediction. Normalised B-factor is a measurement of the mobility of the residues. Values higher than 0 reflect less stable residues in experimental structures. Predicted secondary structure with H in red indicates helix secondary structure, S in green indicates Strand structure and C in black indicates coil structure. Pink box indicates the same differential region between models, white arrow in the

protein predictions. F) PsLIP1 normalised B-factor (blue line) and secondary structure prediction. Normalised B-factor is a measurement of the mobility of the residues. Values higher than 0 reflect less stable residues in experimental structures. Predicted secondary structure with H in red indicates helix secondary structure, S in green indicates Strand structure and C in black indicates coil structure. Pink box indicates the same differential region between models, white arrow in the protein predictions.

Figure 4.15 A and C show that AtCOP1 contains a well-structured helix (blue color in A) that is missing in PsLIP1 (Figure 4.15 B and D). This region corresponds to the N-terminal region of low conservation (Figure 4.13). The C-terminal WD40 repeat domain in AtCOP1 (Red-orange-yellow structure in A) and PsLIP1 WD40 domain (Red-orange -yellow structure in B), highly conserved at the sequence level, also has a very similar structural configuration in both proteins. When comparing both proteins from a different angle (Figure 4.15 C and D), a notable difference is observed in which AtCOP1 has another structure (indicated with white arrow in C and D) that is not so well-constructed in PsLIP1. Although there is a similarity in spatial configuration, the secondary structure in this region is different between proteins (Figure 4.15 E and F indicated with pink box) leading to a poorly-defined circular structure in this region (between 200-350 residues, indicated with pink box). These protein models suggest that the WD40 repeat domain is extremely conserved both in amino acid sequence and secondary and 3D protein structure but, the rest of the protein may have regions of lower similarity in secondary structure and spatial configuration. In order to characterise the WD40 repeat region in detail, a more precise 3D prediction model was performed for both AtCOP1 and PsLIP1 (Figure 4.16).

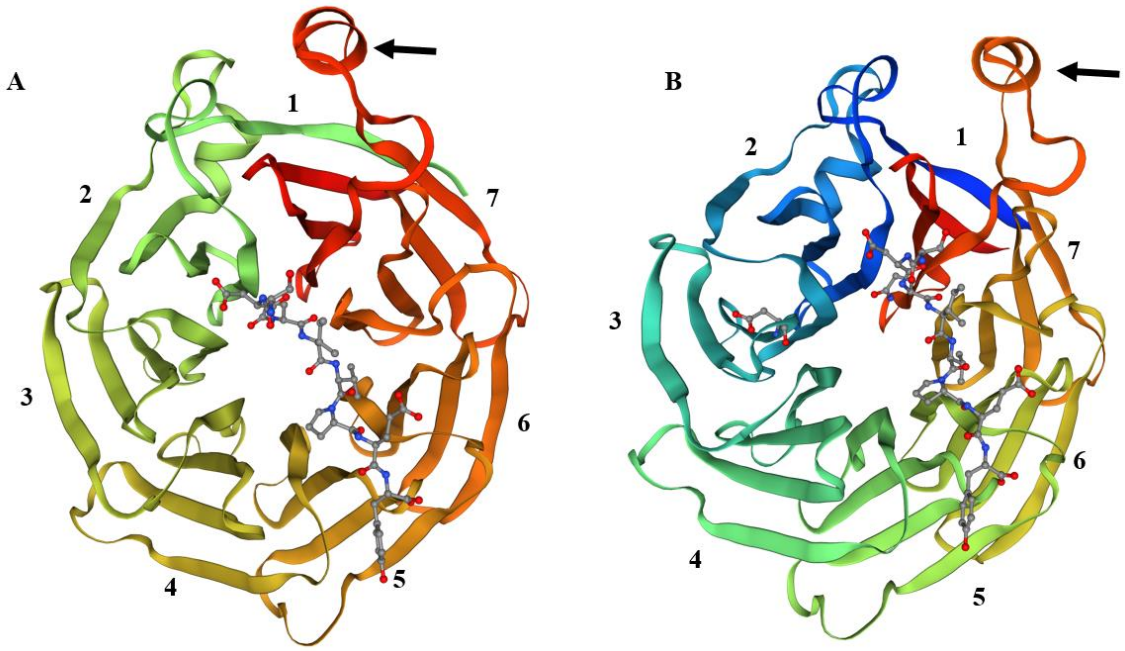

Figure 4.16. Protein structural model prediction of WD40 repeat domain for AtCOP1 and PsLIP1.

Protein prediction was performed with SWISS-MODEL (Waterhouse et al., 2018) that simulates structural homology-models of proteins. Black arrow indicates characteristic loop of AtCOP1, and numbers indicated the seven-blade β-propeller structure. A) AtCOP1 3D protein structural model. B) PsLIP1 3D protein structural model.

Both protein models have highly similar 3D configurations. In Figure 4.16 A, the strands forming the blade β-propeller structure in AtCOP1 (indicated with 1-7 numbers) are more defined than in LIP1 (Figure 4.16 B) but there are still the same number of them. In both models, a characteristic loop specific to *Arabidopsis* COP1 and not present in the human COP1, indicated with a black arrow, is observed in the C-terminal end. These protein predictions confirm a high degree of similarity between LIP1 and AtCOP1 in this WD40 domain, consistent with a highly conserved set of interacting substrate proteins. Similarly, the phylogeny studies and protein predictions suggest that the RING finger domain is highly conserved in pea, both in sequence and structure, suggesting a preserved function of E3 ubiquitin ligase. On the other hand, the coiled-coil domain responsible for SPAs interaction and COP1 homo-dimerization in *Arabidopsis*, is the least conserved region leading to inquire the conservation of the protein interaction domain in the pea LIP1.

4.4 Discussion

The precedent for *COP1* participation in photoperiodic flowering is founded on the differential regulation of CO protein stability in LD and SD in *Arabidopsis* (Jang et al., 2008). COP1 is a direct regulator of CO but it is also known to interact with other components of the pathway, controlling GI protein stability or interacting with FKF1 under specific light conditions. This study has examined the participation of *LIP1*, the *COP1* ortholog in pea, in photoperiod response and flowering regulation in this legume system. Considering that other important functions of *LIP1* are highly conserved with its *Arabidopsis* ortholog, specifically the seedling photomorphogenesis development (Sullivan and Gray, 2000), and the characterization of any flowering role of LIP1 in pea was of high relevance.

4.4.1 Effects of *LIP1* on development and flowering

Unlike other flowering mutants, *COP1* null mutants are lethal and therefore, its characterization has been based in partial loss of function mutants, whether in *Arabidopsis* or for orthologs in other species like rice *PPS,* or pea *LIP1,* where the only known mutant has an impaired function due to partial duplication (McNellis et al., 1994; Podolec and Ulm, 2018; Sullivan and Gray, 2000; Tanaka et al., 2011). We confirm a dwarf phenotype at maturity in *lip1* mutants, consistent with previously observations in pea (Frances et al., 1992; Sponsel et al., 1996) and rice (Tanaka et al., 2011) and the dwarfing effect of *Arabidopsis cop1* (reduction in total plant height and petiole elongation) (Rolauffs et al., 2012). In pea *lip1* dwarf phenotype was explained by a reduction on internode length that also reduced the internode expansion in the mutant (Sponsel et al., 1996). Here we also detect an effect of *lip1* on growth rate and attempt to relate it to node development (Figure 4.4 D).

In this study, the developmental effects of *lip1* have been evaluated, focusing on flowering time and comparisons with previous research on *Arabidopsis* COP1. A key observation is a small but clear effect of *lip1* on flowering. Early flowering of the mutant was seen in both LD and SD conditions and on both NGB5839 and Torsdag genetic backgrounds, but the mutant retained an essentially normal the ability to respond to photoperiod (Figure 4.4 A and Figure 4.5). This differs from the strong SD specific flowering phenotype of the *Arabidopsis cop1* mutant but, it is important to highlight that this characterization was especially focussed on the weak mutant alleles *cop1-4* and *cop1-6* analysing rosette leaves (McNellis et al., 1994; Yu et al., 2008). Remarkably, there is also some literature evidence of an earlier flowering phenotype in *cop1-4*

allele in both LD and SD conditions when total leaf number is studied as flowering measurement (Jang et al., 2008; McNellis et al., 1994). These data support the suggestion that photoperiod responsiveness is variable for each *cop1* allele, and it is also consistent with the phenotype observed in *lip1* mutant, an early flowering phenotype irrespective of photoperiod when NFI is analysed.

The assessment of flowering time (DTF) revealed a loss of correlation with NFI in both genetic backgrounds studied (Figure 4.4 C and Figure 4.5 D), finding in both conditions that *lip1* mutants flowered at a similar time to the LIP1/het genotype class (44 days in LD and 63 days in SD conditions). None of the *cop1* alleles studied in *Arabidopsis* followed this pattern: *cop1-1, cop1-4* and *cop1-6* performed an early date of flowering correlated with early flowering (measured as rosette leaves) in SD (McNellis et al.,1994; Yu et al., 2008). Interestingly, observation data collected from a sowing in a hot summer, represented in Figure 4.6, revealed a reduced difference in NFI between genotypes and an effect in date of flowering in SD between WT/Het and *lip1* plants. The early flowering pattern regarding NFI is observed, and the correlation between NFI and DTF is also lost as previously presented, but the important remark in this data is the effect of higher temperatures in the vegetative development and the induction of flowering. High temperatures are known to induce flowering in *Arabidopsis* earlier than colder temperatures (Balasubramanian et al., 2006; Wigge, 2013). Moreover, a role for *COP1* connecting photoperiodic and ambient temperature regulation of flowering in *Arabidopsis* has also been proposed (Jang et al., 2015). COP1 was described as a regulator of GI protein turnover depending on temperature, affecting *FT* expression through an independent *CO* pathway. This observation is indicative of a possible *LIP1* effect in flowering response to high temperatures in pea and further studies on the matter are of great interest.

The lack of correlation between NFI and DTF observed in the *lip1* mutant prompted an examination of its effect on the rate of node development, particularly as some previous research had reported differences in both in internode length and rate of node development (Sponsel et al., 1996). The data obtained for this thesis supports the conclusion that *LIP1* does indeed influence the rate of development, specifically from week 3 onwards, with a reduction in the rate of node expansion in the *lip1* mutant of up to 20%. This compensated for the earlier flowering node to result in a flowering date similar to WT/Het despite a lower NFI earlier developed node (Figure 4.4 D and Figure 4.5 C). From these experiments, it appeared that the effect of *lip1* on node development is robust, unaffected by the *le-3* mutation, and also not directly related to photoperiod responsiveness. The fact that flowering occurs at the same time in WT and *lip1*

genotypes despite a difference in node of flowering initiation suggests that the critical determinant for flowering initiation is more strongly related to elapsed time than developmental status.

In order to establish the relation between flowering induction and development, *FT* gene expression was analyzed using leaves at an equivalent developmental stage instead of on the same date. *FTb2* was found to be more strongly expressed than *FTa1* (Figure 4.7), as previously reported by Hecht et al., (2011). Interestingly, both *FTb2* and *Fta1* genes were more highly expressed at node 13 in *lip1* than WT, node at which the mutant develops the first flower but WT/Het is still vegetative, suggesting that the induction of flowering has already been initiated in the mutant.

4.4.2 *LIP1* genetic interactions

COP1 has been characterised as a multifunctional protein able to interact with many other components forming multimeric protein complex with high regulatory capabilities (Kim et al., 2017). COP1 is highly regulated by light trough the action of many photoreceptors like PHYA, and it is able to integrate light signalling to the photoperiodic flowering network, through regulation of CO protein (Podolec and Ulm, 2018). It is also participating in flowering regulation in a more indirect manner through the control of GI protein stability when forming a regulatory complex with ELF3, connecting circadian clock regulation to the pathway (Yu et al., 2008). Therefore, *COP1* acts as a decisive regulatory component in the control of flowering time. This section has examined genetic interactions of *lip1* with other pathway components to explore whether other functional relationships are maintained even in the absence of a role for *CO*. Components like *PHYA*, *LATE1 (PsGI)* or *HR (PsELF3a)* are clearly important, and the question of whether *LIP1(PsCOP1)* might interact with them genetically is therefore of interest.

In pea, *PHYA* has well-known effects on light response and flowering time (Weller et al., 1997a, 2004). Specifically, the gain of function mutation *phyA-3D* shows displayed exaggerated photomorphogenic responses, early-photoperiod independent flowering and dwarfism, (Weller et al., 2004), and the similarity of these effects to those of *lip1* suggested that both genes might participate in a common genetic pathway for flowering.

The genetic interaction study between *LIP1* and *PHYA* reveals a genetic connection in different biological processes in pea: flowering time and photomorphogenesis development (Figure 4.8)(Figure 4.9) The flowering characterization found that double mutant (*lip1 phyA-1)* flowered as late as *phyA-1* single mutants and had a closely similar developmental phenotype (Figure 4.8),

indicating that loss of *lip1* does not substantially affect the action of PHYA. As the weak early-flowering phenotype of *lip1* is not seen in the *phyA-1* background*,* this might formally suggest that *phyA* is epistatic to *lip1* and imply that they participate in the same genetic network to control flowering, and also that *PHYA* is acting downstream of *LIP1* in flowering regulation. Previous research in *Arabidopsis* described blue light regulating COP1 activity and effect in flowering regulation (Lee et al., 2017; Zuo et al., 2011). However, a regulatory feedback connection between PHYA and COP1 in *Arabidopsis* has been also described, but the implications of this for the mechanism of flowering time are not well understood (Xu et al., 2016).

The study of photomorphogenesis response revealed a different genetic interaction since the double mutant (*lip1 phyA-1)* displayed an intermediate phenotype under FR light, more similar to WT (Figure 4.9). In this experiment, *phyA-1* mutants developed a common skotomorphogenic phenotype with long internodes and therefore elongated hypocotyls, with a large and angled apical hook and, closed and small undeveloped leaves. The *lip1* single mutant developed expanded leaves and short internodes, resembling a WT light-grown phenotype but with no chlorophyll accumulation. This distinctive skotomorphogenic development of *lip1* mutants was previously reported by Weller et al., (2009b). The study of photomorphogenic response in mutants for other *COP1* orthologs, like *PPS* in rice, indicates that a suppression of internode length and increased leaf/cotyledon expansion are distinctive phenotypic consequences of reduced *COP1* activity during photomorphogenesis (Tanaka et al., 2011). The double mutant (*lip1 phyA-1)* displayed a more similar internode length and leaf expansion area to the single mutant *lip1* (especially similar in leaf expansion area)*,* consistent with the interpretation that *LIP1* is largely epistatic to *PHYA* for this response*.* In this respect, the fact that the double mutant is still somewhat intermediate and similar to WT could reflect some residual activity of *LIP1*, considering that *lip1* is probably only a partial impaired mutant (Sullivan and Gray, 2000). Overall, the *LIP1* and *PHYA* interaction study confirms a genetic interaction for both traits, but the contrasting nature of these interactions is consistent with there being distinct mechanistic basis for the interaction in the two cases. In this respect, it is likely to be relevant that even in *Arabidopsis*, the COP1-PHYA relationship is known to involve at least two distinct interactions that constitute a regulatory feedback: a well characterised inhibition of *COP1* activity by light-activated PHYA, and a light induced degradation of PHYA protein degradation mediated by COP1 (Podolec and Ulm, 2018; Seo et al., 2004).

Returning to the focus on flowering, one elaboration of the *Arabidopsis* model has suggested that *COP1* is able to participate in flowering regulation through a second distinct and partially *CO*-independent route, in which it associates with ELF3 as an adaptor in a protein interaction with GI

that contributes to regulation of GI protein stability (Yu et al., 2008). The genetic characterization in *Arabidopsis* indicates that *GI* acts downstream of *COP1* and *gi* is epistatic to *elf3* (Koornneef et al., 1991; Yu et al., 2008). Published research describes the GI-COP1 interaction occurring in the N-terminal region of COP1 protein (RING finger domain and Coiled-coil domain) which is in general less conserved (as demonstrated above for LIP1, Figure 4.2) which could imply some degree of functionality and/or interaction capability impairment (Yu et al., 2008). In this study of flowering response, the double mutant *lip1 late1-2* revealed an intermediate phenotype regarding NFI and RN (Figure 4.10) which suggests an additive effect and independent regulation of node development and flower initiation in pea. In this same experiment, date of flowering represented an additive phenotypic effect, with extremely dwarf plants that flower even later, combining the two traits of the single mutants and giving support to the independent action of *LIP1* and *LATE1* in flowering time regulation in pea. The study of double mutant *late1-2 hr* illustrated a similar pattern, an intermediate phenotype for NFI and RN (Figure 4.12), indicating again an additive effect of the two genes and independent action of *LATE1* and *HR* in flowering regulation in pea. Finally, the study of *lip1* in an *HR/hr* background indicated and additive but subtle effect, suggesting some functional redundancy between *LIP1* and *HR* (Figure 4.11). In this case the double mutant *lip1 h*r did not display an intermediate phenotype for NFI but did for RN, suggesting a more distinctive role in node developmental control from *LIP1*. Overall, although each component affects photoperiod response in pea, it is implied they are involved in the pathway regulation in different ways, and that the effect of *LIP1* on flowering in pea is relatively minor.

4.4.3 High conservation of *LIP1*

The phylogeny study of *LIP1* indicates high level of conservation in this gene both in the structure, finding 13 exons and 12 introns in all the orthologs sequences and also conservation in the nature of the mutations, commonly finding lethal mutants in different orthologs (McNellis et al.,1994; Tanaka et al., 2011). The conservation level extends to the protein level, finding high conservation in aminoacid sequence, more than 89% similarity between legumes sequences and up to 61% conservation level in other plant species. The protein structure of LIP1 revealed a high conservation in the three protein domains finding the coiled-coil domain the least conserved, followed by the RING finger domain and being the WD40 repeat the most conserved domain (Figure 4.13). The analysis of protein structure model prediction also confirms a significant conservation level, in aminoacid sequence and even in configuration in the space in this WD40 domain (Figure 4.15)(Figure 4.16) suggesting a preservation in functionality in the WD40 domain,

commonly associated with the interaction of substrates and photoreceptors (Hoecker, 2017; Uljon et al., 2016). More recently this domain was related with a competitive binding site formed by VP peptide motif able to mediate in photoreceptor and other interactors affinities with COP1-WD40 domain (Lau et al., 2019; Ponnu and Hoecker, 2021). The conservation in this protein domain in LIP1 suggests a conservation in this competitive binding mechanism of great interest to understand the molecular interactions of LIP1 in the pea system.

4.4.4 Conclusions and future directions

The phylogenetic study presents a high level of conservation among *COP1* orthologs, specifically between legumes, with conservation extending to sequence structure, nature of mutants, protein structure and domains and, flowering response and photomorphogenesis development. The flowering and plant development study indicates that *LIP1* is participating and affecting the rate of plant development and show that a photoperiod response is retained but not affecting the date of flowering. The non-functional partial duplication in pea *LIP1* does confer early flowering in both photoperiods, similar to some *Arabidopsis* literature and rice *PPS* (*COP1 ortholog*) (Jang et al., 2008; Tanaka et al., 2011). The mutant has a slower rate of development which leads to flowering occurring at the same time in WT and *lip1* genotypes despite a difference in node, indicating that the critical determinant of flowering initiation is related more strongly to elapsed time than developmental status.

It is important to consider the nature of the mutation in the interpretation of results since there can be residual function of *LIP1*. Another important consideration is the ability to identify heterozygote and WT homozygote genotypes in the progenies because it could mask some greater differences between genotypes. In *Arabidopsis*, the main function of *COP1* is related with its protein interaction abilities, and an analysis of physical interactions, could in future provide more insight into the effects of *LIP1* on vegetative development and flowering. Such studies might focus on the potential of LIP1 to form homo-dimers and to interact with FKF1, which are both important features of *COP1* function in *Arabidopsis*. As featured in other chapters in this thesis, the use of another legume model system for isolation and functional comparison of *COP1* orthologs could also be valuable.

Chapter 5 - Examining the potential role of *FKF1* and the interactions of FKF1-GI complex in pea flowering

5.1. Introduction

Many photoperiod-response flowering genes are responsible of the variation in geographical adaptation and flowering response. Therefore, characterizing the known key flowering genes from *Arabidopsis* genetic pathway in other crops and plant species is of great interest. *FKF1 (FLAVIN-BINDING, KELCH REPEAT, F-BOX, 1)* and *GI (GIGANTEA)* are main components of the transcriptional regulatory genetic network in *Arabidopsis*, where their interaction in some photoperiodic conditions is able to regulate expression of flowering decisive genes like *CO* or *FT* (Song et al., 2014, 2015). The recent research on *Arabidopsis FKF1* and *GI* molecular mechanism regulating flowering describes diverse pathways, not always including *CO* participation, but always regulating *FT* expression and inducing flowering in LD, supporting their key role in flowering time. Some of these mechanisms include *GI* participation in microRNA172 regulation (Jung et al., 2007), mediating gibberellin (GA) responses by *FKF1* (Yan et al., 2020) or the direct regulation of *FT* by the FKF1 or GI direct binding to *FT* promoter regions (Sawa and Kay, 2011).

These *CO*-independent regulatory mechanisms could be the main controlling pathways for flowering time in species lacking the *CO* role, like temperate legumes. Therefore, the characterization of *FKF1* and *GI* in legume models, specially in LDP like pea, could explain the flowering genetic components, their genetic interaction and explain the interconnection in the molecular network.

5.1.1 *FKF1 (FLAVIN-BINDING, KELCH REPEAT, F-BOX, 1)*

5.1.1.1 FKF1 first characterization: light implications in Arabidopsis

FKF1 gene was first isolated in *Arabidopsis* as a late-flowering mutant in LD that retained responsiveness to vernalization and gibberellin (Nelson et al., 2000). The initial study of the mutant revealed a LD-dependent late-flowering phenotype similar to *gi* mutants suggesting the function of *FKF1* might be related to *GI,* potentially participating in photoperiod response and circadian clock regulation (Nelson et al., 2000; Sawa et al., 2007). The mutant phenotype included effects on hypocotyl elongation, a common light-dependent phenotype of photoreceptors (Nelson et al., 2000). *FKF1* sequence analysis suggested a photoreceptor role related with

ubiquitin degradation (Nelson et al., 2000), and advanced studies with the mutant revealed its primary function in light signalling.

The study of *FKF1* expression revealed an increase during plant development and localisation in leaves, sepals and root tips (Nelson et al., 2000). In leaves its expression was reported to be rhythmic with peaks of expression around ZT10 in LD and ZT7 in SD (Imaizumi et al., 2003; Nelson et al., 2000). These peaks of expression seemed to be influenced by the quality and quantity of light, especially blue and red light, acting as direct regulators of *FKF1* (Imaizumi et al., 2003).

FKF1 contains a LOV (Light, Oxygen, Voltage) domain which has the ability to bind a flavin mononucleotide chromophore (Imaizumi et al., 2003). The LOV domain is effectively a flavoprotein photoreceptor for blue light and confers blue-light activation on *FKF1* function. Further characterization revealed that the role of *FKF1*, particularly in flowering regulation, is independent of other blue-light photoreceptors such as cryptochromes or phototropins, characterizing its role as a self-sufficient blue-light photoreceptor (Imaizumi et al., 2003; Sawa et al., 2007). All the regulatory roles of *FKF1* are dependent of light activation creating a direct light-dependent control of flowering time which has been implicated in the light-directed regulation of *CO* expression and CO protein stability that leads to *FT* regulation (Hwang et al., 2019; Song et al., 2012).

5.1.1.2. FKF1 participation in flowering regulation at multiple levels

FKF1 expression is regulated by circadian clock and was shown to have a similar diurnal pattern to *GI* expression, further pointing to a possible functional interaction between these genes (Imaizumi et al., 2003; Sawa et al., 2007; Sawa and Kay, 2011). The *Arabidopsis fkf1* mutant was characterised with low levels of *FT* expression in LD conditions explaining the late flowering phenotype (Song et al., 2012). Observing that *FT* and *CO* expression were altered in *fkf1* mutant, *FKF1* function was firstly considered to have a transcriptional regulatory role in the photoperiod pathway together with *GI* (Imaizumi et al., 2003). Further studies showed that FKF1 protein was a light-dependent interactor of GI, mainly acting at dusk in LD, forming the FKF1-GI complex which actively regulates flowering gene induction by targeting repressive transcription factors for degradation (Ito et al., 2012a; Song et al., 2012). More specifically, this mechanism regulates the stability of CDF1 (CYCLIC DOF FACTOR 1) and prevents it from repressing *CO* and *FT* transcription under LD, leading to flowering induction. The three components (FKF1, GI and CDF1) interact physically though different specific domains in a blue-light dependent manner (Hwang et al., 2019; Ito et al., 2012a;

Sawa et al., 2007; Song et al., 2012). More detailed recent studies have described *fkf1* mutant under high R:FR "lab" LD conditions and low R:FR "natural" LD conditions, finding that the mutant retains *FT* expression in the morning of natural LD leading to an early flowering phenotype in these conditions (Hwang et al., 2019). Furthermore, it was described that the difference in daily temperature and R/FR ratio were the main controllers of the differences in flowering time between lab and natural LD conditions.

In addition to FKF1 physical protein interaction with GI and CDFs to regulate *CO* transcription, FKF1 is also able to interact with and regulate a wider range of other flowering pathway components and its involvement in flowering regulation is also thought to include post-transcriptional effects through the interaction with COP1. FKF1 is able to interfere in COP1 dimerization and function, blocking the *COP1*-dependent degradation of CO protein in LD (Lee et al., 2017, 2019). It also appears that FKF1 acts to stabilize CO protein in the afternoon also through a direct protein interaction. This interaction occurs via the FKF1 LOV domain, is dependent of blue light and it may take place at the *FT* promoter region (Andrés and Coupland, 2012; Hwang et al., 2019; Ito et al., 2012a; Song et al., 2012). *FKF1*-dependent promotion of flowering in LD is also reported to be associated with Gibberellin (GA) signalling and its ability to physically interact with and regulate the stability of DELLA (aspartic acid [D]–glutamic acid [E]–leucine [L]–leucine [L]–alanine [A]) proteins (Yan et al., 2020).

Overall, *FKF1* participation in *Arabidopsis* flowering regulation can thus be described as five distinct roles: 1) promoting *CO* transcription by direct regulation of CDFs, 2) directly stabilizing CO protein in the LD afternoon 3) interfering with COP1 function, also leading to CO stabilization. 4) interacting with the *FT* promoter region directly to promote its expression. 5) de-stabilizing DELLA protein leading to flowering promotion (Hwang et al., 2019; Lee et al., 2017, 2019; Sawa et al., 2007; Sawa and Kay, 2011; Yan et al., 2020).

5.1.1.3 FKF1 protein structure and interactions

The characterization of FKF1 protein revealed three functional domains: a LOV domain as mentioned above; an F-box domain characteristic of ubiquitin ligase subunits and involved in substrate recognition; and a Kelch repeat motif which also acts in protein-protein interactions and substrate recognition (Imaizumi et al., 2005; Nelson et al., 2000). Each domain has particular characteristics as shown in Figure 5.1. Blue-light absorption through the flavin mononucleotide chromophore in the LOV domain promotes interaction with other flowering-related proteins like

GI or CO, or self-interaction (Pudasaini et al., 2017; Song et al., 2012). The study of FKF1 quaternary conformation *in vitro* also revealed FKF1 can form homodimers, which feature an antiparallel conformation of LOV domains (Ito et al., 2012a; Nakasako et al., 2005; Nakasone et al., 2010). The F-box domain, functions as the ubiquitin ligase unit when associated in ubiquitin ligase protein complex. Finally, the Kelch repeat domain is also assisting in target identification and is key for interaction with several different proteolytic targets. One of the most reported proteolytic target is CDF1 which acts as repressor of *CO* transcription. This interaction requires the formation of the FKF1-GI complex and in the case of GI, this interaction is light-dependent, and it is achieved between the LOV domain of FKF1 and the N-terminal region of GI in specific conditions (Sawa et al., 2007). The interaction with COP1 also takes place through the F-box and Kelch domains (Lee et al., 2017). FKF1-COP1 interaction does not affect COP1 protein stability but impairs COP1 function by disrupting COP1 homo-dimerization (Lee et al., 2017, 2019).

Some *FKF1* homologs like ZEITLUPE (ZTL) and LOV KELCH PROTEIN 2 (LKP2) proteins, have similar protein structure. For instance, they contain a well-conserved LOV domain (Baudry et al., 2010; Zoltowski and Imaizumi, 2014). The structure conservation is also present in the F-box domain with a well-characterised F-box ubiquitin mechanism, specifically the ZTL's SCF (Skp/Cullin/F-box) complex via interaction with ASK1 (Apoptosis Signal-Regulating Kinase 1), which links different targets to the ubiquitin unit directing the proteolysis of many circadian clock components (Han et al., 2004). Similarly, the F-box domain of FKF1 is responsible for the degradation of CDF1 in *Arabidopsis* (Imaizumi et al., 2005). The *FKF1* homologs *ZTL* and *LKP2* are also involved in CDF regulation and can interact with GI, and are also able to interact with FKF1 through its Kelch repeat domain and keep it localised in the cytosol (Baudry et al., 2010; Song et al., 2013; Takase et al., 2011).

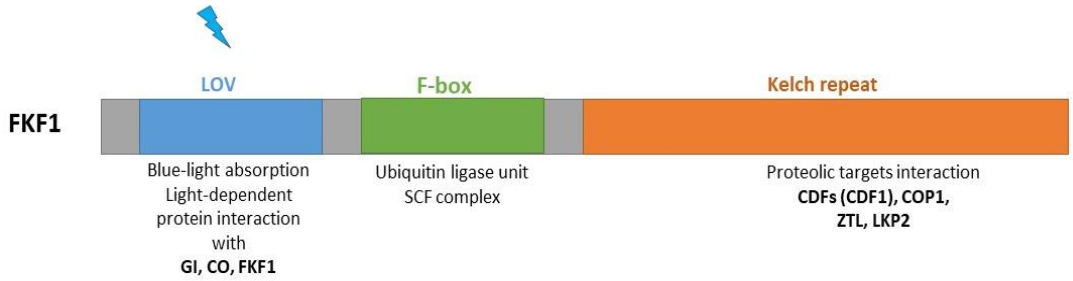

Figure 5.1 FKF1 protein domains and interactors.

FKF1 protein contains three main domains: LOV domain (blue), a F-box domain (green) and a Kelch repeat domain (orange). The LOV domain is characterised as the blue-light absorbance site and where specific light protein-protein interactions take place with proteins like GI, CO or homodimerization with FKF1. The F-box domain participates in ubiquitin ligase activity when forms the SCF complex. The Kelch repeat domain is characterised as the interactive region between FKF1 and different targets for proteolysis like CDFs, including the most characterised CDF1.

5.1.1.4 FKF1 orthologs

The characterization of *FKF1* orthologs in diverse species has indicated a high level of conservation in the amino acid sequence of the proteins, which in some cases, has also been associated with a conservation in function. Most *FKF1* orthologs appear to show a conserved diurnal pattern of regulation that is responsive to circadian clock and highly regulated by light, specifically blue light. For instance, the rice ortholog *OsFKF1* retains circadian rhythmicity and blue light regulation of expression and is able to control the expression of diverse rice flowering genes, as in *Arabidopsis*. OsFKF1 also participates interacting with OsGI and OsCDF1, but with an opposite regulatory output; i.e., flowering is promoted in SD trough the GI-CO-FT homolog pathway with changes in the expression of the rice florigens *Hd3a* and *RFT1* (Han et al., 2015; Hayama et al., 2003; Sawa et al., 2007). Interestingly, *OsFKF1* is also able to induce flowering independently of photoperiod by an autonomous pathway (Han et al., 2015).

In other species characterization has been more limited but does indicate some dissimilarities with *AtFKF1*. For example, in onion or tomato (*AcFKF1* and *SlFKF1* respectively), circadian patterns of expression are present but with some variation regarding daylength response in the case of onion (Taylor et al., 2010), or suppression of expression in response to blue-light in tomato (Shibuya et al., 2021). In this case, *SlFKF1* expression was suppressed by blue light and the low *FKF1* expression has an effect in flowering displaying a late-flowering phenotype in an RNA-interference supressed line, even though flowering is not controlled by photoperiod in tomato (Shibuya et al., 2021). Soybean *FKF1* homologs *GmFKF1* and *GmFKF2* are highly similar to *AtFKF1* (Li et al., 2013) and

show diurnal patterns of expression. Ectopic expression of these genes in *Arabidopsis* promoted flowering in SD (Li et al., 2013).

5.1.2 *GIGANTEA (GI)*

5.1.2.1 Characterization in Arabidopsis

In *Arabidopsis*, light signalling is initiated by light perception by photoreceptors and interacts with the circadian clock to promote flowering time in LD (Valverde et al., 2004). One of the main links between the circadian clock and flowering time regulation appears to be GIGANTEA (GI), a key element which itself participates in the clock and also regulates the CO-FT module (Lee et al., 2005; Mishra and Panigrahi, 2015; Suárez-López et al., 2001).

The initial identification of *GI* in *Arabidopsis* involved the characterization of late flowering *gi* mutants (Koornneef et al., 1991; Rédei, 1962) which in addition to flowering time control (Fowler et al., 1999; Mishra and Panigrahi, 2015; Park et al., 1999) include influences on starch accumulation (Eimert et al., 1995), drought tolerance (Riboni et al., 2013), salt tolerance (Park et al., 2013), cold tolerance (Fornara et al., 2015), microRNA regulation (Jung et al., 2007), hormone signalling (Nohales and Kay, 2019), light signalling (Martin-Tryon et al., 2007), circadian clock control (Lee et al., 2005) and among others.

The analysis of multiple *gi* allele mutants helped to understand the function of this gene, finding most of the mutants to have a phenotype in hypocotyl length, altered circadian rhythmicity and late flowering phenotype in LD (Mishra and Panigrahi, 2015). At the molecular level, GI was identified as a large (1173 amino-acid) protein (Fowler et al., 1999) of unclear function, predicted to contain 11 transmembrane domains. However, its action is understood to be mainly localised in the nuclei, where it is known to form light-dependent nuclear bodies (NBs) with COP1 facilitated by other circadian clock-related proteins such as ELF3 and ELF4 (Huq et al., 2000; Kim et al., 2013c; Yu et al., 2008).

5.1.2.2 GI expression and regulation

The precise control of *GI* gene expression and protein stability through the daily cycle is essential for its correct function in circadian clock, photoperiod responsiveness, light signalling and other processes (Mishra and Panigrahi, 2015; Nohales and Kay, 2019). A major regulator of *GI* expression is the circadian clock itself, in which it participates through multiple feedback loops of regulation

(Kawamura et al., 2008; Park et al., 1999). *GI* is actively transcribed during the day and has a peak of mRNA accumulation around midday, when its direct repressor *CCA1 (CIRCADIAN CLOCK ASSOCIATED 1)* is being repressed by *TOC1 (TIMING OF CAB EXPRESSION 1)*(Lu et al., 2012). During the night, repressive effects of *CCA1* and *ELF3* predominate (Fowler et al., 1999; Hayama and Coupland, 2004). However, other factors can impact on this clock regulation, including sucrose levels, salt stress or cold temperatures which can alter *GI* rhythmicity (Cao et al., 2005; Dalchau et al., 2011; Fornara et al., 2015). Another important regulator of *GI* is light, and both quality and quantity of light influence its expression (Mishra and Panigrahi, 2015; Paltiel et al., 2006).

In addition to transcriptional rhythms, it has also been reported that the GI protein has an independent cyclic pattern of regulation, suggesting another layer of regulatory control that refines GI protein level and activity (David et al., 2006). GI protein level is regulated by photoperiod, via a signalling network that controls its degradation by the 26S proteosome in the dark (David et al., 2006). Another component of its protein regulation involves the flowering pathway and circadian clock, since COP1 is able to ubiquitinate GI and regulates its protein abundance when interacting with ELF3 (Yu et al., 2008). A number of different plant stresses are also reported to influence GI protein regulation. For instance, heat shock induces the SUMOylation of GI protein, preventing protein degradation and leading to early flowering under heat stress (López-Torrejón et al., 2013). In contrast, under saline conditions GI protein degradation is enhanced leading to a delay of flowering (Park et al., 2013).

5.1.2.3 GI roles in plant development: light signalling and circadian clock

The elongated hypocotyl of some *gi* mutant alleles growing under red light indicated a *GI* participation in light signalling (Huq et al., 2000). Analysis of the interaction with phytochromes suggested that *GI* could be acting downstream of both PHYA and PHYB in this response but independently of circadian clock regulation (Oliverio et al., 2007).

The circadian clock was identified as an interconnecting network of proteins maintaining feedback loops of regulation, where *LHY (LATE ELONGATED HYPOCOTYL)* / *CCA1* and TOC1 are the main components of a central regulatory loop (de Montaigu et al., 2010). Analysis of circadian periods in various *gi* mutants suggested a role in period length control (Park et al., 1999), while studies of natural variation for circadian leaf movement also implicated *GI* as a candidate in the circadian system (Swarup et al., 1999). This was confirmed by the demonstration that expression of the core circadian clock genes *CCA1* and *LHY* was affected in *gi* mutants under different photoperiods

(Fowler et al., 1999). *GI* appears to be an important regulator of *TOC1*, together with the blue-light photoreceptor *ZTL*, and may be a major site for light input into the clock (Kim et al., 2007; Locke et al., 2005).

Study of the effect of *gi* mutants on clock properties have also shown that *GI* contributes to the regulation of period length and amplitude, and also is responsible for the clock rhythmicity start in early development (de Montaigu et al., 2010; Huang et al., 2012a; Lu et al., 2012; Park et al., 1999; Salomé et al., 2008). A further important role of *GI* is as a component that mediates temperature compensation (Gould et al., 2006), the effects of sucrose signalling (Dalchau et al., 2011) and the interaction with iron homeostasis in the maintenance of circadian rhythms (Chen et al., 2013).

5.1.2.4 GI participation in flowering time regulation

Most of the known *gi* mutant alleles develop a late flowering phenotype under LD and expression analyses revealed an important effect of *GI* on the expression of *CO*, the key flowering regulator in *Arabidopsis* (Koornneef et al., 1991; Rédei, 1962; Suárez-López et al., 2001). In this respect the rhythmic regulation of *GI* is important, as explained above in section *5.1.2.2*, because it allows *GI* expression to coincide with *FKF1* leading to the well-described CDF regulation by the GI-FKF1 complex (Fornara et al., 2009; Mishra and Panigrahi, 2015; Sawa et al., 2007).

In parallel with this mechanism, *GI* may also influence flowering in other ways. For example, it appears to stabilize the *FKF1* homolog *ZTL*, which participates as a photoreceptor in circadian clock regulation (Kim et al., 2007). *ZTL* mediates photoperiodic flowering in many ways, some of them redundant to *FKF1*, and it is able to interact with GI (Fornara et al., 2009; Song et al., 2014). The GI-ZTL interaction participates in flowering control due to the ability of ZTL to directly interact and regulate CO protein stability (Kim et al., 2007; Song et al., 2014).

GI is also involved in regulation of flowering via post-transcriptional mechanisms. GI is commonly localised in the nucleus but shows a highly dynamic sub-localization which is thought to have an important role in its function. GI can form light-dependent nuclear bodies with diverse proteins as a sequestration regulatory mechanism directed by specific post-translational modifications (Huq et al., 2000; Kim et al., 2013c). Some well-described GI nuclear body formations with flowering regulatory impact are the one formed with ELF4 that leads to suppress *CO* expression (Kim et al., 2013c); or the ELF3-mediated COP1-GI interaction in nuclear bodies that leads to GI protein regulation and degradation (Yu et al., 2008). Furthermore, GI has been reported to act as

a negative regulator of CO stability both by direct interaction GI-CO and indirectly through FKF1 interaction (Krahmer et al., 2019; Song et al., 2014). GI has also been shown to interact and regulate many *FT* repressors like SHORT VEGETATIVE PHASE (SVP) or TEMPRANILLO (TEM1) and (TEM2), to influence *FT* expression independently of *CO* (Castillejo and Pelaz, 2008; Osnato et al., 2012).

More interestingly for legume models, there has been characterization of a *GI* flowering regulatory role independent from the CO-FT module. Some of the *CO*-independent mechanisms include the regulation of microRNA172 by GI which is able to regulate the maturation of microRNA172 rather than the transcription, leading to the induction of *FT* expression and the control of photoperiodic flowering with the absent of a functional *CO* or any type of *CO* regulation (Jung et al., 2007). Another *CO*-independent pathway involves the apparent direct regulation of *FT* expression by GI when recruited to the *FT* promoter region (Pin and Nilsson, 2012; Sawa and Kay, 2011).

5.1.2.5 GI orthologs and LATE1 as GI ortholog in Pea

Several of the important roles of *Arabidopsis GI* in light signalling, circadian clock and flowering time control are known to be conserved in other species (Mishra and Panigrahi, 2015). The better-studied examples are from crop species, both monocots like barley, maize, rice and wheat, and dicots like tomato, morning glory, potato and legumes such as soybean or pea. The identification of a *GI* ortholog in the liverwort *Marchantia polymorpha* shows its deeply conserved nature (Kubota et al., 2014). The expression pattern of *GI* ortholog genes with respect to circadian and diurnal rhythms has been shown to be similar to *Arabidopsis*, suggesting a conserved role in flowering regulation with examples in barley *HvGI* (Dunford et al., 2005), wheat *TaGI* (Rousset et al., 2011; Xiang et al., 2005), onion *AcGI* (Taylor et al., 2010) or rice *OsGI* (Izawa et al., 2011). But, *OsGI* performs as a suppressor of flowering in LD in rice described by overexpression experiments when *OsGI* regulates the rice *CO* homolog *Hd1*, which acts contrary to the *Arabidopsis* model and inhibits flowering in LD (Hayama et al., 2002, 2003). In barley, it has been suggested that expression of *HvGI* during dark periods could explain the early flowering in some cultivars (Zakhrabekova et al., 2012). Of two *GI* homologs present in maize (*Zea mays)* there is evidence that one (*ZmGI1)* has a role as flowering repressor in LD with increased expression of *FT-like* and *CO-like* genes in the mutant, involving a *CO-like* regulatory flowering pathway with *GI* participation (Bendix et al., 2013).

GI orthologs described in other dicot species have been linked to other processes. The tomato *SlGI* seems to be inhibiting seed germination by promoting dormancy (Auge et al., 2009), and the sweet potato *IbGI* which conserves regulatory roles in flowering and circadian rhythm but also in high temperature, drought, salt and cold stress (Tang et al., 2017). In SD models like morning glory, *PnGI* is regulated by the circadian clock and participates in flowering by having a supressing effect in *FT (PnFT)* expression when overexpressed (Higuchi et al., 2011). In other species, like Longan tree a subtropical fruit tree, *DlGI* was suggested to be a conserved component of flowering regulation, by participating in floral bud differentiation and floral initiation (Huang et al., 2017).

The functional characterization of *GI* orthologs in legumes is somewhat more detailed due to the existence of loss of function mutants in both soybean and pea. In soybean*, E2* locus is the ortholog of *GI* and one of the genes explaining most of the natural flowering time variation. *E2* also contributes to geographical adaptation participating in seed maturity (Watanabe et al., 2009, 2011). *E2/GmGIa* mutants display early flowering in SD and regulate *FT* paralogs in a similar manner to the rice SD model. There is higher expression of *FTs* in the *e2* mutant lines (Watanabe et al., 2011), and was later identified as able to regulate *GmFT2a* (florigen gene in soybean). More research in this area described other *GI* orthologous genes in soybean, adopting a new labelling strategy: *GmGI1* (which has two alternative splicing forms named *GmGI1α* and *GmGI1β), GmGI2* and *GmGI3* (Li et al., 2013). Not all of the homologous genes had similar expression rhythmicity to *AtGI*, finding *GmGI2* the most similar with regulation from circadian clock and photoperiod. Otherwise, *GmGI1* and *GmGI3* differed in their response to light regulation (Li et al., 2013).

In the LDP legume pea the *LATE1 (LATE BLOOMER 1)* locus was identified as the *AtGI* ortholog, on the basis of six induced mutant alleles. The *late1* mutants were isolated based on their late-flowering phenotypes under LD conditions, and were also shown to affect seedling photomorphogenesis, and circadian gene expression (Hecht et al., 2007; Liew et al., 2009), maintaining rhythmic expression patterns like in *Arabidopsis* and being able to control expression of *FT-like* genes and as a final output, regulating the mobile flowering signal. Information on *LATE1(PsGI)* expression in pea has been supplemented by results from another LD legume species, *Medicago truncatula*, where *MtGI* expression is regulated by temperature and light (Paltiel et al., 2006) and shows a distinct diurnal pattern of expression between LD and SD, consistent with a role in flowering time regulation (Thomson et al., 2019).

5.1.3 FKF1-GI interaction and protein complex role

The ability of FKF1 and GI to interact in specific light conditions is crucial for a precise control of flowering induction through the transcriptional pathway. In *Arabidopsis*, there are tightly regulated expression peaks of *GI* and *FKF1* towards the end of the day in LD (around ZT10), which facilitates a temporal coincidence and interaction of the two proteins (Sawa et al., 2007; Song et al., 2012, 2013). The complex FKF1-GI formed mediates CDF degradation, leading to the activation of *CO* expression. In contrast, in SD, the expression peaks of *GI* and *FKF1* do not coincide, preventing the complex formation and CDF degradation, thus maintaining CDF repression of *CO* transcription (Mishra and Panigrahi, 2015; Sawa et al., 2007; Song et al., 2012, 2013). In LD when the expression of FKF1 and GI proteins coincides, as represented in Figure 5.2, the interaction takes place between the light-activated FKF1 LOV domain and the N-terminal region of the GI protein (de Montaigu et al., 2010; Sawa et al., 2007). This complex is then able to physically interact with CDF proteins via the FKF1 Kelch domain and the GI N-terminus. This FKF1-GI-CDF complex can be found in both nucleus and cytosol but has been shown to localize to the *CO* promoter region (Hwang et al., 2019; Imaizumi et al., 2005; Kim et al., 2013a; Sawa et al., 2007). Other studies have indicated that both GI and FKF1 can bind to the promoter region of *FT*, raising the possibility that that their physical interaction might also be important for direct regulation of *FT* expression (Sawa and Kay, 2011; Song et al., 2012).

The specific protein domains involved in the interaction of *Arabidopsis* FKF1 and GI were determined through yeast two-hybrid assays and have been confirmed in other species such as soybean (Li et al., 2013). As mentioned above soybean contains two *FKF1* homologs and three *GI* homologs which follow the same pattern of interaction as *Arabidopsis* in which the LOV domain from the GmFKF1 proteins is able to interact with the N-terminal region of the GmGI proteins. It has been suggested that the Kelch domain of GmFKF1 proteins is then interacting with GmCDF1. Yeast-two hybrid experiments have also shown homo and hetero-dimer interactions between the N-terminal regions of GmGI2 and GmGI3 (Krahmer et al., 2019; Li et al., 2013).

Interestingly, ZTL (homolog of *FKF1*) has implications in the interaction and function of the FKF1-GI complex in *Arabidopsis*. ZTL is able to interact with both GI and FKF1, and the interaction with GI is blue-light dependent leading to the regulation of *CO* expression (Kim et al., 2007, 2013a). This interaction also occurs through the LOV domain of ZTL and, ZTL protein levels are strongly stabilized with this GI interaction (Kim et al., 2007). Moreover, ZTL also regulates the distribution and sublocalization of GI between cytosol and nucleus, and this localization is guided by the ability to interact specifically in the cytosol (Hwang et al., 2019; Kim et al., 2013a).

One intriguing aspect of FKF1 and GI function is that although the interaction between FKF1 and GI leads to an induction of *CO* expression, their individual roles in the control of CO protein are antagonistic: GI destabilizes CO and FKF1 is able to stabilize CO protein independently of CDF participation (Song et al., 2014). Moreover, it has recently been reported that GI is able to control FKF1 protein stability but FKF1 is not a direct regulator of GI protein even though it can interfere in GI localization and protein stability (Hwang et al., 2019). It is clear that there is more to be learned about this complex interaction and its implications for flowering control.

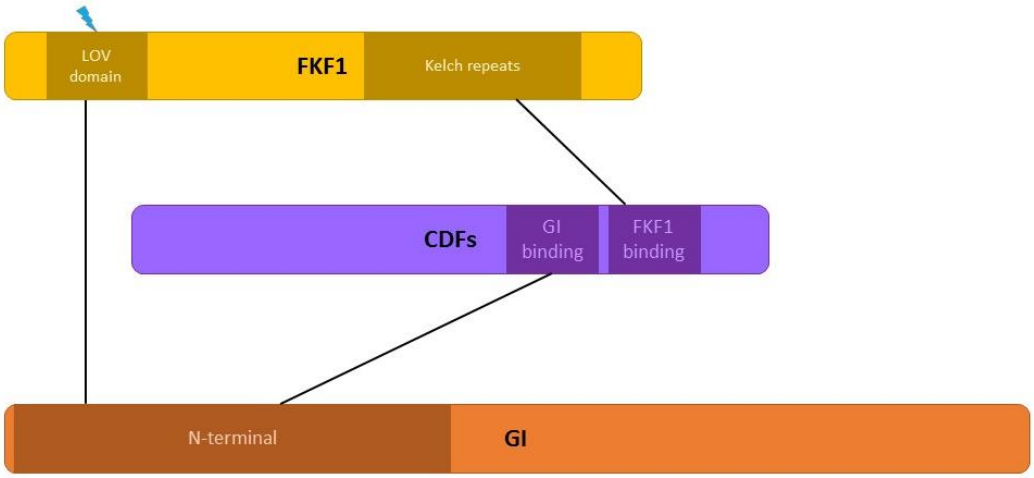

Figure 5.2 FKF1, GI and CDFs interaction.

FKF1 protein interacts trough the LOV domain (brown box) with GI, specifically in its N-terminal region (dark orange box). The same N-terminal region in GI is able to interact with CDFs. CDFs have a GI binding site (purple box) located close by the FKF1 binding site (purple box). FKF1 Kelch repats (brown box) is responsible for the CDF interaction. The three proteins are able to interact and form a regulatory complex dependent of blue-light (blue lighting).

5.1.4 Aims

This chapter aims to give insight into the role that *FKF1* may play in the photoperiodic control of flowering in the temperate legumes, pea and *Medicago*, making use of induced mutants in both species. The chapter also includes a further characterization of *PsGI/LATE1* with the study of the nature of some alleles and protein characterization. Finally, it examines the previously untested question of whether FKF1 and LATE1 interact physically, extending previous studies on interactions of FKF1 with PsCDFc1/LATE2 (Ridge et al., 2016).

5.2 Specific materials and methods

This section describes specific details of materials and methods for research included in this chapter. General materials and methods that are also relevant are described in Chapter 2.

5.2.1 Plant material used

The research in this chapter is based on *Pisum sativum* and *Medicago truncatula.* Details of the pea plant lines used for the experiments presented in this chapter are outlined in Table 5.1.

Table 5.1 Details of pea plant material presented in this chapter.

Target gene	Genotype	Purpose
FKF1	*fkf1-1*	Mutant containing a substitution in a conserved region for *FKF1* gene. Originated by EMS mutagenesis of cv. *Cameor* and obtained by TILLING screen. Further mutation description and mutant characterization regarding flowering response, photoperiodic development and photomorphogenesis response is included in this chapter.
LATE1	*late1-1*	Mutant containing a A530T substitution for *LATE1* gene described by Hecht et al., 2007. Originated by EMS mutagenesis of NGB5839. Genotype used for protein studies including structural configuration predictions and Western Blot, included in this chapter.
LATE1	*late1-2*	Null mutant for *LATE1* gene described by Hecht et al., 2007. Originated by EMS mutagenesis of NGB5839. Genotype used for protein studies including structural configuration predictions and Western Blot, included in this chapter.
LATE1	*late1-3*	Mutant containing a G239E substitution for *LATE1* gene described by Hecht et al., 2007. Originated by EMS mutagenesis of NGB5839. Genotype used for protein studies including structural configuration predictions and Western Blot, included in this chapter.
LATE1	*late1-4*	Null mutant for *LATE1* gene described by Hecht et al., 2007. Originated by EMS mutagenesis of NGB5839. Genotype used for protein studies including structural configuration predictions and Western Blot, included in this chapter.
LATE1	*late1-5*	Mutant for *LATE1* gene (this study). Originated by EMS mutagenesis of NGB5839. Genotype analysed for mutant characterization and protein studies including structural configuration predictions and Western Blot, included in this chapter.
LATE1	*late1-6*	Mutant for *LATE1* gene (this study). Originated by EMS mutagenesis of NGB5839. Genotype used for protein studies including structural configuration predictions and Western Blot, included in this chapter.

Details of the *Medicago* plant lines used for the experiments presented in this chapter are described in Table 5.2.

Table 5.2 Details of *Medicago* plant material presented in this chapter.

Target gene	Genotype	Original line	Purpose
FKF1	*MtFKF1*	NF17817	WT genotype for *FKF1* originated from *Medicago Tnt1* database. Genotype used for *Medicago* flowering and vernalization characterization analysis included in this chapter.
FKF1	*Mtfkf1*	NF17817	Mutant containing a *Tnt1* retrotransposon in its intron. Mutant genotype for *FKF1* originated from *Medicago Tnt1* database. Genotype used for *Medicago* flowering and vernalization characterization analysis included in this chapter.

5.2.2 Plant growth conditions

Plants were either grown in the University of Tasmania Controlled Environment Facility (CEF) phytotron with the photoperiod conditions described in Chapter 2 or in controlled environment growth cabinets at 20°C under fluorescent light for the full photoperiod.

For the different photoperiod experiment included in this chapter, plants were grown in pots in different light conditions specified in Table 3.3, with temperature and water regime controlled as specified in Chapter 2.

For the specific photomorphogenesis experiment in this chapter, plants were grown in pots for 2 weeks in different light conditions specified in Table 5.3. Plants were grown in growth rooms in a double-door isolated space at the CEF of the University of Tasmania where temperature and water regime were controlled. After 14 days, photos of the plants were taken together with the respective photomorphogenesis measurements explained in Chapter 2.

Table 5.3 Details of light conditions used in photomorphogenesis experiment in this chapter.

Light condition	Label	Description
Dark	D	Complete darkness
Blue 0.3	B0.3	Constant blue light at 0.3 µmol m^{-2} s^{-1}
Blue 1	B1	Constant blue light at 1 µmol m^{-2} s^{-1}
Blue 3	B3	Constant blue light at 3 µmol m^{-2} s^{-1}
Blue 10	B10	Constant blue light at 10 µmol m^{-2} s^{-1}1
Red	R	Constant red light at 10 µmol m^{-2} s^{-1}
Red and Blue 10	R+B10	Constant red light with blue light at 10 µmol m^{-2} s^{-1}
White	W	Constant white light at 100 µmol m^{-2} s^{-1}

5.2.3 Primer details

The genotyping of the *fkf1* mutant alleles was performed with HRM markers specified in Table 5.4.

Table 5.4 Details of primers used in this chapter.

Gene	Purpose	Primer name	Primer sequence	Temp
FKF1	*fkf1-1* HRM marker	PsFKF1-4F	TCTTGTTTTTACAGCCGGTTC	60ºC
		PsFKF1-4R	CTAATCTCCGACACCACAACC	
MtFKF1	PCR Genotyping	MtFKF1-F1	AGCCCTTGGTCGTAACTGG	60ºC
		MtFKF1-R1	GCGGTTCAAGTCTATGTTTGC	
		MtFKF1-F1	AGCCCTTGGTCGTAACTGG	60ºC
		MtTnt1-R	CAGTGAACGAGCAGAACCTGTG	
		MtTnt1-F	ACAGTGCTACCTCCTCTGGATG	60ºC
		MtFKF1-R1	GCGGTTCAAGTCTATGTTTGC	
LATE1	*Late1-5* allele characterization	GI-13F	AGCCAATTTCCTCACAATGG	60ºC
		GI-13R	TACGCAAACCCGTTAGTTCC	

LATE1	*Late1-6* allele characterization	GI-8F	CTTAACCCTCCTAATTCAGG	58ºC
		GI-7R	GCTCACTAGTTGTTGCAAGG	
		GI-16F	GAGATTTGGAAGCTTTTCATGGCT	58ºC
		GI-10R	GTCGAAGGCACGAGTTGAGG	
		GI-4F	CAGAACAGTGGGCTCTGG	58ºC
		GI-L12R	AACCGCCCAAAGGTTCATGC	
		GI-6F	TGAGCATCTTGTTGCTGG	58ºC
		GI-L11-R	CTTGCTTCCACTGAATTGG	
		GI-L11-F	AGGTCCTGGAATATCTCC	58ºC
		GI-3b	TCAACTTGTGCCATAGTAGG	
		GI-13F	AGCCAATTTCCTCACAATGG	58ºC
		GI-12R	CCTTGGCTATCCAGGGTTGC	
		GI-13F	AGCCAATTTCCTCACAATGG	58ºC
		GI-13R	TACGCAAACCCGTTAGTTCC	
		GI-13F	AGCCAATTTCCTCACAATGG	58ºC
		GI-14R	AAGTTCATGGTGAACGTCTGC	
		GI-9Fa	GGGAATAGTTTGAGATTTGGAAGC	58ºC
		GI-10R	GTCGAAGGCACGAGTTGAGG	
LATE1	Yeast-two-Hybrid N-terminal *LATE1* vector	GI-15F	ATGGCTTCTACTATGGCTGCT	58ºC
		GI-C-15R	TCAATCAGCAGCTATGCCAGC	
LATE1	Yeast-two-Hybrid complete *LATE1* vector	GI-15F	ATGGCTTCTACTATGGCTGCT	58ºC
		GI-13R	TACGCAAACCCGTTAGTTCC	
LATE1	Colony PCR for *LATE1* Yeas-two-hybrid vectors	pDEST32-F	CGCTACTCTCCCAAAACCAA	55ºC
		GI-7R	GCTCACTAGTTGTTGCAAGG	
LATE1	Colony PCR for *LATE1* Yeas-two-hybrid vectors	pDEST22-F	TGAAGATACCCCACCAAACC	56ºC
		GI-7R	GCTCACTAGTTGTTGCAAGG	

5.2.4 Yeast-two-Hybrid

5.2.4.1 Design of vectors

Yeast two-hybrid analysis was conducted using the ProQuest™ Two-Hybrid System (Invitrogen Corporation, Carlsbad, CA, USA). For the yeast two-hybrid assay, full-length coding sequence and N-terminal region sequence of *PsLATE1* and *AtGI* (Sawa et al., 2007; amino acids 1 to 319 in AG-N-terminal region) were amplified from leaf tissue from wild-type pea cv NGB5839 cDNA and from *Arabidopsis thaliana* (Col-0) cDNA. The amplification was performed by high fidelity PCR specified in Chapter 2 from wild-type cDNA using specific primer detailed in Table 5.4. Successful PCR products were purified, and a poly-A tail was added to PCR products using MangoTaq™ DNA polymerase (Bioline, Alexandria, NSW, Australia) in a reaction mix containing 40µL PCR product, 10µL of 5x reaction buffer, 1µL of dNTPs (10mM) and 0.1µL of MangoTaq™ DNA polymerase, incubated at 72°C for 10 minutes. A-tailed PCR products were purified again, cloned into an entry vector for the Gateway® system using the pCR®8/GW/TOPO® TA Cloning® Kit (Invitrogen Corporation, Carlsbad, CA, USA) and transformed into One Shot® TOP10 Chemically Competent *E. coli* (Invitrogen Corporation, Carlsbad, CA, USA) with heat shock and selection of transformants on LB agar plates containing 100mg/L spectinomycin (for selection of TOPO vector) and 50mg/L streptomycin (for selection of TOP10 *E. coli*), in accordance with the manufacturer's instructions.

These sequences cloned in-frame into the pCR8/GW/TOPO entry vector (Invitrogen) were then transferred by Gateway® LR Clonase™ II Enzyme Mix (Invitrogen Corporation, Carlsbad, CA, USA) to shuttle gene inserts from entry vectors into destination vectors following manufacturer's instructions. Both destination vectors, pDEST32 (bait; BD) and pDEST22 (prey; AD) (Invitrogen) details are specified in Table 5.5. Transformants were selected on antibiotics containing medium according to Table 5.5. Full coding sequences of *PsFKF1*, *PsLATE2* and *Pslate2* and *Arabidopsis AtFKF1, AtCDF* were already available in the group as bait and prey clones (Ridge et al., 2016).

Table 5.5. Details of destination vectors for Yeast-two-Hybrid designed in this thesis.

Vector name	Type of vector used	Purpose	Antibiotic	Concentration (mg/L)
LATE1-BD	pDEST32	Full-length pea LATE1 in bait vector	Gentamicin	10
LATE1-AD	pDEST22	Full-length pea LATE1 in prey vector	Ampicillin	100
LATE1-N-BD	pDEST32	N-terminal region of pea LATE1 in bait vector	Gentamicin	10
LATE1-N-AD	pDEST22	N-terminal region of pea LATE1 in prey vector	Ampicillin	100
PsFKF1-BD	pDEST32	Full-length pea FKF1 in bait vector	Gentamicin	10
PsFKF1-AD	pDEST22	Full-length pea FKF1 in prey vector	Ampicillin	100
AtGI-N-BD	pDEST32	N-terminal region of *Arabidopsis* GIGANTEA in bait vector	Gentamicin	10
AtGI-N-AD	pDEST22	N-terminal region of *Arabidopsis* GIGANTEA in prey vector	Ampicillin	100

Colony PCR was performed at each cloning step using gene specific PCR primers in combination with vector-specific primers (Table 5.4). Plasmid DNA was purified from selected colonies using Promega Wizard Plus SV Mini-preps DNA Purification System (Promega, Madison, WI, USA) according to the manufacturer's instructions. Clones were sequenced using the Sanger method by Macrogen Inc. (Seoul, Korea), to confirm correct coding sequence, reading frame, and orientation of inserts for each entry and destination construct.

5.2.4.2 Yeast transformation and mating

Following the methodology described by Folter and Immink 2011 and previously used in the pea model by Ridge et al., (2016), the haploid yeast strains PJ69-4α and PJ69-4A were transformed with bait and prey constructs, respectively. Transformation was performed with 1µg of plasmid DNA (bait and prey vectors respectively), 100µg of denatured sheared salmon sperm and 100µL of yeast strain suspension previously diluted to OD600 of 0.4 in 50ml YPAD media. Yeast growth media was made using pre-prepared powder mixes from Sunrise Science Products (San Diego, CA,

USA). Rich, routine growth medium (YPAD) comprised 20 g/L peptone, 10g/L yeast extract, 20g/L dextrose and 40 mg/L adenine. This was manually supplemented with 60 mg/L adenine hemisulfate. Dropout media was prepared from dropout base (1.71 g/L yeast nitrogen base, 5 g/L ammonium sulfate and 20 g/L dextrose) combined with dropout mixes with a Synthetic Complete/Hopkins (SC) mixture base (21 mg/L adenine, 85.6 mg/L of each of L-alanine, L-arginine, L-asparagine, L-aspartic acid, L-cysteine, glutamine, L-glutamic acid, glycine, L-histidine, myo-inositol, L-isoleucine, L-lysine, L-methionine, L-phenylalanine, L-proline, L-serine, L-threonine, L-tryptophan, L-tyrosine, uracil and L-valine, 173.4 mg/L L-leucine and 8.6 mg/L para-aminobenzoic acid) with certain amino acids omitted as appropriate for each purpose. Dropout media was used for transformation (SC-Leu-Trp), testing for URA3 reporter gene induction (SC-Leu-Trp-Ura), and testing for HIS3 reporter gene induction (SC-Leu-Trp-His supplemented with 1-50mM 3AT). A negative transformation control (without bait and prey constructs) was included with each batch of transformations, in accordance with the manufacturer's instructions (ProQuest™ Two-Hybrid System, Invitrogen Corporation, Carlsbad, CA, USA). The transformed yeast was grown in selective plates for 4 days at 30°C. Selective media SC lacking leucine (L) (SC-L) and SC lacking tryptophan (W) (SC-W) were used for PJ69-4α and PJ69-4A yeast strains respectively as indicated by the manufacturer's instructions.

For each interaction to be tested, the mating step to create diploid colonies containing both interaction partners took place following Ridge et al., 2016 methodology, using replication plates with YPAD media (not selective) and selective plates with SC-L-W [SC medium lacking leucine (L) and tryptophan (W)]. Individual colonies were then suspended in 200 µL water and were directly spotted onto nonselective medium (SC -L -W) and selective medium also lacking histidine (SC -L -W -His) with 35 mM 3-amino-1,2,4-triazole (3AT) added and grown at 30°C for 4 days to test interactions. Each interaction was tested in both directions, for example: LATE1-BD as bait with putative interactor as prey, putative interactor as bait with LATE1-AD as prey. Two clones for each kit interaction control were obtained using constructs provided with the Invitrogen ProQuest™ Two-Hybrid System (strong positive interaction control pEXP32/Krev1 with pEXP22/RalGDS-WT; weak positive interaction control pEXP32/Krev1 pEXP22/RalGDS-m1; negative interaction control pEXP32/Krev1 pEXP22/RalGDS-m2) and two clones containing empty bait and prey vectors were obtained as negative activation controls. Interactions were considered to be 'negative' if a majority of clones tested negative for all three tests. If clones tested positive for URA3 induction, but not HIS3 or X-gal tests, results were considered to be 'false positive'.

5.2.5 Western blot

5.2.5.1 Protein extraction and sample preparation

The extraction protocol is based on the indications from the manufacturer (Agrisera, Sweden). 100mg of plant tissue (leaf or apex tissue from pea plants) was collected and stored at -80°C until processing. Frozen tissue samples were ground using mortar and pestle. Samples were stabilised with 500µL of 1x PEB Buffer (Agrisera buffer with protease inhibitor, pH 8.5) and kept cold at all times. Samples were sonicated three times for 1 min and frozen in liquid nitrogen between each sonication step to keep the sample cold. When samples were processed, the insoluble material was removed after centrifugation at 10000g during 3 min. The protein concentration in each sample measured using NanoDrop 8000 Spectrophotometer (Thermo Fisher Scientific, Wilmington, DE, USA) in accordance with the manufacturer's instructions.

Protein extracts in 1xPEB were prepared for gel loading in equal volumes and amounts (0.5-10µg in 10µL) with Laemli buffer (4%SDS, 20% glycerol, 0.2% bromophenol blue, 0.125M Tris-HCl, pH 6.8) and 0.5µL of β-mercaptoethanol per sample. Prepared samples were heated at 70°C for 10 min prior to gel loading.

5.2.5.2 SDS-PAGE gel and membrane transfer

Mini polyacrylamide gels were freshly prepared following instructions from the manufacturer (BioRad). The components and volumes for separating and stacking mini gels shown in Table 5.6 were mixed by inversion and pour in the Bio-Rad gel cassette according to manufacturer's instructions. A layer of isopropanol was added on top of the separating gel to facilitate solidification and was removed before pouring the stacking gel solution.

Table 5.6 Polyacrylamide gel components and volumes to cast one mini-gel.

	Separating gel		Stacking gel
	10% (1gel)	**12% (1gel)**	**4% (1 gel)**
Mili-Q water	4.1 ml	3.4 ml	3 ml
1.5 M Tris-HCl (pH 8.8)	2.5 ml	2.5 ml	
0.5 M Tris-HCl (pH 6.8)			1.25ml
29% Acrylamide: 1% N,N'-Methylenebisacrylamide	3.3 ml	4 ml	0.665ml
10% (w/v) SDS	100 µL	100 µL	100 µL
10% (w/v) Ammonium Persulfate (APS)	50 µL	50 µL	50 µL
TEMED	10 µL	10 µL	10 µL

After polymerization, the gel was assembled in the electrophoresis holder which was filled with Running buffer (25mM Tris Base, 192mM Glycine, 0.1% (w/v) SDS). The gel was run at a constant 120V for 1hour. Once the samples were separated, they were transferred on nitrocellulose membrane (BioRad) following manufacturer's instructions. The transfer was performed at 20V overnight in a submerge cold tank with 1xTBS-T buffer (20mM Tris Base, 137mM NaCl, 0.1% Tween 20, pH 7.6).

5.2.5.3 Membrane blocking and detection

The antibody used for this thesis was a polyclonal GIGANTEA antibody (AS12 1864A), produced in rabbit from an *Arabidopsis thaliana* protein and predicted reactivity in *Pisum sativum* (Agrisera, Sweden).

Membrane blocking and antibody incubation (dilution 1/1000) was performed using IncuBlocker kit (Agrisera, Sweden) according to manufacturer instructions (Agrisera, Sweden). Detection was performed using Agrisera ECL kit for chemiluminescent detection following manufacturer's instructions (Agrisera, Sweden). After 20 minutes of exposition, X-ray films were used to print the chemiluminescent portrait.

5.3 Results

5.3.1 *FKF1* phylogeny in legumes

The components of the flowering transcriptional regulatory pathway have been studied in multiple species, and in legumes, the majority of research has focussed on *GI* orthologs (e.g., the pea ortholog *LATE1* (Hecht et al., 2007) or the soybean *E2* gene (Watanabe et al., 2011)) with some research also looking into the role of *CDFs* orthologs in legumes (e.g., the pea ortholog *LATE2* (Ridge et al., 2016) or the *Medicago MtCDFd1_1* (Zhang et al., 2019)).

Although *FKF1* orthologs have been identified and studied in a number of species, their phylogeny within the legume family has not been examined in much detail. Some research in the SD legume soybean described two orthologs of *FKF1,* with similar genomic sequence and protein domains to *AtFKF1* and maintaining diurnal pattern of expression, suggesting a possible role in flowering promotion in SD (Li et al., 2013). *FKF1* phylogenetic analysis in other legume species including *Medicago*, pea and soybean has previously been described (Ridge et al., 2016).

In this section we have expanded the phylogenetic analysis to a wider range of legume FKF1 protein family, including *ZTL* orthologs using the sequences specified in Table 5.7. Sequence alignment shown in Figure 5.3 illustrates the conservation within the FKF1 and ZTL protein families. The FKF1 sequences share more than 62.7% of amino acid identities (the lowest registered between SlFKF1 and OsFKF1) and the ZTL sequences share above 79.4% amino acid identities (the lowest registered between AtZTL and SlZTL). The two subgroups have more differences in their sequences grouping them in two distinguishable subfamilies, finding a conservation in amino acid identities above 56.42% (the lowest registered between AtZTL and SlFKF1, not including AtLKP2 which is less similar [shares 50,54% amino acid identities with SlFKF1]). The protein sequences are similar in length ranging from 606 (ZmFKF1) to 648 (GmFKF1a) amino acids among the FKF1 sequences and ranging from 552 (SlZTL) to 618 (both GmZTL2a and GmZTL2b) amino acids, with no major structural differences apparent. The regions of high conservation correspond to the three characterized domains of AtFK1: LOV/PAS domain, F-box domain and Kelch repeat, highly conserved in both subgroups and are featured with color in Figure 5.3

Table 5.7. FKF1 and ZTL sequences identified in online sequences resources including legumes and other characterised species.

Name	Species	Locus ID
AtFKF1	*Arabidopsis thaliana*	At1g18050
AtLKP2		At2g18915
AtZTL		At5g57360
CaFKF1	*Cicer arietinum*	XP_004503344.1
CaZTL		XP_004487946.1
CcFKF1	*Cajanus cajan*	XP_020221838.1
CcZTL		XP_020228526.1
GmFKF1a	*Glycine max*	Glyma.05G239400.1
GmFKF1b		Glyma.08G046500.1
GmZTL1a		Glyma.09G056100
GmZTL1b		Glyma.15G162300
GmZTL2a		Glyma.13G097600
GmZTL2b		Glyma.17G062000
LjFKF1	*Lotus japonicus*	Lj4g0027300.1
LjZTL		Lj6g0012192.1
MtFKF1	*Medicago truncatula*	Medtr8g105590.1
MtZTL		Medtr2g036510
OsFKF1	*Oryza sativa*	Os11g34460.1
PsFKF1	*Pisum sativum*	PsCam049028 - Psat7g007600
PsZTL		PsCam048993 - Psat1g146560
PvFKF1	*Phaseolus vulgaris*	Phvul.002G321800.1
PvZTL		Phvul.009G239400.1
SlFKF1	*Solanum lycopersicum*	Solyc01g005300.2.1
SlZTL		Solyc07g017750.2.1
ZmFKF1	*Zea mays*	Zm00008a010164

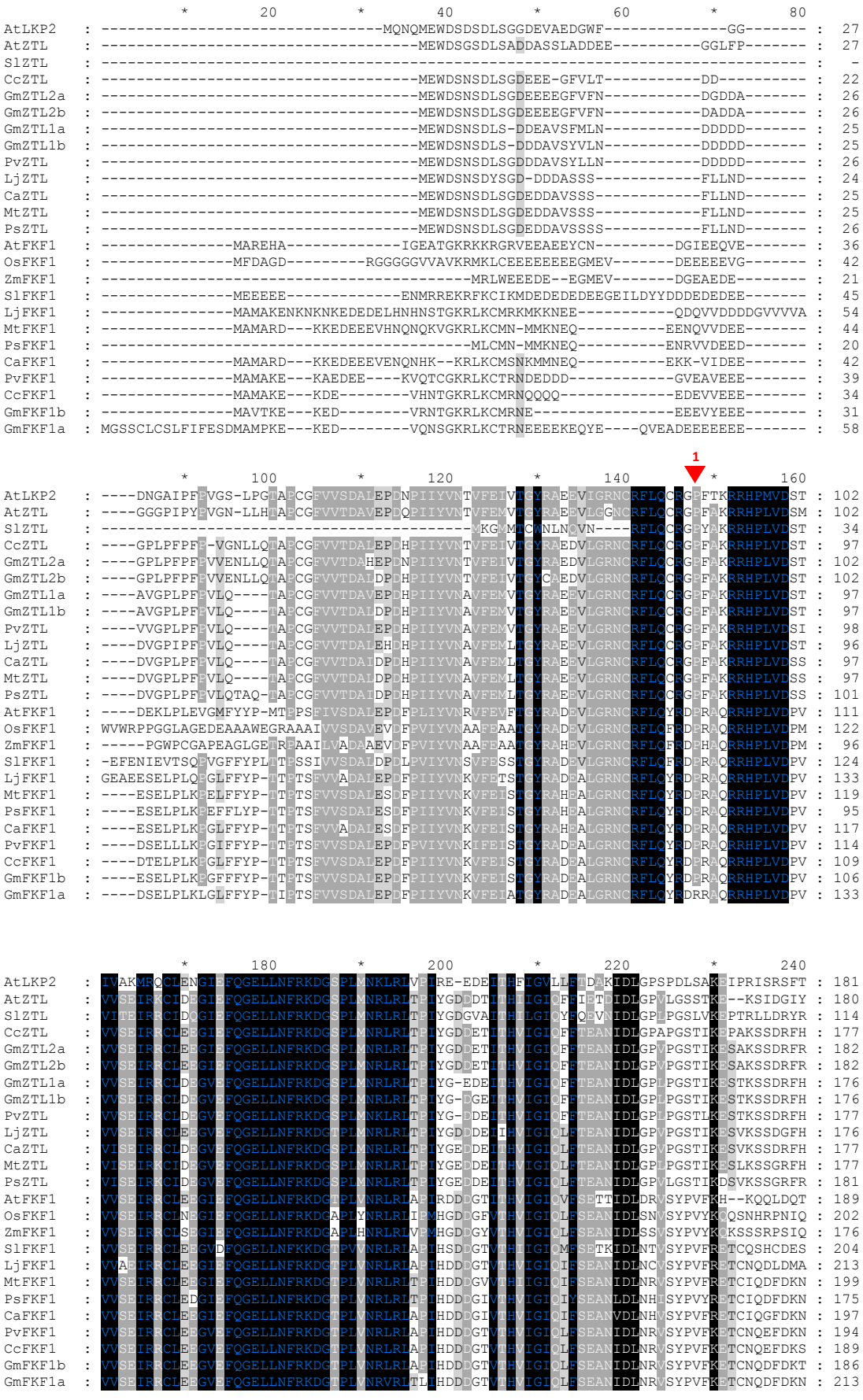

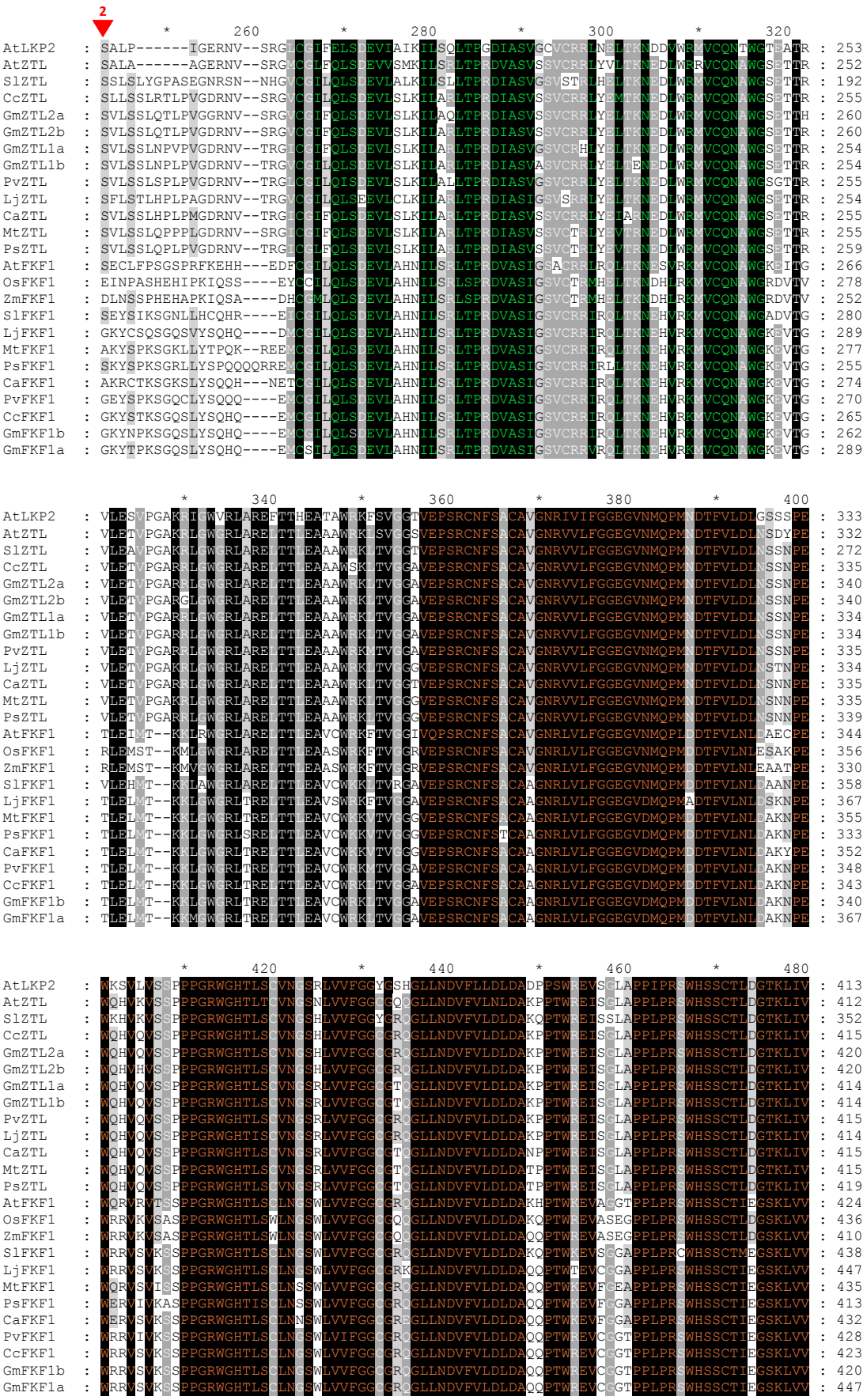
2
AtLKP2
AtZTL
SlZTL
CcZTL
GmZTL2a
GmZTL2b
GmZTL1a
GmZTL1b
PvZTL
LjZTL
CaZTL
MtZTL
PsZTL
AtFKF1
OsFKF1
ZmFKF1
SlFKF1
LjFKF1
MtFKF1
PsFKF1
CaFKF1
PvFKF1
CcFKF1
GmFKF1b
GmFKF1a

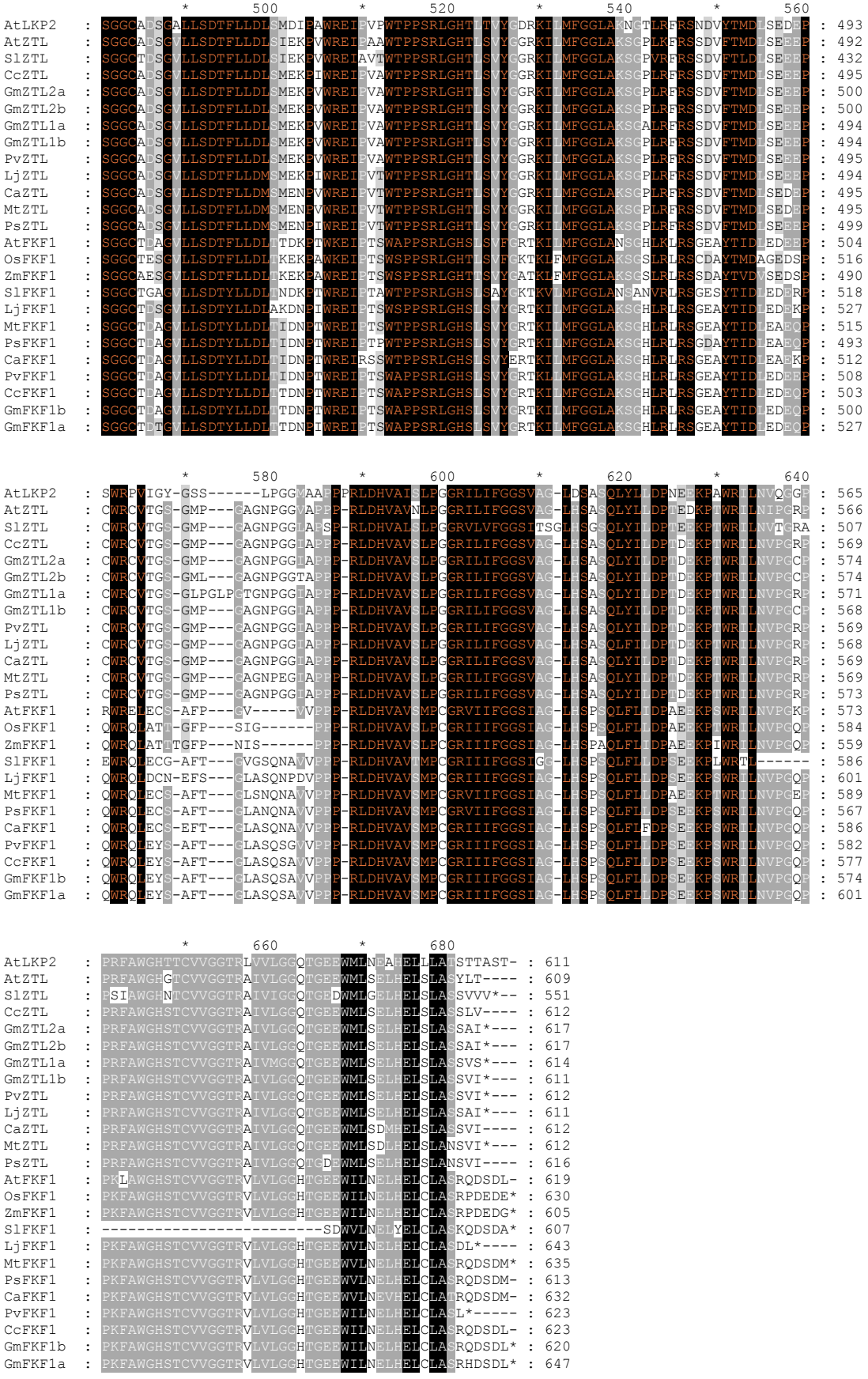

Figure 5.3 Amino acid sequence alignment of FKF1 and ZTL proteins.

A ClustalX alignment (Thompson et al., 1994) was conducted with full-length predicted protein sequences and adjusted with GeneDoc (Nicholas and Nicholas, 1997). The degree of conservation for the aminoacids are identified with shade degree: black for 100% conserved, dark grey for 80% conserved and light grey for 60% conserved. The abbreviation names followed the previous described species in Table 5.7. Locations are indicated for LOV/PAS domain (blue), F-box domain (green) and Kelch repeat domain (orange). The numbered red triangles indicate the location of the pea *fkf1* alleles mutations respectively.

Figure 5.4 shows the phylogenetic relationship between these sequences. As expected, the legume sequences formed a discrete group from the other species, and within this group the SD and LD legume sequences cluster separately. The FKF1 legume family divides in SD (GmFKF1a, GmFKF1b, CcFKF1 and PvFKF1) and LD (LjFKF1, CaFKF1, MtFKF1 and PsFKF1) subgroup. The lotus (LjFKF1) sequence seems to be less related to any other legumes sequence. In the ZTL branch, the division SDP/LDP follows a similar pattern, but in this case the lotus sequence (LjZTL) clusters together with the LDP species (*Cicer*, *Medicago* and pea).

This study is focussed on the characterization of *PsFKF1*, and its closest relative in *Medicago MtFKF1*.

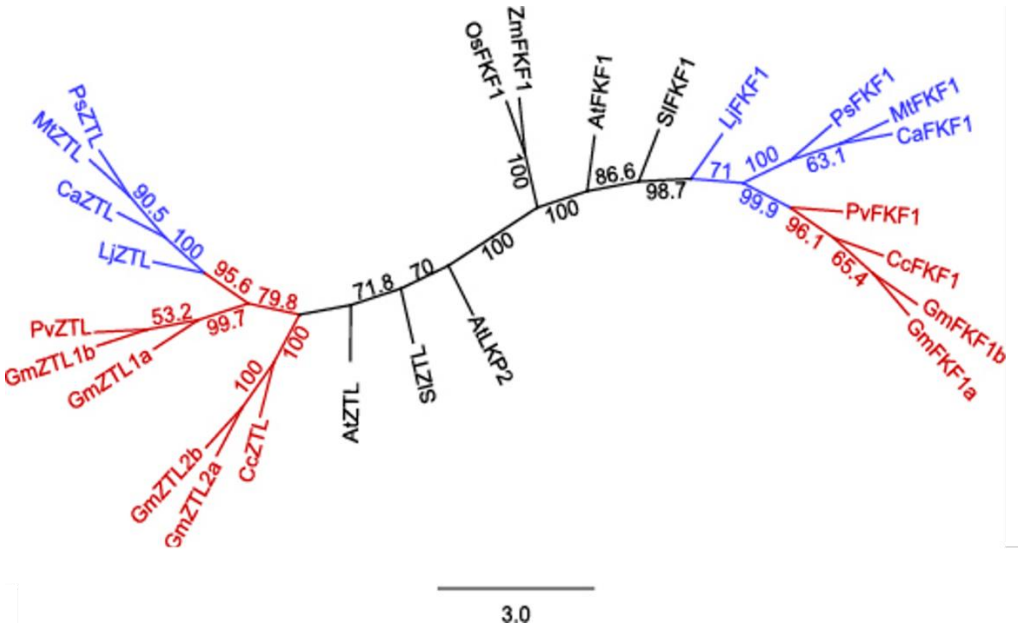

Figure 5.4 Phylogenetic neighbour-joining tree of FKF1 and ZTL protein sequences.

The phylogram was constructed from full length predicted protein sequences of FKF1 and ZTL genes identified in Table 5.7 and align in Figure 5.3. Species names are indicated in Table 5.7. The phylogenetic tree was performed using a neighbour-joining method and with a bootstrap of 1000. Blue color indicates LD legume groups and red color indicates SD legume species.

5.3.2 Functional characterisation of the pea *FKF1* gene: *PsFKF1*

5.3.2.1 PsFKF1 gene structure

The pea *FKF1* gene (Psat7g007600) is similar to the *Arabidopsis* gene, with two exons and one intron as shown in Figure 5.5. A TILLING (Targeted Induced Local Lesions IN Genomes) screen of a pea EMS population in cv. *Cameor* (Dalmais et al., 2008) identified two *PsFKF1* substitution mutant alleles in exon 2. The C to T change at position 176bp in the CDS results in amino acid change from P to L in the highly conserved LOV domain for *Psfkf1-1* and an A to T substitution at position 454pb results in amino acid change of S to C for *Psfkf1-2*. Viable seeds were only obtained for *Psfkf1-1*, and this mutant was backcrossed three times to NGB5839 to generate the material used for evaluation.

Figure 5.5 *PsFKF1* gene diagram.

Schematic representation of *PsFKF1* gene, and location of mutations. Blue box represents exons and grey line represents gDNA.

5.3.2.2 Characterization of PsFKF1 mutants

In order to characterize the pea *fkf1-1* flowering phenotype, a BC_3F_2 population was grown in LD conditions. Flowering traits such as node of flower initiation (NFI), number of reproductive nodes (RN), number of days to flower (DTF) and Flower-Leaf Relativity (FLR) were measured in segregants and results are shown in Figure 5.6.

Figure 5.6 A shows that the *fkf1-1* and WT segregants are similar, reaching the same developmental stage at same time. No significant difference (p-value>0.05) was observed between genotypes for NFI (~16), RN (~6) or DTF (~61 DTF). FLR was also not significantly different between the genotypes of this BC_3F_2 population (Figure 5.6 E). The distribution of the number of days to first flower (DTF) in this segregating progeny covers a period of 8 days (59 to 67 days) with no clear visible differences between genotypes (Figure 5.7), consistent with the conclusions from Figure 5.6.

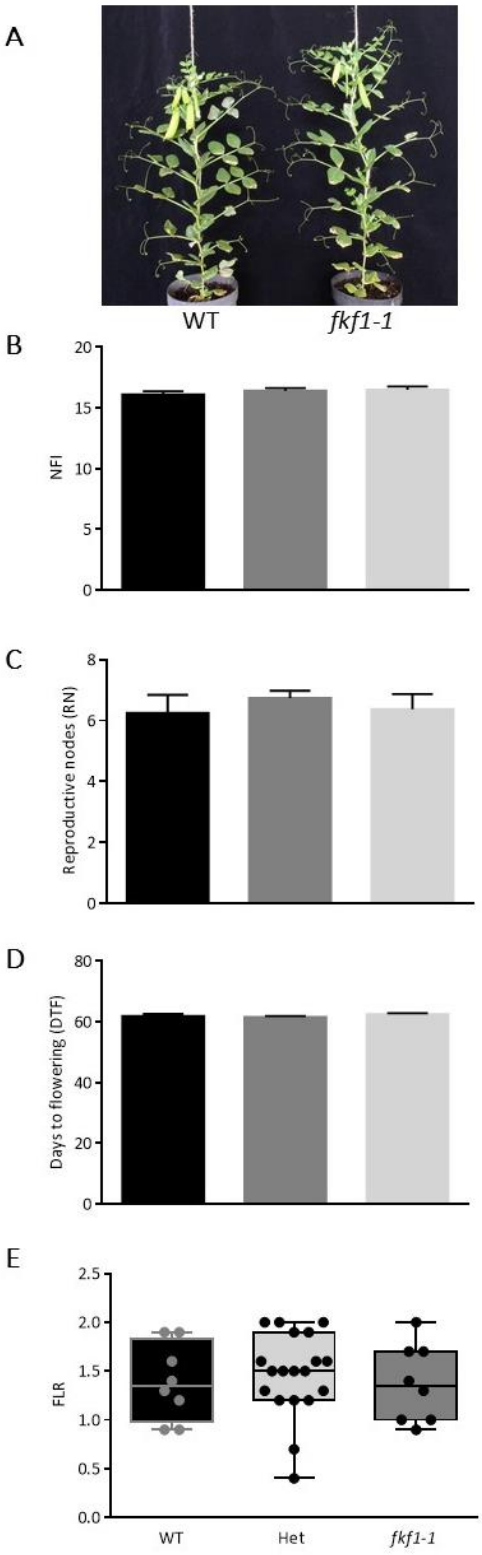

Figure 5.6 Flowering phenotype of *fkf1-1*.

Flowering characteristics of a NGB5839 x *fkf1-1* (*Cameor*) BC_3F_2 population A) Representative plants of WT (left) and *fkf1-1* mutant (right). B-E) Flowering phenotypes of segregants (WT, heterozygous, *fkf1)* B) Node of flowering initiation (NFI). C) Number of reproductive nodes (RN). D) Days to first open flower (DTF). E) Flower-Leaf Relativity index (FLR). Values represent mean ± SE for N=8-19 plants. No significant difference between genotypes were detected (p-value>0.05).

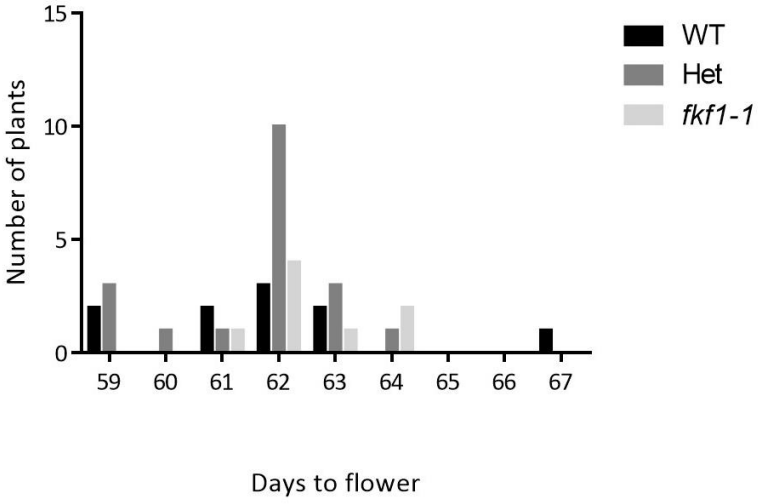

Figure 5.7 Frequency distribution of segregants for *fkf1-1* regarding days to flower (DTF).

Distribution of flowering time for *fkf1-1* segregants from a BC_3F_2. N=8-19 plants per genotype under LD conditions. The WT segregants flowers covering from 59 to 67 days, Hets flowering between 59 and 64 days and *fkf1-1* mutants flowering between 61 and 65 days.

The limited range of photoperiod conditions tested could be reflected in the observed lack of *FKF1* effect in photoperiodic control of flowering time in pea. Therefore, a wider range of photoperiodic conditions were considered to further explore the possible role of *FKF1* in pea flowering regulation. Diverse flowering traits were studied in WT and *fkf1-1* segregants under five different photoperiod conditions specified in Table 3.3 including three different LD conditions (12h LD+ 8h extension, 8h Incandescent -LDI-, Fluorescent -LDF- and Natural LD from the apron in the glasshouse facility), continuous cool-white fluorescent light (CF) and SD conditions(8h light/16h dark).

These experiments used WT and *fkf1-1* families from a BC_3F_3 population together with NGB5839 control plants. As shown in Figure 5.8 A, under LDI, Natural LD and CF conditions, the *fkf1-1* mutant flowered at a significantly later node than the WT plants from the same population segregants (NFI 16.5 compared to 15.2 in LDI, 16 compared to 15 in Natural LD and 16.8 compared to 15.5 in CF) (p-value<0.05 for all comparisons). In LDF and SD conditions no significant difference was seen between the mutant and the WT segregant, although a significant difference (p-value=0.0016) was observed between the NGB5839 controls in LDF.

In contrast, for flowering time (DTF) *fkf1-1* mutants were observed to be statistically later than WT plants only in CF and SD conditions (40.2 DTF compared to 38.1 DTF in CF [p-value = 0.028], and 58.4 DTF compared to 56 DTF in SD [p-value<0.05]; Figure 5.8 B). In both conditions, *fkf1-1* mutant was more similar to NGB5839 controls than to the WT. It is important to note that DTF data for SD conditions includes a reduced sample size due to errors in data collection. Interestingly, both LDI and LDF display a later date of flowering for *fkf1-1* in relation to WT and the external control NGB5839 but without statistical support (p-value >0.05).

Lastly, the Flower-Leaf Relativity (FLR) was again measured as a potential indication of physiological differences related to reproductive vigour, even when node or time of flowering are similar. In SD conditions, FLR values were higher for all genotypes (Figure 5.8 C), indicating a stronger orientation towards vegetative development (more nodes and expanding leaves) instead of reproductive development (flower induction). Statistically significant differences between WT and *fkf1-1* were observed under LDI (p-value= 0.0043) and Natural LD (p-value=0.0008) (Figure 5.8 C). This is consistent with the fact noted above, that in these conditions, NFI in *fkf1-1* was also later than in WT and the FLR score is related to this trait.

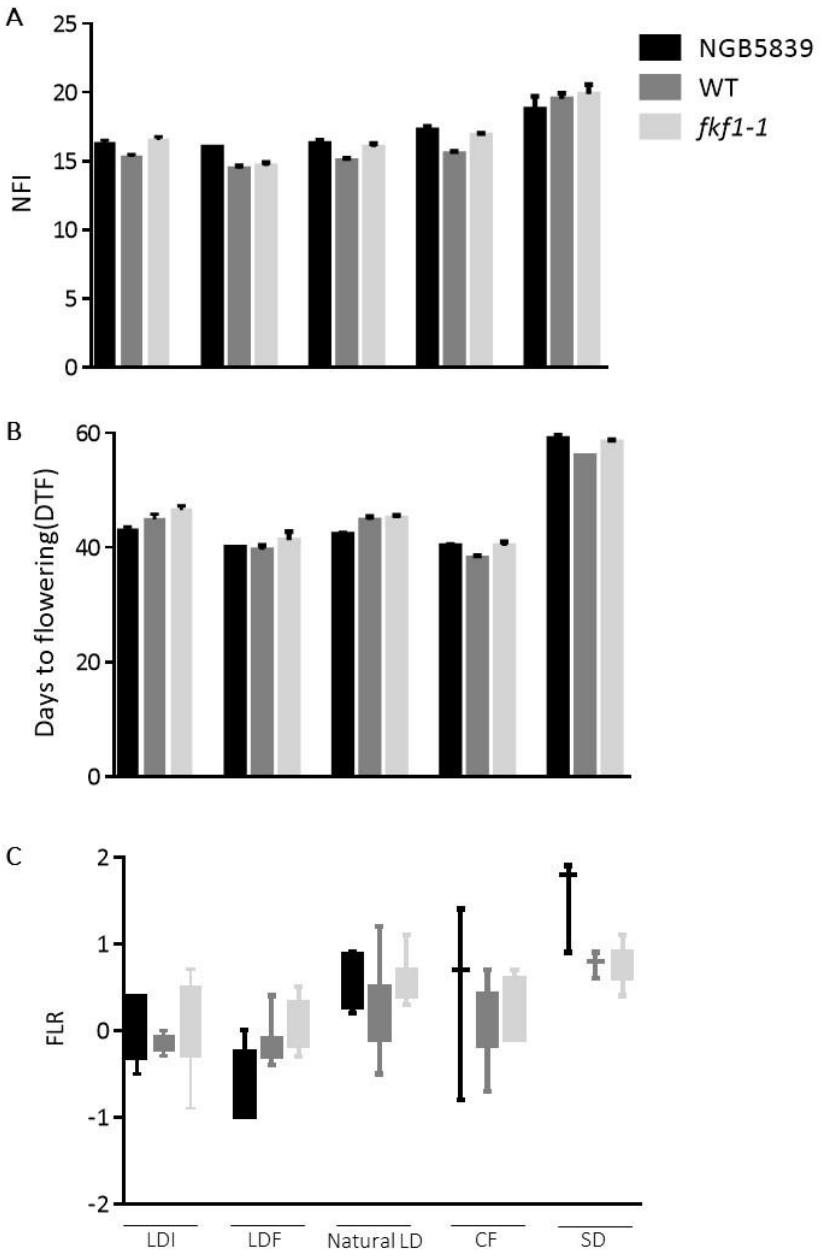

Figure 5.8 Phenotypic comparison of flowering time of WT and *fkf1-1* families in different photoperiod conditions.

Phenotypic characterization of WT and *fkf1-1* from BC_3F_3 populations and comparison to NGB5839 WT control under different photoperiod conditions detailed in Table 3.3. Values represent mean ± SE for n =8 plants in each genotype (WT and *fkf1-1*) and n=4 plants for NGB5839. A) Node of Flowering Initiation (NFI). Statistical differences found between WT and *fkf1-1* in LDI (p-value=0.0028), in Natural LD (p-value=0.0095) and CF (p-value=0.0011). B) Days to flowering (DTF). Statistical differences found between WT and *fkf1-1* in CF (p-value=0.0285) and SD (p-value=0.00006). C) Flower-Leaf Relativity (FLR). Statistical differences found between WT and *fkf1-1* in LDI (p-value= 0.0043) and Natural LD (p-value=0.0008).

5.3.2.3 Effect of Psfkf1-1 on photomorphogenesis

Studies in the *Arabidopsis fkf1* mutant revealed short hypocotyl phenotypes under blue and red light, suggesting a role in photomorphogenic light perception and/or signaling under both blue and red light conditions (Nelson et al., 2000). It was therefore of interest to examine whether the pea *fkf1-1* mutant might show similar effects on seedling development. To test this, WT and *fkf1-1* plants from BC_3F_3 progeny were grown in darkness and 7 different continuous light conditions (specified in Table 5.3) to examine the effects of blue and red light in comparison to white light and darkness on hypocotyl elongation and leaf area.

Results are shown in Figure 5.9. In dark conditions, WT and *fkf1-1* mutant were observed to have similar phenotypes, with elongated hypocotyls and small unexpanded leaves, suggesting that the mutant has an intact etiolation response. These two genotypes also showed a similar phenotype in white light conditions, with a short hypocotyl and a fully-expanded green leaf and therefore a greater leaf area than in dark condition, suggesting a normal de-etiolation response, at least to white light.

The irradiance dependence of the response to blue light was also examined as previously reported for *Arabidopsis fkf1* (Imaizumi et al., 2003; Nelson et al., 2000), considering that any potential effect of the pea *fkf1-1*mutant might be apparent only under a specific irradiance range. As expected, across the irradiance range, plant phenotypes were intermediate between those seen in dark and white light, but there was no evidence for a significant difference between WT and *fkf1-1*mutant under any of the blue light conditions. In *Arabidopsis* the *fkf1* mutant also shows a photomorphogenic effect under red light, again with a shorter hypocotyl than WT. However, in pea, there was also no significant difference in internode length between WT and the *fkf1-1* mutant under red, despite some variation in leaf area, (Figure 5.9). Finally, a combination of red light and blue (R+B10) condition was tested to reveal any possible effect of blue light in "phytochrome-saturated" red light conditions. Once again, no significant difference was detected (Figure 5.9).

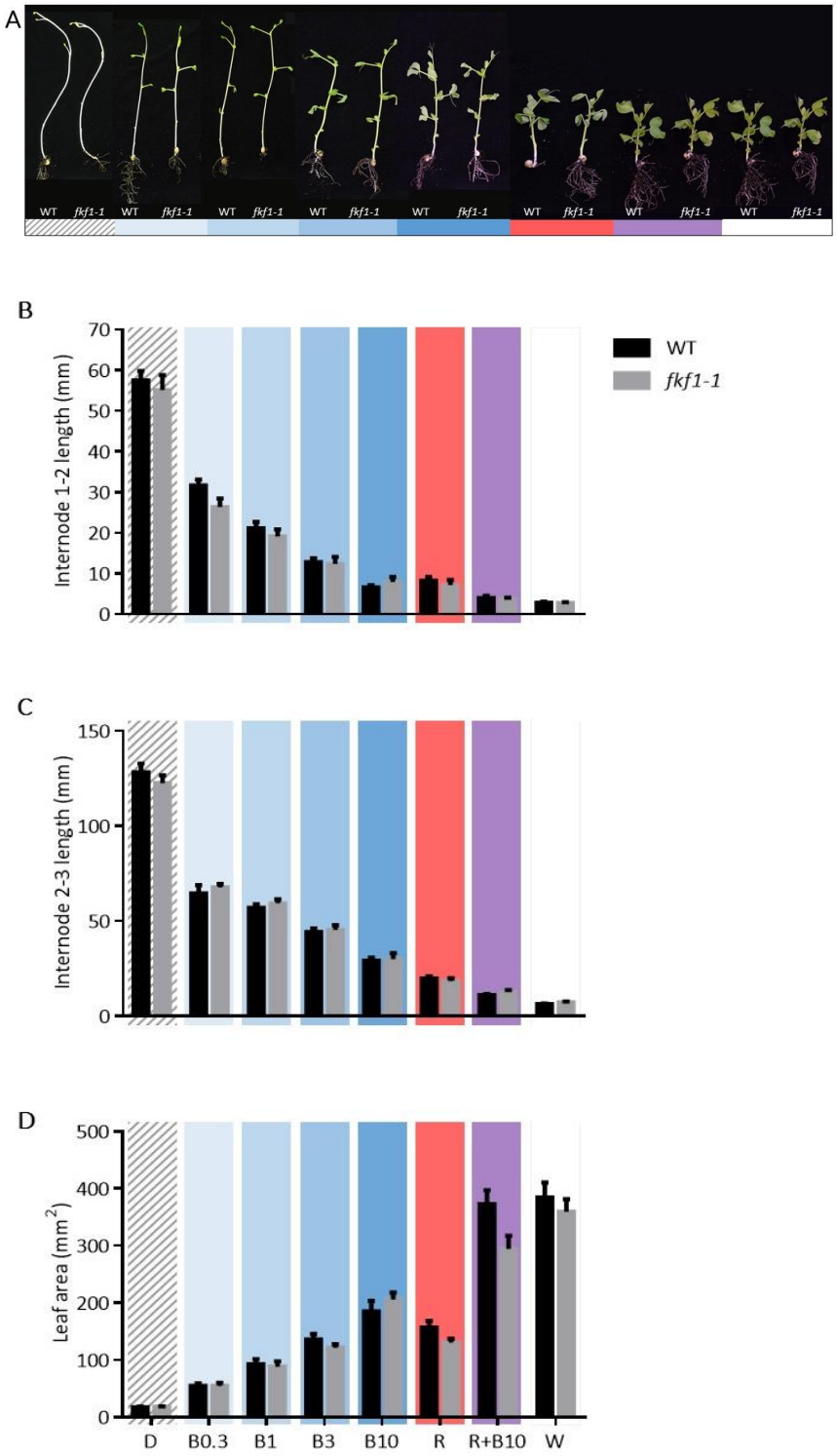

Figure 5.9 Photomorphogenic phenotype of WT and *fkf1-1* under different light regimes.

The photomorphogenic development under different light conditions (dark (D), 4 intensities of blue light (B0.3, B1, B3, B10), red light (R), red and blue light (R+B10), white light (W)). A) Phenotype of WT and *fkf1-1* plants developed for 14 days under the different light conditions indicated by shading boxes B) Internode 1-2 length (mm). C) Internode 2-3 length (mm). D) Leaf area (mm^2). N=12 of each genotype: WT (5839) and *fkf1-1*. No significant differences between genotypes in any light condition were observed (p-value>0.05).

5.3.3 Functional characterisation of *Medicago FKF1*: *MtFKF1*

5.3.3.1 MtFKF1 gene structure

In view of the minimal phenotypic differences between the pea *fkf1-1* mutant and WT, we considered whether the role of this gene could be tested in another related legume system. As outlined in Chapter 3 *Medicago truncatula* has emerged as a temperate LDP legume model with the advantage that it has a high-quality fully annotated genome and substantial genetic resources, including a *Tnt1* retrotransposon insertion mutant platform (Lee and Mysore, 2018). We were able to obtain a putative *FKF1* insertion line (NF17817) carrying a *Tnt1* insertion in the single intron of the *MtFKF1* gene as shown in Figure 5.10.

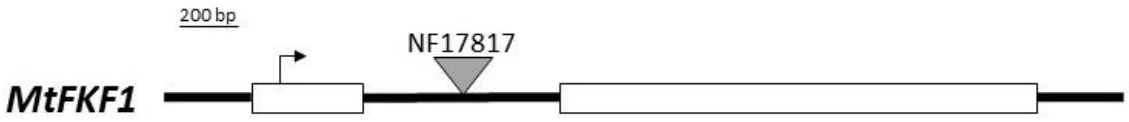

Figure 5.10 *MtFKF1* gene and *Tnt1* insertion scheme.

Representation of line NF17817 containing a *Tnt1* insertion in the first intron of the *MtFKF1* gene. White boxes represent exons and the grey triangle locates the *Tnt1* insertion in the intron.

Seeds from a heterozygous progeny were obtained from the Noble Foundation, sown and plants were genotyped for the presence of the *Tnt1* transposon in the *MtFKF1* intron using a PCR screen with primer pairs detecting presence or absence of the insertion (details in Table 5.4). Progeny from these individual plants were then used for subsequent characterization. The flowering time examination was analysed in LD conditions complemented with a vernalization exposure, which is able to maximize the possible effect of *FKF1* on photoperiod response in *Medicago*.

5.3.3.2 Characterisation of MtFKF1 mutant

The study of *MtFKF1* role in flowering was conducted using WT and *Mtfkf1* mutant families generated from the line NF17817, were named *MtFKF1* (WT- no *Tnt1* insertion in *MtFKF1* gene) and *Mtfkf1* (mutant - insertion of *Tnt1* in *MtFKF1*). Both genotypes were grown in LD condition without (LD+NV group) or after a previous exposure to vernalization (LD+V group).

Flowering time was scored as the date of flowering (DTF). This data is presented in Figure 5.11, showing WT and mutant plants from the LD+NV group, developing a bushy appearance with a short primary shoot axis, prostrate lateral branches and large leaflets, and showing no visible floral buds at 30 days after sowing (Figure 5.11 A). On the other hand, both genotypes show a clear response to vernalization (LD+V; Figure 5.11 B) with elongated shoots, reduced leaf biomass and the first appearance of flower buds and flowers (indicated with grey arrows) by 30 days after sowing. Flowering time data shown in in Figure 5.11 C confirms this difference, both genotypes flowering by 60 days after sowing if unvernalized, but around 23 days when vernalized. However, there were no significant differences in flowering time between genotypes in either condition (p-value>0.005). A closer examination of the date of flowering range also gave no indication that there was any effect of the mutation (Figure 5.11 E and F).

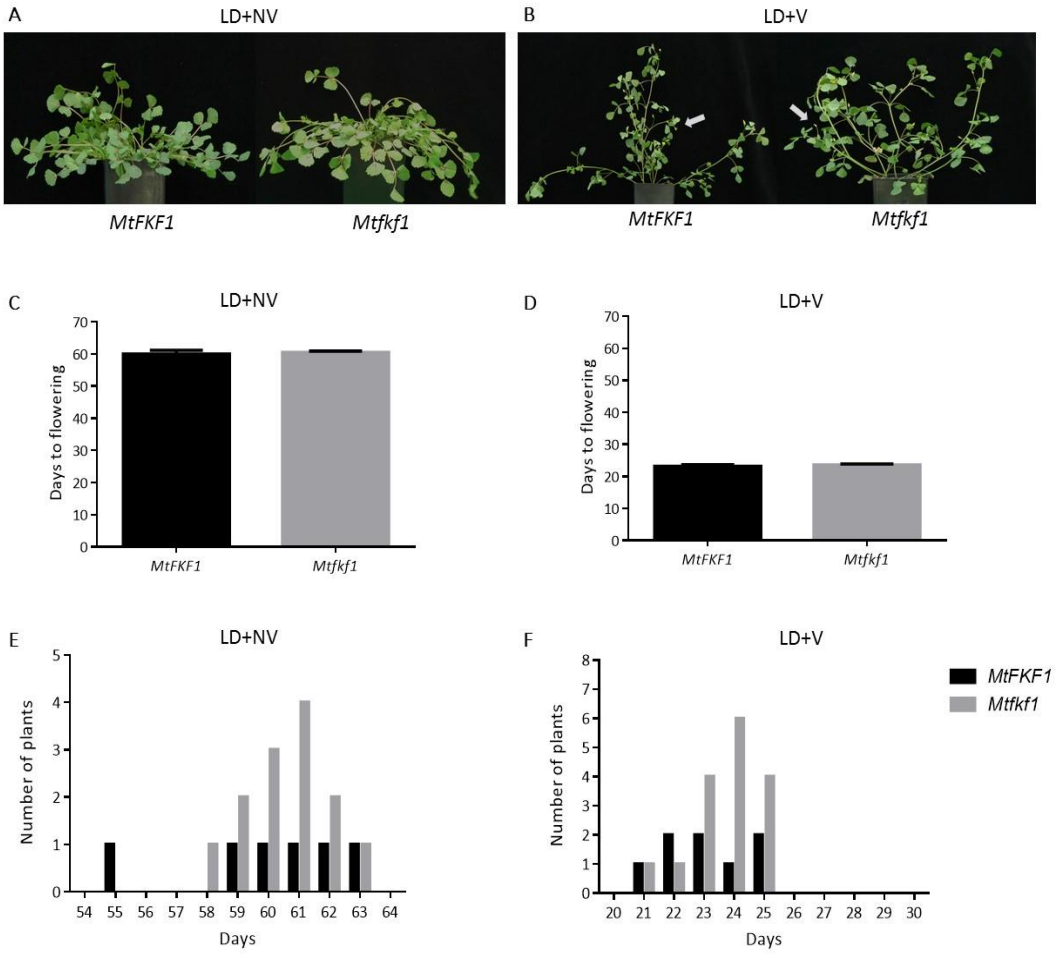

Figure 5.11 Phenotype and flowering time comparison of *MtFKF1* Medicago plants in LD+NV and LD+V treatment.

A) Representative plants of non-vernalized (LD+NV) *MtFKF1* (WT) and *Mtfkf1* (mutant) *Medicago* plants at 30 days after sowing. B) Representative plants of vernalized (LD+V) *MtFKF1* (WT) and *Mtfkf1* (mutant) *Medicago* plants at 30 days after sowing. Flowering time was scored as days to flower (DTF) for LD+NV treatment (C) and LD+V treatment (D). Values represent mean ± SE for N=6-15 plants. There are no significant differences in flowering time between the two genotypes ($p>0.05$). *MtFKF1* (WT) is presented in black and *Mtfkf1* (mutant) in grey. Light grey arrow indicates flowers. (E,F) Distribution of flowering time as number of plants flowering per day for LD+NV (non-vernalized) treatment (E) and for LD+V (vernalized) treatment (F). *MtFKF1* (WT) is presented in black and *Mtfkf1* (mutant) in grey. Values represent frequency of individuals per timepoint for N=6-15 plants.

To provide a further confirmation of this result, the potential effect of the *MtFKF1* insertion was also examined in a segregating population, grown in LD conditions with or without vernalization. The genotype distributions and mean values for flowering time are shown Figure 5.12, finding uneven distribution of genotypes between vernalised and non-vernalised conditions (only 4 *MtFKF1 WT* plants in LD+NV).

Under non-vernalized LD conditions, WT segregants flowered at around 62 days and the heterozygous and mutant segregants both flowered around 58 days, but these differences were not statistically significant (p-value>0.05). For vernalized plants (Figure 5.12 B), the mean flowering time for all genotypes was 25-26 days. The frequency distribution of flowering time in LD+NV treatment seen in Figure 5.12 C also suggests a possible small difference with the WT range 58-66 days, and the range of heterozygotes and mutants between 52-60 days. However, there was no indication of a similar difference in LD+V plants (Figure 5.12 D). This result obtained from segregating progenies is therefore consistent with the earlier results from the homozygous families in the same conditions, and further supports the conclusion that *FKF1* does not play a substantial role in flowering regulation in *Medicago*.

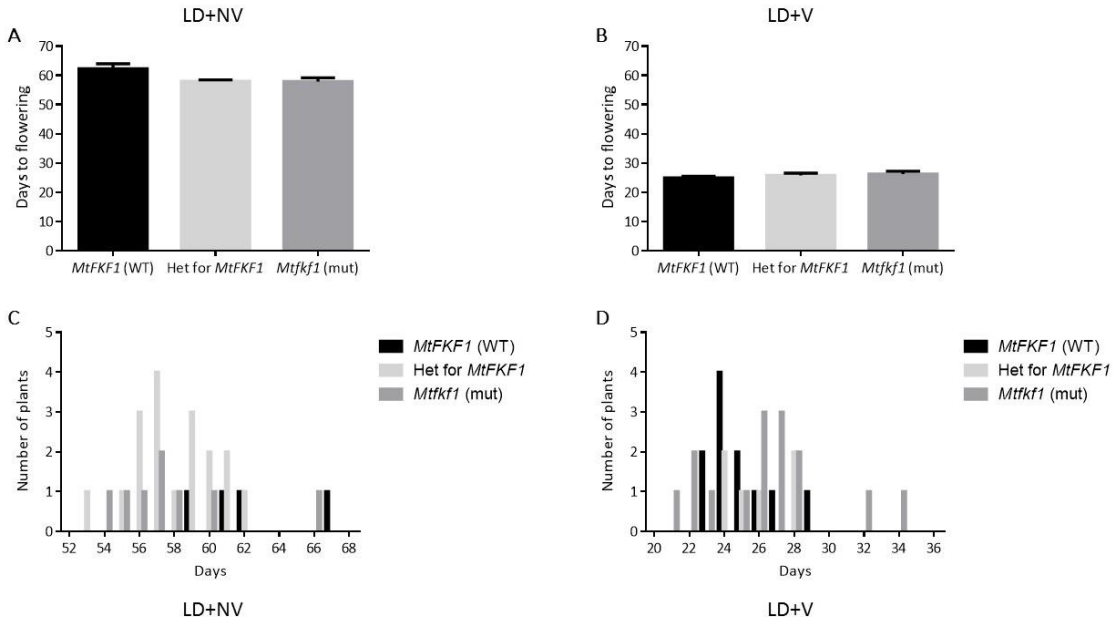

Figure 5.12 Flowering time and frequency distribution of days of flowering of a segregating *MtFKF1* family.

A) Days to Flowering of a segregating family of *MFKF1* in LD+NV (non-vernalized) conditions. B) Days to Flowering of a segregating family of *MFKF1* in LD+V (vernalized) conditions. C) Distribution of flowering time as number of plants flowering per day in LD+NV (non-vernalized) treatment. D) Distribution of flowering time as number of plants flowering per day in LD+V (vernalized) treatment. Values represent mean ± SE for a N= 4-18 plants per genotype. There are no significant differences between the genotypes segregating in the *FKF1* family ($p>0.05$).

A complementary evaluation of possible gene expression in *Mtfkf1* mutant by RT-PCR suggested amplification of *FKF1* gene. This result was not fully confirmed but could be indicative that the *Medicago fkf1* mutant is not a strong mutant for this analysis.

5.3.4 FKF1 protein characterization.

Protein structure prediction software is a useful tool to study structure-based function annotation in uncharacterized proteins and explore the conservation in protein structure, which is possibly associated with conservation in function, among closely related proteins. Following the phylogenetic analysis and *PsFKF1* role characterization in two legume species, a full protein structural prediction was performed in I-TASSER (Yang et al., 2014a; Yang and Zhang, 2015) for the *Arabidopsis*, pea and *Medicago* FKF1 polypeptide sequences (AtFKF1, PsFKF1 and MtFKF1) in order to examine structural diversification potentially related to changes in FKF1 functionality.

The first analysis of the protein predictions in Figure 5.3 revealed similar amino-acid sequence length and protein structure, with high levels of conservation in the three domains: the LOV domain, in charge of light perception and Flavinin binding, the F-box domain, related with ubiquitin activity and substrates recognition, and the Kelch motifs which have a characteristic quaternary structure with each repeat creating a blade formed by four strands of β-sheet (Prag and Adams, 2003). The Kelch domain is commonly recognized as a protein-protein interaction site.

The study of predicted protein configuration is shown in Figure 5.13. Figure 5.13 A shows the characterized blade conformation of each Kelch motif in AtFKF1. This spatial configuration is also observed in PsFKF1 protein prediction (Figure 5.13 C) and in MtFKF1 (Figure 5.13 E), supporting the high conservation in the Kelch domain and suggesting a conserved function between species. On the other hand, the structural predictions for the N-terminal region (Figure 5.13 B, D and F) reveal larger differences in conformation. This region includes the LOV domain known for its light-dependent interaction site with GI, CO or FKF1 homodimerization in *Arabidopsis* (Ito et al., 2012a; Sawa et al., 2007; Song et al., 2012). PsFKF1 and MtFKF1 (Figure 5.13 D and F) are predicted to display a helix structure in this domain, which is not present in AtFKF1 and could interfere in domain accessibility and function.

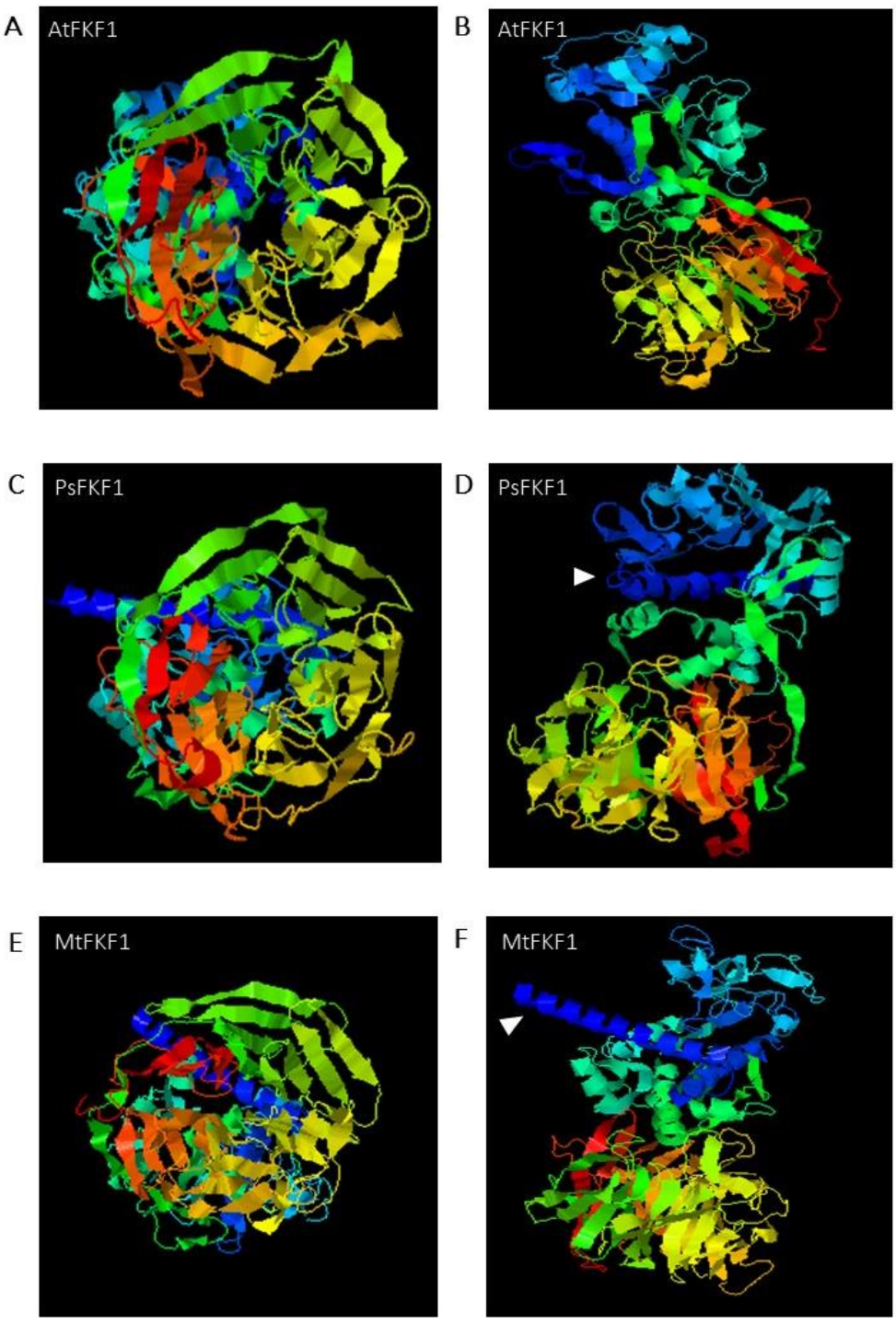

Figure 5.13 Protein structural model prediction for AtFKF1, PsFKF1 and MtFKF1.

Protein prediction was performed with I-TASSER that simulates different structural models and predicts the most confident structural protein model based on C-score (C-score is a confidence measurement of the quality of the protein prediction that is in the range of [-5 to 2]. A high C-score implies a high confidence in the prediction). A) and B) AtFKF1 3D protein simulation with a C-score = -0.86. C and D) PsFK1 3D protein simulation with C-score = -0.58. E) and F) MtFKF1 3D protein simulation with a C-score =-1.86. White triangle indicated the helix structure mentioned in the text.

5.3.5 LATE1 protein analysis and characterization

5.3.5.1 LATE1 gene structure

As previously discussed, *LATE1* is the pea ortholog of the *Arabidopsis GIGANTEA (GI)* gene and has roles in flowering regulation, circadian rhythm maintenance and light signaling (Hecht et al., 2007). Molecular analysis identified six different EMS-induced mutant alleles but focused mainly on one of the strongest alleles, *late1-2*, carrying a nonsense mutation (Hecht et al., 2007). Other characterized alleles carried conserved amino-acid substitutions (*late1-1* and *late1-3*) or a distinct nonsense mutation (*late1-4*) (Hecht et al., 2007). This study examined the two remaining alleles, *late1-5* and *late1-6* DNA sequences. The two alleles were sequenced with primer specified in Table 5.4 but only *late1-5* was successfully characterized. All attempts to characterize *late1-6* allele were unsuccessful. *LATE1* CDS from *late1-6* allele was fully sequenced with multiple combinations of primers, including 5' UTR region of genomic DNA samples, but no mutation in the coding sequence was identified. However, some sequencing results suggested some genomic reorganization in the promoter region of *LATE1* for this allele.

The *LATE1* gene is 9158bp in length and consists of 13 exons (Figure 5.14). The *late1-4* allele was confirmed to carry a nucleotide substitution of G>A in the DNA sequence specifying a codon substitution of W337 to produce a premature stop codon as shown in Figure 5.14. In the *late1-5* allele, a G>A substitution in the last exon predicted an amino acid substitution S1097N (Figure 5.14).

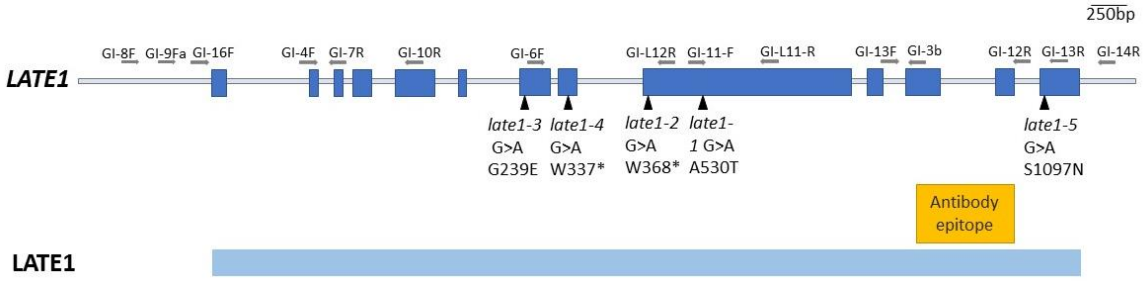

Figure 5.14 *LATE1* molecular allele representation and LATE1 protein representation.

Diagram of the *LATE1* gene in pea showing the location and nature of mutations of *late1* mutant alleles indicated by black triangles. Exons are indicated with blue dark boxes and the grey line represents genomic DNA. The LATE1 protein is represented by a light blue box and the putative antibody epitope recognition site is indicated in yellow.

5.3.5.2 LATE1/GIGANTEA protein characterisation

To describe the predicted LATE1 protein structure and its possible role, a full polypeptide sequence structural prediction was again performed in I-TASSER (Yang et al., 2014a; Yang and Zhang, 2015) for both AtGI and PsLATE1 (Figure 5.15). These two proteins were very similar in length, 1173aa and 1175aa respectively, and their protein structural predictions determine a similar spatial structure with the exception of the middle region where PsLATE1 is proposed to adopt a different conformation. This region is represented in green colour and displays a helix structure in AtGI that differs in LATE1 displaying a blade structural conformation instead (Figure 5.15 C and D, white arrow). Also, AtGI seems to have a more sigmoid shaped conformation in the 3D spatial layer as seen in Figure 5.15 A, and this structural shape is different in PsLATE1 (Figure 5.15 B) finding a more compacted structure with an altered connection between N-terminal region of PsLATE1 (blue colors) and central domains (green tones).

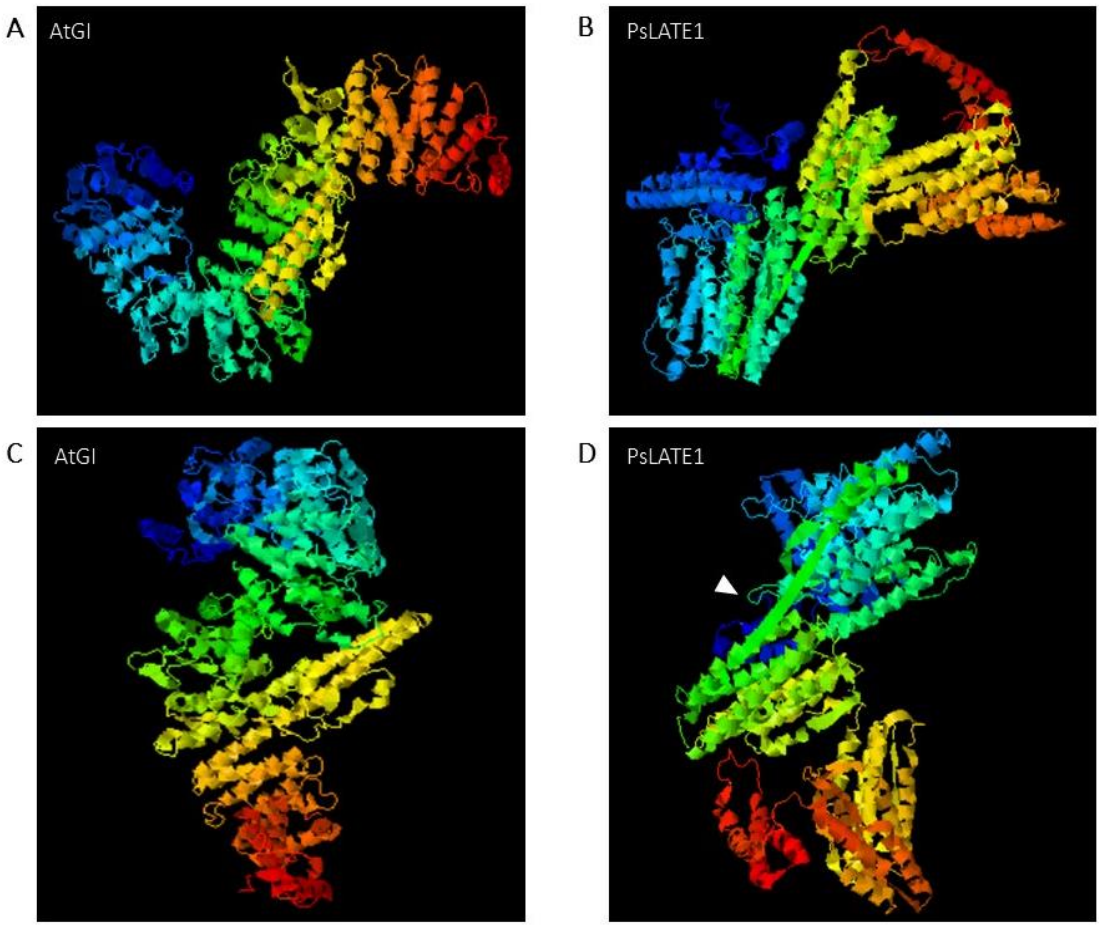

Figure 5.15 Protein structure prediction of AtGI and PsLATE1.

Protein structure prediction was performed with I-TASSER that simulates different structural models and predicts the most confident structural protein model based on C-score (C-score is a confidence measurement of the quality of the protein prediction that is in the range of [-5 to 2]. A high C-score implies a high confidence in the prediction). A) AtGI 3D protein simulation with a C-score = -1.25. B) PsLATE1 3D protein simulation with C-score = -1.31. C) AtGI 3D protein simulation, different angle with a C-score =-1.25.-D) PsLATE1 3D protein simulation, different angle with a C-score =-1.31.White arrow indicates the differential blade structural conformation.

The study of mutant protein predictions, especially in premature codon alleles, is really useful for further protein function and regulation studies. In order to characterize the *late1* alleles, polypeptide sequence structural prediction of all the alleles including the two premature stop codons (*late1-2* and *late1-4*) is displayed in Figure 5.16. LATE1 WT prediction shares similar predicted conformations with *late1-1* and *late1-3* alleles (Figure 5.16 A, C and D respectively) indicating that the amino acid substitutions do not have a substantial impact on the predicted structure. In contrast, the *late1-5* allele also encodes a full-length sequence but clearly affects the predicted structure relative to WT (Figure 5.16 F).

More extreme cases are the *late1-2* and *late1-4* mutants which contain premature stop codons, potentially encoding polypeptides of 368 and 337 amino acid residues respectively. Both conformations (Figure 5.16 C and E respectively) display a low-confidence prediction, probably due to the lack of important protein regions present in LATE1, and have a completely different structural disposition in the space in comparison to the LATE1 WT conformation. Previous research on the GI protein suggests that the central and the terminal region of the protein are the most probable responsible regions for the fine-tuning of circadian clock and its period length, and these regions are missing in these alleles (Mishra and Panigrahi, 2015; Park et al., 1999). Moreover, most of the characterized interactions are described in the N-terminal region of GI which is potentially intact in these alleles if there is viable transcript. An interesting point to note is that the Agrisera antibody epitope used in protein detection in the following result sections, is designed to bind in the predicted C-terminal region of AtGI protein as represented in Figure 5.14.

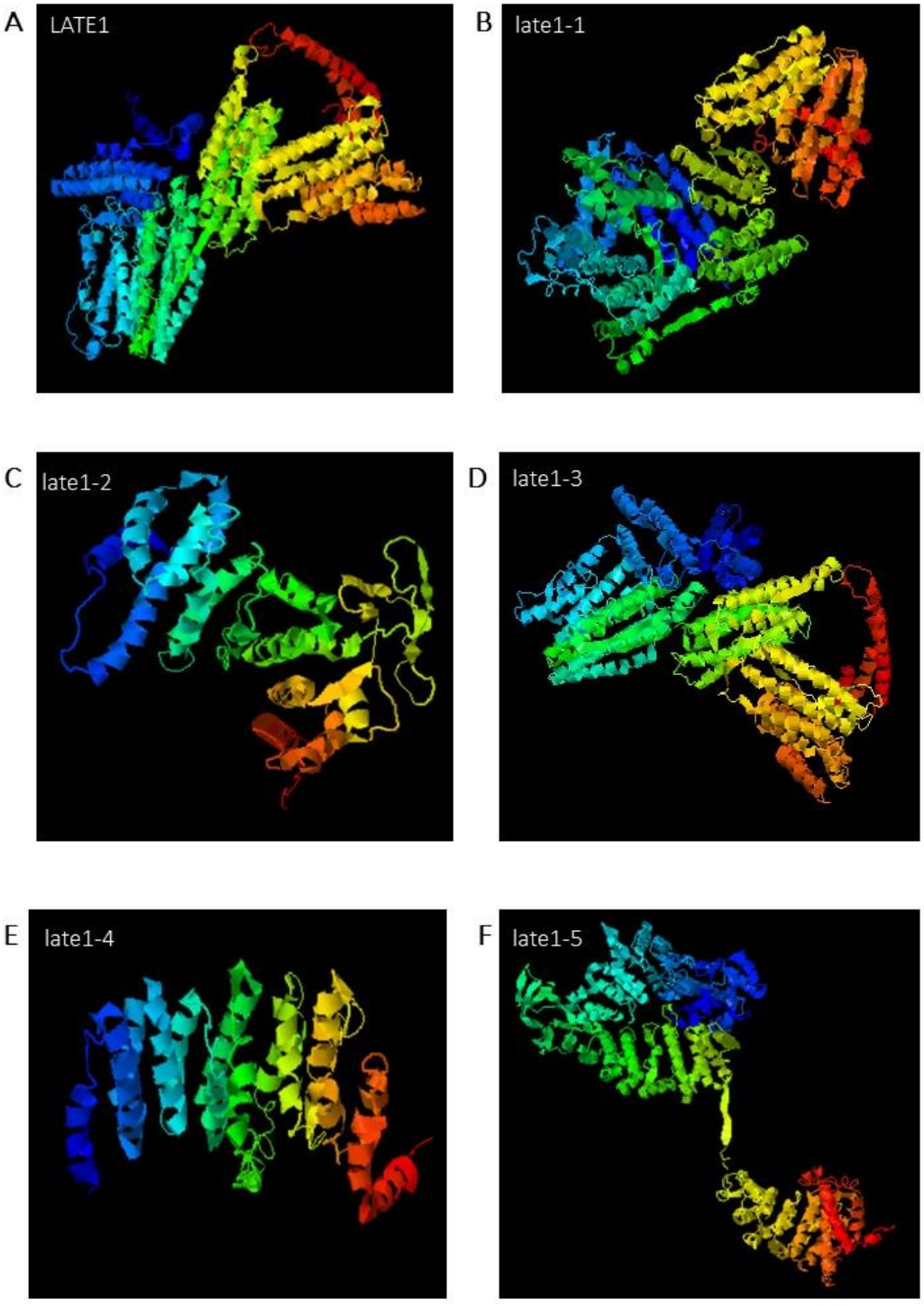

Figure 5.16 Protein structure prediction of PsLATE1 and *late1* mutants.

Protein prediction was performed with I-TASSER that simulates different structural models and predicts the most confident structural protein model based on C-score (C-score is a confidence measurement of the quality of the protein prediction that is in the range of [-5 to 2]. A high C-score implies a high confidence in the prediction). A) LATE1 WT 3D protein simulation with C-score = -1.31. B) Late1-1 3D protein simulation with a C-score= -1.43. C)Late1-2 3D protein simulation with a C-score= -3.83. D) Late1-3 3D protein simulation with a C-score = -1.55. E) Late1-4 3D protein prediction with a C-score= -3.90. D) Late1-5 3D protein prediction with a C-score = -1.32.

5.3.5.3 LATE1 protein detection by Western blotting

The previous research characterizing *LATE1* participation in pea flowering described the nature of the diverse alleles and focused on its expression profile and regulatory outcome in flowering (Hecht et al., 2007), but a protein examination was not included. AtGI protein control is a key mechanism for flowering regulation, finding cyclic AtGI protein levels with accumulation during the day and declining at night due to its proteosome ubiquitin-dependent degradation (Black et al., 2011). Therefore, the study of LATE1 protein in pea is of interest in this thesis.

With the guidance of protein predictions and the previous characterization of *LATE1* function, the study of LATE1 protein was continued with an analysis and detection of protein by Western blot. In *Arabidopsis*, GI protein is characterized with a molecular weight of 120kDa, but smaller bands were identified in Western Blot experiments with molecular weights of 25kDa, 37kDA and 90kDa presumably as degradation products of GI (Black et al., 2011).

The LATE1 protein experiment was designed as a detection method to analyze the protein patterns at different timepoints, different photoperiodic conditions and to fully examine the amount of protein available in different alleles. The method used a polyclonal anti-GI rabbit Agrisera antibody described in section 5.2.5. This antibody was never tested before in pea and was designed to bind in the C-terminal region of GI protein (Figure 5.14).

Firstly, the experiment aimed to study LATE1 WT protein in leaf samples to investigate the efficiency in detection of the method. The WT LATE1 protein detected by Wester blotting is shown in Figure 5.17, with a molecular weight of around 37kDa which is clearly much smaller than the predicted full length protein (around 120kDa). AtGI protein detection experiments reported a degradation product of this same molecular weight, suggesting the detection of a degraded form of LATE1. The Western blot experiment requires a visualization method which in this experiment consisted of a chemiluminescent exposure performed in X-ray films where the molecular weight (MW) could not print a transferable label. Therefore, a visual comparison with the stained membrane was needed for the correct adjustment of MW categorization.

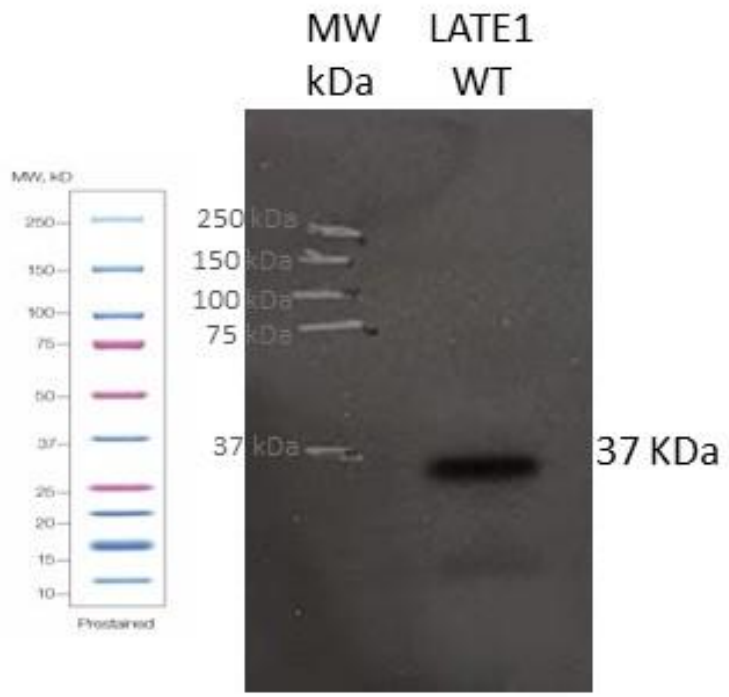

Figure 5.17 LATE1 protein detection by Western Blot.

Western Blot LATE1 film detection by chemiluminescent exposure using anti-GI antibody. The chemiluminescent detection method does not print the Molecular Weight (MW) marker, which is permanently attached to the exposed membrane and manually labelled in the left column after developing.

Due to the detection of a possible degraded polypeptide, multiple troubleshooting attempts were performed with different protein extraction methods, different plants and different samples. In the next experiment, LATE1 WT protein was extracted with two different protocols to avoid and optimize the degradation of the protein and its detection was tested in the following Western Blot, showing both LATE1 WT with a clear band at 37kDa (Figure 5.18). This suggests that the control of LATE1 protein degradation is complicated or that LATE1 protein is truly 37kDa.

Nevertheless, the characterization of the protein in the *late1* mutant alleles was pursued and results are shown in Figure 5.18. Based on protein prediction and characterisation analysis (see above), and on the sequence used as epitope for the production of the antibody (Figure 5.14), the alleles *late1-1* (L1), *late1-3* (L3) and possibly *late1-5* (L5) should all encode a detectable protein by Western Blot with Agrisera anti-GI antibody. On the other hand, the *late1-2* (L2) and *late1*-4 (L4) alleles both contain a premature stop codon and thus encode a

shorter protein and should not be detected. Finally, as *late1-6* (L6) mutation identity is still unknown, the possibility of detecting this mutant form of the protein remains unknown too.

The rest of alleles were extracted following the same protocol as the LATE1 WT sample in the second position in the gel, therefore, their protein detection is comparable to this WT control. Some alleles were detected with a clear band at the same molecular weight like *late1-1 (L1)* and *late1-3 (L3)* indicating protein presence in these mutants. Other alleles, *late1-2 (L2)* and *late1-5 (L5)* display a faint band at the same molecular weight. In the case of *late1-5(L5)*, which was predicted to contain the antibody epitope, this faint band could suggest some protein degradation or the presence of less protein. On the other hand, *late1-2(L2)* is predicted to not create a detectable band due to the lack of the epitope in its amino acid sequence. Therefore, a possible explanation for this faint band might be a gel loading contamination. Lastly, there is no protein detection in *late1-4 (L4)* or *late1-6 (L6),* suggesting the absence of LATE1 detectable protein in these mutants or a total protein degradation during extraction process.

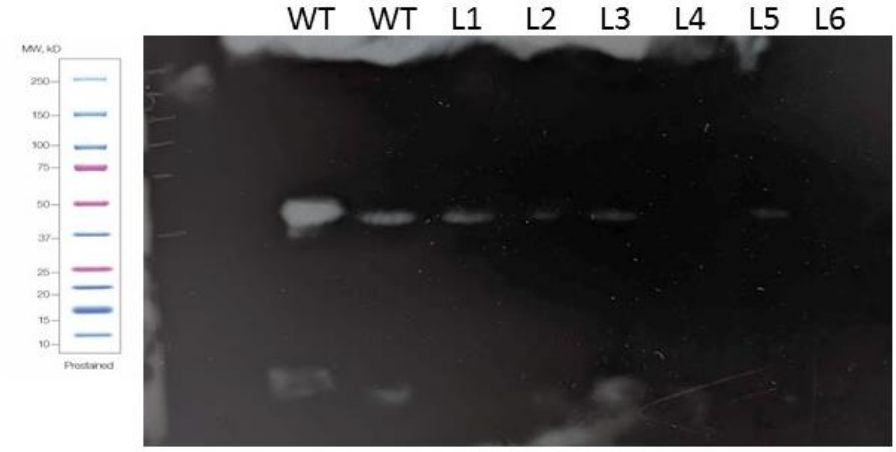

Figure 5.18 *Late1* alleles protein detection by Western Blot.

Western Blot of LATE1 WT and *late1* alleles by chemiluminescent exposure using anti-GI antibody. Molecular weight marker is labelled in the left column and the genotypes are labelled on the top with: LATE1 WT (WT), *late1-1* allele (L1), *late1-2* allele (L2), *late1-3* allele (L3), *late1-4* allele (L4), *late1-5* allele (L5) and *late1-6* allele (L6).

Knowing that LATE1 protein is present and can be detected by anti-GI antibody, the characterization was continued with an examination of the possible LATE1 physical interaction with FKF1.

5.3.6 LATE1 and FKF1 protein interaction.

As discussed in section 5.1., the complex formed by FKF1 and GI In *Arabidopsis* has been extensively studied (Sawa et al., 2007). The interaction FKF1-GI is blue-light controlled and regulates the timing of *CO* expression, via the direct regulation of its transcriptional repressor CDF1 (Mishra and Panigrahi, 2015; Sawa and Kay, 2011). FKF1 is able to interact with CDF1, and its action is dependent of GI. More precisely, the extensive characterization in Sawa et al., 2007 revealed that the N-terminal region of GI protein, from 1 to 139 amino acids, is essential for interaction with FKF1, and the LOV domain in FKF1 is where the interaction occurs (Sawa et al., 2007).

Previous research in pea revealed that LATE2 (*CDF* ortholog) was able to bind to PsFKF1 in a yeast two-hybrid assay (Ridge et al., 2016). Moreover, it was shown that the diurnal expression pattern of *FKF1* coincides with the *LATE1* expression pattern in the middle of the day in LD (Ridge et al., 2016). To continue the characterization of this protein complex and protein interaction, a yeast two-hybrid experiment was designed to study the interaction between LATE1 and FKF1, which domains are involved and confirm the participation of LATE2 in this interaction.

The experiment was designed to test the interaction between the N-terminal region of LATE1 (*GI* ortholog) (i.e. amino acids 1 to 139, corresponding to the region of GI studied by Sawa et al., 2007) with PsFKF1 complete protein sequence. Additionally, LATE2 WT protein and late2 mutant (which contains a R450W substitution that impairs the binding between late2 and PsFKF1 (Ridge et al., 2016)) were included in the experiment and also *Arabidopsis* AtGI-N (just the N-terminal region proven to interact), AtFKF1 and AtCDF were included as interaction controls. The design involved each sequence to be cloned in bait and prey vectors, to test interaction in both directions, together with negative interaction controls. The combinations to test for interaction included: LATE1 complete protein and the LATE1 N-terminal region tested with every other protein in the experiment in both directions, PsFKF1 tested with both LATE1 and AtGI-N in both directions, and AtGI-N tested with every other protein in the experiment also in both directions. These interactions are represented in Table 5.8.

The yeast two-hybrid combination tested, and the results of the interactions are shown in Table 5.8, showing the positive (+) and negative (-) interactions obtained in both directions tested with 3 replicates per test. The interaction analysis seen in Figure 5.19 revealed that LATE1 is able to interact with PsFKF1 and LATE2, indicating that the complex FKF1-GI could form in pea and be able to interact with CDF. The LATE1 N-terminal protein is also able to interact with PsFKF1 and LATE2, indicating that this region is sufficient for the interaction as described in *Arabidopsis* (Sawa et al., 2007). LATE1 is also able to interact with late2, which contains a mutation that impairs late2-PsFKF1 binding but does not interfere in late2-LATE1 binding, consistent with previous knowledge and characterization of the interaction domains (Ridge et al., 2016). Noticeably, both constructs of LATE1 are able to interact with AtGI-N but interact with AtCDF and AtFKF1 in only one orientation of the test. This is a common limitation of the technique also happening in LATE1 and late2 interaction and the test among AtGI-N and AtCDF. PsFKF1 is able to interact with LATE2, LATE1 and with AtGI-N. The *Arabidopsis* controls are consistent with previous literature showing interaction between AtGI-N, AtCDF and AtFKF1.

Table 5.8 Combination of interaction tested in Yeast-two-Hybrid experiment.

Representation of interactions tested in Yeast-Two-Hybrid combinations in both orientations. Prey vectors are specified in columns and bait vectors in rows. Negative interactions are represented with – and positive interactions are represented with + (weak positive), ++ (medium positive interaction) and +++ (strong positive interaction). Blank cells correspond to interactions not tested.

Prey Bait	LATE1	LATE1-N	PsLATE2	Pslate2	PsFKF1	AtGI-N	AtCDF	AtFKF1
LATE1	+++	+++	+++	-	++	+++	-	-
LATE1-N	+++	+++	++	-	++	+++	-	-
PsLATE2	++	+++				++		
Pslate2	++	++				++		
PsFKF1	++	++				++		
AtGI-N	++	++	+++	++	+++	++	++	++
AtCDF	++	+				-		
AtFKF1	+++	+				++		

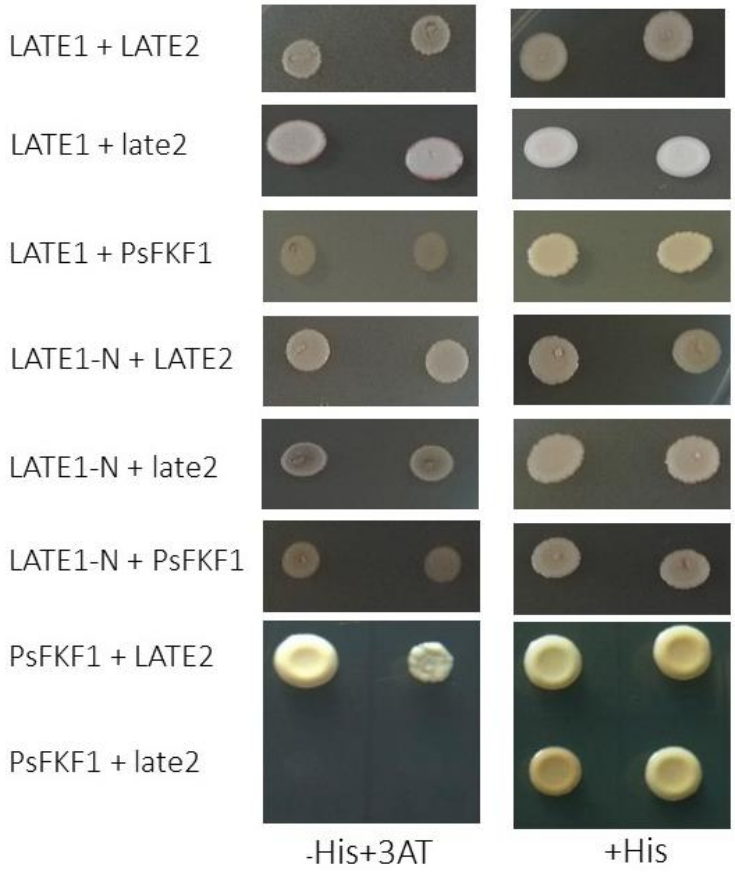

Figure 5.19 Protein interaction combinations tested by yeast two-hybrid analysis.

Yeast two-hybrid analysis of the interaction between pea LATE1 (GI ortholog), FKF1 and LATE2 (CDF ortholog). The previous characterized interaction between PsFKF1 with PsLATE2 and Pslate2 were included (Ridge et al., 2016). Each clone is shown after 4 days of growth at 30°C on selective medium (with 3-amino-1,2,4-triazole added; -His+3AT) and nonselective medium (+His). Each interaction is represented by two colonies. The experiment was performed with respective controls, not shown on this figure.

5.4. Discussion

The *FKF1* and *GI* genes participate in flowering control through several distinct molecular mechanisms, which include both transcriptional and post-transcriptional regulation (Sawa and Kay, 2011; Song et al., 2014). One of these, involving their physical interaction and protein complex formation, is one of the key regulatory pathways for photoperiodic flowering induction in *Arabidopsis* and it is suggested to be a highly conserved mechanism among plant systems (Kim et al., 2013a; Kloosterman et al., 2013; Sawa et al., 2007; Verhage, 2021). It is also relevant to consider that while *GI* is a single-copy gene, *FKF1* has two homologs in *Arabidopsis* (*ZTL* and *LKP2)*, which may also participate in the regulatory pathway, conferring redundancy in *GI* interaction and in function (Baudry et al., 2010; Song et al., 2013).

As one of the two main components has already been functionally characterized in pea (*LATE1 /PsGIGANTEA)*, this study has investigated the other potential member of the complex, *PsFKF1.* This is an important question since *FKF1* might have a key role in mediating light responses in both seedling photomorphogenesis and photoperiod-responsive flowering regulation. This study also included the study of *FKF1* in *Medicago* to examine whether any effect of *FKF1* might be conserved in different LD legume systems. To complement the study of *FKF1* in legumes, some further work on characterization of LATE1 protein and mutant alleles was undertaken.

5.4.1 Effects of *FKF1* on development and flowering

The *PsFKF1* characterization was performed using a mutant allele *fkf1-1* which carries an amino acid substitution in the highly conserved LOV domain of the protein (Figure 5.3)(Figure 5.5). While this is strong evidence for the deleterious nature of the mutation, it cannot be assumed without further functional testing, which in future might involve *Arabidopsis* complementation. The initial examination of development and the study of reproductive traits in LD photoperiod of a BC_3F_2 suggested marginal differences between genotypes indicative of a minor flowering regulatory function of *FKF1* in pea (Figure 5.6)(Figure 5.7).

In view of the known role of *FKF1* as a photoreceptor in *Arabidopsis* and the likely influence of the spectral quality of light on its activity, multiple light/photoperiod conditions were examined in the analysis of flowering response of *fkf1-1* mutant with the objective of testing any possible subtle flowering phenotype that could be accentuated by altering light quality of the photoperiod extension. Some light conditions, in particular CF (continuous cool-white fluorescent light)

indicated a statistically significant late flowering phenotype in NFI, DTF and FLR (Figure 5.8). Other conditions like LDI and natural LD suggested some lateness for NFI and FLR traits but not for DTF, suggesting that the slight effect in flowering time in *FKF1* might be highly dependent on light conditions. Finally, SD conditions did not indicate any flowering phenotype, despite that in *Arabidopsis*, a late flowering phenotype was displayed even in SD when the mutant developed more leaves than WT (Nelson et al., 2000). The *Atfkf1* mutant was characterised as late flowering, in both measurements as days and number of leaves at flowering in LD and with an additional late phenotype in SD. The small phenotypic flowering difference observed in pea supports the possibility of the participation of *PsFKF1* in photoperiodic control of flowering but, further characterization of the light conditions that potentiate its participation are required, together with a fully introgressed *fkf1-1* mutant in the NGB5839 genetic background to exclude other genetic components complicating the results.

A well characterised function of *FKF1* is the blue-light photoreceptor activity with the LOV domain specifically responsible for light perception (Imaizumi et al., 2003; Nelson et al., 2000), and in *Arabidopsis* it has been shown that photomorphogenesis in *fkf1* mutant seedlings is hypersensitive to blue and red light conditions (Nelson et al., 2000). Further experiments confirmed that blue light was the most effective wavelength to activate *FKF1* function, in control of flowering and *FT* expression (Imaizumi et al., 2003), whereas red light was shown not to be effective. The photomorphogenesis study in the pea *fkf1-1* mutant showed that it etiolated normally in dark conditions and de-etiolated normally in response to light (Figure 5.9), like the *Arabidopsis* mutant (Nelson et al., 2000). However, unlike *Arabidopsis*, the mutant also responded normally across a range of intensities, with only a suggestive tendency towards slightly shorter internode length in *fkf1-1* (Figure 5.9). The same trend is observed in the other light treatments, with minimal phenotypic differences in red light conditions or in the combination of red and blue light, indicating that pea *FKF1* has a small effect in photomorphogenesis development. This result suggests that other components could participate redundantly in this regulation and supports previous studies where other pea clock-related genes, like *PPD (ELF3* ortholog) and *DNE (DIE NEUTRALIS* which is *ELF4* ortholog) do not present a considerable effect on seedling elongation, differing from *Arabidopsis* (Rubenach et al., 2017).

The unexpectedly minor effect of *PsFKF1* on both flowering and photomorphogenesis indicates a possible redundancy in pea where other components of the same family could be involved in these developmental processes. A suggested gene is *ZTL,* which presents high conservation level in its sequence and specifically in the LOV, F-box and Kelch repeat domains (Figure 5.4). The subsequent

study of phylogenetic relationships exhibits a clear separation between FKF1 and ZTL families and a diversification within of SD and LD legume group (Figure 5.4). This classification follows a previous description of the FKF1 and ZTL family in legumes (Ridge et al., 2016) and indicates substantial similarity in sequence between the two groups supporting possible redundancy in function as seen in *Arabidopsis* (Baudry et al., 2010; Song et al., 2014).

Finally, an analysis of *Medicago FKF1* flowering response was included studying a *Tnt1 Medicago* mutant line which contains the disruptive insertion in the intron (Figure 5.10). The study of *Medicago FKF1* flowering response indicated a minor, if any, role of *MtFKF1* in flowering regulation (Figure 5.11)(Figure 5.12) even in a segregating family experiment and after a vernalization exposure which is an enhancer of flowering phenotypes in other mutants (Jaudal et al., 2020). This result complements the observations in pea: *FKF1* seems to have a minimal role in flowering regulation in these two LD legumes suggesting that other similar genetic components could redundantly participate in flowering time control.

5.4.2 FKF1 and LATE1 protein characterization

Pea *LATE1* characterization included an extensive study of *late1* flowering mutants, focussing on the late-flowering phenotype of the diverse mutant alleles, the diurnal expression patterns and the regulatory effect on other circadian genes' expression (Hecht et al., 2007). The characterization included the expression profiles of *CO-like* and *FT-like* genes in pea revealing the important role in flowering time regulation that *LATE1* has in the pea model (Hecht et al., 2007; Liew et al., 2009). But, the protein characteristics of this key component was not yet explored in terms of interactions or regulation.

Six mutant alleles (Figure 5.14) were examined in this thesis, describing the nature of the mutation of 5 of them since *late1-6* involves low expression of the gene and difficulty in its sequencing, with indications of possible mutations in the promoter region of the gene. The rest of mutant alleles (*late1-1* to *late1-5)* were studied by their protein profiles including protein structural predictions (Figure 5.15)(Figure 5.16) and protein detection (Figure 5.17)(Figure 5.18). LATE1 and GI are both large proteins with similar structural conformation supporting a conservation in function (Figure 5.15). The anti-GI antibody was designed to bind in the terminal region of GI protein with binding affinity in the same region of LATE1 (Figure 5.14), expecting no binding in the alleles *late1-2* and *late1-4* which contain stop premature codon and which protein structural predictions have low confidence in the structural model (Figure 5.16). On the other hand, the other alleles (*late1-1* and

late1-3) maintain similar length and protein structure to LATE1 WT, however, the amino acid substitution in *late1-5* is predicted to cause a major structural change and could affect the anti-GI binding region (Figure 5.14)(Figure 5.16).

The protein detection experiment revealed that Agrisera GI antibody can be used in pea to detect LATE1 (Figure 5.17) but it detects a possible degradation band of 37kDa instead of an expected band of 127.9kDa, similar molecular weight to characterised 37kDA GI degraded products (Black et al., 2011). Even though different extraction protocols were examined, there was no detection of the expected band of 127.9kDa. The subsequent protein detection study in the different alleles supported the previous observations, presenting a 37kDa band for *late1-1, late1-3* and *late1-5.* Interestingly, the *late1-5* allele shows protein detection in the Western result indicating that the epitope region could be recognised in this allele but with less intensity which could be due to protein degradation or less protein (Figure 5.18). The Western experiment has some conflicting results since the epitope was detected in lines homozygous for alleles where the protein is predicted to be truncated such as *late1-2* this may be due to sample contamination. Therefore, further testing of protein extraction protocol and confirmation of this *late1-2* band results are needed in order to fully integrate this protein detection method for pea LATE1.

The next possible study on this project was the interactive examination of PsFKF1 and LATE1 (FKF1 and GI pea orthologs) in the pea regulatory pathway, since this complex is the main transcriptional regulatory route in *Arabidopsis* model and it is composed of characterised members in the pea model, for which there is evidence of interaction (Sawa et al., 2007; Sawa and Kay, 2011). With the previous knowledge of a Yeast-two-Hybrid interaction between LATE2 (CDF) and PsFKF1 (Ridge et al., 2016), understanding the complete complex interaction was the final objective of this study.

The Yeast-two-Hybrid examination analysed the interaction by pairs of the three described components PsFKF1 (*FKF1* ortholog), LATE1 (*GI* ortholog) and LATE2 (*CDF* ortholog), revealing positive interaction between all pairwise tests (Table 5.8)(Figure 5.19). Moreover, the interaction follows the same characterization as in *Arabidopsis* and other models, where the N-terminal region of GI (LATE1 in this study) is able to interact with FKF1 (PsFKF1 in this study) and CDF (LATE2 in this study) (Sawa et al., 2007). LATE2 has a characterised FKF1 binding region (Ridge et al., 2016) which is distinct to the binding region to LATE1 (Table 5.8)(Figure 5.19). Further description of the specific interactive region of PsFKF1 is required, knowing that the Kelch domain is responsible for CDF binding and LOV domain is in charge of GI binding in *Arabidopsis*. A complementary study

with the *fkf1-1* mutant (which contains a substitution in the LOV domain) could be of high relevance to describe the specific binding regions of PsFKF1 (Li et al., 2013; Sawa et al., 2007). The complementary study could be extended to integrate *late1* mutants and fully characterise the domains involved in protein interaction in this complex. Moreover, FKF1 and GI interaction is described to be light-dependent in *Arabidopsis* (Sawa et al., 2007), then, the effect of different light conditions in this interaction could also be explored in pea.

5.4.5 Conclusions and future directions

The small effect observed in the examination of *FKF1* in both *Medicago* and pea suggests that its role is not as important as in *Arabidopsis*, giving support to redundant components with similar regulatory roles. In *Arabidopsis*, there is supportive literature regarding a redundant component, *ZTL,* which participates in circadian clock and flowering time control in a similar manner to *FKF1* (Song et al., 2014). *ZTL* is able to interact with the same components than *FKF1* and even is able to capture FKF1 protein when forming homodimers (Takase et al., 2011). Moreover, it is fully characterised with a redundant role to *FKF1* regulating *CO* expression, but interestingly, acting antagonistically in CO protein regulation (Hwang et al., 2019). A critical point to consider is the ZTL ability to interact with GI and FKF1, having opposite regulatory effect depending on the interaction (Hwang et al., 2019; Takase et al., 2011). Therefore, the examination of pea *ZTL* is of high interest to fully understand the role of *FKF1* and *LATE1* in pea flowering time regulation. Also, this gene and its effect in flowering time control have not been explored in any other legumes yet.

As mentioned in previous chapters, the characterization of pea and *Medicago fkf1* mutant should include more light conditions and an extended characterization of the blue-light photoreceptor activity. Another point to consider is the description of diverse lab light conditions and their effect in flowering examination, recent research in *Arabidopsis* suggests that lab conditions could induce expression in flowering genes that are not present in nature LD conditions, in particular the expression of *AtFKF1* (Song et al., 2018).

The protein characterization of FKF1 and LATE1 gives evidence of a conserved interaction as described in *Arabidopsis* (Sawa et al., 2007). Future research should complement this study with the characterization of mutant proteins (*fkf1* and *late1* mutants) and their interaction, describing the key regions of interaction and the regulatory function of this complex in pea. This study could also be extended to other legume models, specially SD legume plants, to examine the conservation of these important proteins in the legume family.

Chapter 6 - General discussion

6.1 Summary of main findings

Understanding the molecular mechanism regulating diverse plant developmental processes is one of the best assets to assist on the advance and improvement of agriculture. This is particularly the case for the shift to reproductive stage, which is a key transition in plant development with critical value for agriculture since it aligns reproductive development with environmental conditions. Previous research has focused on analyzing the genetic mechanism regulating flowering time in relation to daylength using *Arabidopsis* as model plant, but the translation and extension of this molecular knowledge to crop species, including legumes, is still an on-going process. The main goal of this thesis has been to examine certain genetic components and the molecular mechanism participating in photoperiodic flowering time regulation in pea, as a representative and well-studied LD legume species. This research aimed to unravel the genetic mechanism controlling flowering time utilizing outlined genetic components in *Arabidopsis,* which are characterized as transcriptional regulators like the case of *FKF1* and *LATE1* (*GI* homolog), or protein regulators like LIP1 (*COP1* homolog). The characterization of the pea model is also complemented by the study of novel legume regulatory candidates like *E1* gene (Andrés and Coupland, 2012; Weller and Ortega, 2015).

The thesis results in Chapter 5 suggest that the known components of the transcriptional regulatory pathway are conserved in legumes, finding the ortholog components of the well-known regulatory complex FKF1-GI and CDF to be able to interact in the pea system in a similar fashion (Table 5.8), (Figure 5.19)(Sawa et al., 2007). But, the analysis of each component function and participation in flowering regulation differs from *Arabidopsis* model (Song et al., 2014). The diverse studies of *PsFKF1* suggest a small effect in flowering time in pea (Figure 5.6), (Figure 5.7), (Figure 5.8) and minimal participation in light developmental response (Figure 5.9), indicating a possible redundancy with other genetic components yet to characterize in pea. The complementation study of *MtFKF1* supports this lack of flowering participation (Figure 5.11), (Figure 5.12). On the other hand, *LATE1* is known to affect flowering time in this species and control circadian expression of other clock genes (Hecht et al., 2007) but the specific protein patterns of this component are still unclear throughout the day and under different light conditions (Figure 5.17), (Figure 5.18).

Another important flowering regulatory pathway in *Arabidopsis* is composed by COP1 and its photoperiodic flowering repressor function towards protein components, most prominently CO

(Xu et al., 2016). COP1 is a well-characterized ubiquitin ligase, regulated by phytochromes, and able to interact with many key flowering components like GI (LATE1 in pea), ELF3 (HR in pea) or PHYA (Jang et al., 2015; Yu et al., 2008). The examination of the genetic interactions and flowering regulatory function of *LIP1* (*COP1* ortholog in pea) in Chapter 4 supports a differentiation in flowering participation of this component in pea since *LIP1* displays a dwarf phenotype and an early node of flowering initiation in both photoperiods studied (Figure 4.4), (Figure 4.5). This result supports a developmental impairment which interferes with flowering node measurements, finding a slower rate of node development (up to 20% slower) in this mutant (Figure 4.5), (Figure 4.7). *LIP1* characterization also included observations on how this mutant is highly dependent on temperature and healthy status of the plant to display a consistent phenotype (Figure 4.6). The genetic interactions studied supported this differential flowering participation, since *LIP1* acts independently of *LATE1 (GI)* (Figure 4.10) and has a subtle additive effect to *HR (ELF3)* (Figure 4.11). This contrasts the *Arabidopsis* model, in which all these components interact (Jang et al., 2015; Yu et al., 2008). Interestingly, the genetic interaction between *LIP1* and *PHYA* in flowering regulation and photomorphogenesis reveals a conserved connection with a possible inter-regulatory mechanism (Figure 4.8), (Figure 4.9), similar to the *Arabidopsis* model (Xu et al., 2016).

Lastly, this research aimed to examine other flowering components important in other plant models, which are not present in *Arabidopsis*. One of the most notable is *E1*, described as a novel legume transcription factor key in the flowering time regulation in soybean (Xia et al., 2012). *E1* is able to repress flowering in LD under the regulation of phytochromes and directly regulate *FT-like* genes in soybean (Zhai et al., 2014a). In Chapter 3, the evaluation of *E1* indicates a high level of sequence conservation among legumes -SD and LD groups- (Figure 3.17), (Figure 3.18), but the major effect on flowering time is not preserved in temperate legumes (pea and *Medicago*), suggesting at most a minor or subsidiary role in flowering regulation (Figure 3.2), (Figure 3.3), (Figure 3.4), (Figure 3.6). Some recent reports have suggested a small effect on flowering in *Medicago* (Jaudal et al., 2020; Zhang et al., 2016), but this was not detected in this study (Figure 3.12), (Figure 3.15). Moreover, *E1* in pea seems to be also regulated by PHYA but further characterization is needed to confirm this (Figure 3.8).

6.2 Revised flowering model in pea

Based on this thesis results and previous research on the molecular mechanism of photoperiodic flowering time in pea and other legumes, the model of flowering regulation in pea is understood like in Figure 6.1 where light is perceived by photoreceptors, PHYA and PHYB, which are able to regulate the expression levels of *FT-like* genes (Weller et al., 1997a, 2001, 2004). The molecular mechanism is still unclear, but this thesis has evaluated the possible mediating role of *LIP1*, which seems to act independently in photoperiodic flowering control but in the same pathway than PHYA in light developmental processes like photomorphogenesis. On the other side, the transcriptional regulatory pathway appears to involve the same components as in *Arabidopsis*: *LATE1, FKF1* and *LATE2. LATE1* is strongly regulated by the circadian clock, and itself controls the rhythmicity of other clock genes (Hecht et al., 2007). It has an important role regulating flowering time leading to the regulation of *FT-like* genes in pea. In the same pathway, *LATE2* participates downstream of light and circadian clock signaling, regulating *FT-like* gene expression, in particular *FTb2* (Ridge et al., 2016). Similarly to *LATE1*, its function appears to be independent of the transcriptional control of *CO-like* genes, supporting the idea that these components do not mediate photoperiodic flowering control in pea in the same way as *Arabidopsis CO.* The last component is *FKF1*, which seems to have only a small effect and function in the regulation of flowering, possibly due to a redundant function with other similar components. These three components are proven to interact in pea, expanding previous findings and confirming the interaction between the N-terminal region of LATE1 with FKF1, FKF1 interacting to a specific binding region in LATE2 which is different to the binding region of LATE1. Hence, this thesis supports a conservation in the transcriptional regulatory mechanism. And finally, the lack of effect of *E1* indicates that despite of being a legume-specific transcriptional factor with key flowering function in other legumes, it does not replace *CO* as the main integrator of photoperiodic flowering.

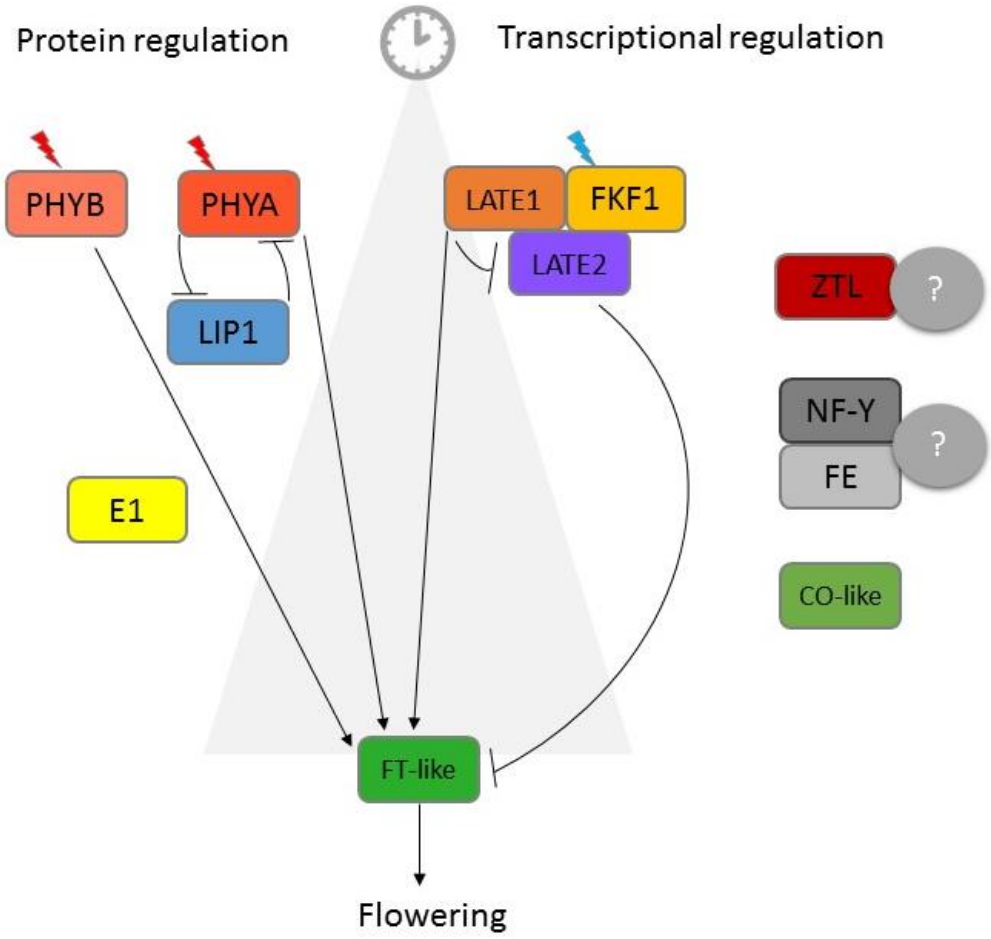

Figure 6.1 Diagram representing photoperiodic flowering genetic network in pea.

Diagrammatic representation of pea flowering model. Components of the pathway are represented in boxes with the acronym names described in this thesis. The left side of the diagram represents protein regulation, and the right side represents the components involved in transcriptional regulation. Components on the outside range and with a question mark represent possible flowering genes still unexamined. Circadian clock involvement is represented by a grey clock. Flat solid arrows indicate direct repression and solid pointy arrows indicate induction. The blue or red lighting represents red or blue light activation.

6.3 Future directions

While the model presented above includes improved understanding of the genetic control of pea flowering time, there are many aspects of this process that remain to be addressed in future studies. A starting point could be a further exploration of light quality effects in the pea system. Recent research has examined the differential molecular behavior of flowering genes in *Arabidopsis* under natural light conditions in spring in comparison to lab light conditions (Song et al., 2018; Wilczek et al., 2009). Interestingly, there were some differential expression patterns in

some key components like *FT* or *FKF1* supporting the importance of the light conditions tested in the characterization of flowering genes. The adjustment of temperature fluctuations and the Red to Far-Red ratio is proven to be sufficient to mimic the expression pattern of *FT* and flowering time outcomes observed in natural LD (Song et al., 2018). This research emphasizes how important the understanding of the light quality effects is in the molecular mechanism and suggests that a deeper examination of light quality and temperature may be critical in further work on photoperiodic flowering in pea and *Medicago*.

It is clear however, that the molecular mechanism regulating flowering time in pea is far from being well-understood and several important functions and potential interactions remain to be tested or described. The initial characterizations of the flowering function in pea of each gene presented here should be complemented with further examination of the conservation in genetic and physical interactions, as done for LATE1-LATE2-FKF1, or *LIP1-PHYA* and *LIP1-LATE1-HR* in this thesis. Thus, further examination of other possible interactions with the known components in pea is highly relevant, specially with well-characterized interactions like FKF1-COP1 in *Arabidopsis*, which is a key flowering regulatory mechanism regulating CO protein and flowering time (Lee et al., 2017; Ponnu and Hoecker, 2021).

Another key step that remains unexplained is the nature of the integrating mechanism, and how photoreceptor and light signals interact to confer photoperiod specific *FT-like* gene expression in the absence of any apparent role for *CO-like* genes (Hecht et al., 2007; Ridge et al., 2016; Weller and Ortega, 2015). This thesis has explored a closer legume flowering genetic network, soybean model, with a key component as intermediate role. The legume-specific *E1* gene has a major integrating role in the SD legume soybean as a direct repressor of *FT* gene expression under LD (Xia et al., 2012), and was initially suggested as a potential candidate for a similar integrator in LD legumes (Zhai et al., 2014a), but the analyses in this thesis do not support this idea. Whether a major role for *E1* is specific to soybean or shared by other SD legumes like common bean or mung bean remains to be determined.

Another gene raised as a possible integrator is *FE,* which acts as *FT* regulator inducing its expression and regulating *FT* transport in the phloem in *Arabidopsis* (Abe et al., 2015; Shibuta and Abe, 2017). A recent study of *MtFE* describes its role in photoperiodic flowering in *Medicago*, where it also regulates *FT-like* gene expression and induces flowering in LD, and may act with NF-Y like proteins in a mechanism similar to that in *Arabidopsis* (Kinoshita and Richter, 2020; Thomson et al., 2021). In future, it will be important to examine whether this effect is conserved in other LDP legumes, with further exploration of the role of *FE* in the legume genetic network. Finally,

several *CO*-independent mechanisms for photoperiod-related *FT* regulation are known in *Arabidopsis* and may be relevant mechanisms to explore in the legume system. These include potential direct roles for *GI* and *FKF1* in *FT* promoter binding and induction (Ito et al., 2012a; Sawa and Kay, 2011; Song et al., 2012), the GI involvement with TEM proteins, which are also known regulators of *FT* (Castillejo and Pelaz, 2008; Sawa and Kay, 2011) or the FKF1-mediated regulation of DELLA proteins leading to flowering promotion (Hwang et al., 2019; Nohales and Kay, 2019; Yan et al., 2020). Future analyses should also consider the *FKF1* paralog *ZTL,* which has similar structure and overlapping functions in circadian clock control and flowering time (Baudry et al., 2010; Song et al., 2014). One final possibility may be the separation of *CO-like* molecular functions into two separate proteins similar to the sugarbeet system where a PRR protein and a B-box zinc finger protein seem to interact simulating the C-terminal and N-terminal domain of CO respectively and regulating flowering together (Dally et al., 2014). A more detailed characterization of PRR and B-box proteins therefore may also be warranted.

6.4 Concluding remarks

The work in this thesis has contributed to the understanding of the molecular mechanism directing photoperiodic flowering time control in pea and provides insight in the role, or lack of function, of diverse genes of the pathway. It has also analysed some molecular components participating in the *Medicago* flowering pathway and together, giving supporting evidence to a flowering legume model without a role for *CO*. While the majority of the information has been negative, in the sense that it argues against conserved roles for genes (*COP1, E1, FKF1*) which have a major effect in other species, this research has nevertheless complemented the knowledge about the LD flowering model, involving *Arabidopsis* information with the exploration of candidate flowering genes and including legume specific components, leading to a better understanding of the flowering response and molecular mechanisms participating in LD legume flowering.

References

Abe, M., Kaya, H., Watanabe-Taneda, A., Shibuta, M., Yamaguchi, A., Sakamoto, T., Kurata, T., Ausín, I., Araki, T., and Alonso-Blanco, C. (2015). FE, a phloem-specific Myb-related protein, promotes flowering through transcriptional activation of FLOWERING LOCUS T and FLOWERING LOCUS T INTERACTING PROTEIN 1. *Plant Journal*, *83*(6), 1059–1068. https://doi.org/10.1111/tpj.12951

Abe, M., Kobayashi, Y., Yamamoto, S., Daimon, Y., Yamaguchi, A., Ikeda, Y., Ichinoki, H., Notaguchi, M., Goto, K., and Araki, T. (2005). FD, a bZIP protein mediating signals from the floral pathway integrator FT at the shoot apex. *Science*, *309*(5737), 1052–1056. https://doi.org/10.1126/science.1115983

Abelenda, A., and Navarro, C. (2014). *Flowering and tuberization : a tale of two nightshades*. *19*(2), 115–122. https://doi.org/10.1016/j.tplants.2013.09.010

Aki, T., Shigyo, M., Nakano, R., Yoneyama, T., and Yanagisawa, S. (2008). Nano scale proteomics revealed the presence of regulatory proteins including three FT-like proteins in phloem and xylem saps from rice. *Plant and Cell Physiology*, *49*(5), 767–790. https://doi.org/10.1093/pcp/pcn049

Alves-Carvalho, S., Aubert, G., Carrère, S., Cruaud, C., Brochot, A. L., Jacquin, F., Klein, A., Martin, C., Boucherot, K., Kreplak, J., Da Silva, C., Moreau, S., Gamas, P., Wincker, P., Gouzy, J., and Burstin, J. (2015). Full-length de novo assembly of RNA-seq data in pea (Pisum sativum L.) provides a gene expression atlas and gives insights into root nodulation in this species. *Plant Journal*, *84*(1), 1–19. https://doi.org/10.1111/tpj.12967

Andrés, F., and Coupland, G. (2012). The genetic basis of flowering responses to seasonal cues. *Nature Reviews. Genetics*, *13*(9), 627–639. https://doi.org/10.1038/nrg3291

Auge, G. A., Perelman, S., Crocco, C. D., Sánchez, R. A., and Botto, J. F. (2009). Gene expression analysis of light-modulated germination in tomato seeds. *New Phytologist*, *183*(2), 301–314. https://doi.org/10.1111/j.1469-8137.2009.02867.x

Balasubramanian, S., Sureshkumar, S., Lempe, J., and Weigel, D. (2006). Potent induction of Arabidopsis thaliana flowering by elevated growth temperature. *PLoS Genetics*, *2*(7), 0980–0989. https://doi.org/10.1371/journal.pgen.0020106

Balcerowicz, M., Kerner, K., Schenkel, C., and Hoecker, U. (2017). SPA proteins affect the subcellular localization of COP1 in the COP1/SPA ubiquitin ligase complex during photomorphogenesis. *Plant Physiology*, *174*(3), 1314–1321. https://doi.org/10.1104/pp.17.00488

Baudry, A., Ito, S., Song, Y. H., Strait, A. A., Kiba, T., Lu, S., Henriques, R., Pruneda-Paz, J. L., Chua, N. H., Tobin, E. M., Kay, S. A., and Imaizumi, T. (2010). F-Box proteins FKF1 and LKP2 act in concert with ZEITLUPE to control Arabidopsis clock progression. *Plant Cell*, *22*(3), 606–622. https://doi.org/10.1105/tpc.109.072843

Beales, J., Turner, A. S., Griffiths, S., Snape, J. W., and Laurie, D. A. (2007). A Pseudo-Response Regulator is misexpressed in the photoperiod insensitive Ppd-D1a mutant of wheat (Triticum aestivum L.). *Theoretical and Applied Genetics*, *115*(5), 721–733. https://doi.org/10.1007/s00122-007-0603-4

Bendix, C., Marshall, C. M., and Harmon, F. G. (2015). Circadian Clock Genes Universally Control Key Agricultural Traits. *Molecular Plant*, *8*(8), 1135–1152. https://doi.org/10.1016/j.molp.2015.03.003

Bendix, C., Mendoza, J. M., Stanley, D. N., Meeley, R., and Harmon, F. G. (2013). The circadian clock-associated gene gigantea1 affects maize developmental transitions. *Plant, Cell and Environment*, *36*(7), 1379–1390. https://doi.org/10.1111/pce.12067

Berardini, T. Z., Reiser, L., Li, D., Mezheritsky, Y., Muller, R., Strait, E., and Huala, E. (2015). The arabidopsis information resource: Making and mining the "gold standard" annotated reference plant genome. *Genesis*, *53*(8), 474–485. https://doi.org/10.1002/dvg.22877

Black, M. M., Stockum, C., Dickson, J. M., Putterill, J., and Arcus, V. L. (2011). Expression, purification and characterisation of GIGANTEA: A circadian clock-controlled regulator of photoperiodic flowering in plants. *Protein Expression and Purification*, *76*(2), 197–204. https://doi.org/10.1016/j.pep.2010.11.009

Blackman, B. K. (2017). Changing responses to changing seasons: Natural variation in the plasticity of flowering time. *Plant Physiology*, *173*(1), 16–26. https://doi.org/10.1104/pp.16.01683

Blümel, M., Dally, N., and Jung, C. (2015). Flowering time regulation in crops-what did we learn from Arabidopsis? *Current Opinion in Biotechnology*, *32*, 121–129. https://doi.org/10.1016/j.copbio.2014.11.023

Böhlenius, H., Huang, T., Charbonnel-Campaa, L., Brunner, A. M., Jansson, S., Strauss, S. H., and Nilsson, O. (2006). CO/FT regulatory module controls timing of flowering and seasonal growth cessation in trees. *Science*, *312*(5776), 1040–1043. https://doi.org/10.1126/science.1126038

Brambilla, V., and Fornara, F. (2013). Molecular Control of Flowering in Response to Day Length in Rice. *Journal of Integrative Plant Biology*, *55*(5), 410–418. https://doi.org/10.1111/jipb.12033

Brambilla, V., and Fornara, F. (2017a). Y flowering? Regulation and activity of CONSTANS and CCT-domain proteins in Arabidopsis and crop species. *Biochimica et Biophysica Acta - Gene Regulatory Mechanisms*, *1860*(5), 655–660. https://doi.org/10.1016/j.bbagrm.2016.10.009

Brambilla, V., Gomez-Ariza, J., Cerise, M., and Fornara, F. (2017b). The importance of being on time: Regulatory networks controlling photoperiodic flowering in cereals. *Frontiers in Plant Science*, *8*(April), 1–8. https://doi.org/10.3389/fpls.2017.00665

Campoli, C., Drosse, B., Searle, I., Coupland, G., and von Korff, M. (2012). Functional characterisation of HvCO1, the barley (Hordeum vulgare) flowering time ortholog of CONSTANS. *Plant Journal*, *69*(5), 868–880. https://doi.org/10.1111/j.1365-313X.2011.04839.x

Cao, D., Li, Y., Lu, S., Wang, J., Nan, H., Li, X., Shi, D., Fang, C., Zhai, H., Yuan, X., Anai, T., Xia, Z., Liu, B., and Kong, F. (2015). GmCOL1a and GmCOL1b Function as Flowering Repressors in Soybean Under Long-Day Conditions. *Plant and Cell Physiology*, *56*(October), 2409–2422. https://doi.org/10.1093/pcp/pcv152

Cao, K., Cui, L., Zhou, X., Ye, L., Zou, Z., and Deng, S. (2016). Four tomato FLOWERING LOCUS T-like proteins act Antagonistically to regulate floral initiation. *Frontiers in Plant Science*, *6*(JAN2016), 1–13. https://doi.org/10.3389/fpls.2015.01213

Cao, S., Ye, M., and Jiang, S. (2005). Involvement of GIGANTEA gene in the regulation of the cold stress response in Arabidopsis. *Plant Cell Reports*, *24*(11), 683–690. https://doi.org/10.1007/s00299-005-0061-x

Castillejo, C., and Pelaz, S. (2008). The Balance between CONSTANS and TEMPRANILLO Activities Determines FT Expression to Trigger Flowering. *Current Biology*, *18*(17), 1338–1343. https://doi.org/10.1016/j.cub.2008.07.075

Catalá, R., Medina, J., and Salinas, J. (2011). Integration of low temperature and light signaling during cold acclimation response in Arabidopsis. *Proceedings of the National Academy of Sciences of the United States of America*, *108*(39), 16475–16480. https://doi.org/10.1073/pnas.1107161108

Causier, B., Ashworth, M., Guo, W., and Davies, B. (2012). The TOPLESS interactome: A framework for gene repression in Arabidopsis. *Plant Physiology*, *158*(1), 423–438. https://doi.org/10.1104/pp.111.186999

Chen, Q., Payyavula, R. S., Chen, L., Zhang, J., Zhang, C., and Turgeon, R. (2018). FLOWERING LOCUS T mRNA is synthesized in specialized companion cells in Arabidopsis and Maryland Mammoth tobacco leaf veins. *Proceedings of the National Academy of Sciences of the United States of America*, *115*(11), 2830–2835. https://doi.org/10.1073/pnas.1719455115

Chen, Y. Y., Wang, Y., Shin, L. J., Wu, J. F., Shanmugam, V., Tsednee, M., Lo, J. C., Chen, C. C., Wu, S. H., and Yeh, K. C. (2013). Iron is involved in the maintenance of circadian period length in Arabidopsis. *Plant Physiology*, *161*(3), 1409–1420. https://doi.org/10.1104/pp.112.212068

Choi, H. H., Phan, L., Chou, P. C., Su, C. H., Yeung, S. C. J., Chen, J. S., and Lee, M. H. (2015). COP1 enhances ubiquitin-mediated degradation of p27Kip1 to promote cancer cell growth. *Oncotarget*, *6*(23), 19721–19734. https://doi.org/10.18632/oncotarget.3821

Clarkson, N. M., and Russell, J. S. (1975). Flowering responses to vernalization and photoperiod in annual medics (Medicago spp.). *Australian Journal of Agricultural Research*, *26*(5), 831–838. https://doi.org/10.1071/AR9750831

Cockram, J., Jones, H., Leigh, F. J., O'Sullivan, D., Powell, W., Laurie, D. A., and Greenland, A. J. (2007). Control of flowering time in temperate cereals: Genes, domestication, and sustainable productivity. *Journal of Experimental Botany*, *58*(6), 1231–1244. https://doi.org/10.1093/jxb/erm042

Corbesier, L., Vincent, C., Jang, S., Fornara, F., Fan, Q., Searle, I., Giakountis, A., Farrona, S., Gissot, L., Turnbull, C., and Coupland, G. (2007). FT protein movement contributes to long-distance signaling in floral induction of Arabidopsis. *Science*, *316*(5827), 1030–1033. https://doi.org/10.1126/science.1141752

Crocco, C. D., Holm, M., Yanovsky, M. J., and Botto, J. F. (2010). AtBBX21 and COP1 genetically interact in the regulation of shade avoidance. *Plant Journal*, *64*(4), 551–562. https://doi.org/10.1111/j.1365-313X.2010.04360.x

Dalchau, N., Baek, S. J., Briggs, H. M., Robertson, F. C., Dodd, A. N., Gardner, M. J., Stancombe, M. A., Haydon, M. J., Stan, G. B., Gonçalves, J. M., and Webb, A. A. R. (2011). The circadian oscillator gene GIGANTEA mediates a long-term response of the Arabidopsis thaliana circadian clock to sucrose. *Proceedings of the National Academy of Sciences of the United States of America*, *108*(12), 5104–5109. https://doi.org/10.1073/pnas.1015452108

Dally, N., Xiao, K., Holtgräwe, D., and Jung, C. (2014). The B2 flowering time locus of beet encodes a zinc finger transcription factor. *Proceedings of the National Academy of Sciences of the United States of America*, *111*(28), 10365–10370. https://doi.org/10.1073/pnas.1404829111

Dalmais, M., Schmidt, J., le Signor, C., Moussy, F., Burstin, J., Savois, V., Aubert, G., Brunaud, V., de Oliveira, Y., Guichard, C., Thompson, R., and Bendahmane, A. (2008). UTILLdb, a Pisum sativum in silico forward and reverse genetics tool. *Genome Biology*, *9*(2). https://doi.org/10.1186/gb-2008-9-2-r43

Dash, S., Campbell, J. D., Cannon, E. K. S., Cleary, A. M., Huang, W., Kalberer, S. R., Karingula, V., Rice, A. G., Singh, J., Umale, P. E., Weeks, N. T., Wilkey, A. P., Farmer, A. D., and Cannon, S. B. (2016). Legume information system (LegumeInfo.org): A key component of a set of federated data resources for the legume family. *Nucleic Acids Research*, *44*(D1), D1181–D1188. https://doi.org/10.1093/nar/gkv1159

David, K. M., Armbruster, U., Tama, N., and Putterill, J. (2006). Arabidopsis GIGANTEA protein is post-transcriptionally regulated by light and dark. *FEBS Letters*, *580*(5), 1193–1197. https://doi.org/10.1016/j.febslet.2006.01.016

de Montaigu, A., Toth, R., and Coupland, G. (2010). Plant development goes like clockwork. *Trends in Genetics*, *26*(7), 296–306. https://doi.org/10.1016/j.tig.2010.04.003

Deng, X. W., Caspar, T., and Quail, P. H. (1991). cop1: A regulatory locus involved in light-controlled development and gene expression in Arabidopsis. *Genes and Development*, *5*(7), 1172–1182. https://doi.org/10.1101/gad.5.7.1172

Dodd, A. N., Salathia, N., Hall, A., Kevei, E., Toth, R., Nagy, F., Hibberd, J. M., Millar, A. J., and Webb, A. A. R. (2005). Plant Circadian Clocks Increase Photosynthesis , Growth , Survival , and Competitive Advantage. *Science*, *July*, 20–25.

Doi, K., Izawa, T., Fuse, T., Yamanouchi, U., Kubo, T., Shimatani, Z., Yano, M., and Yoshimura, A. (2004). Ehd1, a B-type response regulator in rice, confers short-day promotion of flowering

and controls FT-like gene expression independently of Hd1. *Genes and Development*, *18*(8), 926–936. https://doi.org/10.1101/gad.1189604

Dornan, D., Bheddah, S., Newton, K., Inice, W., Frantz, G. D., Dowd, P., Koeppen, H., Dixit, V. M., and French, D. M. (2004). COP1, the negative regulator of p53, is overexpressed in breast and ovarian adenocarcinomas. *Cancer Research*, *64*(20), 7226–7230. https://doi.org/10.1158/0008-5472.CAN-04-2601

Dunford, R. P., Griffiths, S., Christodoulou, V., and Laurie, D. A. (2005). Characterisation of a barley (Hordeum vulgare L.) homologue of the Arabidopsis flowering time regulator GIGANTEA. *Theoretical and Applied Genetics*, *110*(5), 925–931. https://doi.org/10.1007/s00122-004-1912-5

Dyachok, J., Zhu, L., Liao, F., He, J., Huq, E., and Blancaflor, E. B. (2011). SCAR mediates light-induced root elongation in Arabidopsis through photoreceptors and proteasomes. *Plant Cell*, *23*(10), 3610–3626. https://doi.org/10.1105/tpc.111.088823

Eimert, K., Wang Shue-Mei, Lue Wei-Ling, and Chen Jychian. (1995). Monogenic recessive mutations causing both late floral initiation and excess starch accumulation in Arabidopsis. *Plant Cell*, *7*(10), 1703–1712. https://doi.org/10.1105/tpc.7.10.1703

Endo, M., Araki, T., and Nagatani, A. (2016). Tissue-specific regulation of flowering by photoreceptors. *Cellular and Molecular Life Sciences*, *73*(4), 829–839. https://doi.org/10.1007/s00018-015-2095-8

Endo, M., Tanigawa, Y., Murakami, T., Araki, T., and Nagatani, A. (2013). Phytochrome-dependent late-flowering accelerates flowering through physical interactions with phytochrome B and CONSTANS. *Proceedings of the National Academy of Sciences of the United States of America*, *110*(44), 18017–18022. https://doi.org/10.1073/pnas.1310631110

Faure, S., Turner, A. S., Gruszka, D., Christodoulou, V., Davis, S. J., von Korff, M., and Laurie, D. A. (2012). Mutation at the circadian clock gene EARLY MATURITY 8 adapts domesticated barley (Hordeum vulgare) to short growing seasons. *Proceedings of the National Academy of Sciences of the United States of America*, *109*(21), 8328–8333. https://doi.org/10.1073/pnas.1120496109

Folter, S. de, and Immink, R. G. H. (2011). *Chapter 8 Yeast Protein – Protein Interaction Assays and Screens*. 1–8. https://doi.org/10.1007/978-1-61779-154-3

Foo, E., Bullier, E., Goussot, M., Foucher, F., Rameau, C., and Beveridge, C. A. (2005). The branching gene RAMOSUS1 mediates interactions among two novel signals and auxin in pea. *Plant Cell*, *17*(2), 464–474. https://doi.org/10.1105/tpc.104.026716

Fornara, F., de Montaigu, A., and Coupland, G. (2010). SnapShot: Control of flowering in arabidopsis. *Cell*, *141*(3), 3–5. https://doi.org/10.1016/j.cell.2010.04.024

Fornara, F., de Montaigu, A., Sánchez-Villarreal, A., Takahashi, Y., ver Loren Van Themaat, E., Huettel, B., Davis, S. J., and Coupland, G. (2015). The GI-CDF module of Arabidopsis affects freezing tolerance and growth as well as flowering. *Plant Journal*, *81*(5), 695–706. https://doi.org/10.1111/tpj.12759

Fornara, F., Panigrahi, K. C. S., Gissot, L., Sauerbrunn, N., Rühl, M., Jarillo, J. A., and Coupland, G. (2009). Arabidopsis DOF Transcription Factors Act Redundantly to Reduce CONSTANS Expression and Are Essential for a Photoperiodic Flowering Response. *Developmental Cell*, *17*(1), 75–86. https://doi.org/10.1016/j.devcel.2009.06.015

Fowler, S., Lee, K., Onouchi, H., Samach, A., Richardson, K., Morris, B., Coupland, G., and Putterill, J. (1999). GIGANTEA: A circadian clock-controlled gene that regulates photoperiodic flowering in Arabidopsis and encodes a protein with several possible membrane-spanning domains. *EMBO Journal*, *18*(17), 4679–4688. https://doi.org/10.1093/emboj/18.17.4679

Foyer, C. H., Lam, H. M., Nguyen, H. T., Siddique, K. H. M., Varshney, R. K., Colmer, T. D., Cowling, W., Bramley, H., Mori, T. A., Hodgson, J. M., Cooper, J. W., Miller, A. J., Kunert, K., Vorster, J., Cullis, C., Ozga, J. A., Wahlqvist, M. L., Liang, Y., Shou, H., … Considine, M. J. (2016). Neglecting legumes has compromised human health and sustainable food production. *Nature Plants*, *2*(8), 1–10. https://doi.org/10.1038/NPLANTS.2016.112

Frances, S., White, M. J., Edgerton, M. D., Jones, A. M., Elliott, R. C., and Thompson, W. F. (1992). Initial characterization of a pea mutant with light-independent photomorphogenesis. *Plant Cell*, *4*(12), 1519–1530.

Franklin, K. A., and Quail, P. H. (2010). Phytochrome functions in Arabidopsis development. *Journal of Experimental Botany*, *61*(1), 11–24. https://doi.org/10.1093/jxb/erp304

Franssen, S. U., Shrestha, R. P., Bräutigam, A., Bornberg-Bauer, E., and Weber, A. P. M. (2011). Comprehensive transcriptome analysis of the highly complex Pisum sativum genome using

next generation sequencing. *BMC Genomics*, *12*. https://doi.org/10.1186/1471-2164-12-227

Fudge, J. B., Lee, R. H., Laurie, R. E., Mysore, K. S., Wen, J., Weller, J. L., and Macknight, R. C. (2018). Medicago truncatula SOC1 genes are up-regulated by environmental cues that promote flowering. *Frontiers in Plant Science*, *9*(April), 1–11. https://doi.org/10.3389/fpls.2018.00496

Fuller, D. Q., Sato, Y. I., Castillo, C., Qin, L., Weisskopf, A. R., Kingwell-Banham, E. J., Song, J., Ahn, S. M., and van Etten, J. (2010). Consilience of genetics and archaeobotany in the entangled history of rice. *Archaeological and Anthropological Sciences*, *2*(2), 115–131. https://doi.org/10.1007/s12520-010-0035-y

Galvão, V. C., and Fankhauser, C. (2015). Sensing the light environment in plants: Photoreceptors and early signaling steps. *Current Opinion in Neurobiology*, *34*(Figure 1), 46–53. https://doi.org/10.1016/j.conb.2015.01.013

Garner, W. W., and Allard, H. A. (1920). EFFECT OF THE RELATIVE LENGTH OF DAY AND NIGHT AND OTHER FACTORS OF THE ENVIRONMENT ON GROWTH AND REPRODUCTION IN PLANTS. *Monthly Weather Review*, *668*(4), 98–105.

Gnesutta, N., Kumimoto, R. W., Swain, S., Chiara, M., Siriwardana, C., Horner, D. S., Holt, B. F., and Mantovani, R. (2017). CONSTANS imparts DNA sequence specificity to the histone fold NF-YB/NF-YC Dimer. *Plant Cell*, *29*(6), 1516–1532. https://doi.org/10.1105/tpc.16.00864

González-Schain, N. D., Díaz-Mendoza, M., Zurczak, M., and Suárez-López, P. (2012). Potato CONSTANS is involved in photoperiodic tuberization in a graft-transmissible manner. *Plant Journal*, *70*(4), 678–690. https://doi.org/10.1111/j.1365-313X.2012.04909.x

Goodstein, D. M., Shu, S., Howson, R., Neupane, R., Hayes, R. D., Fazo, J., Mitros, T., Dirks, W., Hellsten, U., Putnam, N., and Rokhsar, D. S. (2012). Phytozome: A comparative platform for green plant genomics. *Nucleic Acids Research*, *40*(D1), 1178–1186. https://doi.org/10.1093/nar/gkr944

Gould, P. D., Locke, J. C. W., Larue, C., Southern, M. M., Davis, S. J., Hanano, S., Moyle, R., Milich, R., Putterill, J., Millar, A. J., and Hall, A. (2006). The molecular basis of temperature compensation in the Arabidopsis circadian clock. *Plant Cell*, *18*(5), 1177–1187. https://doi.org/10.1105/tpc.105.039990

Han, L., Mason, M., Risseeuw, E. P., Crosby, W. L., and Somers, D. E. (2004). Formation of an SCFZTL complex is required for proper regulation of circadian timing. *Plant Journal*, *40*(2), 291–301. https://doi.org/10.1111/j.1365-313X.2004.02207.x

Han, S. H., Yoo, S. C., Lee, B. D., An, G., and Paek, N. C. (2015). Rice FLAVIN-BINDING, KELCH REPEAT, F-BOX 1 (OsFKF1) promotes flowering independent of photoperiod. *Plant Cell and Environment*, *38*(12), 2527–2540. https://doi.org/10.1111/pce.12549

Hayama, R., Agashe, B., Luley, E., King, R., and Coupland, G. (2007). A circadian rhythm set by dusk determines the expression of FT homologs and the short-day photoperiodic flowering response in pharbitis. *Plant Cell*, *19*(10), 2988–3000. https://doi.org/10.1105/tpc.107.052480

Hayama, R., and Coupland, G. (2004). The molecular basis of diversity in the photoperiodic flowering responses of arabidopsis and rice. *Plant Physiology*, *135*(2), 677–684. https://doi.org/10.1104/pp.104.042614

Hayama, R., Izawa, T., and Shimamoto, K. (2002). Isolation of rice genes possibly involved in the photoperiodic control of flowering by a fluorescent differential display method. *Plant and Cell Physiology*, *43*(5), 494–504. https://doi.org/10.1093/pcp/pcf059

Hayama, R., Yokoi, S., Tamaki, S., Yano, M., and Shimamoto, K. (2003). Adaptation of photoperiodic control pathways produces short-day flowering in rice. *Nature*, *422*(6933), 719–722. https://doi.org/10.1038/nature01549

He, Y., Chen, T., and Zeng, X. (2020). Genetic and Epigenetic Understanding of the Seasonal Timing of Flowering. *Plant Communications*, *1*(1), 100008. https://doi.org/10.1016/j.xplc.2019.100008

Hearn, T. J., and Webb, A. A. R. (2020). Recent advances in understanding regulation of the Arabidopsis circadian clock by local cellular environment. *F1000Research*, *9*, 1–9. https://doi.org/10.12688/f1000research.21307.1

Hecht, V. (2005). Conservation of Arabidopsis Flowering Genes in Model Legumes. *Plant Physiology*, *137*(4), 1420–1434. https://doi.org/10.1104/pp.104.057018

Hecht, V., Knowles, C. L., vander Schoor, J. K., Liew, L. C., Jones, S. E., Lambert, M. J. M., and Weller, J. L. (2007). Pea LATE BLOOMER1 is a GIGANTEA ortholog with roles in

photoperiodic flowering, deetiolation, and transcriptional regulation of circadian clock gene homologs. *Plant Physiology*, *144*(2), 648–661. https://doi.org/10.1104/pp.107.096818

Hecht, V., Laurie, R. E., vander Schoor, J. K., Ridge, S., Knowles, C. L., Liew, L. C., Sussmilch, F. C., Murfet, I. C., Macknight, R. C., and Weller, J. L. (2011). The pea GIGAS gene is a FLOWERING LOCUS T homolog necessary for graft-transmissible specification of flowering but not for responsiveness to photoperiod. *The Plant Cell*, *23*(1), 147–161. https://doi.org/10.1105/tpc.110.081042

Hicks, K. A., Albertson, T. M., and Wagner, D. R. (2001). EARLY FLOWERING3 encodes a novel protein that regulates circadian clock function and flowering in arabidopsis. *Plant Cell*, *13*(6), 1281–1292. https://doi.org/10.1105/tpc.13.6.1281

Higuchi, Y., Sage-Ono, K., Sasaki, R., Ohtsuki, N., Hoshino, A., Iida, S., Kamada, H., and Ono, M. (2011). Constitutive expression of the GIGANTEA ortholog affects circadian rhythms and suppresses one-shot induction of flowering in pharbitis nil, a typical short-day plant. *Plant and Cell Physiology*, *52*(4), 638–650. https://doi.org/10.1093/pcp/pcr023

Hirose, F., Shinomura, T., Tanabata, T., Shimada, H., and Takano, M. (2006). *Involvement of Rice Cryptochromes in De-etiolation Responses and Flowering*. *47*(7), 915–925. https://doi.org/10.1093/pcp/pcj064

Hoecker, U. (2017). The activities of the E3 ubiquitin ligase COP1/SPA, a key repressor in light signaling. *Current Opinion in Plant Biology*, *37*, 63–69. https://doi.org/10.1016/j.pbi.2017.03.015

Hoecker, U., and Quail, P. H. (2001). The Phytochrome A-specific Signaling Intermediate SPA1 Interacts Directly with COP1, a Constitutive Repressor of Light Signaling in Arabidopsis. *Journal of Biological Chemistry*, *276*(41), 38173–38178. https://doi.org/10.1074/jbc.M103140200

Hoecker, U., Xu, Y., and Quail, P. H. (1998). Spa1: A new genetic locus involved in phytochrome aspecific signal transduction. *Plant Cell*, *10*(1), 19–33. https://doi.org/10.1105/tpc.10.1.19

Holm, M., Ma, L. G., Qu, L. J., and Deng, X. W. (2002). Two interacting bZIP proteins are direct targets of COP1-mediated control of light-dependent gene expression in Arabidopsis. *Genes and Development*, *16*(10), 1247–1259. https://doi.org/10.1101/gad.969702

Hori, K., Matsubara, K., and Yano, M. (2016). Genetic control of flowering time in rice: integration of Mendelian genetics and genomics. *Theoretical and Applied Genetics*, *129*(12), 2241–2252. https://doi.org/10.1007/s00122-016-2773-4

Hu, Y. X., Wang, Y. H., Liu, X. F., and Li, J. Y. (2004). Arabidopsis RAV1 is down-regulated by brassinosteroid and may act as a negative regulator during plant development. *Cell Research*, *14*(1), 8–15. https://doi.org/10.1038/sj.cr.7290197

Hu, Y., Zhou, X., Zhang, B., Li, S., Fan, X., Zhao, H., Zhang, J., Liu, H., He, Q., Li, Q., Ayaad, M., You, A., and Xing, Y. (2021). OsPRR37 Alternatively Promotes Heading Date Through Suppressing the Expression of Ghd7 in the Japonica Variety Zhonghua 11 under Natural Long-Day Conditions. *Rice*, *14*(1), 1–13. https://doi.org/10.1186/s12284-021-00464-1

Huang, F., Fu, Z., Zeng, L., and Morley-Bunker, M. (2017). Isolation and characterization of GI and FKF1 homologous genes in the subtropical fruit tree Dimocarpus longan. *Molecular Breeding*, *37*(7), 1–13. https://doi.org/10.1007/s11032-017-0691-z

Huang, H., Yoo, C. Y., Bindbeutel, R., Goldsworthy, J., Tielking, A., Alvarez, S., Naldrett, M. J., Evans, B. S., Chen, M., and Nusinow, D. A. (2016). PCH1 integrates circadian and light-signaling pathways to control photoperiod-responsive growth in Arabidopsis. *ELife*, *5*(FEBRUARY2016), 1–26. https://doi.org/10.7554/eLife.13292

Huang, W., Pérez-García, P., Pokhilko, A., Millar, A. J., Antoshechkin, I., Riechmann, J. L., and Mas, P. (2012a). Mapping the Core of the Arabidopsis Circadian Clock Defines the Network Structure of the Oscillator. *Science*, *336*(6077), 75–79. https://doi.org/10.1126/science.1219075

Huang, X., Kurata, N., Wei, X., Wang, Z. X., Wang, A., Zhao, Q., Zhao, Y., Liu, K., Lu, H., Li, W., Guo, Y., Lu, Y., Zhou, C., Fan, D., Weng, Q., Zhu, C., Huang, T., Zhang, L., Wang, Y., … Han, B. (2012b). A map of rice genome variation reveals the origin of cultivated rice. *Nature*, *490*(7421), 497–501. https://doi.org/10.1038/nature11532

Huang, X., Ouyang, X., and Deng, X. W. (2014). Beyond repression of photomorphogenesis: Role switching of COP/DET/FUS in light signaling. *Current Opinion in Plant Biology*, *21*, 96–103. https://doi.org/10.1016/j.pbi.2014.07.003

Huq, E., Tepperman, J. M., and Quail, P. H. (2000). GIGANTEA is a nuclear protein involved in phytochrome signaling in Arabidopsis. *Proceedings of the National Academy of Sciences of the United States of America*, *97*(17), 9789–9794. https://doi.org/10.1073/pnas.170283997

Hwang, D. Y., Park, S., Lee, S., Lee, S. S., Imaizumi, T., and Song, Y. H. (2019). GIGANTEA Regulates the Timing Stabilization of CONSTANS by Altering the Interaction between FKF1 and ZEITLUPE. *Molecules and Cells*, *42*(10), 693–701. https://doi.org/10.14348/molcells.2019.0199

Imaizumi, T., Schultz, T. F., Harmon, F. G., Ho, L. A., and Kay, S. A. (2005). Plant science: FKF1 F-box protein mediates cyclic degradation of a repressor of CONSTANS in Arabidopsis. *Science*, *309*(5732), 293–297. https://doi.org/10.1126/science.1110586

Imaizumi, T., Tran, H. G., Swartz, T. E., Briggs, W. R., and Kay, S. A. (2003). FKF1 is essential for photoperiodic-specific light signalling in Arabidopsis. *Nature*, *426*(6964), 302–306. https://doi.org/10.1038/nature02090

Ishikawa, R., Tamaki, S., Yokoi, S., Inagaki, N., Shinomura, T., Takano, M., and Shimamoto, K. (2005). Suppression of the floral activator Hd3a is the principal cause of the night break effect in rice. *Plant Cell*, *17*(12), 3326–3336. https://doi.org/10.1105/tpc.105.037028

Ito, S., Song, Y. H., and Imaizumi, T. (2012a). LOV domain-containing F-box proteins: Light-dependent protein degradation modules in Arabidopsis. *Molecular Plant*, *5*(3), 573–582. https://doi.org/10.1093/mp/sss013

Ito, S., Song, Y. H., Josephson-Day, A. R., Miller, R. J., Breton, G., Olmstead, R. G., and Imaizumi, T. (2012b). FLOWERING BHLH transcriptional activators control expression of the photoperiodic flowering regulator CONSTANS in Arabidopsis. *Proceedings of the National Academy of Sciences of the United States of America*, *109*(9), 3582–3587. https://doi.org/10.1073/pnas.1118876109

Izawa, T. (2007). Adaptation of flowering-time by natural and artificial selection in Arabidopsis and rice. *Journal of Experimental Botany*, *58*(12), 3091–3097. https://doi.org/10.1093/jxb/erm159

Izawa, T., Mihara, M., Suzuki, Y., Gupta, M., Itoh, H., Nagano, A. J., Motoyam, R., Sawad, Y., Yano, M., Hirai, M. Y., Makino, A., and Nagamurad, Y. (2011). Os-GIGANTEA confers robust diurnal rhythms on the global transcriptome of rice in the field. *Plant Cell*, *23*(5), 1741–1755. https://doi.org/10.1105/tpc.111.083238

Izawa, T., Oikawa, T., Sugiyama, N., Tanisaka, T., Yano, M., and Shimamoto, K. (2002). Phytochrome mediates the external light signal to repress FT orthologs in photoperiodic

flowering of rice. *Genes and Development*, *16*(15), 2006–2020. https://doi.org/10.1101/gad.999202

Jang, I. C., Henriques, R., Seo, H. S., Nagatani, A., and Chua, N. H. (2010). Arabidopsis PHYTOCHROME INTERACTING FACTOR proteins promote phytochrome B polyubiquitination by COP1 E3 ligase in the nucleus. *Plant Cell*, *22*(7), 2370–2383. https://doi.org/10.1105/tpc.109.072520

Jang, K., Lee, H. G., Jung, S.-J., Paek, N. C., and Seo, P. J. (2015). The E3 Ubiquitin Ligase COP1 Regulates Thermosensory Flowering by Triggering GI Degradation in Arabidopsis. *Scientific Reports*, *5*(July), 12071. https://doi.org/10.1038/srep12071

Jang, S., Marchal, V., Panigrahi, K. C. S., Wenkel, S., Soppe, W., Deng, X. W., Valverde, F., and Coupland, G. (2008). Arabidopsis COP1 shapes the temporal pattern of CO accumulation conferring a photoperiodic flowering response. *EMBO Journal*, *27*(8), 1277–1288. https://doi.org/10.1038/emboj.2008.68

Jaudal, M., Wen, J., Mysore, K. S., and Putterill, J. (2020). Medicago PHYA promotes flowering, primary stem elongation and expression of flowering time genes in long days. *BMC Plant Biology*, *20*(1), 1–16. https://doi.org/10.1186/s12870-020-02540-y

Jaudal, M., Zhang, L., Che, C., Hurley, D. G., Thomson, G., Wen, J., Mysore, K. S., and Putterill, J. (2016). MtVRN2 is a Polycomb VRN2-like gene which represses the transition to flowering in the model legume Medicago truncatula. *Plant Journal*, *86*(2), 145–160. https://doi.org/10.1111/tpj.13156

Jeong, R. D., Chandra-Shekara, A. C., Barman, S. R., Navarre, D., Klessig, D. F., Kachroo, A., and Kachroo, P. (2010). Cryptochrome 2 and phototropin 2 regulate resistance protein-mediated viral defense by negatively regulating an E3 ubiquitin ligase. *Proceedings of the National Academy of Sciences of the United States of America*, *107*(30), 13538–13543. https://doi.org/10.1073/pnas.1004529107

Jiang, B., Nan, H., Gao, Y., Tang, L., Yue, Y., Lu, S., Ma, L., Cao, D., Sun, S., Wang, J., Wu, C., Yuan, X., Hou, W., Kong, F., Han, T., and Liu, B. (2014). Allelic combinations of soybean maturity loci E1, E2, E3 and E4 result in diversity of maturity and adaptation to different latitudes. *PLoS ONE*, *9*(8). https://doi.org/10.1371/journal.pone.0106042

Johansson, M., and Staiger, D. (2015). Time to flower: Interplay between photoperiod and the circadian clock. *Journal of Experimental Botany*, *66*(3), 719–730. https://doi.org/10.1093/jxb/eru441

Jung, C., and Muller, A. E. (2009). Flowering time control and applications in plant breeding. *Trends in Plant Science*, *14*(10), 563–573. https://doi.org/10.1016/j.tplants.2009.07.005

Jung, J. H., Seo, Y. H., Pil, J. S., Reyes, J. L., Yun, J., Chua, N. H., and Park, C. M. (2007). The GIGANTEA-regulated microRNA172 mediates photoperiodic flowering independent of CONSTANS in Arabidopsis. *Plant Cell*, *19*(9), 2736–2748. https://doi.org/10.1105/tpc.107.054528

Kamran, A., Iqbal, M., and Spaner, D. (2014). Flowering time in wheat (Triticum aestivum L.): A key factor for global adaptability. *Euphytica*, *197*(1), 1–26. https://doi.org/10.1007/s10681-014-1075-7

Kang, C. Y., Lian, H. L., Wang, F. F., Huang, J. R., and Yang, H. Q. (2009). Cryptochromes, phytochromes, and COP1 regulate light-controlled stomatal development in arabidopsis. *Plant Cell*, *21*(9), 2624–2641. https://doi.org/10.1105/tpc.109.069765

Kaur, S., Pembleton, L. W., Cogan, N. O. I., Savin, K. W., Leonforte, T., Paull, J., Materne, M., and Forster, J. W. (2012). Transcriptome sequencing of field pea and faba bean for discovery and validation of SSR genetic markers. *BMC Genomics*, *13*(1), 1–12. https://doi.org/10.1186/1471-2164-13-104

Kawamura, H., Ito, S., Yamashino, T., Niwa, Y., Nakamichi, N., and Mizuno, T. (2008). Characterization of genetic links between two clock-associated genes, GI and PRR5 in the current clock model of Arabidopsis thaliana. *Bioscience, Biotechnology and Biochemistry*, *72*(10), 2770–2774. https://doi.org/10.1271/bbb.80321

Kearse, M., Moir, R., Wilson, A., Stones-Havas, S., Cheung, M., Sturrock, S., Buxton, S., Cooper, A., Markowitz, S., Duran, C., Thierer, T., Ashton, B., Meintjes, P., and Drummond, A. (2012). Geneious Basic: An integrated and extendable desktop software platform for the organization and analysis of sequence data. *Bioinformatics*, *28*(12), 1647–1649. https://doi.org/10.1093/bioinformatics/bts199

Kim, D. H., Doyle, M. R., Sung, S., and Amasino, R. M. (2009). Vernalization: Winter and the timing of flowering in plants. *Annual Review of Cell and Developmental Biology*, *25*, 277–299. https://doi.org/10.1146/annurev.cellbio.042308.113411

Kim, J., Geng, R., Gallenstein, R. A., and Somers, D. E. (2013a). The F-box protein ZEITLUPE controls stability and nucleocytoplasmic partitioning of GIGANTEA. *Development (Cambridge)*, *140*(19), 4060–4069. https://doi.org/10.1242/dev.096651

Kim, J. Y., Song, J. T., and Seo, H. S. (2017). COP1 regulates plant growth and development in response to light at the post-translational level. In *Journal of Experimental Botany* (Vol. 68, Issue 17, pp. 4737–4748). https://doi.org/10.1093/jxb/erx312

Kim, M. Y., Kang, Y. J., Lee, T., and Lee, S. (2013b). Divergence of Flowering-Related Genes in Three Legume Species. *The Plant Genome*, *6*(3). https://doi.org/10.3835/plantgenome2013.03.0008

Kim, W. Y., Fujiwara, S., Suh, S. S., Kim, J., Kim, Y., Han, L., David, K., Putterill, J., Nam, H. G., and Somers, D. E. (2007). ZEITLUPE is a circadian photoreceptor stabilized by GIGANTEA in blue light. *Nature*, *449*(7160), 356–360. https://doi.org/10.1038/nature06132

Kim, W. Y., Hicks, K. A., and Somers, D. E. (2005). Independent roles for EARLY FLOWERING 3 and ZEITLUPE in the control of circadian timing, hypocotyl length, and flowering time. *Plant Physiology*, *139*(3), 1557–1569. https://doi.org/10.1104/pp.105.067173

Kim, Y., Lim, J., Yeom, M., Kim, H., Kim, J., Wang, L., Kim, W. Y., Somers, D. E., and Nam, H. G. (2013c). ELF4 Regulates GIGANTEA Chromatin Access through Subnuclear Sequestration. *Cell Reports*, *3*(3), 671–677. https://doi.org/10.1016/j.celrep.2013.02.021

Kinoshita, A., and Richter, R. (2020). Genetic and molecular basis of floral induction in Arabidopsis thaliana. *Journal of Experimental Botany*, *71*(9), 2490–2504. https://doi.org/10.1093/jxb/eraa057

Kitagawa, S., Shimada, S., and Murai, K. (2012). Effect of Ppd-1 on the expression of flowering-timegenes in vegetative and reproductivegrowth stages of wheat. *Genes and Genetic Systems*, *87*(3), 161–168. https://doi.org/10.1266/ggs.87.161

Kloosterman, B., Abelenda, J. A., Gomez, M. D. M. C., Oortwijn, M., de Boer, J. M., Kowitwanich, K., Horvath, B. M., van Eck, H. J., Smaczniak, C., Prat, S., Visser, R. G. F., and Bachem, C. W. B. (2013). Naturally occurring allele diversity allows potato cultivation in northern latitudes. *Nature*, *495*(7440), 246–250. https://doi.org/10.1038/nature11912

Komiya, R., Ikegami, A., Tamaki, S., Yokoi, S., and Shimamoto, K. (2008). Hd3a and RFT1 are essential for flowering in rice. *Development*, *135*(4), 767–774. https://doi.org/10.1242/dev.008631

Kong, F., Liu, B., Xia, Z., Sato, S., Kim, B. M., Watanabe, S., Yamada, T., Tabata, S., Kanazawa, A., Harada, K., and Abe, J. (2010). Two Coordinately Regulated Homologs of FLOWERING LOCUS T Are Involved in the Control of Photoperiodic Flowering in Soybean. *Plant Physiology*, *154*(3), 1220–1231. https://doi.org/10.1104/pp.110.160796

Kong, S. G., and Okajima, K. (2016). Diverse photoreceptors and light responses in plants. *Journal of Plant Research*, *129*(2), 111–114. https://doi.org/10.1007/s10265-016-0792-5

Koornneef, M., Hanhart, C. J., and van der Veen, J. H. (1991). A genetic and physiological analysis of late flowering mutants in Arabidopsis thaliana. *Molecular & General Genetics : MGG*, *229*(1), 57–66. https://doi.org/10.1007/BF00264213

Koressaar, T., and Remm, M. (2007). Enhancements and modifications of primer design program Primer3. *Bioinformatics*, *23*(10), 1289–1291. https://doi.org/10.1093/bioinformatics/btm091

Krahmer, J., Goralogia, G. S., Kubota, A., Zardilis, A., Johnson, R. S., Song, Y. H., MacCoss, M. J., le Bihan, T., Halliday, K. J., Imaizumi, T., and Millar, A. J. (2019). Time-resolved interaction proteomics of the GIGANTEA protein under diurnal cycles in Arabidopsis. *FEBS Letters*, *593*(3), 319–338. https://doi.org/10.1002/1873-3468.13311

Kreplak, J., Madoui, M. A., Cápal, P., Novák, P., Labadie, K., Aubert, G., Bayer, P. E., Gali, K. K., Syme, R. A., Main, D., Klein, A., Bérard, A., Vrbová, I., Fournier, C., d'Agata, L., Belser, C., Berrabah, W., Toegelová, H., Milec, Z., … Burstin, J. (2019). A reference genome for pea provides insight into legume genome evolution. *Nature Genetics*, *51*(9), 1411–1422. https://doi.org/10.1038/s41588-019-0480-1

Kubota, A., Kita, S., Ishizaki, K., Nishihama, R., Yamato, K. T., and Kohchi, T. (2014). Co-option of a photoperiodic growth-phase transition system during land plant evolution. *Nature Communications*, *5*, 1–9. https://doi.org/10.1038/ncomms4668

Lang, A., Chailakhyan, M. K., and Frolova, I. A. (1977). Promotion and inhibition of flower formation in a dayneutral plant in grafts with a short-day plant and a long-day plant. *Proceedings of the National Academy of Sciences*, *74*(6), 2412–2416. https://doi.org/10.1073/pnas.74.6.2412

Langewisch, T., Lenis, J., Jiang, G. L., Wang, D., Pantalone, V., and Bilyeu, K. (2017). The development and use of a molecular model for soybean maturity groups. *BMC Plant Biology*, *17*(1), 1–13. https://doi.org/10.1186/s12870-017-1040-4

Lau, K., Podolec, R., Chappuis, R., Ulm, R., and Hothorn, M. (2019). Plant photoreceptors and their signaling components compete for COP 1 binding via VP peptide motifs . *The EMBO Journal*, 1–18. https://doi.org/10.15252/embj.2019102140

Lau, O. S., and Deng, X. W. (2012). The photomorphogenic repressors COP1 and DET1: 20 years later. *Trends in Plant Science*, *17*(10), 584–593. https://doi.org/10.1016/j.tplants.2012.05.004

Laubinger, S., Fittinghoff, K., and Hoecker, U. (2004). The SPA quartet: A family of WD-repeat proteins with a central role in suppression of photomorphogenesis in Arabidopsis. *Plant Cell*, *16*(9), 2293–2306. https://doi.org/10.1105/tpc.104.024216

Laurie, R. E., Diwadkar, P., Jaudal, M., Zhang, L., Hecht, V., Wen, J., Tadege, M., Mysore, K. S., Putterill, J., Weller, J. L., and Macknight, R. C. (2011). The medicago Flowering locus T homolog, MtFTa1, is a key regulator of flowering time. *Plant Physiology*, *156*(4), 2207–2224. https://doi.org/10.1104/pp.111.180182

Lazaro, A., Mouriz, A., Piñeiro, M., and Jarillo, J. A. (2015). Red light-mediated degradation of constans by the e3 ubiquitin ligase hos1 regulates photoperiodic flowering in arabidopsis. *Plant Cell*, *27*(9), 2437–2454. https://doi.org/10.1105/tpc.15.00529

Lee, B. D., Cha, J. Y., Kim, M. R., Shin, G. I., Paek, N. C., and Kim, W. Y. (2019). Light-dependent suppression of COP1 multimeric complex formation is determined by the blue-light receptor FKF1 in Arabidopsis. *Biochemical and Biophysical Research Communications*, *508*(1), 191–197. https://doi.org/10.1016/j.bbrc.2018.11.032

Lee, B. D., Kim, M. R., Kang, M. Y., Cha, J. Y., Han, S. H., Nawkar, G. M., Sakuraba, Y., Lee, S. Y., Imaizumi, T., McClung, R. C., Kim, W. Y., and Paek, N. C. (2017). The F-box protein FKF1 inhibits dimerization of COP1 in the control of photoperiodic flowering. *Nature Communications*, *8*(1), 1–10. https://doi.org/10.1038/s41467-017-02476-2

Lee HK., Mysore K.S., W. J. (2018). Tnt1 Insertional Mutagenesis in Medicago truncatula. In *Functional Genomics in Medicago truncatula. Methods in Molecular Biology*. https://www.springer.com/gp/book/9781493986323

Lee, K., Onouchi, H., Mizoguchi, T., Wright, L., Fujiwara, S., Cremer, F., Lee, K., Onouchi, H., Mouradov, A., Fowler, S., Kamada, H., Putterill, J., and Coupland, G. (2005). Distinct roles of GIGANTEA in promoting flowering and regulating circadian rhythms in Arabidopsis. *Plant Cell*, *17*(8), 2255–2270. https://doi.org/10.1105/tpc.105.033464.GI

Lee, R., Baldwin, S., Kenel, F., McCallum, J., and Macknight, R. C. (2013). FLOWERING LOCUS T genes control onion bulb formation and flowering. *Nature Communications*, *4*. https://doi.org/10.1038/ncomms3884

Lee, Y. S., and An, G. (2015). Regulation of flowering time in rice. *Journal of Plant Biology*, *58*(6), 353–360. https://doi.org/10.1007/s12374-015-0425-x

Leijten, W., Koes, R., Roobeek, I., and Frugis, G. (2018). Translating Flowering Time From Arabidopsis thaliana to Brassicaceae and Asteraceae Crop Species. In *Plants* (Vol. 7, Issue 4). https://doi.org/10.3390/plants7040111

Lester, D. R., Ross, J. J., Davies, P. J., and Reid, J. B. (1997). Mendel's stem length gene (Le) encodes a gibberellin 3β-hydroxylase. *Plant Cell*, *9*(8), 1435–1443. https://doi.org/10.1105/tpc.9.8.1435

Lester, D. R., Ross, J. J., Smith, J. J., Elliott, R. C., and Reid, J. B. (1999). Gibberellin 2-oxidation and the SLN gene of Pisum sativum. *Plant Journal*, *19*(1), 65–73. https://doi.org/10.1046/j.1365-313X.1999.00501.x

Li, C., and Dubcovsky, J. (2008). Wheat FT protein regulates VRN1 transcription through interactions with FDL2. *Plant Journal*, *55*(4), 543–554. https://doi.org/10.1111/j.1365-313X.2008.03526.x

Li, F., Zhang, X., Hu, R., Wu, F., Ma, J., Meng, Y., and Fu, Y. F. (2013). Identification and molecular characterization of FKF1 and GI homologous genes in soybean. *PLoS ONE*, *8*(11), 26–28. https://doi.org/10.1371/journal.pone.0079036

Li, L., Li, X., Liu, Y., and Liu, H. (2016). Flowering responses to light and temperature. *Science China Life Sciences*, *59*(4), 403–408. https://doi.org/10.1007/s11427-015-4910-8

Li, Y., and Xu, M. (2017). CCT family genes in cereal crops: A current overview. *Crop Journal*, *5*(6), 449–458. https://doi.org/10.1016/j.cj.2017.07.001

Li, Y. Y., Mao, K., Zhao, C., Zhao, X. Y., Zhang, H. L., Shu, H. R., and Hao, Y. J. (2012). MdCOP1 ubiquitin E3 ligases interact with MdMYB1 to regulate light-induced anthocyanin

biosynthesis and red fruit coloration in apple. *Plant Physiology*, *160*(2), 1011–1022. https://doi.org/10.1104/pp.112.199703

Liew, L. C., Hecht, V., Laurie, R. E., Knowles, C. L., vander Schoor, J. K., Macknight, R. C., and Weller, J. L. (2009). DIE NEUTRALIS and LATE BLOOMER 1 contribute to regulation of the pea circadian clock. *The Plant Cell*, *21*(10), 3198–3211. https://doi.org/10.1105/tpc.109.067223

Liew, L. C., Hecht, V., Sussmilch, F. C., and Weller, J. L. (2014). The Pea Photoperiod Response Gene STERILE NODES Is an Ortholog of LUX ARRHYTHMO. *Plant Physiology*, *165*(2), 648–657. https://doi.org/10.1104/pp.114.237008

Lifschitz, E., and Eshed, Y. (2006). Universal florigenic signals triggered by FT homologues regulate growth and flowering cycles in perennial day-neutral tomato. *Journal of Experimental Botany*, *57*(13), 3405–3414. https://doi.org/10.1093/jxb/erl106

Liu, H., Liu, B., Zhao, C., Pepper, M., and Lin, C. (2011). The action mechanisms of plant cryptochromes. *Trends in Plant Science*, *16*(12), 684–691. https://doi.org/10.1016/j.tplants.2011.09.002

Liu, H., Wang, Q., Liu, Y., Zhao, X., Imaizumi, T., Somers, D. E., Tobin, E. M., and Lin, C. (2013). Arabidopsis CRY2 and ZTL mediate blue-light regulation of the transcription factor CIB1 by distinct mechanisms. *Proceedings of the National Academy of Sciences of the United States of America*, *110*(43), 17582–17587. https://doi.org/10.1073/pnas.1308987110

Liu, L. J., Zhang, Y. C., Li, Q. H., Sang, Y., Mao, J., Lian, H. L., Wang, L., and Yang, H. Q. (2008). COP1-mediated ubiquitination of CONSTANS is implicated in cryptochrome regulation of flowering in Arabidopsis. *Plant Cell*, *20*(2), 292–306. https://doi.org/10.1105/tpc.107.057281

Liu, W., Jiang, B., Ma, L., Zhang, S., Zhai, H., Xu, X., Hou, W., Xia, Z., Wu, C., Sun, S., Wu, T., Chen, L., and Han, T. (2018). Functional diversification of Flowering Locus T homologs in soybean: GmFT1a and GmFT2a/5a have opposite roles in controlling flowering and maturation. *New Phytologist*, *217*(3), 1335–1345. https://doi.org/10.1111/nph.14884

Locke, J. C. W., Southern, M. M., Kozma-Bognár, L., Hibberd, V., Brown, P. E., Turner, M. S., and Millar, A. J. (2005). Extension of a genetic network model by iterative experimentation and mathematical analysis. *Molecular Systems Biology*, *1*(1), 1–9. https://doi.org/10.1038/msb4100018

López-Torrejón, G., Guerra, D., Catalá, R., Salinas, J., and del Pozo, J. C. (2013). Identification of SUMO Targets by a Novel Proteomic Approach in Plants. *Journal of Integrative Plant Biology*, *55*(1), 96–107. https://doi.org/10.1111/jipb.12012

Lu, S. X., Webb, C. J., Knowles, S. M., Kim, S. H. J., Wang, Z., and Tobin, E. M. (2012). CCA1 and ELF3 interact in the control of hypocotyl length and flowering time in arabidopsis. *Plant Physiology*, *158*(2), 1079–1088. https://doi.org/10.1104/pp.111.189670

Lu, S., Zhao, X., Hu, Y., Liu, S., Nan, H., Li, X., Fang, C., Cao, D., Shi, X., Kong, L., Su, T., Zhang, F., Li, S., Wang, Z., Yuan, X., Cober, E. R., Weller, J. L., Liu, B., Hou, X., … Kong, F. (2017). Natural variation at the soybean J locus improves adaptation to the tropics and enhances yield. *Nature Genetics*, *49*(5), 773–779. https://doi.org/10.1038/ng.3819

Lu, X. D., Zhou, C. M., Xu, P. B., Luo, Q., Lian, H. L., and Yang, H. Q. (2015). Red-light-dependent interaction of phyB with SPA1 promotes COP1-SPA1 dissociation and photomorphogenic development in arabidopsis. *Molecular Plant*, *8*(3), 467–478. https://doi.org/10.1016/j.molp.2014.11.025

Luo, X. M., Lin, W. H., Zhu, S., Zhu, J. Y., Sun, Y., Fan, X. Y., Cheng, M., Hao, Y., Oh, E., Tian, M., Liu, L., Zhang, M., Xie, Q., Chong, K., and Wang, Z. Y. (2010). Integration of Light- and Brassinosteroid-Signaling Pathways by a GATA Transcription Factor in Arabidopsis. *Developmental Cell*, *19*(6), 872–883. https://doi.org/10.1016/j.devcel.2010.10.023

Lv, X., Zeng, X., Hu, H., Chen, L., Zhang, F., Liu, R., Liu, Y., Zhou, X., Wang, C., Wu, Z., Kim, C., He, Y., and Du, J. (2021). Structural insights into the multivalent binding of the Arabidopsis FLOWERING LOCUS T promoter by the CO-NF-Y master transcription factor complex. *Plant Cell*, *33*(4), 1182–1195. https://doi.org/10.1093/plcell/koab016

Mao, J., Zhang, Y. C., Sang, Y., Li, Q. H., and Yang, H. Q. (2005). A role for Arabidopsis cryptochromes and COP1 in the regulation of stomatal opening. *Proceedings of the National Academy of Sciences of the United States of America*, *102*(34), 12270–12275. https://doi.org/10.1073/pnas.0501011102

Martin-Tryon, E. L., Kreps, J. A., and Harmer, S. L. (2007). GIGANTEA acts in blue light signaling and has biochemically separable roles in circadian clock and flowering time regulation. *Plant Physiology*, *143*(1), 473–486. https://doi.org/10.1104/pp.106.088757

Matías-Hernández, L., Aguilar-Jaramillo, A. E., Marín-González, E., Suárez-López, P., and Pelaz, S. (2014). RAV genes: Regulation of floral induction and beyond. *Annals of Botany*, *114*(7), 1459–1470. https://doi.org/10.1093/aob/mcu069

McNellis, T. W., von Arnim, A. G., Araki, T., Komeda, Y., Misera, S., and Deng Xing Wang. (1994). Genetic and molecular analysis of an allelic series of cop1 mutants suggests functional roles for the multiple protein domains. *Plant Cell*, *6*(4), 487–500. https://doi.org/10.1105/tpc.6.4.487

Migliorini, D., Bogaerts, S., Defever, D., Vyas, R., Denecker, G., Radaelli, E., Zwolinska, A., Depaepe, V., Hochepied, T., Skarnes, W. C., and Marine, J. C. (2011). Cop1 constitutively regulates c-Jun protein stability and functions as a tumor suppressor in mice. *Journal of Clinical Investigation*, *121*(4), 1329–1343. https://doi.org/10.1172/JCI45784

Miladinović, J., Ćeran, M., Đorđević, V., Balešević-Tubić, S., Petrović, K., Đukić, V., and Miladinović, D. (2018). Allelic variation and distribution of the major maturity genes in different soybean collections. *Frontiers in Plant Science*, *9*(September), 1–8. https://doi.org/10.3389/fpls.2018.01286

Mishra, P., and Panigrahi, K. C. S. (2015). GIGANTEA - an emerging story. *Frontiers in Plant Science*, *6*, 8. https://doi.org/10.3389/fpls.2015.00008

Mizuno, T., Nomoto, Y., Oka, H., Kitayama, M., Takeuchi, A., Tsubouchi, M., and Yamashino, T. (2014). Ambient temperature signal feeds into the circadian clock transcriptional circuitry through the EC night-time repressor in arabidopsis thaliana. *Plant and Cell Physiology*, *55*(5), 958–976. https://doi.org/10.1093/pcp/pcu030

Murfet, I. C. (1973). *FLOWERING IN PISUM . Hr , A GENE FOR HIGH RESPONSE TO PHOTOPERIOD paper (Murfet , 197lc) dealt with the possible physiological action of these genes . It was suggested that Sn produces a flower inhibitor in the*. *31*, 157–164.

Murfet, I. C. (1985). Pisum Sativum. In A. H. Halevy (Ed.), *Handbook of Flowering* (pp. 97–126). CRC Press. https://doi.org/10.1201/9781351072564

Nakamichi, N. (2015). Adaptation to the local environment by modifications of the photoperiod response in crops. *Plant & Cell Physiology*, *56*(4), 594–604. https://doi.org/10.1093/pcp/pcu181

Nakasako, M., Matsuoka, D., Zikihara, K., and Tokutomi, S. (2005). Quaternary structure of LOV-domain containing polypeptide of Arabidopsis FKF1 protein. *FEBS Letters*, *579*(5), 1067–1071. https://doi.org/10.1016/j.febslet.2004.12.078

Nakasone, Y., Zikihara, K., Tokutomi, S., and Terazima, M. (2010). Kinetics of conformational changes of the FKF1-LOV domain upon photoexcitation. *Biophysical Journal*, *99*(11), 3831–3839. https://doi.org/10.1016/j.bpj.2010.10.005

Navarro, C., Cruz-Oró, E., and Prat, S. (2015). Conserved function of FLOWERING LOCUS T (FT) homologues as signals for storage organ differentiation. *Current Opinion in Plant Biology*, *23*, 45–53. https://doi.org/10.1016/j.pbi.2014.10.008

Nelson, D. C., Lasswell, J., Rogg, L. E., Cohen, M. A., and Bartel, B. (2000). FKF1, a clock-controlled gene that regulates the transition to flowering in Arabidopsis. *Cell*, *101*(3), 331–340. https://doi.org/10.1016/S0092-8674(00)80842-9

Nicholas, K. B., and Nicholas, H. B. (1997). *GeneDoc: a tool for editing and annotating multiple sequence alignments*.

Nimmo, H. G., Laird, J., Bindbeutel, R., and Nusinow, D. A. (2020). The evening complex is central to the difference between the circadian clocks of Arabidopsis thaliana shoots and roots. *Physiologia Plantarum*, *169*(3), 442–451. https://doi.org/10.1111/ppl.13108

Nishida, H., Ishihara, D., Ishii, M., Kaneko, T., Kawahigashi, H., Akashi, Y., Saisho, D., Tanaka, K., Handa, H., Takeda, K., and Kato, K. (2013). Phytochrome C is a key factor controlling long-day flowering in barley. *Plant Physiology*, *163*(2), 804–814. https://doi.org/10.1104/pp.113.222570

No, D. H., Baek, D., Lee, S. H., Cheong, M. S., Chun, H. J., Park, M. S., Cho, H. M., Jin, B. J., Lim, L. H., Lee, Y. B., Shim, S. I., Chung, J. il, and Kim, M. C. (2021). High-temperature conditions promote soybean flowering through the transcriptional reprograming of flowering genes in the photoperiod pathway. *International Journal of Molecular Sciences*, *22*(3), 1–12. https://doi.org/10.3390/ijms22031314

Nohales, M. A., and Kay, S. A. (2019). GIGANTEA gates gibberellin signaling through stabilization of the DELLA proteins in Arabidopsis. *Proceedings of the National Academy of Sciences of the United States of America*, *116*(43), 21893–21899. https://doi.org/10.1073/pnas.1913532116

Ogiso-Tanaka, E., Matsubara, K., Yamamoto, S. ichi, Nonoue, Y., Wu, J., Fujisawa, H., Ishikubo, H., Tanaka, T., Ando, T., Matsumoto, T., and Yano, M. (2013). Natural Variation of the RICE FLOWERING LOCUS T 1 Contributes to Flowering Time Divergence in Rice. *PLoS ONE*, *8*(10), 1–22. https://doi.org/10.1371/journal.pone.0075959

Oliverio, K. A., Crepy, M., Martin-Tryon, E. L., Milich, R., Harmer, S. L., Putterill, J., Yanovsky, M. J., and Casal, J. J. (2007). GIGANTEA regulates phytochrome A-mediated photomorphogenesis independently of its role in the circadian clock. *Plant Physiology*, *144*(1), 495–502. https://doi.org/10.1104/pp.107.097048

Olsen, K. M., and Wendel, J. F. (2013). Crop plants as models for understanding plant adaptation and diversification. *Frontiers in Plant Science*, *4*(AUG). https://doi.org/10.3389/fpls.2013.00290

Ordoñez-Herrera, N., Fackendahl, P., Yu, X., Schaefer, S., Koncz, C., and Hoecker, U. (2015). A cop1 spa Mutant Deficient in COP1 and SPA Proteins Reveals Partial Co-Action of COP1 and SPA during Arabidopsis Post-Embryonic Development and Photomorphogenesis. *Molecular Plant*, *8*(3), 479–481. https://doi.org/10.1016/j.molp.2014.11.026

Ortega, R., Hecht, V., Freeman, J. S., Rubio, J., Carrasquilla-Garcia, N., Mir, R. R., Penmetsa, R. V., Cook, D. R., Mi, and Weller, J. L. (2019). Altered expression of an FT cluster underlies a major locus controlling domestication-related changes to chickpea phenology and growth habit. *Frontiers in Plant Science*, *10*(July). https://doi.org/10.3389/fpls.2019.00824

Osnato, M., Castillejo, C., Matías-Hernández, L., and Pelaz, S. (2012). TEMPRANILLO genes link photoperiod and gibberellin pathways to control flowering in Arabidopsis. *Nature Communications*, *3*(May). https://doi.org/10.1038/ncomms1810

Osterlund, M. T., Hardtke, C. S., Ning, W., and Deng, X. W. (2000). Targeted destabilization of HY5 during light-regulated development of Arabidopsis. *Nature*, *405*(6785), 462–466. https://doi.org/10.1038/35013076

Paltiel, J., Amin, R., Gover, A., Ori, N., and Samach, A. (2006). Novel roles for GIGANTEA revealed under environmental conditions that modify its expression in Arabidopsis and Medicago truncatula. *Planta*, *224*(6), 1255–1268. https://doi.org/10.1007/s00425-006-0305-1

Park, D. H., Somers, D. E., Kim, Y. S., Choy, Y. H., Lim, H. K., Soh, M. S., Kim, H. J., Kay, S. A., and Nam, H. G. (1999). Control of circadian rhythms and photoperiodic flowering by the

Arabidopsis GIGANTEA gene. *Science*, *285*(5433), 1579–1582. https://doi.org/10.1126/science.285.5433.1579

Park, H. J., Kim, W. Y., and Yun, D. J. (2013). A role for GIGANTEA: Keeping the balance between flowering and salinity stress tolerance. *Plant Signaling and Behavior*, *8*(7). https://doi.org/10.4161/psb.24820

Peng, L. T., Shi, Z. Y., Li, L., Shen, G. Z., and Zhang, J. L. (2007). Ectopic expression of OsLFL1 in rice represses Ehd1 by binding on its promoter. *Biochemical and Biophysical Research Communications*, *360*(1), 251–256. https://doi.org/10.1016/j.bbrc.2007.06.041

Pfaffl, M. W. (2001). a new mathematical model for relative quantification in real-time RT-PCR. *Nucleic Acids Research*, *29*, 2002–2007.

Pin, P. A., Benlloch, R., Bonnet, D., Wremerth-Weich, E., Kraft, T., Gielen, J. J. L., and Nilsson, O. (2010). An antagonistic pair of FT homologs mediates the control of flowering time in sugar beet. *Science*, *330*(6009), 1397–1400. https://doi.org/10.1126/science.1197004

Pin, P. A., and Nilsson, O. (2012). The multifaceted roles of FLOWERING LOCUS T in plant development. *Plant, Cell and Environment*, *35*(10), 1742–1755. https://doi.org/10.1111/j.1365-3040.2012.02558.x

Platten, J. D., Foo, E., Elliott, R. C., Hecht, V., Reid, J. B., and Weller, J. L. (2005). Cryptochrome 1 contributes to blue-light sensing in pea. *Plant Physiology*, *139*(3), 1472–1482. https://doi.org/10.1104/pp.105.067462

Pnueli, L., Gutfinger, T., Hareven, D., Ben-Naim, O., Ron, N., Adir, N., and Lifschitz, E. (2001). Tomato SP-Interacting Proteins Define a Conserved Signaling System That Regulates Shoot Architecture and Flowering. *The Plant Cell*, *13*(12), 2687–2702. https://doi.org/10.1105/tpc.010293

Podolec, R., and Ulm, R. (2018). Photoreceptor-mediated regulation of the COP1/SPA E3 ubiquitin ligase. *Current Opinion in Plant Biology*, *45*, 18–25. https://doi.org/10.1016/j.pbi.2018.04.018

Ponnu, J., and Hoecker, U. (2021). Illuminating the COP1/SPA Ubiquitin Ligase: Fresh Insights Into Its Structure and Functions During Plant Photomorphogenesis. *Frontiers in Plant Science*, *12*(March), 1–19. https://doi.org/10.3389/fpls.2021.662793

Prag, S., and Adams, J. C. (2003). Molecular phylogeny of the kelch-repeat superfamily reveals an expansion of BTB/kelch proteins in animals. *BMC Bioinformatics*, *4*(May). https://doi.org/10.1186/1471-2105-4-42

Pudasaini, A., Shim, J. S., Song, Y. H., Shi, H., Kiba, T., Somers, D. E., Imaizumi, T., and Zoltowski, B. D. (2017). Kinetics of the LOV domain of ZEITLUPE determine its circadian function in arabidopsis. *ELife*, *6*(1), 1–27. https://doi.org/10.7554/eLife.21646

Purugganan, M. D., and Fuller, D. Q. (2009). The nature of selection during plant domestication. *Nature*, *457*(7231), 843–848. https://doi.org/10.1038/nature07895

Putterill, J., Robson, F., Lee, K., Simon, R., and Coupland, G. (1995). The CONSTANS gene of arabidopsis promotes flowering and encodes a protein showing similarities to zinc finger transcription factors. *Cell*, *80*(6), 847–857. https://doi.org/10.1016/0092-8674(95)90288-0

Putterill, J., and Varkonyi-Gasic, E. (2016). FT and florigen long-distance flowering control in plants. *Current Opinion in Plant Biology*, *33*, 77–82. https://doi.org/10.1016/j.pbi.2016.06.008

Putterill, J., Zhang, L., Yeoh, C. C., Balcerowicz, M., Jaudal, M., and Gasic, E. V. (2013). FT genes and regulation of flowering in the legume Medicago truncatula. *Functional Plant Biology*, *40*(12), 1199–1207. https://doi.org/10.1071/FP13087

Qin, Z., Wu, J., Geng, S., Feng, N., Chen, F., Kong, X., Song, G., Chen, K., Li, A., Mao, L., and Wu, L. (2017). Regulation of FT splicing by an endogenous cue in temperate grasses. *Nature Communications*, *8*, 1–12. https://doi.org/10.1038/ncomms14320

Quiroz, S., Yustis, J. C., Chávez-Hernández, E. C., Martínez, T., Sanchez, M. de la P., Garay-Arroyo, A., Álvarez-Buylla, E. R., and García-Ponce, B. (2021). Beyond the genetic pathways, flowering regulation complexity in Arabidopsis thaliana. *International Journal of Molecular Sciences*, *22*(11). https://doi.org/10.3390/ijms22115716

Ream, T. S., Woods, D. P., and Amasino, R. M. (2012). The molecular basis of vernalization in different plant groups. *Cold Spring Harbor Symposia on Quantitative Biology*, *77*, 105–115. https://doi.org/10.1101/sqb.2013.77.014449

Rédei, G. P. (1962). Supervital Mutants of Arabidopsis. *Genetics*, *47*(4), 443–460. http://www.ncbi.nlm.nih.gov/pubmed/17248096%5Cnhttp://www.pubmedcentral.nih.gov/articlerender.fcgi?artid=PMC1210343

Renau-Morata, B., Carrillo, L., Dominguez-Figueroa, J., Vicente-Carbajosa, J., Molina, R. v., Nebauer, S. G., Medina, J., and Doerner, P. (2020). CDF transcription factors: Plant regulators to deal with extreme environmental conditions. *Journal of Experimental Botany*, *71*(13), 3803–3815. https://doi.org/10.1093/jxb/eraa088

Riboni, M., Galbiati, M., Tonelli, C., and Conti, L. (2013). GIGANTEA enables drought escape response via abscisic acid-dependent activation of the florigens and SUPPRESSOR of OVEREXPRESSION of CONSTANS11[c][w]. *Plant Physiology*, *162*(3), 1706–1719. https://doi.org/10.1104/pp.113.217729

Ridge, S., Deokar, A., Lee, R., Daba, K., Macknight, R. C., Weller, J. L., and Tar'An, B. (2017). The chickpea Early flowering 1 (Efl1) locus is an ortholog of arabidopsis ELF3. *Plant Physiology*, *175*(2), 802–815. https://doi.org/10.1104/pp.17.00082

Ridge, S., Sussmilch, F. C., Hecht, V., vander Schoor, J. K., Lee, R., Aubert, G., Burstin, J., Macknight, R. C., and Weller, J. L. (2016). Identification of LATE BLOOMER2 as a CYCLING DOF FACTOR Homolog Reveals Conserved and Divergent Features of the Flowering Response to Photoperiod in Pea. *The Plant Cell*, *28*(10), 2545–2559. https://doi.org/10.1105/tpc.15.01011

Rolauffs, S., Fackendahl, P., Sahm, J., Fiene, G., and Hoecker, U. (2012). Arabidopsis COP1 and SPA genes are essential for plant elongation but not for acceleration of flowering time in response to a low red light to far-red light ratio. *Plant Physiology*, *160*(4), 2015–2027. https://doi.org/10.1104/pp.112.207233

Romanov, G. A. (2012). Mikhail Khristoforovich Chailakhyan: The fate of the scientist under the sign of florigen. *Russian Journal of Plant Physiology*, *59*(4), 443–450. https://doi.org/10.1134/S1021443712040103

Rousset, M., Bonnin, I., Remoué, C., Falque, M., Rhoné, B., Veyrieras, J. B., Madur, D., Murigneux, A., Balfourier, F., le Gouis, J., Santoni, S., and Goldringer, I. (2011). Deciphering the genetics of flowering time by an association study on candidate genes in bread wheat (Triticum aestivum L.). *Theoretical and Applied Genetics*, *123*(6), 907–926. https://doi.org/10.1007/s00122-011-1636-2

Rubenach, A. J. S., Hecht, V., vander Schoor, J. K., Liew, L. C., Aubert, G., Burstin, J., and Weller, J. L. (2017). EARLY FLOWERING3 Redundancy Fine-Tunes Photoperiod Sensitivity. *Plant Physiology*, *173*(4), 2253–2264. https://doi.org/10.1104/pp.16.01738

Ruffier, M., Kähäri, A., Komorowska, M., Keenan, S., Laird, M., Longden, I., Proctor, G., Searle, S., Staines, D., Taylor, K., Vullo, A., Yates, A., Zerbino, D., and Flicek, P. (2017). Ensembl core software resources: Storage and programmatic access for DNA sequence and genome annotation. *Database*, *2017*(1), 1–11. https://doi.org/10.1093/database/bax020

Salomé, P. A., Xie, Q., and McClung, R. C. (2008). Circadian timekeeping during early arabidopsis development. *Plant Physiology*, *147*(3), 1110–1125. https://doi.org/10.1104/pp.108.117622

Sawa, M., and Kay, S. A. (2011). GIGANTEA directly activates Flowering Locus T in Arabidopsis thaliana. *Proceedings of the National Academy of Sciences of the United States of America*, *2011*(28), 11698–11703. https://doi.org/10.1073/pnas.1106771108/-/DCSupplemental.www.pnas.org/cgi/doi/10.1073/pnas.1106771108

Sawa, M., Nusinow, D. A., Kay, S. A., and Imaizumi, T. (2007). FKF1 and GIGANTEA Complex Formation Is Required for Day-Length Measurement in Arabidopsis. *Science*, *318*(5848), 261–265. https://doi.org/10.1126/science.1146994

Seo, H. S., Watanabe, E., Tokutomi, S., Nagatani, A., and Chua, N. H. (2004). Photoreceptor ubiquitination by COP1 E3 ligase desensitizes phytochrome A signaling. *Genes and Development*, *18*(6), 617–622. https://doi.org/10.1101/gad.1187804

Shaw, L. M., Turner, A. S., Herry, L., Griffiths, S., and Laurie, D. A. (2013). Mutant alleles of Photoperiod-1 in Wheat (Triticum aestivum L.) that confer a late flowering phenotype in long days. *PLoS ONE*, *8*(11). https://doi.org/10.1371/journal.pone.0079459

Sheerin, D. J., Menon, C., Oven-Krockhaus, S. zur, Enderle, B., Zhu, L., Johnen, P., Schleifenbaum, F., Stierhof, Y. D., Huq, E., and Hiltbrunner, A. (2015). Light-activated phytochrome A and B interact with members of the SPA family to promote photomorphogenesis in arabidopsis by reorganizing the COP1/SPA complex. *Plant Cell*, *27*(1), 189–201. https://doi.org/10.1105/tpc.114.134775

Shibuta, M., and Abe, M. (2017). FE Controls the Transcription of Downstream Flowering Regulators Through Two Distinct Mechanisms in Leaf Phloem Companion Cells. *Plant and Cell Physiology*, *58*(11), 2017–2025. https://doi.org/10.1093/pcp/pcx133

Shibuya, T., Nishiyama, M., Kato, K., and Kanayama, Y. (2021). Characterization of the flavin-binding, kelch repeat, f-box 1 homolog slfkf1 in tomato as a model for plants with fleshy

fruit. *International Journal of Molecular Sciences*, *22*(4), 1–12. https://doi.org/10.3390/ijms22041735

Shim, J. S., and Jang, G. (2020). Environmental signal-dependent regulation of flowering time in rice. *International Journal of Molecular Sciences*, *21*(17), 1–15. https://doi.org/10.3390/ijms21176155

Shim, J. S., Kubota, A., and Imaizumi, T. (2017). Circadian clock and photoperiodic flowering in arabidopsis: CONSTANS is a Hub for Signal integration. *Plant Physiology*, *173*(1), 5–15. https://doi.org/10.1104/pp.16.01327

Shin, S. Y., Kim, S. H., Kim, H. J., Jeon, S. J., Sim, S. A., Ryu, G. R., Yoo, C. M., Cheong, Y. H., and Hong, J. C. (2016). Isolation of three B-box zinc finger proteins that interact with STF1 and COP1 defines a HY5/COP1 interaction network involved in light control of development in soybean. *Biochemical and Biophysical Research Communications*, *478*(3), 1080–1086. https://doi.org/10.1016/j.bbrc.2016.08.069

Shrestha, R., Gomez-Ariza, J., Brambilla, V., and Fornara, F. (2014). Molecular control of seasonal flowering in rice, arabidopsis and temperate cereals. *Annals of Botany*, *114*(7), 1445–1458. https://doi.org/10.1093/aob/mcu032

Silva, G. F. F., Silva, E. M., Correa, J. P. O., Vicente, M. H., Jiang, N., Notini, M. M., Junior, A. C., de Jesus, F. A., Castilho, P., Carrera, E., López-Díaz, I., Grotewold, E., Peres, L. E. P., and Nogueira, F. T. S. (2019). Tomato floral induction and flower development are orchestrated by the interplay between gibberellin and two unrelated microRNA-controlled modules. *New Phytologist*, *221*(3), 1328–1344. https://doi.org/10.1111/nph.15492

Song, Y. H., Estrada, D. A., Johnson, R. S., Kim, S. K., Lee, S. Y., MacCoss, M. J., and Imaizumi, T. (2014). Distinct roles of FKF1, GIGANTEA, and ZEITLUPE proteins in the regulation of constans stability in Arabidopsis photoperiodic flowering. *Proceedings of the National Academy of Sciences of the United States of America*, *111*(49), 17672–17677. https://doi.org/10.1073/pnas.1415375111

Song, Y. H., Ito, S., and Imaizumi, T. (2010). Similarities in the circadian clock and photoperiodism in plants. *Current Opinion in Plant Biology*, *13*(5), 594–603. https://doi.org/10.1016/j.pbi.2010.05.004

Song, Y. H., Ito, S., and Imaizumi, T. (2013). Flowering time regulation: Photoperiod- and temperature-sensing in leaves. *Trends in Plant Science*, *18*(10), 575–583. https://doi.org/10.1016/j.tplants.2013.05.003

Song, Y. H., Kubota, A., Kwon, M. S., Covington, M. F., Lee, N., Taagen, E. R., Laboy Cintrón, D., Hwang, D. Y., Akiyama, R., Hodge, S. K., Huang, H., Nguyen, N. H., Nusinow, D. A., Millar, A. J., Shimizu, K. K., and Imaizumi, T. (2018). Molecular basis of flowering under natural long-day conditions in Arabidopsis. *Nature Plants*, *4*(10), 824–835. https://doi.org/10.1038/s41477-018-0253-3

Song, Y. H., Shim, J. S., Kinmonth-Schultz, H. A., and Imaizumi, T. (2015). Photoperiodic Flowering: Time Measurement Mechanisms in Leaves. *Annual Review of Plant Biology*, *66*, 441–464. https://doi.org/10.1146/annurev-arplant-043014-115555

Song, Y. H., Smith, R. W., To, B. J., Millar, A. J., and Imaizumi, T. (2012). FKF1 Conveys Timing Information for CONSTANS Stabilization in Photoperiodic Flowering. *Science*, *336*(6084), 1045–1049. https://doi.org/10.1126/science.1219644

Soo Seo, H., Yang, J. Y., Ishikawa, M., Bolle, C., Ballesteros, M. L., and Chua, N. H. (2003). LAF1 ubiquitination by COP1 controls photomorphogenesis and is stimulated by SPA1. *Nature*, *423*(6943), 995–999. https://doi.org/10.1038/nature01696

Sponsel, V. M., and Reid, J. B. (1992). Use of an acylcyclohexanedione growth retardant, LAB 198 999, to determine whether gibberellin A20 has biological activity per se in dark-grown dwarf (le5839) seedlings of Pisum sativum. *Plant Physiology*, *100*(2), 651–654. https://doi.org/10.1104/pp.100.2.651

Sponsel, V. M., Ross, J. J., Reynolds, M. R., Symons, G. M., and Reid, J. B. (1996). The gibberellin status of lip1, a mutant of pea that exhibits light- independent photomorphogenesis. *Plant Physiology*, *112*(1), 61–66. https://doi.org/10.1104/pp.112.1.61

Suárez-López, P., Wheatley, K., Robson, F., Onouchi, H., Valverde, F., and Coupland, G. (2001). CONSTANS mediates between the circadian clock and the control of flowering in Arabidopsis. *Nature*, *410*(6832), 1116–1120. https://doi.org/10.1038/35074138

Sullivan, J. A., and Gray, J. C. (2000). The Pea light-independent photomorphogenesis1 Mutant Results from Partial Duplication of COP1 Generating an Internal Promoter and Producing Two Distinct Transcripts. *Plant Cell*, *12*(October), 1927–1937.

Summerfield, R. J., Roberts, E. H., Erskine, W., and Ellis, R. H. (1985). Effects of Temperature and Photoperiod on Flowering in Lentils (Lens culinaris Medic .). *Annals of Botany*, *56*(5), 659–671. https://www.jstor.org/stable/42765135

Sun, L., Ge, Y., Bancroft, A. C., Cheng, X., and Wen, J. (2018). FNBtools: A software to identify homozygous lesions in deletion mutant populations. *Frontiers in Plant Science*, *9*(July), 1–11. https://doi.org/10.3389/fpls.2018.00976

Sun, L., Gill, U. S., Nandety, R. S., Kwon, S., Mehta, P., Dickstein, R., Udvardi, M. K., Mysore, K. S., and Wen, J. (2019). Genome-wide analysis of flanking sequences reveals that Tnt1 insertion is positively correlated with gene methylation in Medicago truncatula. *Plant Journal*, *98*(6), 1106–1119. https://doi.org/10.1111/tpj.14291

Sung, S., and Amasino, R. M. (2005). Remembering winter: Toward a molecular understanding of vernalization. *Annual Review of Plant Biology*, *56*, 491–508. https://doi.org/10.1146/annurev.arplant.56.032604.144307

Swarup, K., Alonso-Blanco, C., Lynn, J. R., Michaels, S. D., Amasino, R. M., Koornneef, M., and Millar, A. J. (1999). Natural allelic variation identifies new genes in the Arabidopsis circadian system. *Plant Journal*, *20*(1), 67–77. https://doi.org/10.1046/j.1365-313X.1999.00577.x

Tadege, M., Wen, J., He, J., Tu, H., Kwak, Y., Eschstruth, A., Cayrel, A., Endre, G., Zhao, P. X., Chabaud, M., Ratet, P., and Mysore, K. S. (2008). Large-scale insertional mutagenesis using the Tnt1 retrotransposon in the model legume Medicago truncatula. *Plant Journal*, *54*(2), 335–347. https://doi.org/10.1111/j.1365-313X.2008.03418.x

Takase, T., Nishiyama, Y., Tanihigashi, H., Ogura, Y., Miyazaki, Y., Yamada, Y., and Kiyosue, T. (2011). LOV KELCH PROTEIN2 and ZEITLUPE repress Arabidopsis photoperiodic flowering under non-inductive conditions, dependent on FLAVIN-BINDING KELCH REPEAT F - BOX1. *Plant Journal*, *67*(4), 608–621. https://doi.org/10.1111/j.1365-313X.2011.04618.x

Tamaki, S., Matsuo, S., Wong, H. L., Yokoi, S., and Shimamoto, K. (2007). Hd3a Protein Is a Mobile Flowering Signal in rice. *Science*, *316*(May), 1033–1036.

Tanaka, N., Itoh, H., Sentoku, N., Kojima, M., Sakakibara, H., Izawa, T., Itoh, J.-I., and Nagato, Y. (2011). The COP1 Ortholog PPS Regulates the Juvenile–Adult and Vegetative–Reproductive Phase Changes in Rice . *The Plant Cell*, *23*(6), 2143–2154. https://doi.org/10.1105/tpc.111.083436

Tang, W., Yan, H., Su, Z., Park, S.-C., Liu, Y., Zhang, Y., Wang, X., Kou, M., Ma, D., Kwak, S.-S., and Li, Q. (2017). Cloning and characterization of a novel GIGANTEA gene in sweet potato. *Plant Physiology and Biochemistry*, *116*, 27–35. https://doi.org/10.1016/j.plaphy.2017.04.025

Taoka, K. I., Ohki, I., Tsuji, H., Furuita, K., Hayashi, K., Yanase, T., Yamaguchi, M., Nakashima, C., Purwestri, Y. A., Tamaki, S., Ogaki, Y., Shimada, C., Nakagawa, A., Kojima, C., and Shimamoto, K. (2011). 14-3-3 proteins act as intracellular receptors for rice Hd3a florigen. *Nature*, *476*(7360), 332–335. https://doi.org/10.1038/nature10272

Taylor, A., Massiah, A. J., and Thomas, B. (2010). Conservation of Arabidopsis thaliana photoperiodic flowering time genes in onion (Allium cepa L.). *Plant and Cell Physiology*, *51*(10), 1638–1647. https://doi.org/10.1093/pcp/pcq120

Thakare, D., Kumudini, S., and Dinkins, R. D. (2011). The alleles at the E1 locus impact the expression pattern of two soybean FT-like genes shown to induce flowering in Arabidopsis. *Planta*, *234*(5), 933–943. https://doi.org/10.1007/s00425-011-1450-8

Thomas, B. (2006). Light signals and flowering. *Journal of Experimental Botany*, *57*(13), 3387–3393. https://doi.org/10.1093/jxb/erl071

Thompson, J. D., Higgins, D. G., and Gibson, T. J. (1994). CLUSTAL W: Improving the sensitivity of progressive multiple sequence alignment through sequence weighting, position-specific gap penalties and weight matrix choice. *Nucleic Acids Research*, *22*(22), 4673–4680. https://doi.org/10.1093/nar/22.22.4673

Thomson, G., Taylor, J., and Putterill, J. (2019). The transcriptomic response to a short day to long day shift in leaves of the reference legume Medicago truncatula. *PeerJ*, *2019*(3). https://doi.org/10.7717/peerj.6626

Thomson, G., Zhang, L., Wen, J., Mysore, K. S., and Putterill, J. (2021). The Candidate Photoperiod Gene MtFE Promotes Growth and Flowering in Medicago truncatula. *Frontiers in Plant Science*, *12*(March). https://doi.org/10.3389/fpls.2021.634091

Tiwari, S. B., Shen, Y., Chang, H. C., Hou, Y., Harris, A., Ma, S. F., McPartland, M., Hymus, G. J., Adam, L., Marion, C., Belachew, A., Repetti, P. P., Reuber, T. L., and Ratcliffe, O. J. (2010). The flowering time regulator CONSTANS is recruited to the FLOWERING LOCUS T promoter via a unique cis-element. *New Phytologist*, *187*(1), 57–66. https://doi.org/10.1111/j.1469-8137.2010.03251.x

Tränkner, C., Lehmann, S., Hoenicka, H., Hanke, M. V., Fladung, M., Lenhardt, D., Dunemann, F., Gau, A., Schlangen, K., Malnoy, M., and Flachowsky, H. (2010). Over-expression of an FT-homologous gene of apple induces early xowering in annual and perennial plants. *Planta*, *232*(6), 1309–1324. https://doi.org/10.1007/s00425-010-1254-2

Tsubokura, Y., Matsumura, H., Xu, M., Liu, B., Nakashima, H., Anai, T., Kong, F., Yuan, X., Kanamori, H., Katayose, Y., Takahashi, R., Harada, K., and Abe, J. (2013). Genetic Variation in Soybean at the Maturity Locus E4 Is Involved in Adaptation to Long Days at High Latitudes. *Agronomy*, *3*(1), 117–134. https://doi.org/10.3390/agronomy3010117

Tsubokura, Y., Watanabe, S., Xia, Z., Kanamori, H., Yamagata, H., Kaga, A., Katayose, Y., Abe, J., Ishimoto, M., and Harada, K. (2014). Natural variation in the genes responsible for maturity loci E1, E2, E3 and E4 in soybean. *Annals of Botany*, *113*(3), 429–441. https://doi.org/10.1093/aob/mct269

Tsuji, H., Taoka, K. I., and Shimamoto, K. (2011). Regulation of flowering in rice: Two florigen genes, a complex gene network, and natural variation. *Current Opinion in Plant Biology*, *14*(1), 45–52. https://doi.org/10.1016/j.pbi.2010.08.016

Turck, F., Fornara, F., and Coupland, G. (2008). Regulation and Identity of Florigen: FLOWERING LOCUS T Moves Center Stage. *Annual Review of Plant Biology*, *59*(1), 573–594. https://doi.org/10.1146/annurev.arplant.59.032607.092755

Uljon, S., Xu, X., Durzynska, I., Stein, S., Adelmant, G., Marto, J. A., Pear, W. S., and Blacklow, S. C. (2016). Structural Basis for Substrate Selectivity of the E3 Ligase COP1. *Structure*, *24*(5), 687–696. https://doi.org/10.1016/j.str.2016.03.002

Untergasser, A., Cutcutache, I., Koressaar, T., Ye, J., Faircloth, B. C., Remm, M., and Rozen, S. G. (2012). Primer3-new capabilities and interfaces. *Nucleic Acids Research*, *40*(15), 1–12. https://doi.org/10.1093/nar/gks596

Valverde, F. (2011). CONSTANS and the evolutionary origin of photoperiodic timing of flowering. *Journal of Experimental Botany*, *62*(8), 2453–2463. https://doi.org/10.1093/jxb/erq449

Valverde, F., Mouradov, A., Soppe, W., Ravenscroft, D., Samach, A., and Coupland, G. (2004). Photoreceptor Regulation of CONSTANS Protein in Photoperiodic Flowering. *Science*, *303*(5660), 1003–1006. https://doi.org/10.1126/science.1091761

Verhage, L. (2021). Food for thought – how tuberization and drought tolerance are linked in potato. *Plant Journal*, *105*(4), 853–854. https://doi.org/10.1111/tpj.15175

Wakabayashi, T., Oh, H., Kawaguchi, M., Harada, K., Sato, S., Ikeda, H., and Hiroaki, S. (2014). Polymorphisms of E1 and GIGANTEA in wild populations of Lotus japonicus. *Journal of Plant Research*, *127*(6), 651–660. https://doi.org/10.1007/s10265-014-0649-8

Wang, Q., and Lin, C. (2019a). Photoreceptor signaling: when COP1 meets VPs. *The EMBO Journal*, 1–2. https://doi.org/10.15252/embj.2019102962

Wang, Q., Liu, Q., Wang, X., Zuo, Z., Oka, Y., and Lin, C. (2018). New insights into the mechanisms of phytochrome–cryptochrome coaction. *New Phytologist*, *217*(2), 547–551. https://doi.org/10.1111/nph.14886

Wang, W., Chen, Q., Botella, J. R., and Guo, S. (2019b). Beyond light: Insights into the role of constitutively photomorphogenic1 in plant hormonal signaling. *Frontiers in Plant Science*, *10*(May). https://doi.org/10.3389/fpls.2019.00557

Watanabe, S., Harada, K., and Abe, J. (2011). Genetic and molecular bases of photoperiod responses of flowering in soybean. *Breeding Science*, *61*(5), 531–543. https://doi.org/10.1270/jsbbs.61.531

Watanabe, S., Hideshima, R., Zhengjun, X., Tsubokura, Y., Sato, S., Nakamoto, Y., Yamanaka, N., Takahashi, R., Ishimoto, M., Anai, T., Tabata, S., and Harada, K. (2009). Map-based cloning of the gene associated with the soybean maturity locus E3. *Genetics*, *182*(4), 1251–1262. https://doi.org/10.1534/genetics.108.098772

Waterhouse, A., Bertoni, M., Bienert, S., Studer, G., Tauriello, G., Gumienny, R., Heer, F. T., de Beer, T. A. P., Rempfer, C., Bordoli, L., Lepore, R., and Schwede, T. (2018). SWISS-MODEL: Homology modelling of protein structures and complexes. *Nucleic Acids Research*, *46*(W1), W296–W303. https://doi.org/10.1093/nar/gky427

Wei, N., and Deng, X. W. (1996). The role of the COP/DET/FUS genes in light control of arabidopsis seedling development. *Plant Physiology*, *112*(3), 871–878. https://doi.org/10.1104/pp.112.3.871

Weller, J. L., Batge, S. L., Smith, J. J., Kerckhoffs, L. H. J., Sineshchekov, V. A., Murfet, I. C., and Reid, J. B. (2004). A dominant mutation in the pea PHYA gene confers enhanced responses

to light and impairs the light-dependent degradation of phytochrome A. *Plant Physiology*, *135*(4), 2186–2195. https://doi.org/10.1104/pp.103.036103

Weller, J. L., Beauchamp, N., Kerckhoffs, L. H. J., Damien Platten, J., and Reid, J. B. (2001). Interaction of phytochromes A and B in the control of de-etiolation and flowering in pea. *Plant Journal*, *26*(3), 283–294. https://doi.org/10.1046/j.1365-313X.2001.01027.x

Weller, J. L., Hecht, V., Liew, L. C., Sussmilch, F. C., Wenden, B., Knowles, C. L., and Vander Schoor, J. K. (2009a). Update on the genetic control of flowering in garden pea. *Journal of Experimental Botany*, *60*(9), 2493–2499. https://doi.org/10.1093/jxb/erp120

Weller, J. L., Hecht, V., vander Schoor, J. K., Davidson, S. E., and Ross, J. J. (2009b). Light regulation of gibberellin biosynthesis in pea is mediated through the COP1/HY5 pathway. *The Plant Cell*, *21*(3), 800–813. https://doi.org/10.1105/tpc.108.063628

Weller, J. L., Liew, L. C., Hecht, V., Rajandran, V., Laurie, R. E., Ridge, S., Wenden, B., vander Schoor, J. K., Jaminon, O., Blassiau, C., Dalmais, M., Rameau, C., Bendahmane, A., Macknight, R. C., and Lejeune-Hénaut, I. (2012). A conserved molecular basis for photoperiod adaptation in two temperate legumes. *Proceedings of the National Academy of Sciences of the United States of America*, *109*(51), 21158–21163. https://doi.org/10.1073/pnas.1207943110

Weller, J. L., and Macknight, R. C. (2019). Genetic control of flowering time in legumes. In *The Model Legume Medicago truncatula* (pp. 182–188). https://doi.org/10.1002/9781119409144.ch22

Weller, J. L., Murfet, I. C., and Reid, J. B. (1997a). Pea mutants with reduced sensitivity to far-red light define an important role for phytochrome A in day-length detection. *Plant Physiology*, *114*(4), 1225–1236. https://doi.org/10.1104/pp.114.4.1225

Weller, J. L., and Ortega, R. (2015). Genetic control of flowering time in legumes. *Frontiers in Plant Science*, *6*(April), 207. https://doi.org/10.3389/fpls.2015.00207

Weller, J. L., Reid, J. B., Taylor, S. A., and Murfet, I. C. (1997b). The genetic control of flowering in pea. *Trends in Plant Science*, *2*(11), 412–418. https://doi.org/10.1016/S1360-1385(97)01127-8

Weller, J. L., vander Schoor, J. K., Perez-Wright, E. C., Hecht, V., González, A. M., Capel, C., Yuste-Lisbona, F. J., Lozano, R., and Santalla, M. (2019). Parallel origins of photoperiod adaptation

following dual domestications of common bean. *Journal of Experimental Botany*, *70*(4), 1209–1219. https://doi.org/10.1093/jxb/ery455

Wigge, P. A. (2013). Ambient temperature signalling in plants. *Current Opinion in Plant Biology*, *16*(5), 661–666. https://doi.org/10.1016/j.pbi.2013.08.004

Wilczek, A. M., Roe, J. L., Knapp, M. C., Cooper, M. D., Lopez-Gallego, C., Martin, L. J., Muir, C. D., Sim, S., Walker, A., Anderson, J., Egan, J. F., Moyers, B. T., Petipas, R., Giakountis, A., Charbit, E., Coupland, G., Welch, S. M., and Schmitt, J. (2009). Effects of Genetic Perturbation on Seasonal Life History Plasticity. *Science*, *323*(5916), 930–934. https://doi.org/10.1126/science.1165826

Wong, A. C. S., Hecht, V., Picard, K., Diwadkar, P., Laurie, R. E., Wen, J., Mysore, K. S., Macknight, R. C., and Weller, J. L. (2014). Isolation and functional analysis of CONSTANS-LIKE genes suggests that a central role for CONSTANS in flowering time control is not evolutionarily conserved in Medicago truncatula. *Frontiers in Plant Science*, *5*(September), 486. https://doi.org/10.3389/fpls.2014.00486

Wu, F., Price, B. W., Haider, W., Seufferheld, G., Nelson, R., and Hanzawa, Y. (2014). Functional and evolutionary characterization of the CONSTANS gene family in short-day photoperiodic flowering in soybean. *PLoS ONE*, *9*(1). https://doi.org/10.1371/journal.pone.0085754

Xia, Z., Watanabe, S., Yamada, T., Tsubokura, Y., Nakashima, H., Zhai, H., Anai, T., Sato, S., Yamazaki, T., Lü, S., Wu, H., Tabata, S., and Harada, K. (2012). Positional cloning and characterization reveal the molecular basis for soybean maturity locus E1 that regulates photoperiodic flowering. *Proceedings of the National Academy of Sciences of the United States of America*, *109*(32), E2155-64. https://doi.org/10.1073/pnas.1117982109

Xiang, Y. Z., Mao, S. L., Jia, R. L., Chun, M. G., and Xian, S. Z. (2005). The wheat TaGI1, involved in photoperiodic flowering, encodes an Arabidopsis GI ortholog. *Plant Molecular Biology*, *58*(1), 53–64. https://doi.org/10.1007/s11103-005-4162-2

Xie, X., Kagawa, T., and Takano, M. (2014). The phytochrome B/phytochrome C heterodimer is necessary for phytochrome C-mediated responses in rice seedlings. *PLoS ONE*, *9*(5). https://doi.org/10.1371/journal.pone.0097264

Xing Liang Liu, Covington, M. F., Fankhauser, C., Chory, J., and Wagner, D. R. (2001). ELF3 encodes a circadian clock-regulated nuclear protein that functions in an Arabidopsis PHYB

signal transduction pathway. *Plant Cell*, *13*(6), 1293–1304. https://doi.org/10.1105/tpc.13.6.1293

Xu, D., Zhu, D., and Deng, X. W. (2016). The role of COP1 in repression of photoperiodic flowering. *F1000Research*, *5*(0), 1–6. https://doi.org/10.12688/f1000research.7346.1

Xu, L., Hu, K., Zhang, Z., Guan, C., Chen, S., Hua, W., Li, J., Wen, J., Yi, B., Shen, J., Ma, C., Tu, J., and Fu, T. (2015a). Genome-wide association study reveals the genetic architecture of flowering time in rapeseed (*Brassica napus L.*). *DNA Research*, *23*(December 2015), dsv035. https://doi.org/10.1093/dnares/dsv035

Xu, M., Yamagishi, N., Zhao, C., Takeshima, R., Kasai, M., Watanabe, S., Kanazawa, A., Yoshikawa, N., Liu, B., Yamada, T., and Abe, J. (2015b). Soybean-specific E1 family of floral repressors controls night-break responses through down-regulation of FLOWERING LOCUS T orthologs. *Plant Physiology*, *168*(4), 1735–1746. https://doi.org/10.1104/pp.15.00763

Xue, W., Xing, Y., Weng, X., Zhao, Y., Tang, W., Wang, L., Zhou, H., Yu, S., Xu, C., Li, X. H., and Zhang, Q. (2008). Natural variation in Ghd7 is an important regulator of heading date and yield potential in rice. *Nature Genetics*, *40*(6), 761–767. https://doi.org/10.1038/ng.143

Yamashino, T., Yamawaki, S., Hagui, E., Ueoka-Nakanishi, H., Nakamichi, N., Ito, S., and Mizuno, T. (2013). Clock-controlled and FLOWERING LOCUS T (FT)-dependent photoperiodic pathway in lotus japonicus I: Verification of the flowering-associated function of an FT homolog. *Bioscience, Biotechnology and Biochemistry*, *77*(4), 747–753. https://doi.org/10.1271/bbb.120871

Yan, J., Li, X., Zeng, B., Zhong, M., Yang, J., Yang, P., Li, X., He, C., Lin, J., Liu, X., and Zhao, X. (2020). FKF1 F-box protein promotes flowering in part by negatively regulating DELLA protein stability under long-day photoperiod in Arabidopsis. *Journal of Integrative Plant Biology*, *62*(11), 1717–1740. https://doi.org/10.1111/jipb.12971

Yan, L., Fu, D., Li, C., Blechl, A., Tranquilli, G., Bonafede, M., Sanchez, A., Valarik, M., Yasuda, S., and Dubcovsky, J. (2006). The wheat and barley vernalization gene VRN3 is an orthologue of FT. *Proceedings of the National Academy of Sciences of the United States of America*, *103*(51), 19581–19586. https://doi.org/10.1073/pnas.0607142103

Yang, J., Lin, R., Sullivan, J., Hoecker, U., Liu, B., Xu, L., Xing, W. D., and Wang, H. (2005). Light regulates COP1-mediated degradation of HFR1, a transcription factor essential for light

signaling in Arabidopsis. *Plant Cell*, *17*(3), 804–821. https://doi.org/10.1105/tpc.104.030205

Yang, J., Yan, R., Roy, A., Xu, D., Poisson, J., and Zhang, Y. (2014a). The I-TASSER suite: Protein structure and function prediction. *Nature Methods*, *12*(1), 7–8. https://doi.org/10.1038/nmeth.3213

Yang, J., and Zhang, Y. (2015). I-TASSER server: New development for protein structure and function predictions. *Nucleic Acids Research*, *43*(W1), W174–W181. https://doi.org/10.1093/nar/gkv342

Yang, S., Murphy, R. L., Morishige, D. T., Klein, P. E., Rooney, W. L., and Mullet, J. E. (2014b). Sorghum phytochrome B inhibits flowering in long days by activating expression of SbPRR37 and SbGHD7, repressors of SbEHD1, SbCN8 and SbCN12. *PLoS ONE*, *9*(8). https://doi.org/10.1371/journal.pone.0105352

Yang, Y., Peng, Q., Chen, G. X., Li, X. H., and Wu, C. Y. (2013). OsELF3 Is involved in circadian clock regulation for promoting flowering under long-day conditions in rice. *Molecular Plant*, *6*(1), 202–215. https://doi.org/10.1093/mp/sss062

Yi, C., and Deng, X. W. (2005). COP1 - From plant photomorphogenesis to mammalian tumorigenesis. *Trends in Cell Biology*, *15*(11), 618–625. https://doi.org/10.1016/j.tcb.2005.09.007

Yin, R., and Ulm, R. (2017). How plants cope with UV-B: from perception to response. *Current Opinion in Plant Biology*, *37*, 42–48. https://doi.org/10.1016/j.pbi.2017.03.013

Yu, J. W., Rubio, V., Lee, N. Y., Bai, S., Lee, S. Y., Kim, S. S., Liu, L., Zhang, Y., Irigoyen, M. L., Sullivan, J. A., Zhang, Y., Lee, I., Xie, Q., Paek, N. C., and Deng, X. W. (2008). COP1 and ELF3 Control Circadian Function and Photoperiodic Flowering by Regulating GI Stability. *Molecular Cell*, *32*(5), 617–630. https://doi.org/10.1016/j.molcel.2008.09.026

Yu, Y., Wang, J., Shi, H., Gu, J., Dong, J., Deng, X. W., and Huang, R. (2016). Salt stress and ethylene antagonistically regulate nucleocytoplasmic partitioning of COP1 to control seed germination. *Plant Physiology*, *170*(4), 2340–2350. https://doi.org/10.1104/pp.15.01724

Yu, Y., Wang, J., Zhang, Z., Quan, R., Zhang, H., Deng, X. W., Ma, L., and Huang, R. (2013). Ethylene Promotes Hypocotyl Growth and HY5 Degradation by Enhancing the Movement of

COP1 to the Nucleus in the Light. *PLoS Genetics*, *9*(12). https://doi.org/10.1371/journal.pgen.1004025

Zakhrabekova, S., Gough, S. P., Braumann, I., MuÏler, A. H., Lundqvist, J., Ahmann, K., Dockter, C., Matyszczak, I., Kurowska, M., Druka, A., Waugh, R., Granerd, A., Stein, N., Steuernagel, B., Lundqvist, U., and Hansson, M. (2012). Induced mutations in circadian clock regulator Mat-a facilitated short-season adaptation and range extension in cultivated barley. *Proceedings of the National Academy of Sciences of the United States of America*, *109*(11), 4326–4331. https://doi.org/10.1073/pnas.1113009109

Zeevaart, J. A. D. (2006). Florigen coming of age after 70 years. *The Plant Cell*, *18*(8), 1783–1789. https://doi.org/10.1105/tpc.106.043513

Zhai, H., Lü, S., Liang, S., Wu, H., Zhang, X., Liu, B., Kong, F., Yuan, X., Li, J., and Xia, Z. (2014a). GmFT4, a homolog of FLOWERING LOCUS T, is positively regulated by E1 and functions as a flowering repressor in soybean. *PLoS ONE*, *9*(2). https://doi.org/10.1371/journal.pone.0089030

Zhai, H., Lü, S., Wang, Y., Chen, X., Ren, H., Yang, J., Cheng, W., Zong, C., Gu, H., Qiu, H., Wu, H., Zhang, X., Cui, T., and Xia, Z. (2014b). Allelic variations at four major maturity e genes and transcriptional abundance of the E1 gene are associated with flowering time and maturity of soybean cultivars. *PLoS ONE*, *9*(5). https://doi.org/10.1371/journal.pone.0097636

Zhang, L., Jiang, A., Thomson, G., Kerr-Phillips, M., Phan, C., Krueger, T., Jaudal, M., Wen, J., Mysore, K. S., and Putterill, J. (2019). Overexpression of Medicago MtCDFd1_1 Causes Delayed Flowering in Medicago via Repression of MtFTa1 but Not MtCO-Like Genes. *Frontiers in Plant Science*, *10*(September), 1–14. https://doi.org/10.3389/fpls.2019.01148

Zhang, Q., Li, H., Li, R., Hu, R., Fan, C., Chen, F., Wang, Z., Liu, X., Fu, Y. F., and Lin, C. (2008). Association of the circadian rhythmic expression of GmCRY1a with a latitudinal cline in photoperiodic flowering of soybean. *Proceedings of the National Academy of Sciences of the United States of America*, *105*(52), 21028–21033. https://doi.org/10.1073/pnas.0810585105

Zhang, X., Zhai, H., Wang, Y., Tian, X., Zhang, Y., Wu, H., Lü, S., Yang, G., Li, Y., Wang, L., Hu, B., Bu, Q., and Xia, Z. (2016). Functional conservation and diversification of the soybean maturity gene E1 and its homologs in legumes. *Scientific Reports*, *6*, 29548. https://doi.org/10.1038/srep29548

Zhao, C., Takeshima, R., Zhu, J., Xu, M., Sato, M., Watanabe, S., Kanazawa, A., Liu, B., Kong, F., Yamada, T., and Abe, J. (2016). A recessive allele for delayed flowering at the soybean maturity locus E9 is a leaky allele of FT2a, a FLOWERING LOCUS T ortholog. *BMC Plant Biology*, *16*(1), 20. https://doi.org/10.1186/s12870-016-0704-9

Zhao, J., Huang, X., Ouyang, X., Chen, W., Du, A., Zhu, L., Wang, S., Deng, X. W., and Li, S. (2012). OsELF3-1, an ortholog of arabidopsis EARLY FLOWERING 3, regulates rice circadian rhythm and photoperiodic flowering. *PLoS ONE*, *7*(8), 1–10. https://doi.org/10.1371/journal.pone.0043705

Zhu, D., Maier, A., Lee, J. H., Laubinger, S., Saijo, Y., Wang, H., Qu, L. J., Hoecker, U., and Deng, X. W. (2008). Biochemical characterization of Arabidopsis complexes containing constitutively photomorphogenic1 and suppressor of PHYA proteins in light control of plant development. *Plant Cell*, *20*(9), 2307–2323. https://doi.org/10.1105/tpc.107.056580

Zhu, J., Takeshima, R., Harigai, K., Xu, M., Kong, F., Liu, B., Kanazawa, A., Yamada, T., and Abe, J. (2019). Loss of Function of the E1-Like-b Gene Associates With Early Flowering Under Long-Day Conditions in Soybean. *Frontiers in Plant Science*, *9*(January), 1–13. https://doi.org/10.3389/fpls.2018.01867

Zoltowski, B. D., and Imaizumi, T. (2014). Structure and function of the ZTL/FKF1/LKP2 group proteins in arabidopsis. *Enzymes*, *35*, 213–239. https://doi.org/10.1016/B978-0-12-801922-1.00009-9

Zuo, Z., Liu, H., Liu, B., Liu, X., and Lin, C. (2011). Blue light-dependent interaction of CRY2 with SPA1 regulates COP1 activity and floral initiation in arabidopsis. *Current Biology*, *21*(10), 841–847. https://doi.org/10.1016/j.cub.2011.03.048